

# Effluent Salinity of Pipe Drains and Tube-Wells

A case study from the Indus plain



CENTRALE LANDBOUWCATALOGUS

0000 0873 1602

Promotor: Prof. dr. ir. R.A. Feddes  
Hoogleraar in de bodemnatuurkunde, agrohydrologie en het  
grondwaterbeheer

Co-Promotoren: Dr. ir. Th.M. Boers  
Senior onderzoeker, ILRI, Wageningen

Dr. ir. J.C. van Dam  
Universitair docent, departement omgevingswetenschappen,  
Wageningen Universiteit

Samenstelling promotiecommissie: Prof. dr. ir. J.J. de Vries, Vrije Universiteit, Amsterdam  
Prof. dr. ir. A. Leijnse, Wageningen Universiteit  
Dr. ir. L.K. Smedema  
Dr. ir. M.G. Bos, ILRI, Wageningen

## Propositions

1. Effluent salinity of pipe drains and tube-wells in the Indus plain can be predicted in a computationally efficient way by a combination of the one-dimensional vertical finite-difference model SWAP for the variably saturated zone and a solute impulse response function based on stream functions for the saturated zone. *This Thesis*
2. Drained areas in the Indus plain generally exhibit a time lag between the reclamation of the rootzone, and the reclamation of the complete soil-aquifer system. The implication is that farmers will benefit quickly from the drainage system but that long term solutions are required for the safe use and disposal of the effluent. *This Thesis*
3. The solute impulse response function of the saturated zone for pipe drains in a thin aquifer and for tube-wells with a relatively long well screen, can be described by an exponential distribution that is based on the mixing reservoir approach. *This Thesis*
4. In areas where fresh groundwater is overlying saline groundwater, pipe drains discharge water of lower salinity than skimming wells. *This Thesis*
5. Consultants who propose a sub-surface drainage project because the existing surface drainage system is not working properly due to bad maintenance, should be sent back to primary school.
6. Een bijkomend voordeel van de Engelse taal is dat "you" zowel "je" als "u" vervangt.
7. Overheidsinstellingen die de door haar ontwikkelde producten en diensten niet gratis beschikbaar stellen doen de belastingbetaler tekort.
8. Er bestaat geen verband tussen algemene intelligentie en spelinzicht op het voetbalveld. *Stelling op basis van 10 jaar lidmaatschap van voetbalclub GVC, een vereniging met een relatief hoog percentage aan studenten en afgestudeerden.*
9. Deskundigen vertellen ons dat het consumentenvertrouwen bepalend is voor de groei van de economie. Dit zou betekenen dat recessies simpelweg vermeden kunnen worden door het woordvoerdersgilde en de nieuwsmidia louter met optimisten te bevolken.
10. Eens houdt het op (Maarten Koning in Het Bureau deel 4 door J.J. Voskuil).

T.J. Kelleners. Effluent Salinity of Pipe Drains and Tube-Wells. A case study from the Indus plain. 28 November 2001, Wageningen.

11.12.2001

T.J. Kelleners

## Effluent Salinity of Pipe Drains and Tube-Wells

A case study from the Indus plain

Proefschrift  
ter verkrijging van de graad van doctor  
op gezag van de rector magnificus  
van Wageningen Universiteit,  
Prof. dr. ir. L. Speelman,  
in het openbaar te verdedigen  
op woensdag 28 November 2001  
des namiddags te vier uur in de Aula.

im 1634042

ILRI  
P.O. Box 45  
6700 AA Wageningen  
The Netherlands  
E-mail: [ilri@ilri.nl](mailto:ilri@ilri.nl)

Wageningen University  
Sub-department of Water Resources  
Nieuwe Kanaal 11  
6709 PA Wageningen  
The Netherlands

Thijs Kelleners  
U.S. Salinity Laboratory  
450 W. Big Springs Road  
Riverside, CA 92507-4617  
USA  
Phn: 1 909 369 4868  
Fax: 1 909 342 4964  
E-mail: [tkelleners@ussl.ars.usda.gov](mailto:tkelleners@ussl.ars.usda.gov)

CIP-DATA KONINKLIJKE BIBLIOTHEEK, DEN HAAG

Kelleners, T.J.

Effluent salinity of pipe drains and tube-wells. A case study from the Indus plain. T.J.  
Kelleners  
PhD Thesis Wageningen University. - With ref. - With summary in Dutch.  
ISBN 90-5808-523-6

## Abstract

Kelleners, T.J., 2001. Effluent salinity of pipe drains and tube-wells. A case study from the Indus plain. Doctoral Thesis, Wageningen University, The Netherlands.

Irrigated agriculture in arid and semi-arid zones often suffers from waterlogging and salinity problems. Sub-surface drainage systems can be used to control the groundwater table and to facilitate the leaching of salts from the rootzone. In the Indus plain, pipe drains and tube-wells are used for this purpose. Regional water management requires that the development of the effluent salinity with time of these systems is known in advance. Numerical models based on the Darcy equation and the mass balance equation for water flow and the advection-dispersion equation for solute transport are powerful tools to predict the effluent salinity of pipe drains and tube-wells at field level. In advection-dominated transport problems, however, solute impulse response functions based on stream-functions constitute a more computationally efficient approach.

A new modelling approach is presented that combines the one-dimensional vertical finite-difference SWAP model for the variably saturated zone with a solute impulse response function for the saturated zone. This approach is applied to the Sampla experimental pipe drainage site in Haryana, India, the S-I-B-9 pipe drainage unit of the Fourth Drainage Project, Punjab, Pakistan and the Satiana tube-well Pilot Project, Punjab, Pakistan. Results show that the effluent salinity of pipe drains and tube-wells changes only gradually with time due to the low percolation from the irrigated fields and due to the large quantities of salts stored in the groundwater. Areas with relatively high percolation and a shallow depth of the impermeable layer (pipe drains at Sampla) still require 10 years before the effluent salinity has reduced to equilibrium levels. In contrast, desalinization of the rootzone generally takes only 1-3 years. The implication is that farmers will benefit quickly from the installation of a drainage system. However, for the safe use and disposal of the effluent, long term solutions are required.

In the Indus plain, groundwater salinity usually increases with depth. In water scarce areas, the shallow fresh groundwater may be an important source of irrigation water. In waterlogged areas, where sub-surface drainage is installed to control the groundwater table, the presence of fresh groundwater bodies may result in a relatively low effluent salinity. The finite-element model SUTRA is used to study the behaviour of skimming wells and pipe drains in fresh-saline groundwater systems. The model is calibrated on two documented experiments with a skimming well and a scavenger well at Phularwan research farm, Punjab, Pakistan. Salt water upconing below the skimming well is particularly sensitive to the anisotropy factor of the aquifer. The relationship between aquifer anisotropy and the Electrical Conductivity ( $EC$ ) of the pumped water is non-linear. The skimming well simulations show that water with an  $EC$  of  $\sim 1.7 \text{ dS m}^{-1}$  can be pumped from a thin fresh groundwater body, provided that the pumping rate is low. Under the same circumstances, pipe drains yield a better effluent quality ( $EC$  of  $1.2\text{--}1.3 \text{ dS m}^{-1}$ ). With pipe drains, flow is restricted to the shallow fresh groundwater. The deeper saline groundwater is left untouched. The better effluent quality for pipe drains as compared to skimming wells, must be evaluated against the considerably higher installation costs for pipe drains.

**Keywords:** anisotropy, aquifer, desalinization, effluent salinity, groundwater, irrigation, salt-water upconing, soil salinity, stream-function, subsurface drainage

## Preface

The idea for a study on the relationship between drainage technology and effluent salinity came from Bert Smedema of the International Program for Technology and Research in Irrigation and Drainage (IPTRID). I started working on this subject at ILRI in September 1993 under the guidance of Ruud van Aart. During this first period a literature review was written and two model studies were conducted. At the end of 1996, the original proposal was re-written to facilitate a PhD study. Subsequently, in April 1997, I was appointed as a PhD-student for the sub-department of Water Resources of Wageningen University. My desk, however, remained at ILRI, which also continued to provide all the funds for the study.

Reinder Feddes of the sub-department agreed to serve as my promotor. Jos van Dam, also of the sub-department, and Theo Boers and Hans Boonstra, both of ILRI, completed the support group. All four group members played an important role during the course of the study. Reinder provided detailed comments on all my drafts and, through his generally positive remarks, encouraged me to continue. Jos gave many valuable suggestions and helped me during my initial struggles with the SWAP model. Theo rigorously reviewed all my writings and made numerous suggestions for improvement. Finally, Hans, in his own way, gave a number of valuable comments, especially on the modelling of density-dependent flow. Reinder, Jos, Theo and Hans thanks for all your help!

Writing a thesis can be a lonely job. Luckily, some time was available during the past years to participate in some of the more regular ILRI activities. I was very fortunate to be able to spend some of my time teaching in ILRI's International Course on Land Drainage (ICLD) and in ILRI's tailor-made courses in India. I enjoyed the cooperation with Fons Jaspers (ICLD) and Henk Ritzema, Roland Oosterbaan, Karel Lenselink and Rob Kselik (India). Looking back, I must say that some of my best insights in land drainage developed while preparing or conducting classes (I am under the impression that the one person who learns most from a lecture is the lecturer).

During my study, I cooperated with various individuals from India and Pakistan. I am greatly indebted to Dr M.R. Chaudhry of the International Waterlogging and Salinity Research Institute, Lahore, Pakistan and Drs S.K. Kamra, O.P. Singh, S.K. Gupta, D.P. Sharma and P.S. Kumbhare of the Central Soil Salinity Research Institute, Karnal, India for sharing their data and valuable insights with me. Also many thanks to R.K. Jhorar of the Haryana Agricultural University, Hisar, India for helping me out on many occasions. Much to my dismay, I had to remove all the "Hisar" calculations from Chapter 5 to maintain the overall balance in the thesis. However, part of the data from Hisar are incorporated in the Journal of Hydrology paper which was published in 2000.

This thesis covers only a part of my research efforts over the past years. I also invested quite some time to study the effluent salinity of pipe drains in clay soils. I collected data from Portugal (Lezíria Grande), Egypt (Nile Delta and Fayoum Oasis) and India (Chambal Plain). Part of this work was published in ILRI's annual reports 1996 and 1997. Unfortunately, I did not find the time to write a research paper for an international journal. Hopefully, I will find the time in the near future. Anyway, many thanks to António Pissarra of the Associação de Beneficiários da Lezíria Grande de Vila Franca de Xira, Portugal, Frank Croon of Arcadis-Euroconsult and Drs R.D. Sharma and K.V.G.K. Rao of the Rajasthan Agricultural Drainage Research Project, Kota, India, for all their help.

During the course of this study, two students from Wageningen University collaborated with me as part of their MSc research work. Hugo Oosterkamp collected drainage effluent salinity data in Pakistan and looked at the possibilities for drainage water re-use. Reinier van Hoffen used the SWMS\_2D model to simulate two-dimensional water flow and solute transport to a pipe drain in Egypt. Hugo and Reinier, I enjoyed working with you and I want to thank the both of you for all your hard work. During my study, I also collaborated with Dr D.K. Singh of the Water Technology Centre, New Delhi, India, who visited ILRI for about 6 months. Dr Singh, or rather D.K., you did a fine job in unravelling the mysteries of the SUTRA model for the simulation of density-dependent water flow and solute transport. Chapter 6 could not have been written without your help.

Over the years I received much help from the people of the Haaff library. The persons behind the service desk never complained when I came up with one more list with requested papers. The Haaff proved to be an invaluable source of information for me. Piet, Leni, Petra, Marjan, Mariska and all the others... thanks! Thanks also to Luuk Wielstra and Jan Van Brakel of IAC for solving all my computer problems. Many other persons contributed to this thesis in one way or another. In random order: Hans Van Alphen, Jelle Beekma, Frans Cortenbach, Asher Hussain, Asad Sarwar, Jeroen Alberts, Johan Van Manen, Joop Van Dijk, Wouter Wolters, Willem Vlotman, Elisabeth Rijksen, Shaakeel Hasan, Marcel Schaap, Koen Roest, Meredith Naeff, Elly Verschoor and Rien Bos. I want to thank you all!

For a long time, I was the only "young" person at ILRI. Luckily, this changed during the past year. Within the time frame of a few months, Catharien Terwisscha van Scheltinga, Herco Jansen and Paul-Willem Vehmeyer joined the institute. Our daily lunch break was always a welcome interruption from thesis writing. Catharien, Herco and Paul-Willem, I hope you will enjoy working at ILRI as much as I did!

Thijs Kelleners  
Riverside, October 2001



# Table of Contents

1	Introduction .....	1
1.1	Drainage of irrigated areas in arid and semi-arid zones .....	1
1.2	Drainage and water quality in the Indus plain .....	2
1.3	Scope and objective of this study .....	3
1.4	Limitations of this study .....	4
1.5	Outline of the thesis .....	5
2	Theory of Water Flow and Solute Transport in Porous Media .....	7
2.1	Soil evaporation and crop transpiration .....	7
2.2	Two-dimensional pressure and density driven water flow and solute transport in porous media .....	9
2.3	Two-dimensional water flow in terms of pressure head and hydraulic conductivity .....	11
2.4	One-dimensional vertical water flow and solute transport in the unsaturated zone with root water uptake .....	12
2.5	Description of the soil hydraulic properties .....	14
2.6	Description of a pipe drain in a finite-element mesh .....	15
3	Theory of Solute Travel Time to Pipe Drains and Tube-Wells in Steady-State Flow Fields .....	17
3.1	The stream-function concept in a vertical cross-section .....	18
3.2	Governing equation for two-dimensional flow in a vertical cross-section ..	19
3.3	Governing equation for axi-symmetric flow in a vertical cross-section ....	20
3.4	Analytical solution of the stream function for a pipe drain in a two-layered soil .....	21
3.5	Numerical solution of the stream function for a partially penetrating well in an unconfined aquifer .....	25
3.6	Calculation of solute travel time .....	26
4	Description of the Study Areas in the Indus Plain .....	29
4.1	Location, climate and cropping pattern .....	29
4.2	Geo-hydrology .....	31
4.3	Irrigation and drainage for agriculture .....	32
4.4	Sampla experimental pipe drainage site .....	33
4.5	Satiana tube-well Pilot Project .....	37
4.6	Fourth Drainage Project .....	40
4.7	Conclusions .....	46
5	Prediction of Long Term Effluent Salinity of Pipe Drains and Tube-Wells .....	49
5.1	Introduction .....	49
5.2	New modelling approach for pipe drains .....	50
5.3	Calibration of the soil-aquifer hydraulic properties .....	54
5.4	Case 1: Sampla experimental pipe drainage site .....	55
5.5	Case 2: Unit S-I-B-9 of the Fourth Drainage project .....	65
5.6	New modelling approach for tube-wells .....	72

5.7	Case 1: Satiana Pilot Project tube-well .....	74
5.8	The mixing reservoir approach .....	77
5.9	Conclusions .....	82
6	Density-Dependent Water Flow and Solute Transport to Tube-Wells and Pipe Drains .....	85
6.1	Introduction .....	85
6.2	Phularwan experimental skimming well site .....	88
6.3	Calibration of the SUTRA model for the <i>skimming well</i> experiment .....	90
6.4	Validation of the SUTRA model for the <i>scavenger well</i> experiment .....	98
6.5	Scenario analysis 1: Effluent salinity of a skimming well .....	100
6.6	Scenario analysis 2: Effluent salinity of a pipe drain in fresh-saline groundwater .....	104
6.7	Scenario analysis 3: Effluent salinity of a pipe drain in saline groundwater .....	107
6.8	Conclusions .....	109
7	Summary and Conclusions .....	111
	Samenvatting en conclusies .....	119
	References .....	127
Appendix A	Application of the SWMS_2D Model to Simulate the $q_d(H)$ Relationship for Pipe Drains .....	139
Appendix B	Analysis of Pumping Test Data from Satiana Tube-Well No. 22a with WTAQ .....	141
	List of Symbols .....	145
	Curriculum Vitae .....	151

# 1 Introduction

## 1.1 Drainage of irrigated areas in arid and semi-arid zones

Irrigated agriculture in arid and semi-arid zones often suffers from waterlogging and salinity problems. Excess water in the crop rootzone and high soil salinity reduce transpiration and hence crop yields. The waterlogging problems are due to seepage from irrigation canals and percolation from irrigated fields which bring the groundwater table close to the soil surface. Salts are added to the soil with the irrigation water and through capillary rise from the shallow groundwater. These salts add up to the salts that are naturally present in the soil. Waterlogging and salinity problems occur mainly in areas with a flat topography (low natural drainage) and in local depressions that serve as sinks for water and salts from the surrounding areas. The International Food Policy Research Institute (1995) estimates that worldwide between 0.3 and 1.5 million ha of land are lost each year to waterlogging and salinity. Major affected areas can be found in the Central Asian Republics, China, India, Egypt, Irak, Pakistan and the United States.

Several strategies can be followed when dealing with waterlogging and salinity problems. Improved irrigation design and management may reduce the recharge to the groundwater at regional scale and facilitate a better soil water and soil salinity management at field level (Hanson, 1989; Wolters, 1992). This strategy tackles the source of the problem, and should therefore be considered first. Where high groundwater tables and soil salinities persist, the growing of more salt tolerant crops or trees may maintain some agricultural productivity of the affected fields (Maas, 1990; Heuperman, 1993). This strategy can be described as "living with the problem". The retirement of specific lands with shallow groundwater tables and high levels of salinity has also been proposed (Swain, 1991; Belitz and Phillips, 1995).

If the above measures do not solve the problems, or if the measures are not acceptable from a socio-economic point of view, the installation of sub-surface drainage systems can be considered. A sub-surface drainage system controls the groundwater table and facilitates the leaching of salts from the rootzone. The drainage system may consist of ditches, mole drains, pipe drains or tube-wells. The choice for one of these systems is made on the basis of geo-hydrology, costs and the expected quality of the effluent. With the increasing scarcity of fresh water resources, especially in arid and semi-arid zones, *the effluent quality is becoming increasingly important when drainage options are considered*. Disposal of the effluent should not detriment the water resources downstream (Johnston et al., 1997). Furthermore, drainage effluent may be an important source of irrigation water in dry areas, provided that certain water quality criteria are met (Oster, 1994; Willardson et al., 1997).

In arid and semi-arid zones the drainage effluent quality is determined primarily by the salt content and the ion composition. The water captured by the sub-surface drainage systems is often highly concentrated with the major cations being  $\text{Na}^+$ ,  $\text{Ca}^{2+}$ ,  $\text{Mg}^{2+}$  and to a lesser extent  $\text{K}^+$ . The major anions are  $\text{Cl}^-$ ,  $\text{SO}_4^{2-}$ ,  $\text{HCO}_3^-$  and  $\text{CO}_3^{2-}$  (Westcot, 1997). In regions with high-input agriculture, pesticides and fertilizers may also affect the effluent quality. Locally, toxic trace elements like Arsenic, Boron, Molybdenum and Selenium may cause problems (Ayers and Westcot, 1985). If these natural or man-made pollutants remain stored in the local groundwater

they may not pose a threat. Installation of a sub-surface drainage system, however, mobilizes the pollutants and conveys them into the surface water system.

### 1.2 Drainage and water quality in the Indus plain

The Indus plain forms a typical example of an irrigated area in an arid to semi-arid zone where sub-surface drainage systems are installed to combat waterlogging and salinity problems. The need for sub-surface drainage became urgent when after several decades of irrigation the groundwater table had risen from 30 m below soil surface at pre-irrigation times to ~1.5 m below soil surface (Ahmad and Chaudhry, 1988). The sub-surface drainage systems in the Indus plain consist of either "vertical" tube-wells or "horizontal" pipe drains. Because of the relatively sandy nature of the soil-aquifer system and the associated unstable soils, ditches and mole drains are not used. Also the loss of agricultural land, which is inherent to ditches, is for most farmers not acceptable.

*Salt load and ion composition of the drainage effluent are the primary water quality concerns in the Indus plain.* Problems due to pesticides and fertilizers are still relatively small because agricultural inputs are generally low. Also no difficulties with toxic trace elements are reported. With regard to water quality in the Indus plain, a distinction is made between saline and fresh groundwater areas where the boundary lies at an Electrical Conductivity,  $EC$  of  $1.5 \text{ dS m}^{-1}$ . In saline groundwater areas, drainage is provided by government funded pipe drains and tube-wells. Most of the saline effluent is disposed in surface drains and salt load is the main problem. In fresh groundwater areas, irrigation tube-wells take care of the sub-surface drainage requirements. As the pumped water is relatively high in  $\text{Na}^+$  ions, use of this water for irrigation may not only result in soil salinity problems but may also affect the structure of the soil (Van Hoorn and Van Alphen, 1994; Kuper, 1997).

The continuing development of irrigation tube-wells in the Indus plain is nowadays resulting in over-pumping, leading in many fresh groundwater areas to falling groundwater tables. The bulk of the new tube-wells is installed by farmers who use the pumped water to supplement the limited canal water supplies. In e.g. the Pakistan part of the Indus plain, the number of farmer owned tube-wells has risen from only a few thousand in 1960 to approximately 450,000 at present (Sarwar, 2000). Developments in the Indian part of the Indus plain are probably not much different (e.g. Abrol, 1999). Strictly speaking, because of over-pumping, many fresh groundwater areas in the Indus plain do no longer have a sub-surface drainage problem. As a result of over-pumping, saline groundwater may encroach towards fresh water tube-wells, turning these wells saline.

In the Indus plain, agricultural water quality is expressed through three parameters;  $EC$ , Sodium Adsorption Ratio ( $SAR$ ) and Residual Sodium Carbonate ( $RSC$ ). The  $EC$ , measured at a reference temperature of  $25^\circ\text{C}$ , is an indicator for the total salt concentration. The  $SAR$ , defined as  $\text{Na}^+ / \sqrt{(\frac{1}{2}\text{Ca}^{2+} + \frac{1}{2}\text{Mg}^{2+})}$  (concentrations in  $\text{meq l}^{-1}$ ), is a measure for possible negative effects of  $\text{Na}^+$  on the structure of the soil. The  $RSC$ , defined as  $\text{HCO}_3^- + \text{CO}_3^{2-} - \text{Ca}^{2+} - \text{Mg}^{2+}$  (concentrations in  $\text{meq l}^{-1}$ ), is an indicator of the danger that  $\text{Na}^+$  in the soil solution will increase more than

proportionally owing to the precipitation of especially Calcite  $\text{CaCO}_3$  in the soil. The water quality standards used in Pakistan by the Water and Power Development Authority (WAPDA) are given in Table 1.1. These standards relate primarily to the usability of the water for the irrigation of crops.

**Table 1.1** Water quality standards used in Pakistan by WAPDA to assess the usability of water for irrigation (Beg and Lone, 1992).

Category	EC (dS $\text{m}^{-1}$ )	SAR (meq $\text{l}^{-1}$ ) <sup>0.5</sup>	RSC (meq $\text{l}^{-1}$ )
Usable	0-1.5	0-10	<2.5
Marginal	1.5-2.7	10-18	2.5-5.0
Hazardous	>2.7	>18	>5.0

### 1.3 Scope and objective of this study

It is widely accepted that sub-surface drainage design and management should be based on both water quantity and water quality criteria (Ayars et al., 1997). Many factors should be taken into account such as climate, geo-hydrology, soils and agricultural practices. Because of the large number of factors involved, and because of the large spatial and temporal variability in some of these factors, no fixed set of rules is available for the design and management of a drainage system. In view of these uncertainties, sub-surface drainage systems are often field tested by constructing pilot areas before being implemented on a large scale. These field tests, however, are costly and time consuming, and only allow the study of a limited number of designs and management scenarios.

In the Indus plain, both pipe drains and tube-wells are used to provide sub-surface drainage in saline groundwater areas. It is generally believed that, after a certain reclamation period, pipe drains render a better effluent quality than tube-wells. The flow lines to pipe drains are shorter and therefore originate from usually less saline groundwater layers (Smedema, 1993). A direct comparison between the effluent of both technologies on the basis of field data alone is difficult because of two reasons: (1) pipe drains and tube-wells are generally not applied in the same area; (2) long term monitoring of discharge from the drainage systems and effluent quality is generally not done with sufficient intensity to allow firm conclusions.

Traditionally, steady-state drain spacing and well spacing equations have been used for the design of sub-surface drainage systems (Ritzema, 1994; Boehmer and Boonstra, 1994). For pipe drains also transient drain spacing equations have been developed (e.g. Dumm, 1968). These equations allow a fair judgement of the effect of drainage on waterlogging and salinity in the rootzone. The prediction of drainage water quality, however, requires the use of hydrodynamic models that describe the motion of subsurface water towards the drainage media (Guitjens et al., 1997). Specialized hydrodynamic models also facilitate a more detailed assessment of the moisture and the salinity status of the rootzone in response to drainage and their effect on crop growth (e.g. Šimůnek et al., 1994; Van Dam et al., 1997).

*The objective of this study is to review the relationship between drainage technology (pipe drains and tube-wells) and the effluent salinity in the Indus plain. Field data from existing drainage schemes and pilot areas are combined with hydrodynamic models to quantify this relationship. The hydrodynamic models allow the identification of the most dominant processes and facilitate long term predictions. The results of this study will assist irrigation and drainage engineers with the selection of the proper drainage method, taking into account the expected effluent salinity. Application of the results is however restricted to relatively coarse textured soil-aquifer systems as found in the Indus plain. For clay soils, for example, the dominant processes are likely to be different (e.g. Rycroft and Amer, 1995; Bronswijk et al., 1995; Groen, 1997).*

### 1.4 Limitations of this study

In this study, sub-surface drainage is treated as a local flow problem. This allows a detailed assessment of the flow and transport processes at field level. The aquifer in the Indus plain, however, is extensive and essentially unbounded. This implies that, in reality, regional flow processes will interact with the local flow processes. In saline groundwater areas, exclusion of regional flow is likely to overestimate the reclamation rate of the soil-aquifer system. Regional inflow of saline groundwater into the drained areas will present a continuous source of salts. The extent to which the reclamation rate is overestimated (and the effluent salinity underestimated) depends on the amount of irrigation water that percolates to the groundwater in the drained areas as compared to the surrounding undrained areas and on the local geohydrologic conditions. Examples of studies that include the interaction between local and regional flow processes can be found in Fio and Deverel (1991), Pohll and Guitjens (1994), Eching et al. (1994) and Vaughan et al. (1999).

Several investigations have shown the benefits of integrating irrigation and drainage water management at field level. Careful irrigation water management limits percolation losses to the groundwater and reduces the drainage requirements (Hoffman et al., 1978). Conjunctive use of canal water and drainage water for irrigation may achieve good crop yields while limiting drainage water disposal problems (Rhoades et al., 1992). Shallow or controlled drainage increases the contribution of the shallow groundwater to the crop water requirement, reduces the discharge from the drainage systems and diminishes the need for irrigation water (El-Atfy et al., 1991; Ayars, 1996; Manguerra and Garcia, 1996; Ayars et al., 1999). Although very relevant, these issues are not addressed in this study. In the Indus plain the prospects of integrating irrigation and drainage water management at field level are bleak because of the small landholdings, the rigidity of the Warabandi irrigation system and the generally low degree of organization of the farmers.

Compared to irrigation water, drainage effluent shows elevated levels of all major ions due to concentration of the soil water and the shallow groundwater by evapotranspiration. Also a shift in ion composition can usually be noticed. Percentage-wise,  $\text{Na}^+$  and  $\text{Cl}^-$  increase while  $\text{Ca}^{2+}$ ,  $\text{Mg}^{2+}$ ,  $\text{HCO}_3^-$  and  $\text{SO}_4^{2-}$  decrease. This is due to the leaching of  $\text{Na}^+$  and  $\text{Cl}^-$  from the irrigated soils and the precipitation herein of calcite  $\text{CaCO}_3$ , gypsum  $\text{CaSO}_4 \cdot 2\text{H}_2\text{O}$ , sepiolite  $\text{Mg}_3\text{Si}_6\text{O}_{15}(\text{OH})_2 \cdot 6(\text{H}_2\text{O})$  and others (Christiansen, 1973; Šimůnek et al., 1996; Kuper, 1997).

Exchange of cations between the solid phase adsorption complex and the soil solution, and dissolution processes also result in a shift in the ion composition. In this study, ion composition is only incorporated through the *SAR* and *RSC* parameters discussed in Section 1.2. A more thorough discussion on ion composition with regard to effluent quality is hampered by a lack of reliable field data. For the same reason, the model applications in Chapters 5 and 6 consider only the *EC* of the drainage effluent. Examples of model studies that do incorporate the ion composition can be found in Ayars et al. (1981) and Šimůnek and Suarez (1994).

## 1.5 Outline of the thesis

In Chapter 2 the theory of water flow and solute transport in porous media will be discussed. The presented equations form the basis of the finite-element model SUTRA (Voss, 1984), the finite-element model SWMS\_2D (Šimůnek et al., 1994) and the vertical one-dimensional finite-difference model SWAP (Van Dam et al., 1997), which will all three be used in this study. Chapter 2 also includes a section on the calculation of soil evaporation and crop transpiration.

The theory of solute travel time to pipe drains and tube-wells in steady-state flow fields is treated in Chapter 3. The stream-function concept is explained, which allows the delineation of streamlines in the groundwater. The presented theory facilitates the calculation of solute impulse response functions which describe the transport characteristics of the aquifer in a computationally efficient way.

Chapter 4 describes the study areas in the Indus plain. First, a general description of the Indus plain as a whole is given. Subsequently, the study areas are discussed: the Sampla experimental pipe drainage site, Haryana, India, the Satiana tube-well Pilot Project, Punjab, Pakistan and the Fourth Drainage Project (pipe drains), Punjab, Pakistan. The Phularwan experimental skimming well site, Punjab, Pakistan, which will be used to study density-dependent water flow and solute transport to pipe drains and tube-wells, is discussed in Chapter 6.

In Chapter 5 a new modelling approach is presented that is designed specifically to facilitate long term predictions of soil and effluent salinity in irrigated and drained areas. The general idea is to couple the SWAP model for water flow and solute transport in the variably saturated zone with a solute impulse response function for the saturated zone. The modelling approach is applied to the study areas described in Chapter 4. In Chapter 5, the SWMS\_2D model is used to assist in the calibration of the soil hydraulic properties, especially the horizontal and vertical hydraulic conductivities in the saturated zone.

The modelling of density-dependent water flow and solute transport to pipe drains and tube-wells with the SUTRA model is discussed in Chapter 6. The SUTRA model is calibrated and validated with data from a skimming well experiment and a scavenger well experiment at the earlier mentioned Phularwan site. The calibrated model is subsequently used to study the effluent salinity of skimming wells and pipe drains under conditions where fresh groundwater is overlying saline groundwater. The effluent salinity of pipe drains in a completely saline soil-aquifer system is also simulated.

## Chapter 1

---

Finally, in Chapter 7, the summary and conclusions of this study are presented.



## 2 Theory of Water Flow and Solute Transport in Porous Media

In this chapter, the theory and modelling of water flow and solute transport in porous media is discussed. The chapter starts, however, with a brief section on the calculation of soil evaporation and crop transpiration (Section 2.1). The relationships described in Section 2.1 are incorporated in the one-dimensional vertical finite-difference SWAP model (Van Dam et al., 1997), and are used to describe water fluxes between the porous media and the atmosphere.

The water flow and solute transport equations are presented in Sections 2.2 to 2.4. These equations form the basis of the finite-element model SUTRA (Section 2.2), the finite-element model SWMS\_2D (Section 2.3) and the vertical one-dimensional finite-difference model SWAP (Section 2.4), which will all three be used in this study. All three models use the analytical Mualem-Van Genuchten (MVG) model to describe the soil hydraulic properties. The MVG model is discussed in Section 2.5. Finally, Section 2.6 discusses the description of a pipe drain in a finite-element mesh.

### 2.1 Soil evaporation and crop transpiration

Various methods are available to calculate daily potential evapotranspiration. Generally, the Penman-Monteith method is used which is recommended by the FAO (Smith, 1993; Allen et al., 1998):

$$\lambda_w \rho_w ET_p = \frac{\Delta_v (R_n - G) + \rho_a c_p \frac{(e_s - e_a)}{r_a}}{\Delta_v + \gamma_a \left( 1 + \frac{r_s}{r_a} \right)} \quad (2.1)$$

where  $\lambda_w$  is the latent heat of vaporization [ $L^2 T^{-2}$ ],  $\rho_w$  the density of water [ $M L^{-3}$ ],  $ET_p$  the potential evapotranspiration rate [ $L T^{-1}$ ],  $\Delta_v$  the slope of the saturated vapour pressure curve [ $M L^{-1} T^{-2} \Theta^{-1}$ ],  $R_n$  the net radiation [ $M T^{-3}$ ],  $G$  the soil heat flux [ $M T^{-3}$ ],  $\rho_a$  the air density [ $M L^{-3}$ ],  $c_p$  the specific heat of the air [ $L^2 T^{-2} \Theta^{-1}$ ],  $e_s$  the saturation vapour pressure [ $M L^{-1} T^{-2}$ ],  $e_a$  the actual vapour pressure [ $M L^{-1} T^{-2}$ ],  $\gamma_a$  the psychrometric constant [ $M L^{-1} T^2 \Theta^{-1}$ ],  $r_s$  the crop resistance [ $T L^{-1}$ ] and  $r_a$  the aerodynamic resistance [ $T L^{-1}$ ].

The two crop specific parameters  $r_s$  and  $r_a$  in (2.1) are generally not available. Use of the hypothetical reference crop concept of the FAO circumvents this problem. In this concept, the evapotranspiration of a reference crop is multiplied with crop factors,  $k_c$  [-] to obtain the potential evapotranspiration for a specific crop (Smith, 1993; Allen et al., 1998).

The potential evaporation rate of the soil,  $E_p$  [ $L T^{-1}$ ] depends on the development stage of the crop and can be calculated from (Belmans et al., 1983; Van Dam et al., 1997):

$$E_p = ET_p e^{-\kappa LAI} \quad (2.2)$$

where  $\kappa$  is the extinction coefficient for global solar radiation [-] and  $LAI$  the Leaf Area Index [ $L^2 L^{-2}$ ]. Recent approaches estimate  $\kappa$  as the product of the extinction coefficient for diffuse light, which varies with crop type, and the extinction coefficient for direct visible light (Van Dam et al., 1997). In this thesis a value  $\kappa = 0.6$  is used for all crops as was proposed by Belmans et al. (1983).

The potential transpiration rate of the crop,  $T_p$  [ $L T^{-1}$ ] equals the potential evapotranspiration rate,  $ET_p$  (corrected for the time needed to evaporate interception water), minus  $E_p$  (Van Dam, 2000):

$$T_p = \left( 1 - \frac{P_{ir}}{ET_{p0}} \right) ET_p - E_p \quad (2.3)$$

where  $P_{ir}$  is intercepted precipitation rate [ $L T^{-1}$ ] and  $ET_{p0}$  the potential evapotranspiration rate [ $L T^{-1}$ ] of the wet crop, as calculated with Eq. (2.1), assuming  $r_s = 0$ .

Von Hoyningen-Hüne (1983) and Braden (1985) measured interception of precipitation for various crops. They proposed the following general formula for canopy interception:

$$P_{ir} = a_i LAI \left( 1 - \frac{1}{1 + \frac{b_i P_r}{a_i LAI}} \right) \quad (2.4)$$

where  $P_r$  is precipitation rate [ $L T^{-1}$ ],  $a_i$  an empirical coefficient [ $L T^{-1}$ ] and  $b_i$  the soil cover fraction ( $\approx LAI / 3.0$ ) [-]. In principle  $a_i$  must be determined experimentally. For ordinary agricultural crops it may be assumed that  $a_i = 0.25 \text{ cm d}^{-1}$  (Van Dam et al., 1997).

The actual transpiration rate depends on the root water uptake which will be discussed in Section 2.4. The actual soil evaporation rate,  $E_a$  [ $L T^{-1}$ ] is calculated by:

$$E_a = \min(E_p, E_{\max}, E_{\text{emp}}) \quad (2.5)$$

where  $E_{\max}$  is the maximum evaporation rate [ $L T^{-1}$ ] which the top soil may deliver (calculated from Darcy's law) and  $E_{\text{emp}}$  the evaporation rate [ $L T^{-1}$ ] according to an empirical function.

Empirical soil evaporation functions may be useful if Darcy's law is not valid for the top few centimetres of the soil. At shallow depths, Darcy's law may fail because of splashing rain, crust formation, vapour diffusion through air filled pores and cultivation practices (e.g. Feddes and Bastiaanssen, 1990; Van Dam et al., 1997). In this thesis the Boesten and Stroosnijder (1986) functions are used to calculate  $E_{\text{emp}}$ :

$$\sum E_{\text{emp}} = \sum E_p \quad \text{for} \quad \sum E_p \leq \beta_p^2 \quad (2.6a)$$

$$\sum E_{\text{emp}} = \beta_p (\sum E_p)^{1/2} \quad \text{for} \quad \sum E_p > \beta_p^2 \quad (2.6b)$$

where  $\beta_p$  is the so-called Boesten parameter [ $L^{1/2}$ ].

The parameter  $\beta_p$  must be calibrated for local conditions. From micro-lysimeter studies in the Netherlands, Boesten and Stroosnijder (1986) found  $0.44 \leq \beta_p \leq 0.63 \text{ cm}^{1/2}$ . The Boesten and Stroosnijder functions are reset ( $\sum E_{\text{emp}} = \sum E_p = 0$ ) if rainfall  $\geq 0.5 \text{ cm d}^{-1}$ .

## 2.2 Two-dimensional pressure and density driven water flow and solute transport in porous media

Flow in porous media is generally described by the Darcy equation. For density-dependent flow in a vertical cross-section, this equation may be written as:

$$q_i = -\frac{k_r k_{ij}}{\mu} \left( \frac{\partial p}{\partial x_j} + \rho g \eta_j \right) \quad i, j = 1, 2 \quad (2.7)$$

where  $q_i$  is the specific discharge in the  $i$  direction [ $L \text{ T}^{-1}$ ],  $k_r$  the relative permeability to fluid flow [-],  $k_{ij}$  the permeability tensor [ $L^2$ ],  $\mu$  the fluid viscosity [ $M \text{ L}^{-1} \text{ T}^{-1}$ ],  $p$  the fluid pressure [ $M \text{ L}^{-1} \text{ T}^{-2}$ ],  $x_j$  the  $j$ th coordinate direction [ $L$ ],  $\rho$  the fluid density [ $M \text{ L}^{-3}$ ],  $g$  the gravitational acceleration [ $L \text{ T}^{-2}$ ] and  $\eta_j = 1$  indicates the vertical direction ( $j = 2$ ), while  $\eta_j = 0$  indicates the horizontal direction ( $j = 1$ ). In Eq. (2.7) it is assumed that the vertical coordinate  $x_2 = z$  points positive upwards.

The basic mass balance equation for flow in porous media is expressed as (Bear, 1979):

$$\frac{\partial(\varepsilon S_w \rho)}{\partial t} = -\frac{\partial}{\partial x_i}(\rho q_i) - S_k \quad (2.8)$$

where  $\varepsilon$  is the porosity [-],  $S_w$  the relative saturation [-],  $t$  the time [ $T$ ] and  $S_k$  a sink term [ $M \text{ L}^{-3} \text{ T}^{-1}$ ].

The term on the lefthand side of Eq. (2.8) represents the total change in fluid mass contained in the void space with time. For calculations, it is necessary to express the time derivative in terms of the primary variables  $p$  and  $C$ , where  $C$  is the solute concentration [ $M \text{ M}^{-1}$ ] on mass basis. For  $\rho = \rho(p, C)$ , the time derivative in (2.8) can be expanded so that (Bear, 1979; Voss, 1984):

$$\left( S_w \rho S_{\text{op}} + \varepsilon \rho \frac{\partial S_w}{\partial p} \right) \frac{\partial p}{\partial t} + \left( \varepsilon S_w \frac{\partial \rho}{\partial C} \right) \frac{\partial C}{\partial t} = -\frac{\partial}{\partial x_i}(\rho q_i) - S_k \quad (2.9)$$

where  $S_{op}$  is the specific pressure storativity [ $L T^2 M^{-1}$ ]. The  $S_{op}$  term is determined by the porous matrix compressibility,  $\alpha$  [ $L T^2 M^{-1}$ ] and the fluid compressibility,  $\beta$  [ $L T^2 M^{-1}$ ] according to (Voss, 1984):

$$S_{op} = (1 - \varepsilon)\alpha + \varepsilon\beta \quad (2.10)$$

It should be noted that the concepts upon which the specific pressure storativity is based, do not exactly hold for unsaturated porous media. The error introduced in (2.9) by summing the storativity term with the term involving  $(\partial S_w / \partial p)$  is, however, insignificant as  $(\partial S_w / \partial p) \gg S_{op}$  (Voss, 1984).

Substitution of (2.7) into (2.9) yields the final form of the fluid mass balance equation:

$$\left( S_w \rho S_{op} + \varepsilon \rho \frac{\partial S_w}{\partial p} \right) \frac{\partial p}{\partial t} + \left( \varepsilon S_w \frac{\partial \rho}{\partial C} \right) \frac{\partial C}{\partial t} = \frac{\partial}{\partial x_i} \left( \frac{k_i k_{ij} \rho}{\mu} \left( \frac{\partial p}{\partial x_j} + \rho g \eta_j \right) \right) - S_k \quad (2.11)$$

Solute transport in porous media can be described by the following advection-dispersion equation (after Voss, 1984):

$$\frac{\partial (\varepsilon S_w \rho C)}{\partial t} = - \frac{\partial}{\partial x_i} (\rho q_i C) + \frac{\partial}{\partial x_i} \left( \varepsilon S_w \rho D_{ij} \frac{\partial C}{\partial x_j} \right) - S_k C \quad (2.12)$$

where  $D_{ij}$  is the hydrodynamic dispersion tensor [ $L^2 T^{-1}$ ].

Terms describing solute adsorption and production/decay processes have not been included in (2.12). These processes are not considered in this study (Chapter 1).

The hydrodynamic dispersion tensor,  $D_{ij}$ , is given by (Bear, 1972):

$$\varepsilon S_w D_{ij} = \alpha_T |q| \delta_{ij} + (\alpha_L - \alpha_T) \frac{q_i q_j}{|q|} + \varepsilon S_w D_m \delta_{ij} \quad (2.13)$$

where  $\alpha_L$  and  $\alpha_T$  are the longitudinal and transverse dispersivities [ $L$ ], respectively,  $D_m$  the porous medium ionic or molecular diffusion coefficient [ $L^2 T^{-1}$ ] and  $\delta_{ij}$  the Kronecker delta function [-] ( $\delta_{ij} = 1$  if  $i = j$ , and  $\delta_{ij} = 0$  if  $i \neq j$ ).

Equations (2.10)-(2.13) are generally solved on a fixed spatial grid, so that pressures and concentrations are associated with fixed points or volume elements in space. This is called the Eulerian method (Bear, 1972).

Fluid density, while a weak function of pressure,  $p$  is primarily dependent upon solute

concentration,  $C$ . Using a first order Taylor expansion about a base (reference) density, the fluid density can be given as a linear function of solute concentration (Voss, 1984):

$$\rho = \rho_0 + \frac{\partial \rho}{\partial C}(C - C_0) \quad (2.14)$$

where  $C_0$  is a base solute concentration [ $\text{M M}^{-1}$ ] and  $\rho_0$  the fluid density [ $\text{M L}^{-3}$ ] at  $C = C_0$ . In this study it was assumed that  $\rho_0 = 1000 \text{ kg m}^{-3}$  for  $C_0 = 0$  and that  $\partial \rho / \partial C = 700 \text{ kg m}^{-3}$ .

The equations described in this section form the basis of the U.S. Geological Survey finite-element model SUTRA (Voss, 1984). Initial conditions are  $p(x_i)$  and  $C(x_i)$  for the complete flow domain. Boundary conditions for the flow equation may consist of specified pressure,  $p$  (Dirichlet condition) and specified fluid mass flux,  $q_m$  [ $\text{M L}^{-2} \text{T}^{-1}$ ] (Neumann condition). Boundary conditions for the solute transport equation are strictly related to the boundary conditions for the flow equation. Solute concentration,  $C$  of any fluid that enters the flow domain must be specified. The spatial coordinate system may be either Cartesian ( $x, y$ ) or ( $x, z$ ) or, in case of radial symmetry, radial-cylindrical ( $r, z$ ). Time-dependent boundary conditions can be programmed by the user in a special subroutine of the source code. The SUTRA model may also be used to simulate the transport of thermal energy in the groundwater and solid matrix of the aquifer.

### 2.3 Two-dimensional water flow in terms of pressure head and hydraulic conductivity

If the effects of differences in fluid density can be neglected, water flow is described more conveniently in terms of pressure head,  $h$  [ $\text{L}$ ] and hydraulic conductivity,  $K_{ij}$  [ $\text{L T}^{-1}$ ]. The pressure head is related to the fluid pressure through:

$$h = \frac{p}{\rho_0 g} \quad (2.15)$$

The hydraulic conductivity tensor,  $K_{ij}$  is defined as:

$$K_{ij} = \frac{k_{ij} \rho_0 g}{\mu} \quad (2.16)$$

Combining Eqs. (2.11) and (2.15)-(2.16), neglecting changes in storativity, and redefining the sink term results in the following flow equation for two-dimensional water flow in a vertical cross-section with root water uptake (Bear, 1979; Šimůnek et al., 1994):

$$\frac{\partial \theta}{\partial t} = \frac{\partial}{\partial x_i} \left( K_i K_{ij} \left( \frac{\partial h}{\partial x_j} + \eta_j \right) \right) - S_a(x_i) \quad (2.17)$$

where  $\theta$  is the volumetric water content [-] ( $=\epsilon S_w$ ),  $K_r$  the relative hydraulic conductivity [-], and  $S_a$  the actual soil water extraction rate by plant roots [ $T^{-1}$ ].

Equation (2.17) is the governing flow equation in the U.S. Salinity Laboratory finite-element SWMS\_2D model (Šimůnek et al., 1994). To calculate water flow,  $h(x_i)$  constitutes the initial condition over the entire flow domain. Boundary conditions may consist of prescribed pressure heads,  $h$  (Dirichlet type), and prescribed flux,  $q_v$  [ $L T^{-1}$ ] (Neumann type). These boundary conditions may be time-dependent. In addition, the model facilitates the specification of an atmospheric boundary condition, a head-discharge relationship (Cauchy type) and a free drainage boundary condition. The SWMS\_2D model is also capable of simulating solute transport with the advection-dispersion equation.

#### 2.4 One-dimensional vertical water flow and solute transport in the unsaturated zone with root water uptake

For one-dimensional vertical water flow in the unsaturated zone, Eq. (2.17) may be written as (Richards, 1931; Feddes et al., 1988):

$$\frac{\partial \theta}{\partial t} = C_d(h) \frac{\partial h}{\partial t} = \frac{\partial}{\partial z} \left[ K_r K_s \left( \frac{\partial h}{\partial z} + 1 \right) \right] - S_a(z) \quad (2.18)$$

where  $C_d$  is the differential water capacity ( $d\theta/dh$ ) [ $L^{-1}$ ],  $z$  the vertical coordinate [ $L$ ] and  $K_s$  the saturated hydraulic conductivity [ $L T^{-1}$ ]. Note that  $h + z = \phi$ , the hydraulic head [ $L$ ].

The actual root water flux in (2.18) can be calculated from (Van Dam et al., 1997):

$$S_a(z) = \alpha_{rw} \alpha_{rs} S_p(z) \quad (2.19)$$

where  $\alpha_{rw}$  is a reduction factor due to water stress [-],  $\alpha_{rs}$  a reduction factor due to salinity stress [-] and  $S_p$  the potential soil water extraction rate by plant roots [ $T^{-1}$ ]. In this study,  $S_p$  linearly declines with depth according to (Prasad, 1988):

$$S_p(z) = \frac{2T_p}{|z_r|} \left( 1 - \frac{|z|}{|z_r|} \right) \quad (2.20)$$

where  $T_p$  is the potential transpiration rate [ $L T^{-1}$ ] and  $z_r$  is the depth of the root zone [ $L$ ].

The relative importance of water and salinity stresses on root-water uptake for conditions where both stresses occur simultaneously is still unclear (e.g. Homaei, 1999). In this thesis the water and salinity stresses are considered multiplicative (Eq. 2.19). The reduction factor  $\alpha_{rw}$  is a function of soil water pressure head,  $h$  and potential transpiration rate,  $T_p$  (Fig. 2.1). The reduction factor  $\alpha_{rs}$  is a function of the Electrical Conductivity of the saturation extract,  $EC_e$  of

the soil water (Fig. 2.2).

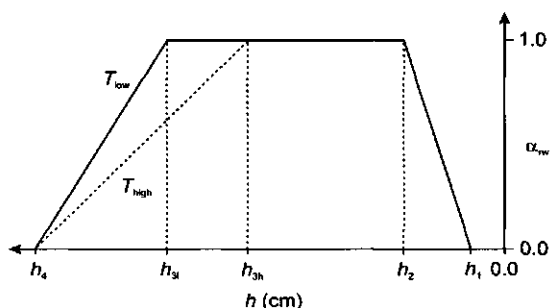


**Figure 2.1** Reduction function for root water uptake,  $\alpha_w$  as a function of soil water pressure head,  $h$  for different potential transpiration rates,  $T_p$  (after Feddes et al., 1978).

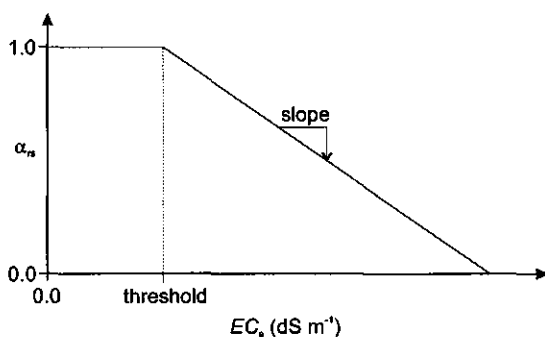


**Figure 2.2** Reduction function for root water uptake,  $\alpha_s$  as a function of soil salinity,  $EC_e$ .

The actual transpiration rate,  $T_a$  [ $L T^{-1}$ ] can now be calculated as:

$$T_a = \int_{-z_r}^0 S_a(z) dz \quad (2.21)$$

For vertical solute transport in the unsaturated zone with root water uptake, and with the volume-based solute concentration  $c$  [ $M L^{-3}$ ] instead of the mass-based solute concentration  $C$  [ $M M^{-1}$ ], Eqs. (2.12) and (2.13) may be combined into the following advection-dispersion equation (neglecting fluid density effects):

$$\frac{\partial(\theta c)}{\partial t} = -\frac{\partial(qc)}{\partial z} + \frac{\partial}{\partial z} \left( \theta \left( D_m + \alpha_l \left| \frac{q}{\theta} \right| \right) \frac{\partial c}{\partial z} \right) - \alpha_{cf} S_a(z)c \quad (2.22)$$

where  $\alpha_{cf}$  is a root uptake concentration factor [-]. In this study it is assumed that  $\alpha_{cf} = 0$ .

The Millington and Quirk (1961) relationship can be used to calculate the porous medium diffusion coefficient,  $D_m$ :

$$D_m = D_w \frac{\theta^{7/3}}{\varepsilon^2} \quad (2.23)$$

where  $D_w$  is the solute diffusion coefficient in free water [ $L^2 T^{-1}$ ].

The equations discussed in this section form the basis of the one-dimensional vertical finite-difference SWAP model which is a joint development of Alterra and Wageningen University (Feddes et al., 1978; Van Dam et al., 1997; Kroes et al., 1999). Initial conditions for the water flow and solute transport calculations with SWAP consist of  $h(z)$  and  $c(z)$ , respectively. The soil surface constitutes the top boundary. The boundary condition at the top boundary depends on the soil moisture status of the soil and on the direction and magnitude of the surface fluxes. During the iterative solution of Richards' equation the boundary condition may switch from flux-controlled ( $q$ ) to pressure head-controlled ( $h$ ), and vice versa. A schematic overview of the criteria is given by Van Dam et al. (1997) and Van Dam (2000).

The bottom boundary of the vertical one-dimensional SWAP model is either in the unsaturated zone or in the upper part of the saturated zone where the transition takes places to three-dimensional groundwater flow. The bottom boundary condition can be of the following types (Van Dam et al., 1997): (1) specified pressure head,  $h$  or groundwater level as a function of time (Dirichlet type); (2) specified flux,  $q$  as a function of time (Neumann type); (3) a head-discharge relationship (Cauchy type); (4) free drainage; and (5) free outflow at a soil-air interface. The boundary conditions for the solute transport equation are strongly related to the boundary conditions for the water flow equation. Solute concentration,  $c$  of any flux that enters the flow domain must be specified.

## 2.5 Description of the soil hydraulic properties

The numerical models mentioned in the previous sections require information on the relationship between  $S_w$ ,  $p$  and  $k_r$  (SUTRA), or alternatively,  $\theta$ ,  $h$  and  $K_r$  (SWMS\_2D and SWAP). In principle, these relationships can be given in tabular format. Description of the soil hydraulic properties with the functions of Mualem (1976) and Van Genuchten (1980) is however more convenient, as only a few parameters are required. Also several databases exist that describe the soil hydraulic properties of different soils with the MVG functions (e.g. Carsel and Parrish, 1988; Leij et al., 1996; Wösten et al., 1998; Wösten et al., 2001).



First, a dimensionless saturation,  $S_e$  is defined:

$$S_e = \frac{S_w - S_{wr}}{1 - S_{wr}} = \frac{\theta - \theta_r}{\theta_s - \theta_r} \quad (2.24)$$

where  $S_{wr}$  is the residual saturation [-],  $\theta_r$  the residual volumetric water content [-] and  $\theta_s$  the saturated volumetric water content [-].

The relationship between  $S_w$  and  $p$  (SUTRA) and between  $\theta$  and  $h$  (SWMS\_2D and SWAP) is written as (Van Genuchten, 1980):

$$S_e(p) = \frac{1}{(1 + |\alpha_p p|^n)^m} \quad \text{for } p \leq 0 \quad (2.25a)$$

$$S_e(p) = 1 \quad \text{for } p > 0 \quad (2.25b)$$

$$S_e(h) = \frac{1}{(1 + |\alpha_h h|^n)^m} \quad \text{for } h \leq 0 \quad (2.25c)$$

$$S_e(h) = 1 \quad \text{for } h > 0 \quad (2.25d)$$

where  $\alpha_p$  [ $M^{-1} L T^2$ ],  $\alpha_h$  [ $L^{-1}$ ],  $n$  [-] and  $m$  [-] are empirical parameters, with  $m = 1-1/n$ .

The relationship between  $S_w$  and  $k_r$ , and between  $\theta$  and  $K_r$  is written as (Mualem, 1976; Van Genuchten, 1980):

$$k_r(S_e) = K_r(S_e) = S_e^\lambda [1 - (1 - S_e^{\frac{1}{m}})^m]^2 \quad (2.26)$$

where  $\lambda$  is an empirical parameter [-].

## 2.6 Description of a pipe drain in a finite-element mesh

The description of a pipe drain in a two-dimensional ( $x, z$ ) finite-element mesh has been discussed by Fipps et al. (1986). Basically two approaches can be followed: (1) The drain is represented by a hole in the finite element mesh. This requires extremely small elements near the drain in order to obtain accurate flow rates (e.g. Gureghian and Youngs, 1975; Zaradny and Feddes, 1979;

De Vos, 1997); (2) Description of the drain by a single node. Accurate drain flow rates may be obtained with this approach by adjusting the permeability (or hydraulic conductivity) of the elements surrounding the drain using results from electric analog experiments (Vimoke et al., 1962; Rogers and Fouss, 1989; Šimůnek et al., 1994). In this study the single node approach was followed because it is computationally efficient.

Adjustment of the permeability,  $k$  (SUTRA) or the hydraulic conductivity,  $K$  (SWMS\_2D) of the elements surrounding the drain is as follows:

$$k_{\text{drain}} = k C_{\text{drain}} \quad (2.27a)$$

$$K_{\text{drain}} = K C_{\text{drain}} \quad (2.27b)$$

where  $k_{\text{drain}}$  is the adjusted permeability [ $L^2$ ],  $K_{\text{drain}}$  the adjusted hydraulic conductivity [ $L T^{-1}$ ] and  $C_{\text{drain}}$  the correction factor [-].

The correction factor,  $C_{\text{drain}}$  is a function of the effective drain diameter,  $d_{\text{eff}}$  [L] and the side length of the square formed by the elements surrounding the drain. For the exact calculation of  $C_{\text{drain}}$ , the reader is referred to Vimoke et al. (1962). Values of  $d_{\text{eff}}$  for different drain tubes are provided by Mohammad and Skaggs (1983). Rogers and Fouss (1989) have shown that  $C_{\text{drain}}$  must be reduced by a factor 2 in order to obtain consistency between the finite-element model and the electric analog experiments of Vimoke et al. (1962).

### 3 Theory of Solute Travel Time to Pipe Drains and Tube-Wells in Steady-State Flow Fields

Numerical models that use a combination of the Darcy equation and the basic mass balance equation and the advection-dispersion equation in  $(x,z)$  or  $(r,z)$  coordinates (Chapter 2) perform well if the solute transport is dispersion-dominated. In advection-dominated transport problems, however, these models suffer from numerical dispersion and artificial oscillations, especially in the region of sharp concentration fronts (Kinzelbach, 1986; Bear and Verruijt, 1987). In order to minimize numerical errors, small discretization in time and space is needed, which requires considerable and sometimes prohibitive computational effort, especially when considering field-scale problems (Crane and Blunt, 1999).

In irrigated agriculture, solutes are distributed along the soil surface with the irrigation water or are initially present in the soil-aquifer system. *Pipe drains or partially penetrating tube-wells usually present small and isolated outflow surfaces.* For such flow systems, *outflow concentrations are controlled almost exclusively by advective mixing*, resulting from the convergence of the flow towards the drainage media (Duffy and Lee, 1992). Under these circumstances, Lagrangian methods constitute a computationally more efficient approach to describe solute transport than the Euler methods discussed in Chapter 2.

In Lagrangian methods, solute concentration is associated with fluid elements which move with the prevailing velocity field. The positions that are occupied by the elements as time passes constitute a path-line (Bear, 1972). As a fluid element moves along its pathline, its concentration, provided the transport is purely advective, does not change (Crane and Blunt, 1999). The travel time,  $\tau$  [T] between some reference point  $s_0$  and some point  $s$  on a path-line, is given by:

$$\tau = t - t_0 = \int_{s_0}^s \frac{1}{v} ds \quad (3.1)$$

where  $v$  is the advective displacement velocity [ $L T^{-1}$ ].

Equation (3.1) is valid for transient flow fields. Solution of (3.1) still requires elaborate computations as  $v$  changes both in space and time. Considering the long solute travel times which are generally found for pipe drains and tube-wells in extensive aquifers, it is practical to assume that the flow field is at steady-state (e.g. Jury, 1975; Raats, 1978; Kamra et al., 1991a). For steady-state flow fields, path-lines coincide with streamlines. Where streamlines are defined as instantaneous curves that are at every point tangent to the direction of the velocity at that point. The condition of tangency can be expressed mathematically as (Frind and Matanga, 1985):

$$q_i \times ds = 0 \quad i=1,2,3 \quad (3.2)$$

Streamlines can be calculated using the stream-function concept (Bear, 1972). The required stream-function values can be determined analytically (for some specific cases) or numerically.

Both methods will be discussed in this chapter. The actual calculation of solute travel times from the streamline pattern is explained in Section 3.6.

### 3.1 The stream-function concept in a vertical cross-section

For flow in a vertical cross-section, the vector product in (3.2) can be expanded as:

$$\begin{vmatrix} q_x & q_z \\ dx & dz \end{vmatrix} = 0 \quad (3.3)$$

so that:

$$q_x dz - q_z dx = 0 \quad (3.4)$$

where  $x$  is the horizontal coordinate [L],  $q_x$  the specific discharge [ $L T^{-1}$ ] in the  $x$ -direction and  $q_z$  the specific discharge [ $L T^{-1}$ ] in the  $z$ -direction.

The stream-function  $\psi = \psi(x, z)$  [ $L^2 T^{-1}$ ] is defined, which is a constant along a streamline (Bear, 1972):

$$d\psi = \frac{\partial \psi}{\partial x} dx + \frac{\partial \psi}{\partial z} dz = 0 \quad (3.5)$$

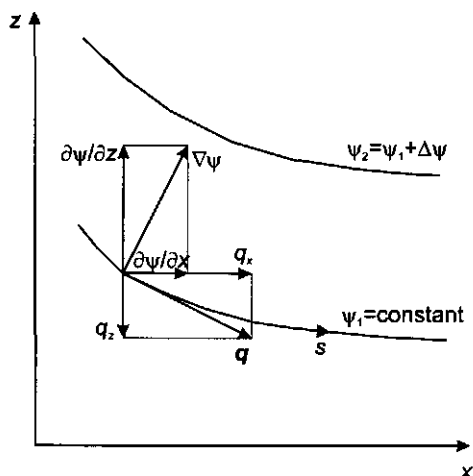


**Figure 3.1** Relationship between Darcy flux and stream function (after Frind and Matanga, 1985).

Comparison of (3.4) and (3.5) leads to (see also Fig 3.1):

$$q_x = -\frac{\partial \psi}{\partial z} \quad (3.6a)$$

$$q_z = \frac{\partial \psi}{\partial x} \quad (3.6b)$$

In a two-dimensional system, a stream-tube is defined by its two bounding streamlines, say  $\psi_1$  and  $\psi_2$  (where  $\psi_2 = \psi_1 + \Delta\psi$ ). It can be shown that the flux through this stream-tube is equal to  $\Delta\psi$  (Anderson and Woessner, 1992). In other words, the Darcy discharge through a stream-tube is equal to the numerical difference between the two bounding streamlines (Frind and Matanga, 1985). A drawback of using the stream-function concept is the fact that sources and sinks inside the flow domain generally cannot be handled (Fogg and Senger, 1985).

### 3.2 Governing equation for two-dimensional flow in a vertical cross-section

The derivation of the partial differential equation of the stream function is generally based on the assumption that the flow is irrotational, i.e. that the curl of the hydraulic gradient vector ( $\nabla \times \nabla \phi$ ) is equal to zero (Bear, 1972; Matanga, 1993).

Because  $-\nabla \phi = q_i / K_{ij}$  (Darcy equation),  $\nabla \times \nabla \phi$  can be written as (Frind and Matanga, 1985):

$$\nabla \times \left( \frac{q_i}{K_{ij}} \right) = 0 \quad (3.7)$$

where  $K_{ij}$  is the hydraulic conductivity [ $L T^{-1}$ ] tensor. In matrix notation,  $K_{ij}$  is given as:

$$K_{ij} = \begin{bmatrix} K_{xx} & K_{xz} \\ K_{zx} & K_{zz} \end{bmatrix} \quad (3.8)$$

For groundwater flow in a vertical cross-section:

$$\frac{q_i}{K_{ij}} = \frac{1}{|K|} \begin{bmatrix} K_{zz} & -K_{xz} \\ -K_{zx} & K_{xx} \end{bmatrix} \begin{bmatrix} q_x \\ q_z \end{bmatrix} \quad (3.9)$$

where  $|K| = K_{xx}K_{zz} - K_{xz}K_{zx}$ .

Expansion of (3.7) for a vertical cross-section results in:

$$\left| \begin{array}{cc} \frac{\partial}{\partial x} & \frac{\partial}{\partial z} \\ \left( \frac{K_{zz}}{|K|} q_x - \frac{K_{xz}}{|K|} q_z \right) & \left( -\frac{K_{zx}}{|K|} q_x + \frac{K_{xx}}{|K|} q_z \right) \end{array} \right| = 0 \quad (3.10)$$

so that:

$$\frac{\partial}{\partial x} \left( -\frac{K_{zx}}{|K|} q_x + \frac{K_{xx}}{|K|} q_z \right) - \frac{\partial}{\partial z} \left( \frac{K_{zz}}{|K|} q_x - \frac{K_{xz}}{|K|} q_z \right) = 0 \quad (3.11)$$

Substitution of (3.6) into (3.11) yields:

$$\frac{\partial}{\partial x} \left( \frac{K_{xx}}{|K|} \frac{\partial \psi}{\partial x} + \frac{K_{zx}}{|K|} \frac{\partial \psi}{\partial z} \right) + \frac{\partial}{\partial z} \left( \frac{K_{zz}}{|K|} \frac{\partial \psi}{\partial x} + \frac{K_{xz}}{|K|} \frac{\partial \psi}{\partial z} \right) = 0 \quad (3.12)$$

If the coordinate axes are oriented along the principal directions of permeability, Eq. (3.12) reduces to:

$$\frac{\partial}{\partial x} \left( \frac{1}{K_{zz}} \frac{\partial \psi}{\partial x} \right) + \frac{\partial}{\partial z} \left( \frac{1}{K_{xx}} \frac{\partial \psi}{\partial z} \right) = 0 \quad (3.13)$$

Equation (3.13) is valid for inhomogeneous anisotropic media (Bear, 1972). The equation can be solved numerically with standard groundwater flow codes after minor adjustments in the input (Anderson and Woessner, 1992). The equation can also be solved with a spreadsheet (Olsthoorn, 1998). Solution of the more general Eq. (3.12) requires a specialized flow code (e.g. Frind and Matanga, 1985).

### 3.3 Governing equation for axi-symmetric flow in a vertical cross-section

For axi-symmetric flow in a vertical cross-section, Eq. (3.6) can be re-written as:

$$q_r = -\frac{1}{2\pi r} \frac{\partial \psi}{\partial z} \quad (3.14a)$$

$$q_z = -\frac{1}{2\pi r} \frac{\partial \psi}{\partial r} \quad (3.14b)$$

where  $r$  is the radial coordinate [L] and  $q$ , the specific discharge [L T<sup>-1</sup>] in the  $r$ -direction.

The stream-function  $\psi = \psi(r, z)$  has dimensions  $[L^3 T^{-1}]$ . With  $(r, z)$  coordinates instead of  $(x, z)$  coordinates, the derivations as given in Eqs. (3.7)-(3.11), result in the following alternative expression for (3.12):

$$\frac{\partial}{\partial r} \left( \frac{1}{2\pi r} \left( \frac{K_{rr}}{|K|} \frac{\partial \psi}{\partial r} + \frac{K_{rz}}{|K|} \frac{\partial \psi}{\partial z} \right) \right) + \frac{\partial}{\partial z} \left( \frac{1}{2\pi r} \left( \frac{K_{rz}}{|K|} \frac{\partial \psi}{\partial r} + \frac{K_{zz}}{|K|} \frac{\partial \psi}{\partial z} \right) \right) = 0 \quad (3.15)$$

With the coordinate axes oriented along the principal directions of permeability, (3.15) becomes:

$$\frac{\partial}{\partial r} \left( \frac{1}{2\pi r K_{zz}} \frac{\partial \psi}{\partial r} \right) + \frac{\partial}{\partial z} \left( \frac{1}{2\pi r K_{rr}} \frac{\partial \psi}{\partial z} \right) = 0 \quad (3.16)$$

Unlike Eq. (3.13), Eq. (3.16) cannot be used directly because of the  $1/r$  factor in the first term on the lefthand side of (3.16). This problem is solved by differentiating the first term on the lefthand side of (3.16) with respect to  $r$  (Olsthoorn, 1998):

$$-\frac{1}{2\pi r^2 K_{zz}} \frac{\partial \psi}{\partial r} + \frac{1}{2\pi r} \frac{\partial}{\partial r} \left( \frac{1}{K_{zz}} \frac{\partial \psi}{\partial r} \right) + \frac{1}{2\pi r} \frac{\partial}{\partial z} \left( \frac{1}{K_{rr}} \frac{\partial \psi}{\partial z} \right) = 0 \quad (3.17)$$

to yield:

$$-\frac{1}{r K_{zz}} \frac{\partial \psi}{\partial r} + \frac{\partial}{\partial r} \left( \frac{1}{K_{zz}} \frac{\partial \psi}{\partial r} \right) + \frac{\partial}{\partial z} \left( \frac{1}{K_{rr}} \frac{\partial \psi}{\partial z} \right) = 0 \quad (3.18)$$

Equation (3.18) is again valid for inhomogeneous anisotropic media (Bear, 1972). The equation can be solved with a spreadsheet as discussed by Olsthoorn (1998).

### 3.4 Analytical solution of the stream function for a pipe drain in a two-layered soil

Several investigators derived analytical expressions for the stream function in pipe-drained soils for various conditions. A summary is given in Table 3.1. All studies mentioned in Table 3.1 describe the pipe-soil system by considering a vertical cross-section perpendicular to the alignment of the drains. Studies concerning sloping lands and interceptor drainage have not been included in the table (see Van der Ploeg et al., 1999).

**Table 3.1** Summary of analytical expressions for the stream function in pipe-drained soils.

Field conditions	Reference
-Pipe drain in a single-layered soil under ponded conditions	Kirkham (1949)
-Pipe drain in a two-layered soil under ponded conditions	Kirkham (1951)
-Pipe drain in a two-layered soil underlain by an artesian aquifer under ponded conditions	Kirkham (1954)
-Pipe drain in a single-layered soil	Kirkham (1958)
-Pipe drain in a single-layered soil underlain by an artesian aquifer	Hinesly and Kirkham (1966)
-Pipe drain in a two-layered and a three-layered soil	Töksöz and Kirkham (1971)
-Pipe drain in a single-layered aquifer of infinite depth	Ernst (1973)
-Pipe drain which is part of a dual-pipe subirrigation-drainage system	Kirkham and Horton (1992)
-Dual-depth pipe drainage system under ponded conditions	Kirkham et al. (1997)
-Pipe drain in soil of finite depth and in soil with infinite depth under partial ponding	Youngs and Leeds-Harrison (2000)

*In this study, the expressions for seepage to a pipe drain in a two-layered soil developed by Toksöz and Kirkham (1971) are used.* The geometry of the pipe-soil system used by these authors provides the most accurate representation of field conditions for the study areas (Chapter 4). The geometry of the system is shown in Fig. 3.2. Because of symmetry, only the left part of the flow domain is actually used in the calculations. The following assumptions are made: (1) Both soil layers below drain level are homogeneous and isotropic; (2) The groundwater table is at, or above, drain level; (3) The pipe drain is running half full; (4) The loss in hydraulic head between the groundwater table and drain level is negligible compared with the head loss in the remainder of the region; (5) Vertical fictitious frictionless membranes in this zone (dotted lines in Fig. 3.2) force the water to flow vertically downwards at a uniform rate.

In the analysis of Toksöz and Kirkham (1971), assumptions (4) and (5) imply that streamlines will be equally spaced along the horizontal line connecting the drain centres. This is a simplification of reality. In most cases, flow between the groundwater table and drain level will be two-dimensional. The pipe drain itself, is represented by a slit drain of supposed thickness zero and width  $\zeta$  (Fig. 3.2, left part). During the derivation of the stream-function for the first layer it is assumed that  $\zeta \rightarrow 0$ , so that the drain becomes a line sink perpendicular to the  $(x, z)$  plane. It should be noted that the definition of the  $z$ -coordinate in Fig 3.2 (positive downward, origin at drain level) differs from the previous definition in Eq. (2.7) ( $z$  positive upward).



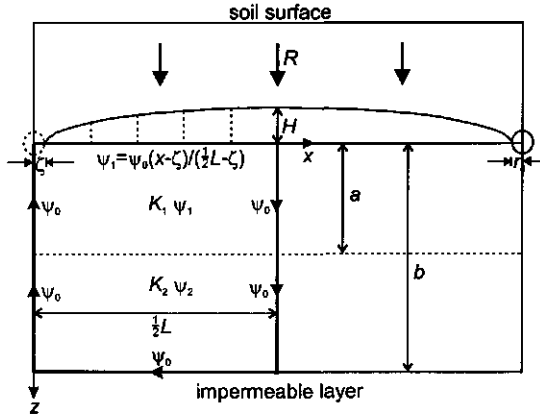


**Figure 3.2** Geometry of pipe drains in a two-layered soil (after Töksoz and Kirkham, 1971).

The stream function for the first layer,  $\psi_1$  [ $L^2 T^{-1}$ ] is:

$$\psi_1 = \psi_0 - \frac{2\psi_0}{\pi} \sum_{m=1}^{\infty} \left( \frac{1}{m} \sin\left(\frac{2m\pi x}{L}\right) \frac{\sinh\left[m\pi \frac{2(a-z)}{L}\right]}{\sinh\left(\frac{2m\pi a}{L}\right)} + B_m \sin\left(\frac{2m\pi x}{L}\right) \frac{\sinh\left(\frac{2m\pi z}{L}\right)}{\sinh\left(\frac{2m\pi a}{L}\right)} \right) \quad (3.19)$$

where  $\psi_0 = R \times \frac{1}{2} L$  [ $L^2 T^{-1}$ ], with  $R$  being the recharge rate [ $L T^{-1}$ ] and  $L$  the drain spacing [ $L$ ].

The stream function for the second layer,  $\psi_2$  [ $\text{L}^2 \text{T}^{-1}$ ] is:

$$\psi_2 = \psi_0 - \frac{2\psi_0}{\pi} \sum_{m=1}^{\infty} C_m \sin\left(\frac{2m\pi x}{L}\right) \frac{\sinh\left[m\pi \frac{2(b-z)}{L}\right]}{\cosh\left[m\pi \frac{2(b-a)}{L}\right]} \quad (3.20)$$

The constants  $B_m$  [-] and  $C_m$  [-] are evaluated with help of the potential function,  $\Phi$  [ $L^2 T^{-1}$ ] ( $\Phi = K\phi$ ) (see Toksöz and Kirkham, 1971). The  $B_m$  term is given by:

$$B_m = \frac{1}{m} \frac{1}{\sinh\left(\frac{2m\pi a}{L}\right)} \frac{1}{\left(\frac{K_1}{K_2}\right) \coth\left[m\pi \frac{2(b-a)}{L}\right] + \coth\left(\frac{2m\pi a}{L}\right)} \quad (3.21)$$

and  $C_m$  by:

$$C_m = \frac{1}{m} \frac{1}{\sinh\left(\frac{2m\pi a}{L}\right)} \frac{1}{\left(\frac{K_1}{K_2}\right) + \tanh\left[m\pi \frac{2(b-a)}{L}\right] \coth\left(\frac{2m\pi a}{L}\right)} \quad (3.22)$$

Equations (3.19)-(3.22) are exact analytical solutions of Laplace's equation for the stream function,  $\nabla^2 \psi = 0$  and the potential function,  $\nabla^2 \Phi = 0$  in the first and second layer (Toksöz and Kirkham, 1971). Because of this, the effect of soil anisotropy on the stream functions of the first and second layer can be accounted for by coordinate transformation (Maasland, 1957). By transformation of coordinates, the anisotropic soil is converted to a fictitious isotropic soil for which Eqs. (3.19)-(3.22) apply. Both the  $x$ -coordinates and the  $z$ -coordinates can be used for conversion. Transformation of the  $z$ -coordinates is generally more practical (Boumans, 1979). With the coordinate axes located along the principal directions of hydraulic conductivity, the dimensions of the fictitious isotropic soil become:

$$a' = a \sqrt{\frac{K_{xx1}}{K_{zz1}}} \quad (3.23a)$$

$$(b-a)' = (b-a) \sqrt{\frac{K_{xx2}}{K_{zz2}}} \quad (3.23b)$$

where  $a'$  is the converted thickness [L] of the first layer and  $(b-a)'$  the converted thickness [L] of the second layer.

The hydraulic conductivities of the first and second layer for the fictitious isotropic soil are calculated as:

$$K_1 = \sqrt{K_{xx1} K_{zz1}} \quad (3.24a)$$

$$K_2 = \sqrt{K_{xx2} K_{zz2}} \quad (3.24b)$$

As an example, the analytical expressions discussed in this section are used to draw streamlines in a two-layered anisotropic soil with pipe drains (Fig. 3.3). In Fig. 3.3, each stream-tube represents 10% of the total discharge. Because of the neglect of the hydraulic head loss between the groundwater table and drain level (assumption 4) and the assumption of vertical frictionless membranes in this zone (assumption 5), *the shape of the streamlines is independent of the recharge,  $R$ .*

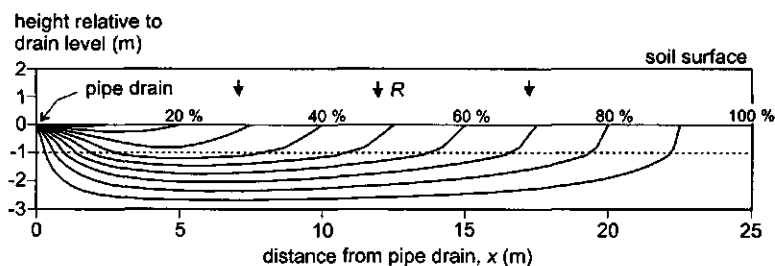


**Figure 3.3** Streamlines towards a pipe drain in a two-layered soil. Analytical solution of Töksoz and Kirkham (1971). Drain spacing 50 m, drain depth 2.0 m below soil surface and impermeable layer at 3.0 m below drain level. The soil below drain level consists of two layers; thickness of layer 1 is 1 m ( $K_{xx1} = 1 \text{ m d}^{-1}$ ,  $K_{zz1} = 0.2 \text{ m d}^{-1}$ ), thickness of layer 2 is 2 m ( $K_{xx2} = 5 \text{ m d}^{-1}$ ,  $K_{zz2} = 1 \text{ m d}^{-1}$ ).

### 3.5 Numerical solution of the stream function for a partially penetrating well in an unconfined aquifer

Exact analytical solutions of the stream function for fully penetrating wells in a vertical cross-section have been given by Khan and Kirkham (1971) and Khan et al. (1971). For partially penetrating wells, which will be considered in this study, no analytical solutions are available. The stream function to a partially penetrating well will therefore be calculated numerically using Eq. (3.18). The discretisation of (3.18) through a finite-difference scheme can be found in Olsthoorn (1998). Actual computations are conducted with a spreadsheet.

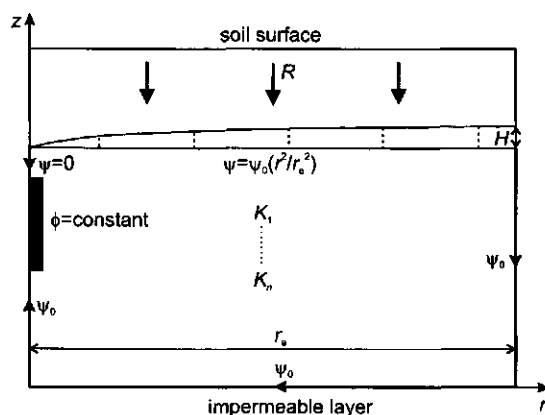


**Figure 3.4** Geometry of a partially penetrating well in a multi-layered aquifer.

The geometry of the well-aquifer system is shown in Fig. 3.4, where  $\psi_0 = R\pi r_e^2 [L^3 T^{-1}]$  with  $r_e$

being the radial distance [L] to the water divide. The partially penetrating well constitutes a constant head boundary, allowing relatively large inflow into the well at the edges of the well screen (Muskat, 1937). In a spreadsheet, a constant head boundary can be included by adding an extra row or column to the sides of the model and giving them very high hydraulic conductivity (Olsthoorn, 1998). The outer radial boundary is treated as a water divide, which is the appropriate boundary condition for a well that is part of a complete well-field. It is assumed that the drawdown regions of neighboring wells do not overlap.

Single wells in large continuous aquifers might draw their water from much greater distances than  $r_c$ . These last type of wells will not be considered in this study. Similar to the pipe drainage case, it is assumed that the loss in hydraulic head in the arch shaped region below the groundwater table is negligible compared with the head loss in the remainder of the flow region. Again fictitious, frictionless membranes are assumed in this zone that force the water to flow vertically downwards at a uniform rate (see Section 3.4).

As an example, streamlines are calculated for a partially penetrating well in a homogeneous anisotropic aquifer (Fig. 3.5). Each stream-tube represents 10 % of the total discharge. In contrast to the case for pipe drainage, the starting points of the streamlines are no longer spaced equally along the horizontal plane. This is due to the use of radial coordinates to describe the well.

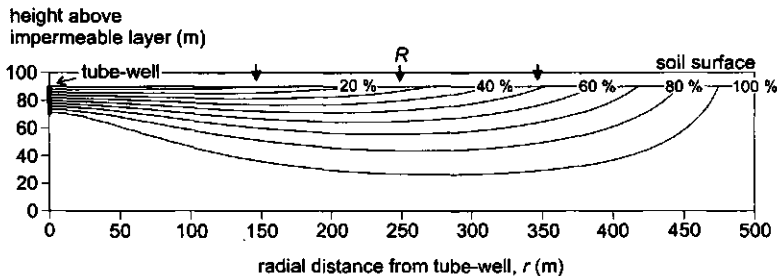


**Figure 3.5** Streamlines towards a partially penetrating well in a homogeneous unconfined anisotropic aquifer. Numerical solution according to Olsthoorn (1998). Radial distance to the water divide is 500 m. Depth of the impermeable layer is 100 m below soil surface ( $K_r = 20 \text{ m d}^{-1}$ ,  $K_z = 1 \text{ m d}^{-1}$ ). The horizontal boundary plane (see Chapter 5) is located at 10 m depth.

### 3.6 Calculation of solute travel time

For flow in two dimensions, the travel time  $\tau$  [T] of a fluid particle moving from  $s_0$  to  $s$  through a stream tube is given by:

$$\tau = \frac{n_e}{\Delta \psi} \int_{s_0}^s w(s) ds \quad (3.25)$$

where  $w$  is the width [L] of the stream tube and  $n_e$  the effective porosity [-].

To solve Eq. (3.25) in  $(x,z)$  coordinates, the cross-sectional area of each stream tube must be determined. This cross-sectional area can be calculated by numerical integration along the two bounding streamlines of each stream tube, using the composite Simpson's rule (Faires and Burden, 1993). In the present case, numerical integration requires that for a given  $\psi$  and  $x$ ,  $z$  is calculated. Unfortunately, Eqs. (3.19) and (3.20), which describe the relationship between  $(x,z)$  and  $\psi$  for pipe drains, cannot be rewritten to calculate  $z$  directly. Therefore, each  $z$ -coordinate has to be found from (3.19) and (3.20) by trial and error. To speed up calculations, a computer program, written in FORTRAN by the present author, is used to carry out the necessary computations.

For axi-symmetric flow in a vertical cross-section, Eq. (3.25) changes into:

$$\tau = \frac{2\pi n_e}{\Delta\psi} \int_{s_0}^s r w(s) ds \quad (3.26)$$

Equation (3.26) cannot be solved easily because both  $r$  and  $w$  change as the solute progresses through the stream tube. Furthermore, no analytical expressions are available to relate  $(r,z)$  to  $\psi$ , for cases other than fully penetrating wells. For axi-symmetric flow, it is therefore more convenient to calculate the solute travel time by particle tracing in the flow field. The required velocity of the solute particles is calculated as:

$$v_r = \frac{q_r}{n_e} = - \frac{1}{2\pi m_e} \frac{\partial \psi}{\partial z} \quad (3.27a)$$

$$v_z = \frac{q_z}{n_e} = \frac{1}{2\pi m_e} \frac{\partial \psi}{\partial r} \quad (3.27b)$$

With known velocities of the solute particles, the particles can be followed through the flow field with integration methods. Four methods are commonly used: semi-analytical, Euler, Runge-Kutta, and Taylor series expansion (Anderson and Woessner, 1992). In this study, the Euler integration formulas are used:

$$r_p = r_0 + (v_r)_0 \Delta t \quad (3.28a)$$

$$z_p = z_0 + (v_z)_0 \Delta t \quad (3.28b)$$

where  $(r_0, z_0)$  is the initial position of the particle,  $(v_r)_0$  and  $(v_z)_0$  are the velocities at the initial position in radial and vertical direction, respectively, and  $(r_p, z_p)$  is the position of the particle

after time step  $\Delta t$ . With Euler integration, small time steps are required to limit numerical errors.

Equations (3.27a)-(3.28b) can be used to calculate solute travel time to tube-wells with help of the BV11-2-5 code of Bear and Verruijt (1987). The original program was adjusted by the present author (in FORTRAN) to facilitate its use in  $(r,z)$  coordinates. The two most important modifications were: (1) incorporation of Eqs. (3.27a) and (3.27b) to calculate velocity; (2) insertion of a bi-cubic interpolation scheme (Press et al., 1992) to calculate inter-nodal values of the stream function. Bi-cubic interpolation requires the input of  $\psi$ ,  $\partial\psi/\partial r$ ,  $\partial\psi/\partial z$ , and  $\partial^2\psi/(\partial r\partial z)$  for each nodal point. The bi-cubic scheme replaces the original iso-parametric interpolation algorithm in BV11-2-5 which uses only  $\psi$  to interpolate linearly. Linear interpolation in radial coordinates will give poor results. Note that the bi-cubic interpolation scheme as given by Press et al. (1992) can only be used for rectangular grid systems. For deformed grids, bi-cubic interpolation can be implemented by using iso-parametric finite elements in conjunction with Hermitian basis functions (Van Genuchten et al., 1977; Frind, 1977).

To calculate solute transport to pipe drains and tube-wells, *cumulative outflow can be used as a substitute for solute travel time*. This allows the flow regime to be transient (Van Ommen et al., 1989). Solute breakthrough follows from a direct comparison of the cross-sectional area (pipe drains) or volume (tube-wells) of the stream tubes on the one hand and cumulative outflow on the other. This requires that the shape of the stream tubes is time-invariant, which is true if the head loss in the arch-shaped region below the groundwater table is neglected (Sections 3.4 and 3.5). For pipe drains, the cross-sectional area,  $A_i$  [ $L^2$ ] of each stream tube,  $i$  is equal to the  $\int w(s)ds$  term in Eq. (3.25) which is determined by numerical integration. For tube-wells, the volume  $V_i$  [ $L^3$ ] of each stream tube  $i$  is equal to the  $2\pi\int rw(s)ds$  term in Eq. (3.26) which can be calculated indirectly, after solute travel time has been determined with Eqs. (3.27a)-(3.28b).

## 4 Description of the Study Areas in the Indus Plain

This chapter starts with a general description of the hydrological characteristics of the Indus plain. Subsequently, in Sections 4.4 to 4.6, three study areas are discussed. These study areas will be used in Chapter 5 to assess long term soil and effluent salinity of pipe drains and tube-wells. The 9-ha Sampla experimental pipe drainage site (Section 4.4), represents a case where high soil and groundwater salinity have made the area unfit for crop production. The Sampla site provides a good opportunity to follow the reclamation process after the introduction of drainage. The Satiana tube-well Pilot Project (40,000 ha) is representative for a typical public tube-well drainage project in Pakistan (Section 4.5). High discharge government tube-wells as the ones in the Satiana Project were installed in great numbers in Pakistan in between 1960 and 1990. Section 4.6 discusses the Fourth Drainage Project. This large scale pipe drainage project (120,000 ha) is the third in a row of seven government pipe drainage projects which were initiated in Pakistan from 1977 onwards. Finally, in Section 4.7, some conclusions are drawn. The Phularwan experimental skimming well site, which will be used to study density-dependent water flow and solute transport to pipe drains and tube-wells, is discussed in Chapter 6.

### 4.1 Location, climate and cropping pattern

The Indus river and its tributaries are shown in Fig. 4.1. The Indus river system transports water from the Himalayas and the Hindukush in the north and from the Baluchistan mountains in the west to the Arabian sea. The Indus plain occupies three main administrative areas; Punjab Province and Sindh Province in Pakistan, and the State of Punjab in India. Haryana State in India, is part of both the Indus river system and the Ganges river system. Figure 4.1 also shows the location of the study areas. Note that, strictly speaking, the Sampla experimental pipe drainage site is not part of the Indus plain, but situated in between the Indus and the Ganges plain.

The climate of the Indus plain ranges from arid in Sindh to semi-arid in the Punjab. Rainfall is unevenly distributed over the year. Most of the rain falls during the monsoon period (July to September) when storms originating from the bay of Bengal reach the plain. Average annual rainfall ranges from ~100 mm in Sindh Province to ~1000-1400 mm in the north-eastern parts of Punjab State (India) and Haryana State. Temperatures range from just above 0 °C in winter to above 45 °C in summer. Monthly fluctuations in rainfall and reference crop evapotranspiration,  $ET_{ref}$  can be read from the three climatograms which are shown in Fig. 4.2 (Smith, 1993). The climate allows to grow two crops per year, provided sufficient irrigation water is available. In the Rabi winter season (October-May) the main crops are wheat, berseem and mustard. In the Kharif summer season (June-September) the main crops are cotton, rice, maize and sorghum. Sugarcane is cropped year round.

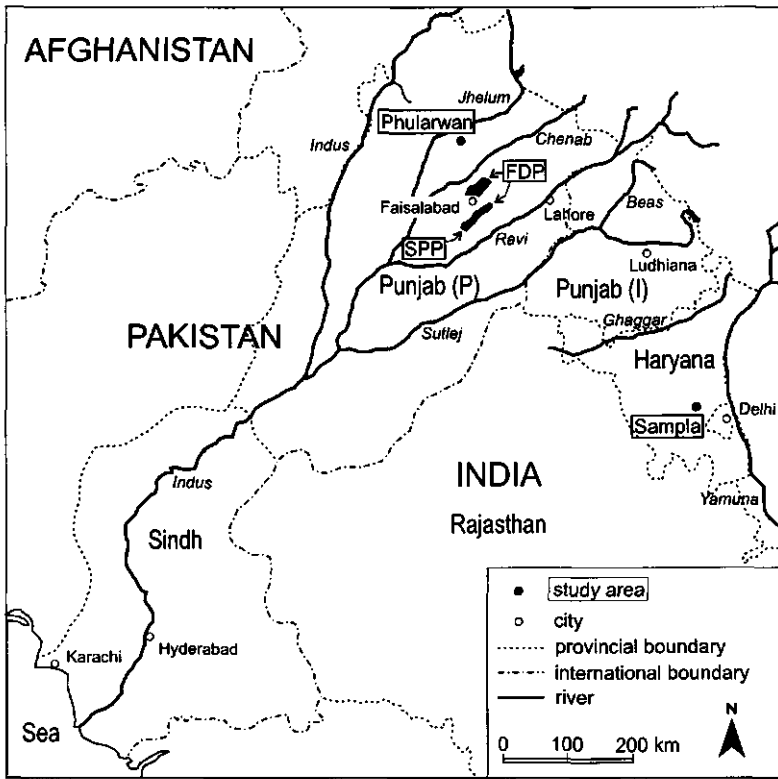


**Figure 4.1** The Indus river system in Pakistan and India. Locations of the study areas are indicated. The abbreviations FDP and SPP stand for Fourth Drainage Project (pipe drains) and Satiana Pilot Project (tube-wells), respectively. Note that the Ghaggar river ends inland.

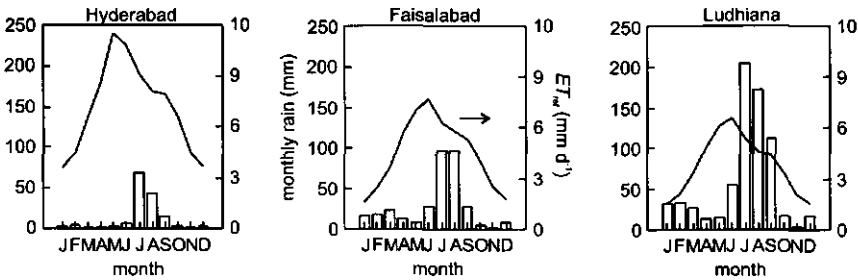


**Figure 4.2** Climate in the Indus plain. The abbreviation  $ET_{ref}$  stands for reference crop evapotranspiration (Smith, 1993). The locations of the three cities are shown in Fig. 4.1.



## 4.2 Geo-hydrology

The Indus plain consists of alluvial deposits of variable thickness. The alluvial complex of the Indus plain represents the latest phase of sedimentation in a subsiding trough, at the boundary of the rising Himalayas. The sediments consist mainly of sand intersected by silt and clay. Due to the relatively unsorted sedimentation in a fluvial environment, the individual layers have little continuity. An inhomogeneous aquifer system formed in such a way can be expected to have a rather uniform regionally-effective permeability. Local layers with extremely low or high permeabilities have no far reaching influence. Thickness of the aquifer ranges from a few metres close to rock outcrops to a few kilometres at the centre of the plain (Bender and Raza, 1995).

Soils in the Indus plain range mainly from loamy sand to silty clay loam, except for the Indus delta near the Arabian sea where clay soils predominate. In the plain, the occurrence of a particular soil type is related to its physiographic position. A distinction is made between Pleistocene river terraces which occupy the highest positions in the landscape, abandoned flood plains which take an intermediate position, and active flood plains which occupy the lowest positions near the rivers. In the field, the differences between the various landforms are often hardly visible, partly because of the large scale land development which has taken place in the Indus plain. Subtle differences in the physiographic position, however, may have considerable influence on the soil dynamics as represented by soil moisture status, salt accumulation and leaching of soluble salts. In some areas, wind blown sands occurring as sand dunes are overlying the alluvium (e.g. Rao et al., 1986).

Large tracts of the Indus plain are underlain by shallow groundwater at a depth of 1 to 3 m. Groundwater quality varies considerably. For Punjab Province, Pakistan, Swarzenski (1968) describes a clear pattern in groundwater salinity measured from tube-wells. Salinity is relatively low in the northern part of the Province where rainfall is relatively high ( $> 400 \text{ mm a}^{-1}$ ) and along the rivers where recharge has created fresh water zones. Salinity is relatively high in the centres of the inter-fluvial areas where groundwater is stagnant and near the confluents of the rivers, where upward moving groundwater is lost to evapotranspiration. Similar patterns are reported for Punjab State India (Minhas and Gupta, 1992) and for Haryana State (Agarwal and Roest, 1996). In Sindh province, which receives little rainfall, fresh groundwater areas only occur close to the river Indus.

Seiler et al. (1988) used isotopic (Deuterium, Oxygen-18 and Tritium) and conventional methods ( $\text{Cl}^-$  and  $\text{EC}$ ) to investigate the origin of the shallow and deep groundwater in the Faisalabad area (Fig. 4.1). The conclusions most relevant for this study were: (1) the residence time of the groundwater above the pre-irrigation groundwater table ( $\sim 30 \text{ m}$  depth) is more than 10-30 years; (2) the replenishment rate of the deeper groundwater ( $> 150 \text{ m}$  depth) is negligible; (3) the rise of the groundwater table is mainly due to the infiltration from the canal system. The contribution from the irrigated fields and rainfall is  $< 30 \%$ ; and (4) the salinity of the groundwater in the area is mainly due to the dissolution of salts from the sediments and partly due to heavy evaporation from the shallow groundwater table. No evidence was found of old marine groundwater.

### 4.3 Irrigation and drainage for agriculture

The present day irrigation canal network in the Indus plain was developed during the 19<sup>th</sup> and 20<sup>th</sup> century. In total about 16 million ha falls in the canal commanded areas (Ahmad and Chaudhry, 1988; Singh, 1993). Both perennial and non-perennial canals exist. The irrigation water is distributed through the so-called Warabandi system. Under Warabandi, farmers receive water according to a fixed rotation schedule. The farmer's entitlement to water is proportional to landholding. In practice, there is insufficient canal water to irrigate all land. Quality of the canal water is generally excellent ( $EC \sim 0.2-0.5 \text{ dS m}^{-1}$ ). In the south-west part of Haryana State India, consisting of upland areas, a number of lift irrigation schemes are in operation (Agarwal and Roest, 1996).

After independence in 1947, India and Pakistan signed the Indus Water Treaty in 1960. The treaty assigned the water of the three eastern tributaries of the Indus (Sutlej, Beas and Ravi) to India, and the three western tributaries (upper Indus, Jhelum and Chenab) to Pakistan. Implementation of the treaty required a major rescheduling of the canal irrigation system, especially in Pakistan's Punjab province. Amongst others, link canals were dug in Punjab to transport water from the Western rivers to the Ravi and the Sutlej rivers (Ahmad and Chaudhry, 1988). In India, part of the water from the Beas and Sutlej rivers is being directed towards the state of Rajasthan to develop 1,393,000 ha of new land (Hooja et al., 1995).

To supplement the irrigation supplies many government and private tube-wells have been installed in the Indus plain during the second half of the 20<sup>th</sup> century. These tube-wells can be found both in the canal commands and outside the canal commands. Due to the availability of tube-well water, overall cropping intensities in the Indus plain have gone up from ~60 % to ~150-200 %. Continued expansion of groundwater use, however, is becoming a major concern in the face of over-exploitation (Abrol, 1999). Excessive lowering of the groundwater table means that farmers spend more on pumping, while the well-water quality is deteriorating.

The Indus plain is provided with an extensive network of surface drains to carry off stormwater. The efficiency of this network, however, is generally low due to the flat topography of the plain and due to poor maintenance. Furthermore, most surface drains are shallow, and as a result, do little to control the groundwater table. Haryana State is a particularly difficult area with regard to drainage. The central part of this state constitutes a topographical depression with no natural drainage outlet. Stormwater in this part of Haryana is disposed by pumping it into the irrigation canals (Boumans et al., 1988).

In Pakistan, large-scale sub-surface drainage projects called Salinity Control And Reclamation Projects (SCARPs) were started in 1959 to combat waterlogging and salinity. Under the SCARP programme, 12,226 deep tube-wells were installed in fresh groundwater areas in Punjab and Sindh (providing both irrigation and drainage), 2,726 deep tube-wells were installed in saline groundwater areas and 70,875 ha were fitted with pipe drains (World Bank, 1997). Of the 2,726 deep tube-wells in the saline groundwater areas, 376 tube-wells in Sindh are of the scavenger-well type. These Scavenger wells have two well screens. The upper screen is located in the shallow relatively fresh groundwater, delivering water for irrigation. The lower screen is located



Soil type is sandy loam up to a depth of 1.8 m, below which a more permeable loamy sand layer is found up to a depth of 3.0 m. The underlying sandy loam soil layer, which starts at 3.0 m depth, was treated as an impermeable layer during the design process. Pre-drainage groundwater tables varied from 0 m depth (soil surface) during the rainy season to 1.5 m depth at the end of summer. Average soil salinity before drainage, expressed in  $EC_e$ , varied from  $\sim 50 \text{ dS m}^{-1}$  at the soil surface to  $\sim 15 \text{ dS m}^{-1}$  at 1.5 m depth. The  $EC$  of the shallow groundwater varied between 10 to  $40 \text{ dS m}^{-1}$  (Rao et al., 1986; Rao, 1996; Sharma et al., 2000).

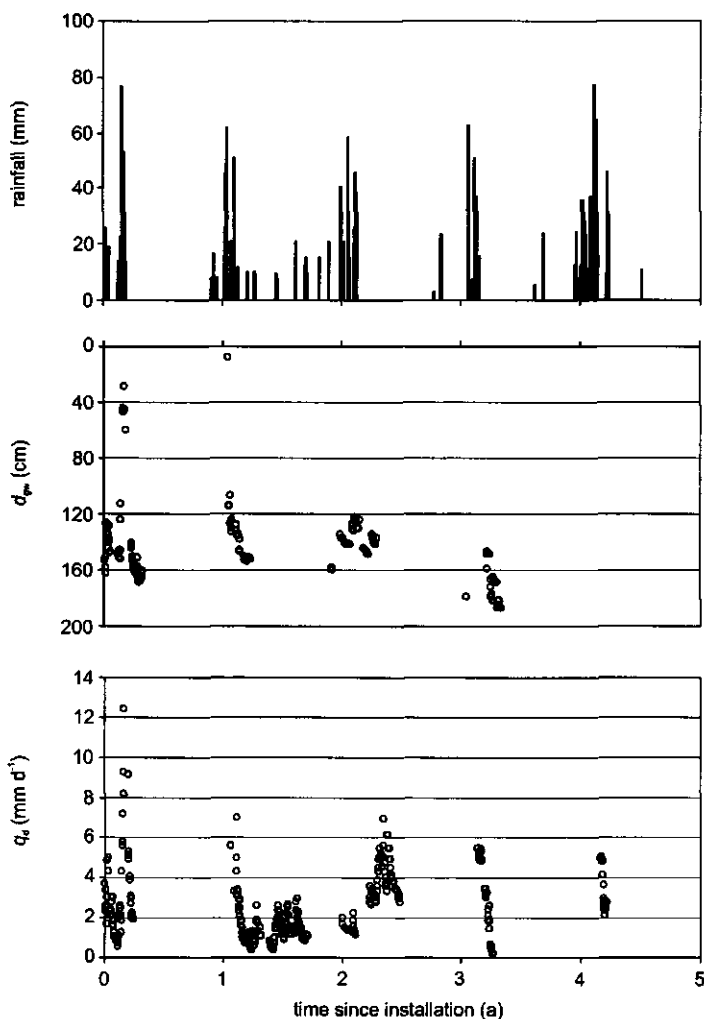


**Figure 4.4** Rainfall, depth of the groundwater table,  $d_{gw}$  and drain flux,  $q_d$  for the 50 m spacing area of the Sampla experimental pipe drainage site.

At the start of drainage, the experimental site was barren. Cropping was initiated in the 1984-85 winter season, after the monsoon rains. In the first four years, wheat, barley and sorghum were grown in winter, while pearl millet, sorghum and cotton were grown in summer. The site was irrigated with canal water with an  $EC$  of  $0.5 \text{ dS m}^{-1}$ . The total canal water availability was  $\sim 375 \text{ mm a}^{-1}$ . In subsequent years, several water management experiments were conducted at Sampla. In one experiment, conducted between 1990 and 1992, irrigation applications were limited and pumping of drainage water was suspended temporarily to increase the contribution of groundwater to satisfy crop water requirements (Rao et al., 1992). In another experiment, conducted between 1986 and 1993, drainage water was used to irrigate crops (Sharma and Rao, 1998). The latter experiment was confined to the area with drain spacing of 25 m.

A wealth of field data has been collected from the Sampla site. Amongst others, rainfall, depth of the groundwater table, drain discharge, soil salinity, effluent salinity and crop yields have been measured. A detailed description of the monitoring program can be found in Rao et al. (1986) and Sharma et al. (2000). Unfortunately, not all data could be retraced from the paper files by the present author. Rainfall, depth of the groundwater table,  $d_{gw}$  and drain flux,  $q_d$  for the 50 m spacing area are shown in Fig. 4.4. After the cessation of rain, the groundwater dropped quickly to drain level (or deeper). The deeper groundwater tables cannot be properly recognized from Fig. 4.4 because the frequency of groundwater table measurements was greatly reduced in dry periods. Observed groundwater table fluctuations for the 25 and 75 m spacing areas were very similar (Kamra et al., 1991b; Rao, 1996).

The relationship between the height of the groundwater table above drain level,  $H$  and drain flux,  $q_d$  for the 50 m spacing area is shown in Fig. 4.5. Data from the complete 5-year monitoring period were used, covering several different rainfall events. An almost linear relationship is found, indicating that flow to the drains mainly occurs below drain level (Dieleman and Trafford, 1976). This can be explained best with the help of the well-known Hooghoudt equation (Ritzema, 1994):

$$q_d = \frac{8K_b d_e H + 4K_a H^2}{L^2} \quad (4.1)$$

where  $d_e$  is the equivalent depth [L], an imaginary thickness below drain level proposed by Hooghoudt (1940) to correct for differences in flow pattern between open ditches and pipe drains,  $L$  is the drain spacing [L] and  $K_a$  and  $K_b$  are the saturated hydraulic conductivities [ $\text{L T}^{-1}$ ] above and below drain level, respectively.

The  $8K_b d_e H$  term above the division line in (4.1) describes flow to the drains below drain level, while the  $4K_a H^2$  term describes flow to the drains above drain level. If flow to the drains is mainly taking place below drain level, the  $4K_a H^2$  term can be neglected, and a linear relationship results between  $q_d$  and  $H$ . Similar to the 50 m spacing area at Sampla, the 25 m and 75 m spacing areas also yielded linear relationships. Fig. 4.5 shows that the drainage resistance,  $\gamma (=H/q_d)$  is 133 days. Calculated  $\gamma$  values for the 25 m and 75 m spacing areas are 38 days and 116 days, respectively.

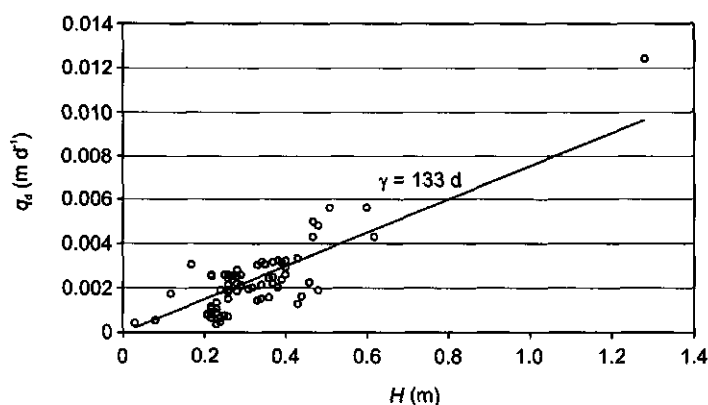


**Figure 4.5** Relationship between the height of the groundwater table above drain level at mid-spacing,  $H$  and drain flux,  $q_d$  for the 50 m spacing area at the Sampla experimental pipe drainage site. Height of the groundwater table above drain level was calculated from observation well c5. Drain flux is the average of laterals 5 and 6. Data recorded between 4 July 1984 and 22 September 1988.

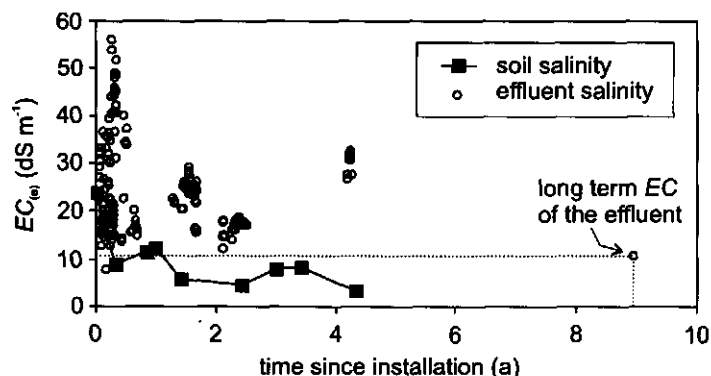


**Figure 4.6** Development of soil salinity,  $EC_e$  (0-1.0 m) and effluent salinity versus time since installation of the drainage system for the 50 m spacing area at the Sampla experimental pipe drainage site. Electrical conductivity of the effluent is the average of laterals 5 and 6.

The development of soil salinity,  $EC_e$  (0-1.0 m) and effluent salinity,  $EC_{dw}$  against time for the 50 m spacing area is shown in Fig. 4.6. Long term effluent salinity for the Sampla area as a whole, obtained from the irrigation experiment of Sharma and Rao (1998), is also shown. Figure 4.6 shows that average soil salinity reduced from 22.4 to 3.6  $dS\ m^{-1}$  in 4.5 years. Effluent salinity reduced at a slower rate, from ~20-60 to ~10.5  $dS\ m^{-1}$  in about 9 years. Shortly after the start of

drainage, effluent salinity fluctuated considerably. These fluctuations are an indicator for preferential flow phenomena, as it is unlikely that the groundwater salinity near the pipe drains shows this type of variation. Preferential flow might come from flow through macropores that developed during land preparation (ploughing and levelling) and from flow through the drain trench. The relatively slow reduction in effluent salinity over the years is attributed partly to the inflow of saline groundwater from the area surrounding the experimental site which is undrained (Sharma et al., 1995). Similar trends in soil and effluent salinity are observed for the 25 m and 75 m spacing areas.

#### 4.5 Satiana tube-well Pilot Project

The 71 tube-wells of the Satiana Pilot Project (SPP) were installed from 1975 to 1977. The project area covers about 40,000 ha of irrigated land in what is considered to be a saline groundwater area. Fifty wells were constructed alongside the three main surface drains, and 21 wells were constructed alongside the Lower Gugera branch canal and the Burala branch canal (Fig. 4.7). Pumpage from the wells alongside the surface drains is disposed directly in the drainage system. Pumpage from the wells alongside the irrigation canals is diverted to the irrigation system. The average depth of the wells is 60 m, with the length of the screen being about 40 m. The design discharge rate of the wells is  $4,893 \text{ m}^3 \text{ d}^{-1}$ . During 1988-89, most of the wells were still in working order, although their efficiency was reduced (Boonstra et al., 1991).

Soils in the area are mainly loam to silt loam, underlain by a highly conductive, deep, loamy sand to sandy loam aquifer. Estimates of the effective depth of the aquifer range from 100 to 300 m. At greater depths, permeabilities tend to be relatively low, owing to the compression and compaction of the aquifer material (Bennett et al., 1967). Groundwater tables vary between 1 and 4 m below soil surface. Groundwater salinity shows distinct patterns. Alongside the branch canals  $EC$  is low ( $<1.5 \text{ dS m}^{-1}$ ) due to seepage losses from the unlined canals. The width of this fresh water zone varies from 1 to 2 km. In the remainder of the area,  $EC$  is relatively high ( $>2.7 \text{ dS m}^{-1}$ ).

Table 4.1 shows the average  $EC$ ,  $SAR$  and  $RSC$  values of the tube-wells between 1979-81 and 1989-90 (data from SCARP Monitoring Organization, SMO). A distinction is made between the drainage tube-wells and the irrigation tube-wells. Averages are taken only for the tube-wells that were sampled during all four surveys. The distinct differences in well water quality between the two well-types are as expected. Temporal changes in water quality are minor. Over the 10-year period,  $EC$  for the drainage tube-wells decreased slightly (from  $3.3$  to  $3.1 \text{ dS m}^{-1}$ ), while  $RSC$  for both well types showed an increasing trend with time (from  $5.9$  to  $6.8 \text{ meq l}^{-1}$  for drainage tube-wells and from  $0.6$  to  $1.2 \text{ meq l}^{-1}$  for irrigation tube-wells).

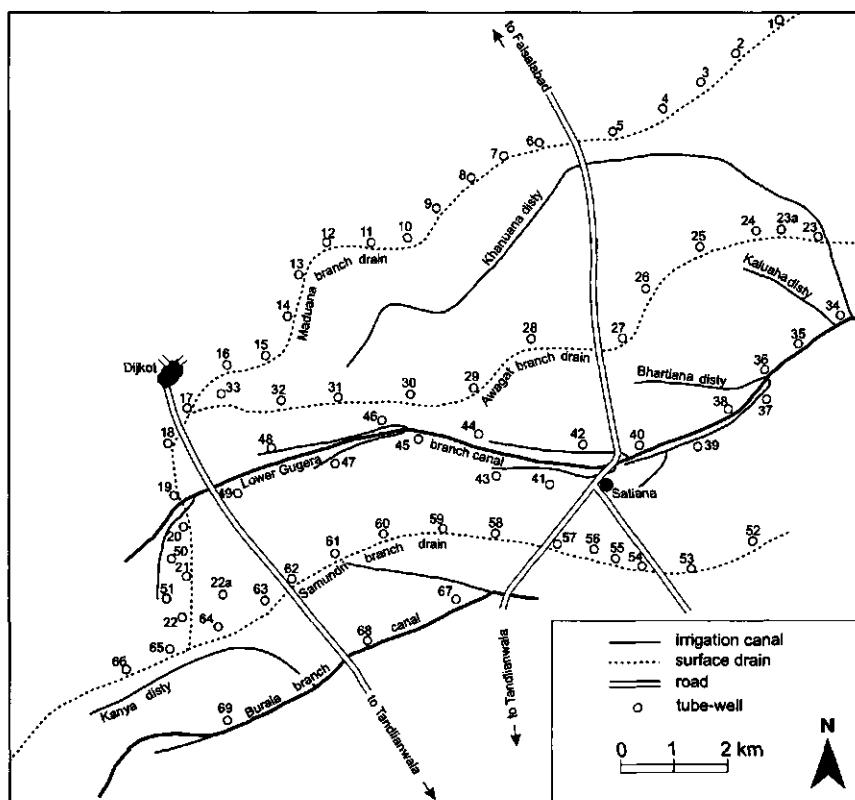


**Figure 4.7** Lay-out of the Satiana tube-well Pilot Project, Punjab Province, Pakistan.

**Table 4.1** Average *EC*, *SAR* and *RSC* values for Satiana Pilot Project tube-wells alongside surface drains (drain TW; 34 wells) and alongside irrigation canals (irrig TW; 18 wells). Values between brackets denote standard deviations.

Year	<i>EC</i> (dS m <sup>-1</sup> )		<i>SAR</i> (meq l <sup>-1</sup> ) <sup>0.5</sup>		<i>RSC</i> (meq l <sup>-1</sup> )	
	drain TW	irrig TW	drain TW	irrig TW	drain TW	irrig TW
1979-81	3.3 (1.4)	0.6 (0.4)	17.6 (5.1)	2.5 (3.3)	5.9 (4.0)	0.6 (1.9)
1983-84	3.2 (1.4)	0.6 (0.3)	16.6 (5.6)	3.0 (3.1)	6.2 (3.9)	1.1 (1.8)
1984-85	3.2 (1.2)	0.6 (0.3)	16.8 (4.7)	2.6 (2.9)	6.6 (3.5)	1.0 (1.9)
1989-90	3.1 (1.4)	0.6 (0.4)	17.6 (6.9)	2.6 (3.0)	6.8 (3.7)	1.2 (2.1)

The findings for the SPP tube-wells correspond with the findings of Beg and Lone (1992) for the SCARP 1 tube-well project which is located in the same inter-fluvial area. Beg and Lone studied water quality data that were taken over a 25-year period (1960-1985) from 1,901 tube-wells, and



found that water quality changed relatively little over time. Only the *RSC* values tended to increase. The relatively small temporal changes in water quality are due to the dampening effects of the deep, highly conductive aquifer. Water pumped from one point in the aquifer is replaced by water of comparable quality from the direct vicinity.

Figure 4.8 shows details of individual tube-wells. Data from all of the SPP tube-wells that were sampled in 1979-81 and in 1989-90 (52 wells) are plotted against each other for the *EC*, the *SAR* and the *RSC*. Again, a distinction is made between drainage tube-wells and irrigation tube-wells. The 1:1 lines in the figure indicate the situation in which no change occurs. Figure 4.8 shows that over the 10-year period only a limited number of wells show considerable change. The *EC* ranges from  $\sim 0$  to  $\sim 6 \text{ dS m}^{-1}$ . Tube-wells with the most saline water ( $EC > 5 \text{ dS m}^{-1}$ ) are situated alongside the Maduana branch drain, which lies approximately in the middle of the inter-fluvial area between the rivers Ravi and Chenab, where deep groundwater salinity is highest. One tube-well (number 67) shows a deviating behaviour. This irrigation tube-well has relatively high *EC*, *SAR* and *RSC* values.

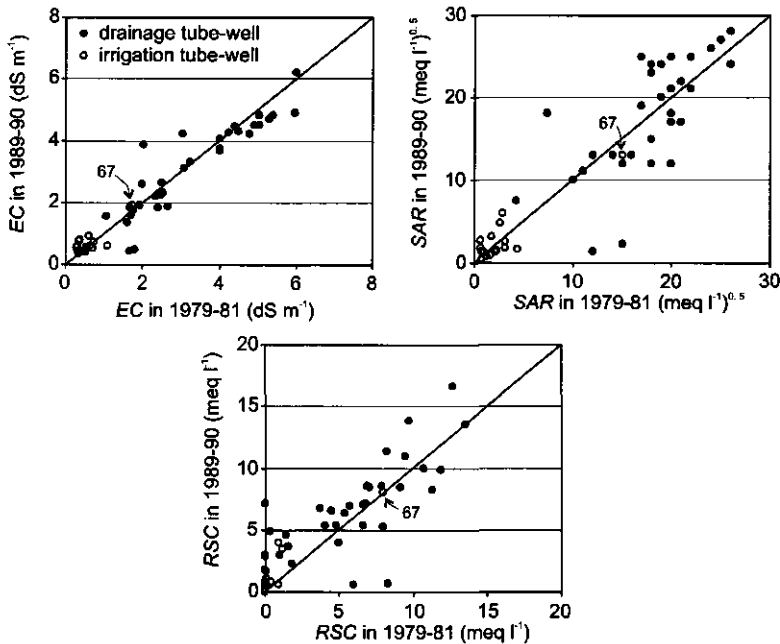


**Figure 4.8** Electrical Conductivity, *SAR* and *RSC* values of tube-well water in 1979-81 and 1989-90 from the Satiana Pilot Project, Punjab Province, Pakistan. A distinction is made between drainage tube-wells and irrigation tube-wells. The 1:1 lines indicate no change. Tube-well No. 67 shows a deviating behaviour.

#### 4.6 Fourth Drainage Project

Construction of the Fourth Drainage Project (FDP) was started in 1988 and completed in 1994. The project area covers 120,000 ha of irrigated land, of which 30,000 ha is equipped with pipe drains, divided over 79 units (Fig. 4.9). A typical drainage unit covers between 200 and 400 ha. Generally, it consists of subsurface laterals that discharge into a sump through subsurface collectors. Both laterals and collectors are of corrugated PVC, are perforated, and are surrounded by a gravel envelope. The design depth of the laterals is 2.4 m. The collectors are installed between 3 and 4 m depth. The spacing between the laterals varies from 100 to 750 m. From the sumps, the water is pumped into surface drains. Note that the FDP and SPP areas partly overlap (Figs 4.7 and 4.9). Geo-hydrological conditions in the FDP area are approximately similar to those of the SPP area.

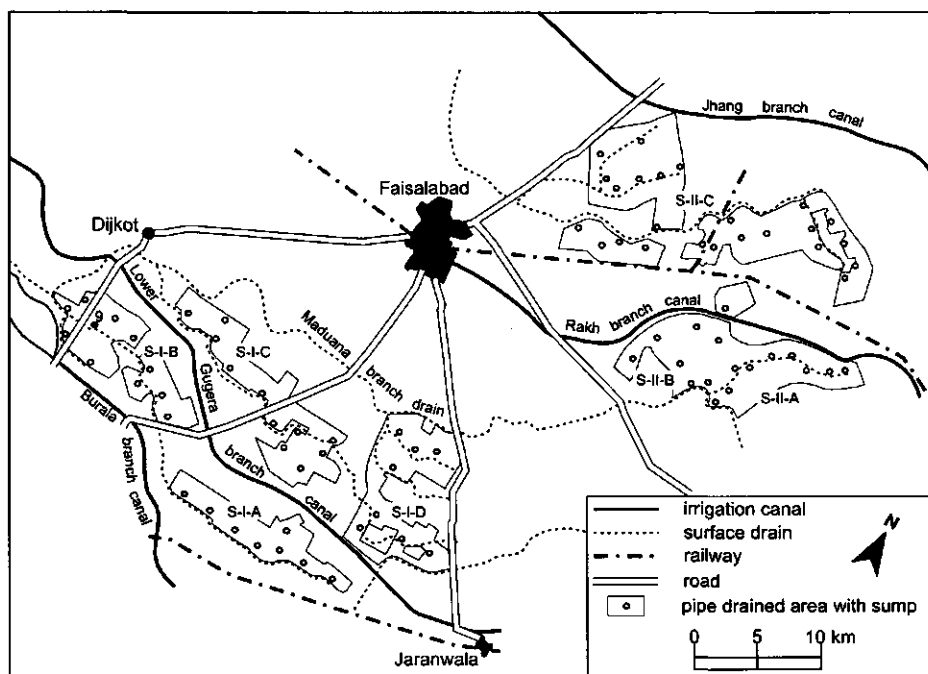


**Figure 4.9** Lay-out of the Fourth Drainage Project, a 30,000 ha pipe drainage project in Punjab Province, Pakistan. The black dot represents sump unit S-I-B-9.

Effluent quality of the 79 sump units is monitored by SMO. Due to differences in the construction date, and due to differences in the length of the monitoring period, not all sump units have a sufficiently long data record. Average *EC*, *SAR* and *RSC* of 18 sump units that were monitored between 1988-91 and 1994-95, a period of approximately 5 years, are shown in Table 4.2. The table shows that, on average, *EC* remained about constant over the 5-year period while *SAR* and *RSC* seemed to increase. Comparison with the SPP *drainage* tube-wells (Table 4.1),

which are situated in similar areas as the sump units, learns that pipe drains have lower overall salinity levels. The difference is explained by the fact that tube-wells attract groundwater from greater depths, which is generally more saline. The *EC*, *SAR* and *RSC* values for individual sump units are shown in Fig. 4.10.

**Table 4.2** Average *EC*, *SAR* and *RSC* for 18 selected sump units of the Fourth Drainage Project. Values between brackets denote standard deviations.

Year	<i>EC</i> (dS m <sup>-1</sup> )	<i>SAR</i> (meq l <sup>-1</sup> ) <sup>0.5</sup>	<i>RSC</i> (meq l <sup>-1</sup> )
1988-91	2.3 (0.9)	11.5 (4.9)	4.8 (3.5)
1994-95	2.4 (0.9)	14.5 (5.2)	5.6 (2.9)

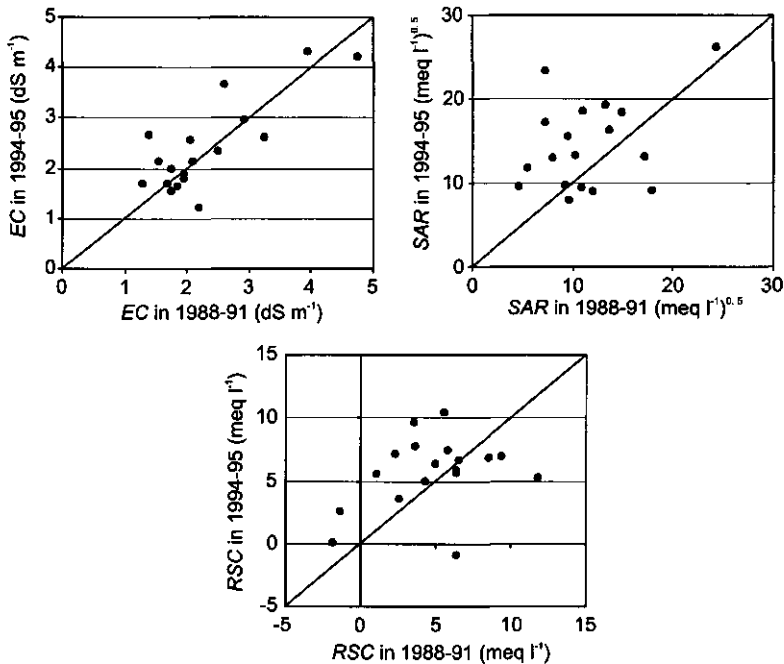


**Figure 4.10** Electrical Conductivity, *SAR* and *RSC* values of 18 selected sump units in 1988-91 and 1994-95 from the Fourth Drainage Project. The 1:1 lines indicate no change.

The International Waterlogging and Salinity Research Institute (IWASRI), carried out detailed investigations in sump unit S-I-B-9 of the FDP area (see Fig. 4.9). The layout of the 225-ha area is shown in Fig. 4.11. Actual depths of the laterals varies between 1.6 and 3.2 m. The diameter of the laterals ranges from 0.15 to 0.25 m. The average depth of the collector is 3.1 m. The sub-surface interceptor drain in Fig. 4.11, serves to stabilize the side slope of the surface drain, and

to prevent seepage from the surface drain back to the drained area. The unit became operational during June 1989 (Vlotman et al., 1994).

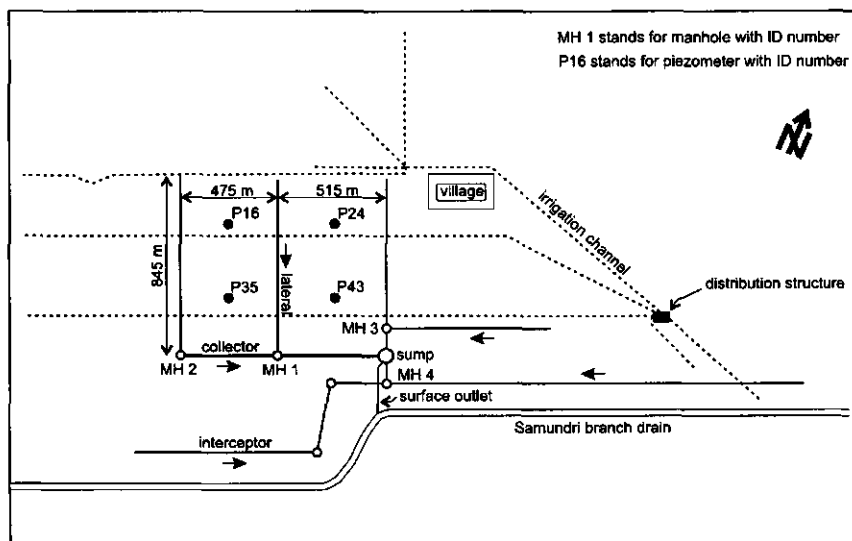


**Figure 4.11** Lay-out of pipe drainage unit S-I-B-9 of the Fourth Drainage Project, Punjab Province, Pakistan. The black dots represent the piezometers used in this study.

The S-I-B-9 unit provides drainage to over 500 agricultural fields. Main crops are maize, sorghum and cotton in summer, and wheat and berseem in winter. Sugarcane is cropped year round. The total canal water available for crop growth is  $\sim 450 \text{ mm a}^{-1}$ . Due to the limited availability of canal water, about 25 % of the area is abandoned. Furthermore, in summer, 25 % of the area is fallow. In winter about 9 % of the area is fallow. The quality of the canal water is excellent ( $EC \sim 0.2 \text{ dS m}^{-1}$ ;  $SAR < 2 \text{ (meq l}^{-1})^{0.5}$ ;  $RSC \sim 0 \text{ meq l}^{-1}$ ).

Many data have been collected from the S-I-B-9 area, like weather data, depth of the groundwater table, drain discharge, soil salinity, effluent salinity and crop yields. A detailed description of the measurement programme can be found in Vlotman et al. (1994) and Sarwar (2000). Rainfall, depth of the groundwater table,  $d_{gw}$  and drain flux,  $q_d$  for the S-I-B-9 area are shown in Fig. 4.12. Depth of the groundwater table is only shown for piezometer P35. The groundwater fluctuations measured by the other piezometers were practically the same. Note that the drain flux was derived from discharge measurements at the point where the collector enters the sump (Vlotman et al., 1994). Only a few discharge measurements were taken at the outlet of the central lateral drain (Sarwar, 2000). The  $q_d(H)$  relationship for the central lateral drain is shown in Fig. 4.13. The relationship is approximately linear, indicating that flow to the drains mainly occurs below drain level. Similar observations were made earlier for the Sampla experimental pipe drainage site (Section 4.4). Drainage resistance,  $\gamma$  in the present case is 625 days.

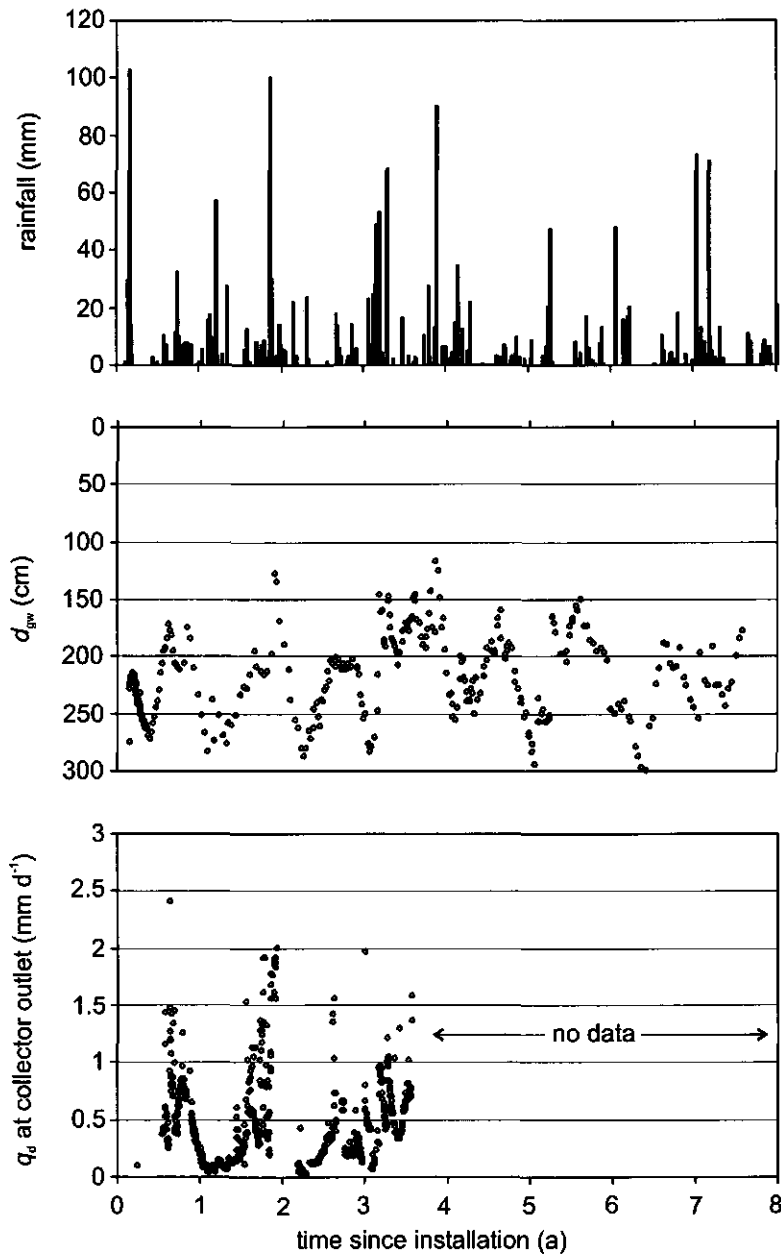


**Figure 4.12** Rainfall, depth of the groundwater table,  $d_{gw}$  and drain flux,  $q_d$  at the collector outlet for the S-I-B-9 drainage unit of the Fourth Drainage Project. Depth of the groundwater table was taken from piezometer P35.

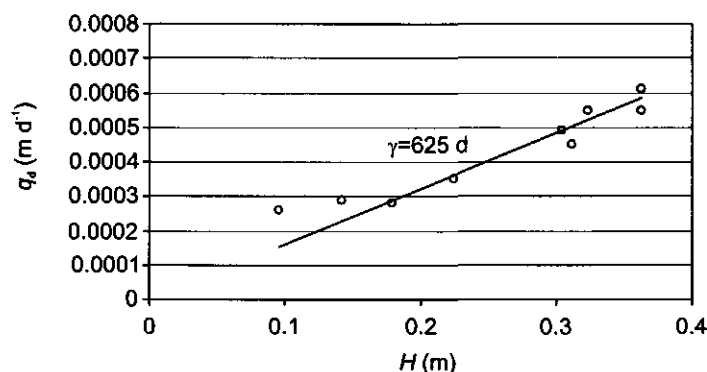


**Figure 4.13** Relationship between height of the groundwater table above drain level at mid-spacing,  $H$  and drain flux,  $q_d$  for the central lateral drain at the S-I-B-9 sump unit of the Fourth Drainage Project. Head above drain level is the average of 4 piezometers (P16, P24, P35 and P43). Drain flux was calculated from discharge measurements at the central lateral drain (Sarwar, 2000).

The development of effluent salinity with time for the S-I-B-9 area is shown in Fig. 4.14. Samples were taken from the sump water. Figure 4.14 shows that the  $EC$ ,  $SAR$  and  $RSC$  are relatively constant in time. The average  $EC$  of the S-I-B-9 sump water is  $\sim 3.1 \text{ dS m}^{-1}$ , the average  $SAR$  is  $\sim 14.5 (\text{meq l}^{-1})^{0.5}$  and the average  $RSC$  is  $\sim 5.2 \text{ meq l}^{-1}$ . On two days in August and September 1989, water samples from the sump showed extraordinary values. There is no explanation for this other than human error. Fluctuation in the  $EC$ ,  $SAR$  and  $RSC$  values are relatively small (compare with Fig. 4.6). The primary reason for these small fluctuations is the dampening effect of the deep aquifer. The fact that effluent salinity in S-I-B-9 is influenced by management practices from over 500 fields, by several watercourses, by seepage from the surface drain and possibly by regional inflow through the aquifer also contributes to the small fluctuations. Development of soil salinity is not shown in Fig. 4.14. At S-I-B-9, each of the 500 fields has its own specific soil salinity level, depending on the cropping history (Hendrickx et al., 1992). Regular EM38 measurements around the central lateral drain ( $\sim 3400$  grid points) between September 1989 and May 1995 showed no significant changes in soil salinity (unpublished data).

Figure 4.15 shows detailed measurements of the effluent salinity of the sump water and of individual sections of the pipe drainage system (see also Fig. 4.11). It is clear from Fig. 4.15 that temporal variations are again limited. Samples from Manhole 3 which receives water from the north-east part of the drained area, showed the lowest values (average  $EC$  of  $2.8 \text{ dS m}^{-1}$ ). Samples from Manhole 2, which receives water from the western part of the area, have the highest values ( $EC$  of  $3.3 \text{ dS m}^{-1}$ ) (Oosterkamp, 1997). Similar to the sump water, the water from the manholes is of a mixed type.

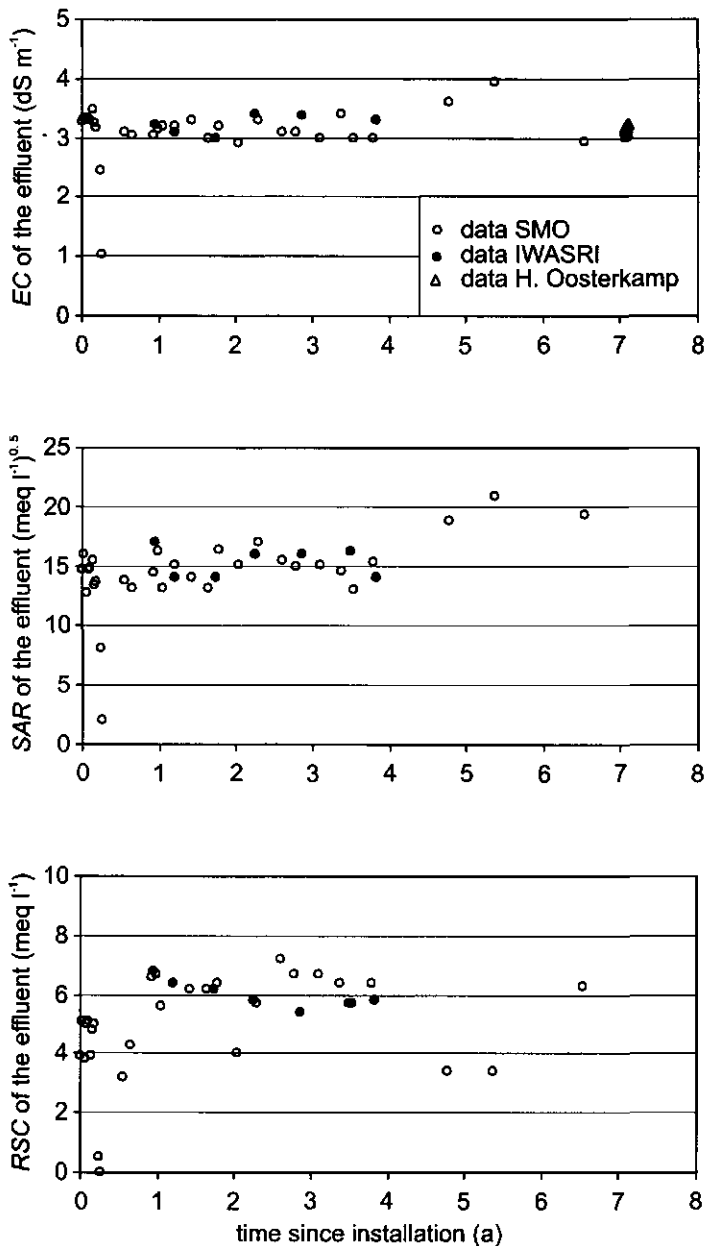


**Figure 4.14** Electrical Conductivity, SAR and RSC values for the sump water at unit S-I-B-9 of the Fourth Drainage Project.

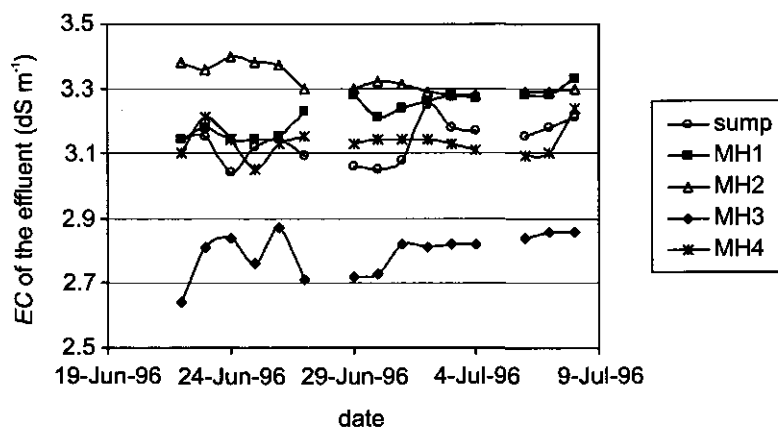


**Figure 4.15** Electrical conductivity of Sump water and Manhole water at unit S-I-B-9 of the Fourth Drainage Project (Oosterkamp, 1997).

#### 4.7 Conclusions

The  $q_d(H)$  relationships for the Sampla experimental pipe drainage site and the S-I-B-9 pipe drainage unit show that in the relatively light textured soil-aquifer systems of the northern Indus plain, flow to pipe drains mainly occurs below drain level. This implies that the schematization of Tököz and Kirkham (1971) (Fig. 3.2) is applicable. Measured drainage resistance,  $\gamma$  for the Sampla site of between 38 and 133 days are considerably lower than those for the S-I-B-9 unit ( $\gamma = 625$  days). The differences in  $\gamma$  are due to the larger drain spacing at S-I-B-9 (495 m against 25-75 m for Sampla) which offsets the higher transmissivity of the zone below drain level at S-I-B-9.

The Sampla experimental pipe drainage site shows that soil salinity drops quickly in response to drainage. Two years after the installation of the drainage system the rootzone may be considered reclaimed. Improved control over the groundwater table and the presence of an outlet, facilitate the leaching of the topsoil by rainfall and irrigation water. In contrast, effluent salinity reacts slowly. At Sampla, it takes ~9 years before the EC of the effluent has reduced from 20-60 dS m<sup>-1</sup> to 10.5 dS m<sup>-1</sup>. The slow development in effluent salinity for Sampla is partly due to the influence of regional inflow.

For the SPP tube-wells and the FDP pipe drainage units effluent salinity does not change significantly with time. The lack of change is attributed mainly to the dampening effects of the deep, highly conductive aquifer. Comparison of the irrigation tube-wells and the drainage tube-wells of the SPP on the one hand, and the pipe drainage units of the FDP on the other, shows the relative influence of drainage technology and pre-drainage groundwater salinity on effluent salinity. On average, irrigation tube-wells, which are situated in fresh groundwater areas, have an EC of 0.6 dS m<sup>-1</sup>, while drainage tube-wells, which are situated in saline groundwater areas,



have an *EC* of 3.1-3.3 dS m<sup>-1</sup>. This difference is as expected. The higher average *EC* of the *drainage* tube-wells as compared to the *EC* of the pipe drainage units (2.3-2.4 dS m<sup>-1</sup>), is attributed to the fact that tube-wells attract groundwater from greater depths, which is generally more saline.

Effluent of the SPP tube-wells and the FDP pipe drainage units exhibits an increase of *RSC* with time (Tables 4.1 and 4.2). Comparison between the ion composition of the canal irrigation water and the ion composition of the drainage effluent shows that the increase in *RSC* is due to a disproportional increase in  $\text{HCO}_3^-$  in the drainage water as compared to  $\text{Ca}^{2+}$  and  $\text{Mg}^{2+}$  ( $\text{CO}_3^{2-}$  concentrations are ~0 meq l<sup>-1</sup>). Near the rootzone,  $\text{HCO}_3^-$  concentrations may increase due to the presence of  $\text{CO}_2$  (root activity) which reacts with water. This, however, does probably not explain the relatively strong increase in  $\text{HCO}_3^-$  concentrations in the effluent, as the drainage systems in the Indus plain generally attract groundwater from considerable depths (Chapter 5). The most likely explanation for the increase in *RSC* with time is that more ( $\text{Ca}^{2+} + \text{Mg}^{2+}$ ) precipitates in the soil-aquifer system than  $\text{HCO}_3^-$ .

The development of soil and effluent salinity for the Sampla experimental pipe drainage site, the SPP tube-wells and the S-I-B-9 unit of the FDP are studied in more detail during the modelling exercise in Chapter 5.



## 5 Prediction of Long Term Effluent Salinity of Pipe Drains and Tube-Wells

### 5.1 Introduction

In irrigated agriculture, solutes are distributed along the soil surface with the irrigation water or are initially present in the soil-aquifer system. Transport of these solutes to pipe drains or tube-wells can be described in various ways. In the past, several investigators used stream functions to assess steady-state flow patterns to pipe drains and tube-wells and the associated solute transport. The stream functions were obtained either analytically (e.g. Table 3.1) or numerically. The transport of solutes along the streamlines was calculated assuming piston flow (Luthin et al., 1969; Ortiz and Luthin, 1970; Jury, 1975; Van der Molen, 1987; Quinn, 1991; Youngs and Leeds-Harrison, 2000), advective-dispersive transport (Kamra et al., 1991a; Yu and Konyha, 1992) or a series of mixing reservoirs (Rao and Leeds-Harrison, 1991). The stream function approach facilitates long term predictions of effluent quality of both pipe drains and tube-wells with limited computational resources.

Van Ommen (1985), using Dupuit assumptions, showed that the solute breakthrough curve of a field with parallel canals or fully penetrating wells can be described by a simple exponential function. This exponential function is identical to the solute breakthrough curve of a completely mixing reservoir. The assumption of a completely mixing reservoir has also been used to predict outflow water quality for aquifer systems (e.g. Gelhar and Wilson, 1974; McLin and Gelhar, 1979; Prendergast et al., 1994; Oosterbaan, 1998). The great advantage of the mixing reservoir approach is its simplicity, as the aquifer is characterized by only three parameters: the saturated thickness of the aquifer,  $B$  [L], the effective porosity of the aquifer,  $n_e$  [-] and the initial solute concentration in the aquifer,  $c_0$  [M L<sup>-3</sup>]. The mixing reservoir approach does not provide information about the spatial pattern of flow or concentration within the aquifer (Duffy et al., 1990).

Two- or three-dimensional numerical models based on the Darcy equation for water flow and the advection-dispersion equation for solute transport provide the most complete description currently available to simulate water flow and solute transport to pipe drains and tube-wells (Pickens et al., 1979; Nour el-Din et al., 1987; Šimůnek et al., 1994; Nieber and Misra, 1995; De Vos, 1997; Mohanty et al., 1998). Numerical models allow the specification of complex aquifer geometries, temporally variable boundary conditions and spatially variable hydraulic properties and solute concentrations. Application of these models in transient mode is generally restricted to a few drainage events only. Long term calculations tend to be very time consuming, even on present-day personal computers.

A quasi three-dimensional numerical model was developed by Garcia et al. (1995). The model solves Richards' equation and the advection-dispersion equation for one-dimensional vertical water flow and solute transport in the unsaturated zone above the groundwater table. It also solves the depth-averaged Boussinesq equation and the two-dimensional advection-dispersion equation for areal flow and transport in the fully saturated zone below the groundwater table. The model facilitates the specification of spatially variable land use (Manguerra and Garcia, 1995).

In a later development, (Manguerra and Garcia, 1997) incorporated a fully three-dimensional representation of water flow and solute transport in the saturated zone. This modification was made to allow a more accurate calculation of drainage water quality.

In this chapter, a *new modelling approach* is presented that facilitates long term predictions of soil and effluent salinity. The general idea is to *couple the SWAP model for water flow and solute transport in the variably saturated zone with a solute impulse response function for the saturated zone*. The solute impulse response function is derived from two-dimensional (pipe drains) and three-dimensional (tube-wells) streamline patterns. The resulting quasi three-dimensional modelling set-up is similar to the set-up as used by Manguerra and Garcia (1997), only without the possibility to specify spatially variable land use. The use of stream functions for the saturated zone implies that the modelling approach has also links with older studies that used steady-state streamlines to predict effluent quality (especially Jury, 1975).

The modelling approach is explained in Section 5.2. Subsequently, the calibration procedure is described in Section 5.3. The modelling approach is applied to the Sampla experimental pipe drainage site and the S-I-B-9 pipe drainage unit in Sections 5.4 and 5.5. In Section 5.6, the modelling approach for tube-wells is presented. The tube-well case is illustrated with calculations for a Satiana Pilot Project tube-well in Section 5.7. The applicability of the mixing reservoir approach to calculate the solute impulse response of the saturated zone is discussed in Section 5.8. Finally, conclusions are drawn in Section 5.9. It should be noted that in the calculations, solute concentrations are expressed in  $\text{mg l}^{-1}$ . Results, however, are presented in Electrical Conductivity,  $EC$ , having units  $\text{dS m}^{-1}$ . During all calculations it was assumed that  $1 \text{ dS m}^{-1} = 700 \text{ mg l}^{-1}$  (e.g. Van Hoorn and Van Alphen, 1994).

### 5.2 New modelling approach for pipe drains

A schematic representation of the modelling approach for pipe drains is given in Fig. 5.1. The flow region is divided into two zones: one above drain level where only vertical flow is assumed, and one below drain level where flow is two-dimensional. This schematization follows the geometry of the soil-pipe-aquifer system as used by Toksöz and Kirkham (1971) (Fig. 3.2). *The underlying assumption is that groundwater flow to pipe drains occurs only below drain level*. In Chapter 4 it was shown that this is generally true for the relatively coarse textured soil-aquifer system in the Indus plain.

Water flow and solute transport in the zone above drain level is described with the SWAP model (Van Dam et al., 1997). This transient one-dimensional model predicts the solute concentration as a function of depth and time using Richards' equation and the advection-dispersion equation. The SWAP model simulates the water and solute fluxes at mid-spacing. The fact that the groundwater table is generally curved, i.e. the height of the groundwater table near the drain is lower than at mid-spacing, is neglected. The zone below drain level is characterized by the stream functions of Töksoz and Kirkham (1971). In the stream-tubes, piston flow is assumed. Solute breakthrough from each stream-tube  $i$  is calculated by evaluating cumulative drainage against  $n_e A_i / (dx)_i$ , with  $n_e$  being the effective porosity [-] in the zone below drain level,  $A_i$  the

cross-sectional area  $[L^2]$  of stream-tube  $i$  and  $(dx)_i$  the horizontal distance  $[L]$  between the two bounding streamlines of tube  $i$ , measured at drain level.

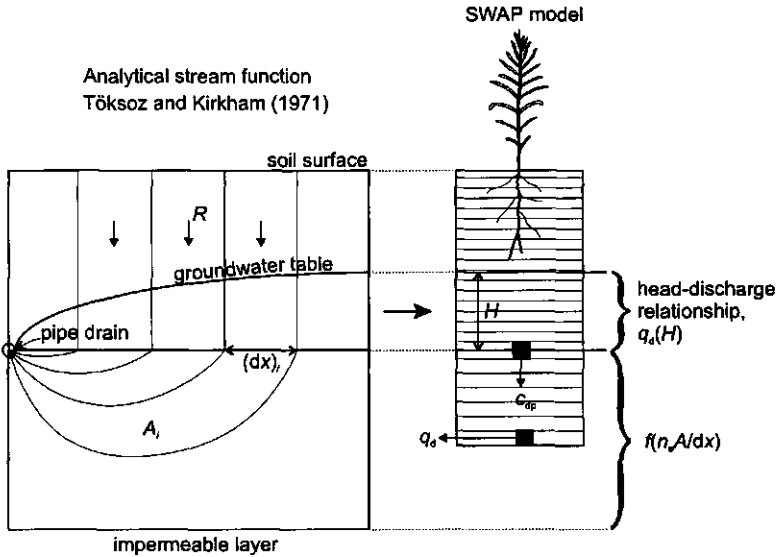


**Figure 5.1** Schematic representation of the modelling approach for pipe drains. The left side of the figure represents the geometry of the soil-pipe-aquifer system as used by Töksoz and Kirkham (1971). The right side of the figure represents the SWAP model, with  $f(n_e A/dx)$  representing the solute impulse response function of the zone below drain level.

The solute concentration of the effluent from the pipe drains,  $c_{dw}$   $[M L^{-3}]$  is calculated by convolution of the solute input from the zone above drain level with the solute impulse response function of the zone below drain level. The convolution integral is given by (after Jury and Roth, 1990):

$$c_{dw}(t) = g_w \left( \frac{2dx}{L} \right) \int_0^t c_{dp}(D(t) - D(t')) f[D(t') - \Delta W(D(t) - D(t'))] q_d(t') dt' \quad (5.1)$$

where  $g_w(2dx/L)$  is a weighting function  $[-]$ , with  $L$  being the drain spacing  $[L]$ ,  $c_{dp}$  is the solute concentration  $[M L^{-3}]$  of the downward soil water flux at drain level,  $D$  the cumulative drainage  $[L]$ ,  $f(D)$  the cumulative drainage probability density function  $[L^{-1}]$  (= impulse response function),  $\Delta W$  the change in water storage  $[L]$  below drain level and  $q_d$  the drain flux  $[L T^{-1}]$ . Note that Eq. (5.1) is valid for transient water flow. The weighting function  $g_w$  is incorporated to account for the relative influence of each stream tube  $i$  on the effluent salinity,  $c_{dw}$ .

The cumulative drainage,  $D$  at time  $t$  is calculated from:

$$D(t) = \int_0^t q_d(t) dt \quad (5.2)$$

For the zone below drain level,  $D(t')$  is equivalent to  $n_e A / (dx)$ . Therefore:

$$f(D(t')) = f\left(\frac{n_e A}{dx}\right) \quad (5.3)$$

Flow to pipe drains requires that the groundwater table is above drain level. Hence, during drain flow, the zone below drain level is always saturated:

$$\Delta W(D(t) - D(t')) = 0 \quad (5.4)$$

Insertion of Eqs. (5.2)-(5.4) in (5.1) results in:

$$c_{dw}(t) = g_w \left( \frac{2dx}{L} \right) \int_0^t c_{dp} \left( \int_0^t q_d(t) dt - \frac{n_e A}{dx} \right) f\left(\frac{n_e A}{dx}\right) q_d(t') dt' \quad (5.5)$$

Taking into account the initial solute concentration of the zone below drain level,  $c_0$  [ $M L^{-3}$ ], Eq. (5.5) can be written in discrete form as:

$$c_{dw}(t) = \frac{\sum_{i=1}^N c_i(t)(dx)_i}{\sum_{i=1}^N (dx)_i} = \frac{2 \sum_{i=1}^N c_i(t)(dx)_i}{L} \quad (5.6)$$

where:

$$c_i(t) = c_0 \quad \text{for} \quad \int_0^t q_d(t) dt < \frac{n_e A_i}{(dx)_i} \quad (5.7)$$

$$c_i(t) = c_{dp} \left( \int_0^t q_d(t) dt - \frac{n_e A_i}{(dx)_i} \right) \quad \text{for} \quad \int_0^t q_d(t) dt \geq \frac{n_e A_i}{(dx)_i} \quad (5.8)$$

where  $N$  is the total number of stream-tubes and  $c_i$  is the solute concentration [ $M L^{-3}$ ] of stream-

tube  $i$  at the point where it enters the drain. Note that Eqs. (5.6) to (5.8) are solved only for times  $t$  at which  $q_d > 0$ .

Overall, the modelling approach assumes that: (1) the initial solute concentration,  $c_0$  and effective porosity below drain level,  $n_e$  are space-invariant, (2) the shape of the stream-tubes is time-invariant (valid under the assumptions of Toksöz and Kirkham (1971), Section 3.4) and (3) solute transport in the zone below drain level can be described by advection only, neglecting the effects of dispersion and diffusion. According to Duffy and Lee (1992), assumption (3) is reasonable for hydrological systems in which solute input or initial solute concentrations are distributed in space, while the outflow surface is small or isolated.

The value of the drain flux,  $q_d$  is calculated from the  $q_d(H)$  relationship, where  $H$  is the height of the groundwater table above drain level. SWAP assumes that  $q_d$  leaves the model at the bottom compartment. The vertical dimension modelled with SWAP is extended to below drain level (Fig. 5.1). This allows the groundwater table to drop below drain level in periods where capillary rise predominates. Under these circumstances, the value of  $q_d$  is set to zero. Drain flow resumes, when recharge from the zone above drain level raises the groundwater table to above drain level. Note that the drain flux,  $q_d$  has a solute concentration,  $c_d$  [ $M L^{-3}$ ] which is not necessarily equal to  $c_{dp}$  in Fig. 5.1. In the calculations the value of  $c_d$  is ignored. The fact that solutes are allowed to leave the model through the bottom compartment in SWAP is essential in preventing unrealistic accumulation of the solutes in the lower part of the model.

Equations (5.6)-(5.8) do not account for the effect of capillary rise on the solutes within the stream-tubes below drain level. This results in assumption (4): upward vertical solute transport in the stream-tubes due to depletion of the groundwater by capillary rise, is balanced by downward vertical solute transport during the subsequent recharge period(s). In other words, no vertical solute transport is assumed in the stream-tubes other than that predicted by the stream functions of Toksöz and Kirkham (1971).

The modelling approach has several strong features. The SWAP model provides a state-of-the-art description of water flow and solute transport processes in the zone above drain level, including the interaction with crop growth. The transient nature of the flow and transport processes in this zone is fully recognized (e.g. Nielsen et al., 1986). This warrants a good approximation of the drainable surplus at field level. The use of stream functions for the zone below drain level, gives an accurate description of the transport of solutes towards the drains. Computational requirements are low because no transient two- or three-dimensional numerical models are used to describe water flow and solute transport below drain level. Treating the zone below drain level differently from the zone above drain level, is supported by the observation that flow and transport processes in the groundwater can usually be approximated by a steady-state approach (e.g. Jury, 1975; Raats, 1978; Kamra et al., 1991a).

### 5.3 Calibration of the soil-aquifer hydraulic properties

The prediction of long term soil and effluent salinity for the experimental pipe drainage sites requires a number of steps. Verification of the soil hydraulic properties, both above and below drain level, is the most difficult task. Vertical water flow and solute transport above drain level is particularly sensitive to the vertical saturated hydraulic conductivity,  $K_s$ , and the unsaturated soil hydraulic properties. In contrast, two-dimensional flow to pipe drains below drain level, and therefore  $f(n_e A/dx)$ , mainly responds to the horizontal saturated hydraulic conductivity,  $K_{xx}$  and the vertical saturated hydraulic conductivity,  $K_{zz}$ . Note that  $K_s$  and  $K_{zz}$  are the vector and tensor representation, respectively of the same parameter (Chapter 2).

Estimation of the soil hydraulic properties under variably saturated conditions usually comes from laboratory experiments on undisturbed soil samples (e.g. Van Dam et al., 1994). However, direct application of the soil hydraulic parameters derived from these small scale experiments to the larger scale of a drained area often leads to disappointing results (Beekma et al., 1995; Smets et al., 1997; Sarwar, 2000). Spatial variability in the soil hydraulic properties plays a major role in the failure to obtain suitable parameter values. Several investigators have tried to solve this problem by taking multiple samples of each soil horizon (in the order of 20 or more), and by using a scaling procedure (e.g. Warrick et al., 1977; Hopmans and Stricker, 1989; Clausnitzer et al., 1992). A scaling procedure was also conducted for the S-I-B-9 unit of the Fourth Drainage Project. The number of samples, however, was too small, and the variability in soil type too large, to claim that field conditions were described accurately (Kelleners et al., 1999).

Alternatively, the soil hydraulic properties under variably saturated conditions can be determined by inverse modelling of an experimental field plot, using the SWAP model. This requires that the top and bottom boundary conditions in SWAP can be estimated with reasonable accuracy from field data. The soil hydraulic properties can be found by either matching measured and simulated volumetric water contents, pressure heads, or groundwater table depths, or a combination of these. Soil salinity data may also assist in the verification of the soil hydraulic properties. The inverse modelling technique was applied with reasonable success at the S-I-B-9 unit of the Fourth Drainage Project (Beekma et al., 1995; Kelleners, 1996; Sarwar, 2000).

Spatial differences between the experimental plot scale (0.01-0.2 ha) and the scale of the complete drained area (2.0-125.0 ha) imply, however, that there is no guarantee that calibrated plot scale parameters will yield satisfactory results at the larger scale. Spatial differences might stem from differences in soil type and differences in soil profile layering. In this thesis, therefore, a more general approach is followed, in which the *soil hydraulic properties are tuned by trial and error to match measured and simulated groundwater table depths and drain fluxes at the scale of the drained area*. The soil profiles used in the SWAP model are generalized compared to the soil profiles found in the plot scale studies (some soil layers are put together). Estimates of individual parameters values in the MVG model are based on the above mentioned inverse modelling studies, and on existing databases for various soil texture classes (Rawls et al., 1982; Carsel and Parrish, 1988; Leij et al., 1996; Wösten et al., 1998; Wösten et al., 2001).

The saturated hydraulic conductivities,  $K_{xx}$  and  $K_{zz}$  can be determined through an inverse



procedure by matching measured and simulated  $q_d(H)$  relationships. This procedure is attractive because it results in area-averaged values of hydraulic conductivity as the complete area between the (parallel) drains is considered (Oosterbaan and Nijland, 1994). In principle, simulated  $q_d(H)$  relationships might be obtained from a relationship given by Töksoz and Kirkham (1971), or from the steady-state drainage equation of Hooghoudt (Eq. 4.1). For anisotropic soils ( $K_{xx} \neq K_{zz}$ ) this would require a coordinate transformation (Smedema et al., 1985; Kelleners et al., 2000). In this study, however, *the two-dimensional numerical SWMS\_2D code (Šimůnek et al., 1994) is used to match measured and simulated  $q_d(H)$  relationships*. This code provides a complete description of the soil-pipe-aquifer system without any simplifying assumptions about the flow regime. SWMS\_2D is only run for single drainage events, which keeps the computation time in check. Details about the application of SWMS\_2D are given in Appendix A.

The actual calibration of the soil hydraulic properties for a particular site, consists of a SWMS\_2D model run to test the  $q_d(H)$  relationship as well as a SWAP model run to test the groundwater tables and the drain fluxes. *The final result of the calibration procedure consists of a MVG parameter set for each soil-aquifer layer plus  $K_{xx}$  and  $K_{zz}$  for each soil-aquifer layer.*

#### 5.4 Case 1: Sampla experimental pipe drainage site

Calculations for the Sampla experimental pipe drainage site were conducted for all three drain spacings: 25 m, 50 m and 75 m. The simulation period covered almost 15 years (4/7/1984-31/5/1999), with 4/7/1984 being the date that the drainage system became operational.

##### *Top boundary condition in the SWAP model*

It was mentioned earlier that cropping at Sampla was initiated after the first monsoon period that followed after the installation of the drainage system. Unfortunately, cropping patterns and irrigation water management were not monitored continuously. Project reports (e.g. Rao et al., 1986) indicate that several different crops were grown at the same time, even within a particular drain spacing area. It was mentioned earlier that the modelling approach can only deal with one crop at a time. In the SWAP model the heterogeneous land use at Sampla was therefore simplified to one representative crop rotation consisting of pearl millet in summer and wheat in winter. In the first 5 months of the simulation period no crop was defined to represent the initial barren period. The simplification of land use implies that the model results do not represent the actual field conditions. A close match between measured and simulated groundwater tables depths and drain fluxes can therefore only be expected for the initial barren period. Measured and simulated long term trends in soil and effluent salinity, however, should be approximately the same.

Rainfall at Sampla was measured at a nearby meteorological station. Reference crop evapotranspiration was taken from the Climwat database which uses the Penman-Monteith method (Eq. 2.1; Smith, 1993). For the Indus plain, however, it has been found that the Penman-Monteith method overestimates the potential evapotranspiration, especially at high evaporation rates (Kumar and Bastiaanssen, 1993; Sarwar, 2000). Although the Penman-Monteith method is preferred from a physical viewpoint, insufficient watering of the surroundings of

meteorological stations in dry areas, often results in non-representative relative humidity and temperature measurements, limiting the applicability of the Penman-Monteith method.

Instead, the Priestley-Taylor method was used in this study to calculate reference crop evapotranspiration (Priestley and Taylor, 1972). This method, which relies more on radiation than on turbulent momentum, heat and vapour transport, is less sensitive to non-representative relative humidity and temperature measurements (only the slope of the saturated vapour pressure curve,  $\Delta_v$  is affected) (Bastiaanssen et al., 1996). Use of the Priestley-Taylor method implies that crop factors,  $k_c$  are needed to convert the reference crop evapotranspiration,  $ET_{ref}$  to a crop specific potential evapotranspiration,  $ET_p$  (e.g. Allen et al., 1998).

Reference crop evapotranspiration,  $ET_{ref}$  [ $L\ T^{-1}$ ] according to the Priestley-Taylor method is calculated as (Priestley and Taylor, 1972):

$$\lambda_w \rho_w ET_{ref} = 1.26(R_n - G) \frac{\Delta_v}{\Delta_v + \gamma_a} \quad (5.9)$$

where  $\lambda_w$  is the latent heat of vaporization [ $L^2\ T^{-2}$ ],  $\rho_w$  the density of water [ $M\ L^{-3}$ ],  $R_n$  the net radiation [ $M\ T^{-3}$ ],  $G$  the soil heat flux [ $M\ T^{-3}$ ],  $\Delta_v$  the slope of the saturated vapour pressure curve [ $M\ L^{-1}\ T^{-2}\ \Theta^{-1}$ ] and  $\gamma_a$  the psychrometric constant [ $M\ L^{-1}\ T^{-2}\ \Theta^{-1}$ ].

It was assumed that both the pearl millet crop and the wheat crop receive a pre-irrigation of 100 mm. Irrigation scheduling during the growing periods of the crops was based on the criterion that relative transpiration,  $T_a/T_p \geq 0.95$ . If the transpiration ratio fell below 0.95, an irrigation application of fixed depth (75 mm) was simulated by SWAP. This type of deficit irrigation is common in areas where canal water availability is limited (only ~375 mm  $a^{-1}$  at Sampla). Note that the growing period of a particular crop starts with the emergence of the crop (not sowing). The growing period ends with harvest.

A summary of the SWAP input data with regard to crop data and irrigation data is given in Table 5.1. Two crop specific parameters, notably crop factor,  $k_c$  and Leaf Area Index,  $LAI$ , are given as a function of the crop development stage. The  $k_c$  values were derived from Allen et al. (1998). Basal crop factors were used that relate only to crop transpiration and not to soil evaporation (soil evaporation is treated separately by SWAP; Van Dam et al., 1997). In Table 5.1, the three  $k_c$  values for each crop relate to the initial crop development stage, the mid-season stage and the final value at the late season stage, respectively. Similarly, the four  $LAI$  values for each crop relate to the start of the initial stage (emergence), the end of the initial stage, the mid-season stage and the end of the late season stage, respectively. Threshold  $EC_e$  and Slope were taken from Maas (1990), who provides salt tolerance data for a large variety of crops.

**Table 5.1** Crop and irrigation data for the SWAP model for the Sampla experimental pipe drainage site.

<i>General</i>		
Simulation period	4/7/1984-31/5/1999	
Assumed crop rotation	pearl millet-wheat (first 5 months in 1 <sup>st</sup> year barren)	
Boesten parameter, $\beta_p$ (cm <sup>1/2</sup> )	0.54	
Irrigation water quantity (mm)	100 (pre-irrigation); 75 (growing period)	
EC of irrigation water (dS m <sup>-1</sup> )	0.5	
<i>Crop specific</i>	pearl millet	wheat
Pre-irrigation date	1/6	20/12
Growing period	18/6-30/9	5/1-9/5
Crop factor, $k_c$	0.15-0.95-0.2	0.15-1.1-0.3
Leaf Area Index, LAI (-)	0.05-0.5-6.0-3.0	0.05-0.5-5.0-2.5
Max. rooting depth (cm)	120	110
$h_1, h_2, h_{3h},$	-0.1, -1.0, -300,	-0.1, -1.0, -500,
$h_{3l}, h_4$ (cm)	-2500, -10000	-900, -16000
Threshold $EC_e$ (dS m <sup>-1</sup> )	6.8	6.0
Slope % per dS m <sup>-1</sup>	16.0	7.1

#### **Hydraulic characteristics of the drained area**

The soil hydraulic properties for the Sampla experimental pipe drainage site as determined through the procedure mentioned in Section 5.3, are given in Table 5.2. Parameters describing the drainage system are also given. The soil parameters were determined by assuming that the soil-aquifer hydraulic properties for all three drain spacing areas are the same. The horizontal saturated hydraulic conductivities,  $K_{xx}$  of 1.0 and 3.0 m d<sup>-1</sup> for the topsoil and subsoil, respectively compare reasonably well with field measurements of Kamra and Rao (1985) using the auger-hole method and the piezometer method. Measured  $K_{xx}$  for the topsoil ranged between 0.1 and 2.4 m d<sup>-1</sup> (50 % log-normal probability value 0.9 m d<sup>-1</sup>), while  $K_{xx}$  for the subsoil ranged from 1.3 to 22.5 m d<sup>-1</sup> (50 % log-normal probability value 7.4 m d<sup>-1</sup>). A comparison between the measured and simulated  $q_d(H)$  relationship for the 50 m spacing area at Sampla is shown in Fig. 5.2.

Figure 5.2 shows that the comparison between the measured and simulated  $q_d(H)$  relationship is satisfactory. As could be expected, measured values show more scatter than simulated values, for SWMS\_2D simulates an irrigation event under idealized circumstances (no spatial variability; only redistribution). The simulated values show a slight upward curvature, indicating that in the SWMS\_2D model, flow to the drains from above drain level is not entirely zero. The simulated  $q_d(H)$  relationship for the 50 m spacing area translates into a drainage resistance,  $\gamma = 108$  d. Measured and simulated  $\gamma$  values for all drain spacings at Sampla are given in Table 5.3. Because the measured  $\gamma$  value of 116 d for the 75 m spacing area is lower than the measured  $\gamma$  value of 133 d for the 50 m spacing area, it is impossible to obtain a good match between all measured and simulated values. Assuming, of course, that the soil-aquifer hydraulic properties for all three drain spacing areas are the same.

**Table 5.2** Parameters describing the drainage system and the soil hydraulic properties for the Sampla experimental pipe drainage site.

<i>Drainage system</i>		
Drain depth, $d$ (m)	1.75	
Drain spacing, $L$ (m)	25, 50, 75	
Effective drain diameter, $d_{\text{eff}}$ (m)	0.1	
<i>Soil</i>	topsoil	subsoil
Depth of layer (m)	0-1.8	1.8-3.0
Soil texture	sandy loam	sand/loamy sand
Res. water content, $\theta_r$	0.02	0.01
Sat. water content, $\theta_s$	0.36	0.36
Shape parameter, $\alpha_h$ ( $\text{cm}^{-1}$ )	0.017	0.021
Shape parameter, $n$	1.45	2.0
Shape parameter, $\lambda$	0.5	0.5
Hor. sat. hydr. cond., $K_{xx}$ ( $\text{m d}^{-1}$ )	1.0	3.0
Vert. sat. hydr. cond., $K_{zz}$ ( $\text{m d}^{-1}$ )	0.25	0.75

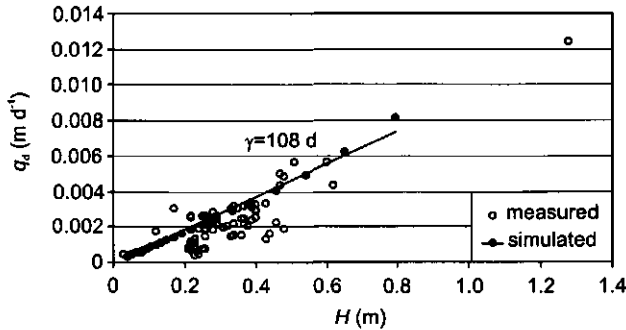


**Figure 5.2** Measured and SWMS\_2D simulated head-discharge,  $q_d(H)$  relationship for the 50 m spacing area of the Sampla experimental pipe drainage site.

**Table 5.3** Measured and simulated drainage resistance,  $\gamma(d)$  for the Sampla experimental pipe drainage site.

	$L=25$ m	$L=50$ m	$L=75$ m
Measured	38	133	116
Simulated	34	108	213

Simulated streamlines towards the pipe drain for the 50 m spacing area are shown in Fig. 5.3. The streamlines are calculated by means of Eqs. (3.19) - (3.22). Ten stream-tubes are drawn, each conveying 10 % of the total discharge. Figure 5.3 shows that flow towards the pipe drain is mainly horizontal. Radial flow is restricted to  $x$  over  $\frac{1}{2}L$  ratios  $< 0.1$ , where  $L$  is the drain spacing. Streamline patterns for the other drain spacings at Sampla (not shown) are comparable. Note that the calculated streamline pattern is sensitive to the depth of the restrictive layer. If this depth becomes larger than the present value of 3.0 m below soil surface, the difference between the horizontal flow region and the radial flow region will become less pronounced.

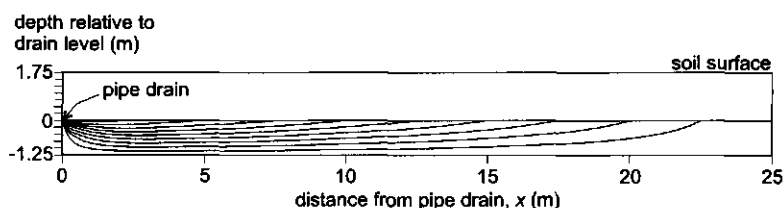


**Figure 5.3** Calculated streamline pattern below drain level for the 50 m spacing area of the Sampla experimental pipe drainage site. Each stream tube represents 10 % of the total discharge. Results of the analytical expressions for the stream function of Töksoz and Kirkham (1971).

### Salinity parameters

The parameters used in the solute transport calculations are summarized in Table 5.4. The transport of salts through the zone above drain level is sensitive to the value of dispersion length,  $\alpha_L$  in SWAP. The value of  $\alpha_L$  typically ranges from about 0.5 cm or less for laboratory scale experiments involving disturbed soils, to about 10 cm or more for field scale experiments (Nielsen et al., 1986). Kamra et al., (1991b), using a steady-state approach, adopted  $\alpha_L=80$  cm for the Sampla site. For transient simulations this value is probably too high. Considering the above information, an  $\alpha_L$  value of 10 cm was selected for the Sampla site. Solute transport in the unsaturated zone is generally not very sensitive to the value of the diffusion coefficient,  $D_w$  (Beven et al., 1993).

**Table 5.4** Parameters for the calculation of solute transport for the Sampla experimental pipe drainage site.

Initial soil $EC_e$ (dS m <sup>-1</sup> )	50.7 (soil surface) - 15.5 (175 cm depth)
Initial $EC$ groundwater (dS m <sup>-1</sup> )	27.0
Dispersion length, $\alpha_L$ (cm)	10.0
Diffusion coef. in water, $D_w$ (cm <sup>2</sup> d <sup>-1</sup> )	0.72
Avg. Saturation Percentage, $SP$ (%)	39.5
Avg. dry bulk dens., $\rho_b$ (g cm <sup>-3</sup> )	1.54
Eff. por. below drain level, $n_e$ (-)	0.33

The Electrical Conductivity,  $EC$  at volumetric water content,  $\theta$  is calculated by:

$$EC_{\theta} = \frac{\rho_b}{\rho_w} \frac{SP}{100} \frac{EC_e}{\theta} \quad (5.10)$$

where  $\rho_b$  is the average dry bulk density [ $M L^{-3}$ ],  $\rho_w$  the density of water [ $M L^{-3}$ ] and  $SP$  the Saturation Percentage (g of water needed to obtain a saturated paste from 100 g of dry soil, expressed as a percentage).

#### ***Depth of the groundwater table and cumulative drainage***

The 5-month barren period which followed directly after the installation of the drainage system is used to assess the reliability of the simulated depth of the groundwater table,  $d_{gw}$  and drain flux,  $q_d$ . As explained earlier, the subsequent cropping seasons cannot be used to check the SWAP model because the simulations are based on an assumed crop rotation and an assumed irrigation schedule. Measured and simulated  $d_{gw}$  and  $q_d$  for the 50 m spacing area at Sampla are shown in Figs. 5.4 and 5.5, respectively. Both  $d_{gw}$  and  $q_d$  are simulated reasonably well. Between 23-Aug-84 and 4-Sep-84, the Sampla site received 354.1 mm of rainfall which raised the groundwater table to the surface. The resulting shallow groundwater tables seem to be exaggerated by the simulations. Possibly more surface runoff occurred in the field than was simulated by SWAP (a maximum ponding layer of 10 cm was set in the model to account for the presence of field bunds).

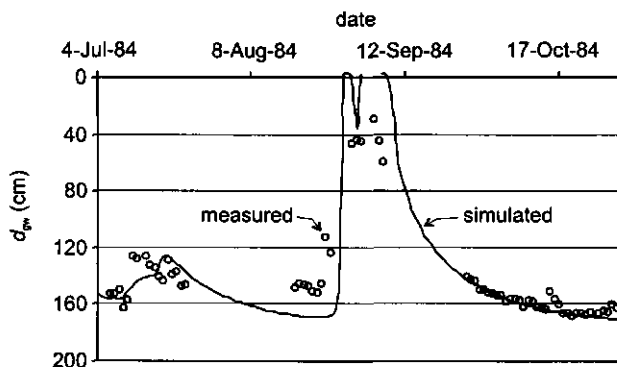


**Figure 5.4** Measured and SWAP simulated depth of the groundwater table,  $d_{gw}$  for the initial barren period at the Sampla experimental pipe drainage site ( $L=50$  m).

Simulated  $d_{gw}$  and cumulative drainage,  $D$  for the complete simulation period for the 50 m spacing area at Sampla are shown in Fig. 5.6. Results for the other drain spacings are comparable. The semi-arid climate, combined with large but infrequent irrigation applications, result in a strongly fluctuating groundwater table. Note that the fluctuations in Fig. 5.6 may be exaggerated due to the simplification of land use (the complete area is assumed to be irrigated at once, while in reality, field plots are irrigated one by one). Figure 5.6 shows that the groundwater table occasionally reaches the soil surface after which it recedes quickly under the influence of the drainage system. Frequently, the groundwater table falls below drain level (at 1.75 m below soil

surface). This also happens in reality (Fig. 4.4). Groundwater table depths,  $d_{gw}$ , of 200 cm and more are, however, not generally observed at Sampla (e.g. Rao et al., 1986; Rao, 1996). The failure of the SWAP model to simulate these deeper groundwater tables correctly is probably due to the inability of the modelling approach to account for regional inflow. Water balance studies at Sampla indicate that the contribution of seepage from the surrounding area ranges from 20 % in the monsoon season to 60 % in the winter season (Rao et al., 1996).

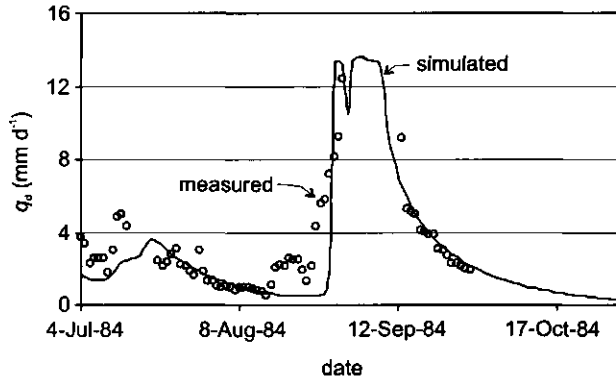


**Figure 5.5** Measured and SWAP simulated drain flux,  $q_d$  for the initial barren period at the Sampla experimental pipe drainage site ( $L=50$  m).

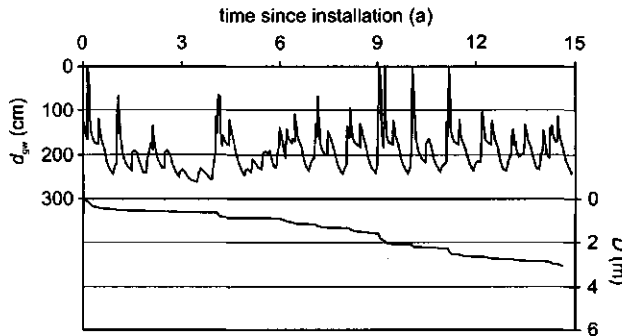


**Figure 5.6** SWAP simulated depth of the groundwater table,  $d_{gw}$  and cumulative drainage,  $D$  for the 50 m spacing area of the Sampla experimental pipe drainage site.

### Soil and effluent salinity

Simulated soil and effluent salinity for the three drain spacings at Sampla are shown in Fig. 5.7. To complete the picture, the salinity of the downward soil water flux at drain level,  $EC_{dp}$  is also given. Results for the three drain spacings are practically the same. Soil salinity,  $EC_e$  (0-1 m depth) drops quickly in response to the installation of the drainage system from  $\sim 24$  to  $\sim 4$  dS  $m^{-1}$

in one year. The strong decrease is the result of the heavy monsoon rainfall in 1984. In subsequent years the  $EC_e$  falls below  $1 \text{ dS m}^{-1}$  for most of the time. Effluent salinity,  $EC_{dw}$ , shows a different behaviour. During the first years after installation of the drainage system,  $EC_{dw}$  shows elevated levels. Only after 4 years  $EC_{dw}$  starts to decrease. The sudden decrease in  $EC_{dw}$  in the 5<sup>th</sup> year is due to heavy monsoon rainfall in 1988. Between 1/7/1988 and 31/8/1988, 546 mm of rainfall was recorded at Sampla. Reclamation of the soil-aquifer system is more or less completed after 10 years when  $EC_{dw}$  has dropped below  $2 \text{ dS m}^{-1}$ .

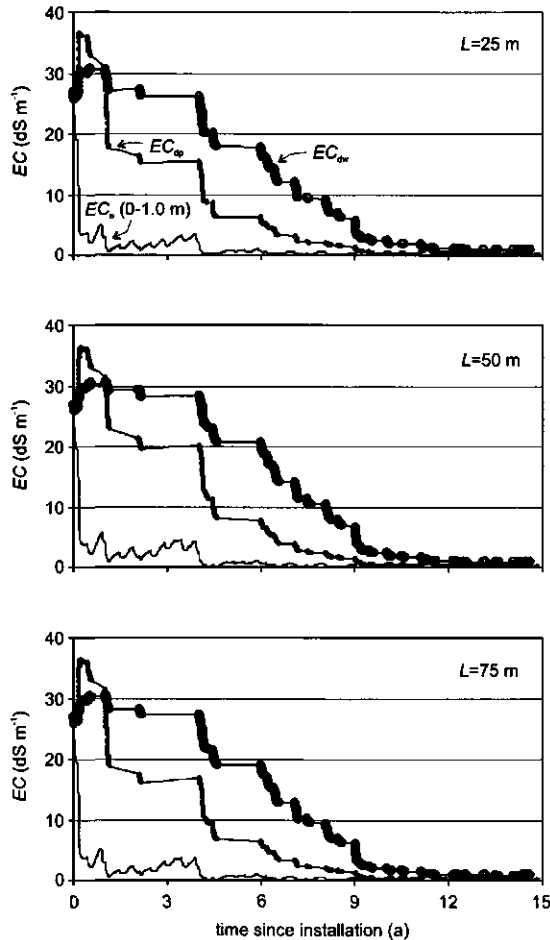


**Figure 5.7** SWAP simulated soil salinity,  $EC_e$ , salinity of the downward flux at drain level,  $EC_{dp}$  and effluent salinity,  $EC_{dw}$  for all three drain spacings at the Sampla experimental pipe drainage site.



Comparison of the simulated  $EC_e$  and  $EC_{dw}$  values for the 50 m spacing area with measured values (Fig. 4.6), shows only a fair agreement. The scatter in the measured  $EC_{dw}$  values is not described by the model because of the neglect of preferential flow phenomena (e.g. mobile-immobile fractions in the unsaturated zone, direct flow to the pipe through the drain trench). Also the measured long term  $EC_{dw}$  value of  $\sim 10 \text{ dS m}^{-1}$  after 9 years of drainage is not reproduced. The latter is attributed to the neglect of regional inflow into the drained area. As explained in Chapter 1, treating drainage as a local flow problem will overestimate the reclamation rate of the soil-aquifer system as, in reality, regional inflow will present a continuous source of salts. *The distinctly different behaviour of  $EC_e$  and  $EC_{dw}$  in response to drainage, however, is described correctly, indicating that the basic processes determining soil and effluent salinity are captured by the modelling approach.*

Drain spacing at Sampla has no effect on the development of  $EC_{dw}$  with time. This can be understood by inspection of Eqs. (5.7) and (5.8). The contribution of a specific stream-tube,  $i$  to  $EC_{dw}$  depends on the proportion of cumulative drainage,  $D$  against  $(n_e A_i)/(dx)_i$ . The value of  $n_e$  is the same for all drain spacings at Sampla, while the value of  $D$  differs only slightly (discussed later). Any difference in  $EC_{dw}$  for the three drain spacings should therefore be attributed to the ratio  $A_i/(dx)_i$ . With a shallow depth of the impermeable layer, and with a practically homogeneous composition of the zone below drain level (Table 5.2), flow to the pipe drains in mainly horizontal (Fig. 5.3). Under these conditions, the relationship between  $A_i$  and  $(dx)_i$  for a particular stream tube  $i$  is approximately linear for different drain spacings. The ratio  $A_i/(dx)_i$ , and hence  $EC_{dw}$ , is more likely to change with drain spacing if the impermeable layer is found at greater depths.

### Water and salt balance

The water balance equation for the soil-pipe-aquifer system reads:

$$\Delta W = P + I - P_i - R_s - T - E - D \quad (5.11)$$

where  $\Delta W$  is the change in water storage [L] over the simulation period,  $P$  the cumulative precipitation [L],  $I$  the cumulative irrigation water [L],  $P_i$  the cumulative intercepted precipitation [L],  $R_s$  the cumulative surface runoff [L],  $T$  the cumulative transpiration [L],  $E$  the cumulative evaporation [L] and  $D$  the cumulative drainage [L].

The water balance for the 5445-days simulation period for the Sampla site is given in Table 5.5. Clearly, the water balance at Sampla is insensitive to drain spacing. Apparently, the differences in drainage resistance,  $\gamma$  of between 38 days and 133 days (Table 5.3) are too small to have a significant impact on the water balance. This concurs with Rao (1996), who states that, for the Sampla site, a drain spacing of 75 m suffices to keep the groundwater table well under control. The simulated irrigation water applications for the three drain spacings of between 359 and 364  $\text{mm a}^{-1}$  are only slightly lower than the actual canal water availability at Sampla ( $375 \text{ mm a}^{-1}$ ). It seems that the selected pearl-millet - wheat crop rotation, combined with the  $T_a/T_p$  ratio of 0.95, and the irrigation water quantity of 75 mm (Table 5.1), represent the farmer practices at Sampla fairly well.

**Table 5.5** Simulated water balance terms over 5445 days for the Sampla experimental pipe drainage site (all values in mm a<sup>-1</sup>).

	<i>L</i> =25 m	<i>L</i> =50 m	<i>L</i> =75 m
Rainfall, <i>P</i>	581	581	581
Irrigation, <i>I</i>	364	359	364
Interception, <i>P<sub>i</sub></i>	23	23	23
Surface runoff, <i>R<sub>s</sub></i>	0	3	1
Crop transpiration, <i>T</i>	563	556	557
Soil evaporation, <i>E</i>	166	167	168
Cumulative drainage, <i>D</i>	207	205	210
Change in water storage, $\Delta W$	-14	-13	-14

The salt balance equation for the soil-pipe-aquifer system can be written as:

$$\Delta \int_{A_{sa}} \theta c dA_{sa} = \frac{1}{2} L \left[ \int_0^t I_i c_{ir} dt - \int_0^t R_{sr} c_s dt - \int_0^t q_d c_{dw} dt \right] \quad (5.12)$$

where  $A_{sa}$  is the cross-sectional area [L<sup>2</sup>] of the soil-aquifer domain,  $I_i$  the irrigation rate [L T<sup>-1</sup>],  $c_{ir}$  the solute concentration [M L<sup>-3</sup>] of the irrigation water,  $R_{sr}$  the surface runoff rate [L T<sup>-1</sup>] and  $c_s$  the solute concentration [M L<sup>-3</sup>] of the surface runoff.

The simulated salt mass balance for the three drain spacings at Sampla is given in Table 5.6. Note that the cross-sectional area of the soil-aquifer domain,  $A_{sa}$  is divided into the zone above drain level and the zone below drain level. In the SWAP model, no distinction is made between surface runoff due to rainfall or surface runoff due to excess irrigation. As a result, the solute concentration of the surface runoff,  $c_s$  is assumed to be zero. Table 5.6 shows that 17.0 to 17.1 t ha<sup>-1</sup> a<sup>-1</sup> of salts are removed from the area. A considerable amount of salt is leached from the zone above drain level, which was highly saline at the start of drainage. The influence of drain spacing on the salt balance is only minor. *At Sampla, variations in drain spacing of between 25 and 75 m do not have a significant effect on the salt loads that must be disposed.*

**Table 5.6** Simulated salt mass balance terms over 5445 days for the Sampla experimental pipe drainage site (all values in t ha<sup>-1</sup> a<sup>-1</sup>).

	<i>L</i> =25 m	<i>L</i> =50 m	<i>L</i> =75 m
Salts in irrigation water	1.3	1.3	1.3
Salts in drainage water	17.1	17.0	17.0
Change in salt storage above drain level	-9.9	-9.9	-9.9
Change in salt storage below drain level	-5.9	-5.9	-5.9

## 5.5 Case 2: Unit S-I-B-9 of the Fourth Drainage project

Calculations for the S-I-B-9 pipe drainage unit of the Fourth Drainage Project area were focussed on the central lateral drain with a drained area of ~42 ha (Fig. 4.11). The simulation period for the S-I-B-9 unit covered 8 years (1/6/1989-31/5/1997), with 1/6/1989 being the data that the drainage system became operational.

### *Top boundary condition in the SWAP model*

The S-I-B-9 unit includes over 500 agricultural fields with an average size of ~0.2 ha. Crops and irrigation applications vary considerably between fields. Because only one crop can be simulated at a time in the SWAP model, the land use was again simplified. Based on the dominant land use in the area, a cotton-wheat rotation was selected, where cotton is grown in summer and wheat in winter. Rainfall was measured at the drainage unit. Reference crop evapotranspiration was derived from the Climwat database (Smith, 1993) using the Priestley-Taylor method (Eq. 5.9). It was assumed that the cotton crop receives two pre-irrigations of 100 mm each and that the wheat crop receives one pre-irrigation of 100 mm (e.g. Smets, 1996). Irrigation scheduling during the growing periods of the crops was based again on the criterion that relative transpiration,  $T_d/T_p \geq 0.95$  (depth of application 75 mm). A summary of the crop and irrigation input data is given in Table 5.7.

**Table 5.7** Crop and irrigation data for the SWAP model for the central lateral drain of the S-I-B-9 pipe drainage unit of the Fourth Drainage Project.

<i>General</i>		
Simulation period	1/6/1989-31/5/1997	
Assumed crop rotation	cotton-wheat	
Boesten parameter, $\beta_p$ (cm <sup>2</sup> )	0.54	
Irrigation water quantity (mm)	100 (pre-irrigation); 75 (growing period)	
EC of irrigation water (dS m <sup>-1</sup> )	0.2	
<i>Crop specific</i>	Cotton	Wheat
Pre-irrigation date	18/5+1/6	20/12
Growing period	18/6-19/12	5/1-9/5
Crop factors, $k_c$	0.15-1.15-0.45	0.15-1.1-0.3
Leaf area index, LAI (-)	0.05-0.5-3.5-1.75	0.05-0.5-5.0-2.5
Max. rooting depth (cm)	140	110
$h_1, h_2, h_{3h}$	-0.1, -1.0, -400,	-0.1, -1.0, -500,
$h_{3l}, h_4$ (cm)	-800, -16000	-900, -16000
Threshold $EC_e$ (dS m <sup>-1</sup> )	7.7	6.0
Slope % per dS m <sup>-1</sup>	5.2	7.1

### *Hydraulic characteristics of the drained area*

In the Fourth Drainage Project, no impermeable layer was identified in the drainage design process (USBR, 1989). Estimates of the depth of the aquifer range from 100 to 300 m (Chapter 4). The vertical extent of the flow domain for pipe drains in the FDP is probably smaller. In a

homogeneous isotropic aquifer the maximum depth that contributes to the drain discharge can be estimated by assuming half-circular streamlines (De Vries, 1975; Van Dam et al., 1997):

$$b = \frac{L}{4} \quad (5.13)$$

The deepest streamline which arrives in the drain, originates from a point at mid-spacing ( $L/2$ ). In the concept of Töksoz and Kirkham (1971), the zone below drain level consists of two (individually homogeneous) sub-zones with thicknesses  $a$  and  $(b-a)$  (Fig. 3.2). Each sub-zone may be characterized by a specific anisotropy factor. High anisotropy factors will result in relatively shallow streamlines to the drains. With the boundary between the two sub-zones parallel to the  $x$ -axis and with the coordinate axis oriented along the principal directions of the hydraulic conductivity, the maximum depth that contributes to the drain discharge becomes (e.g. Maasland, 1957):

$$b' = a \sqrt{\frac{K_{zz1}}{K_{xx1}}} + (b-a) \sqrt{\frac{K_{zz2}}{K_{xx2}}} \quad (5.14)$$

where  $b'$  [L] is the depth of the hypothetical impermeable layer below drain level for the anisotropic two-layered aquifer. Subscripts 1 and 2 denote the first and second layer, respectively. For the central lateral drain of the S-I-B-9 unit, the above procedure results in  $b' = 87.4$  m.

**Table 5.8** Parameters describing the central lateral drain and the soil hydraulic properties for the S-I-B-9 pipe drainage unit of the Fourth Drainage Project.

<i>Drainage system</i>		
Drain depth, $d$ (m)	2.4	
Drain spacing, $L$ (m)	495	
Effective drain diameter, $d_{\text{eff}}$ (m)	0.3	
<i>Soil</i>	Topsoil	Subsoil
Depth of layer (m)	0-2.8	2.8-89.8
Soil texture	silt loam	loamy sand
Res. water content, $\theta_r$	0.02	0.02
Sat. water content, $\theta_s$	0.375	0.34
Shape parameter, $\alpha_h$ (cm <sup>-1</sup> )	0.015	0.014
Shape parameter, $n$	1.23	1.8
Shape parameter, $\lambda$	0.5	0.5
Hor. sat. hydr. cond., $K_{xx}$ (m d <sup>-1</sup> )	0.7	15.0
Vert. sat. hydr. cond., $K_{zz}$ (m d <sup>-1</sup> )	0.175	7.5

The soil hydraulic properties for the S-I-B-9 unit are given in Table 5.8, together with the parameters describing the central lateral drain. The soil water retention curve for the topsoil (0-2.8 m) is compared with field measurements from four field plots at S-I-B-9 in Fig. 5.8. The field

measurements were obtained from tensiometers and neutron probe readings at depths ranging from 15 to 200 cm below soil surface. Of the four field plots, plot 64/01 has a sandy loam to loam texture while the other plots have a loam to silt loam texture. Figure 5.8 shows that the adopted curve for the topsoil fits the data for plots 39/13 and 64/19 reasonably well. The soil water retention of plots 62/07 and 64/01, however, are somewhat overestimated.

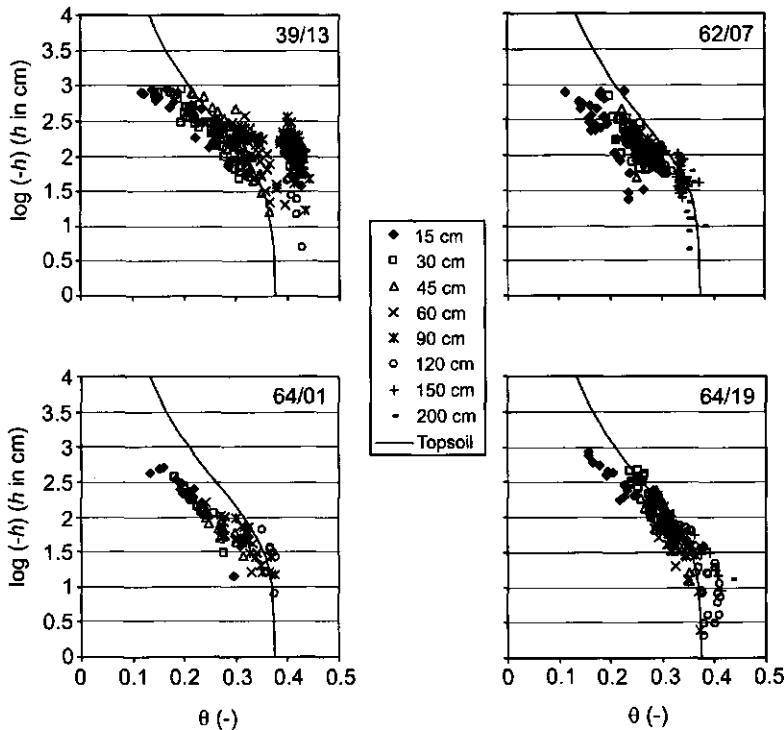


**Figure 5.8** Comparison between the calibrated water retention curve for the topsoil at the S-I-B-9 pipe drainage unit of the Fourth Drainage Project and measured water retention data from four field plots in the drainage unit.

The comparison between the measured and simulated  $q_d(H)$  relationship is satisfactory (Fig. 5.9). Unfortunately, the maximum measured  $H$  value is only 0.36 m. A measured  $q_d(H)$  relationship containing higher values for  $H$  would have allowed a more thorough verification of the soil hydraulic properties. The simulated  $q_d(H)$  relationship translates into a drainage resistance,  $\gamma = 588$  d (measured  $\gamma = 625$  d, Chapter 4). It was mentioned before in Chapter 4 that the relatively high value of  $\gamma$  for the S-I-B-9 unit is mainly due to the relatively large drain spacing,  $L$  of 495 m.

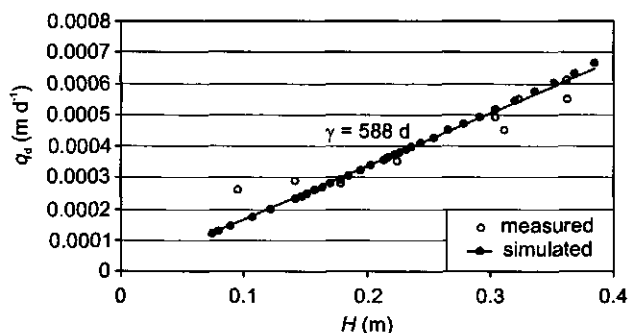


**Figure 5.9** Measured and SWMS\_2D simulated head-discharge,  $q_d(H)$  relationship for the central lateral drain of the S-I-B-9 pipe drainage unit of the Fourth Drainage Project.

Simulated streamlines towards the pipe drain are shown in Fig. 5.10. Again, ten streamlines are drawn, each conveying 10 % of the total discharge. The simulated streamline pattern for S-I-B-9 is less pronounced than the streamline pattern for Sampla ( $L=50$  m) (Fig. 5.3). At S-I-B-9, no clear distinction can be made between horizontal and radial flow regions below drain level. The difference is attributed to the greater depth of the hypothetical impermeable layer at S-I-B-9 as compared to the depth of the impermeable layer at Sampla (87.4 m against 1.25 m below drain level).

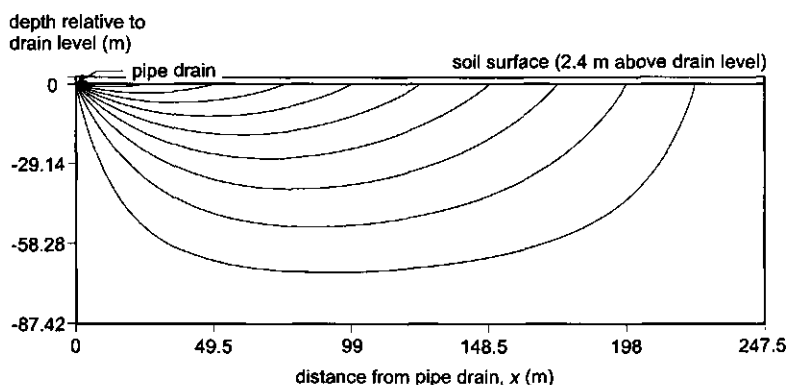


**Figure 5.10** Calculated streamline pattern below drain level for the central lateral drain of the S-I-B-9 pipe drainage unit of the Fourth Drainage Project. Each stream tube represents 10 % of the total discharge. Results of the analytical expressions for the stream function of Töksoz and Kirkham (1971).

It should be noted that the cross-sectional area of the deepest stream-tubes may become unrealistically large, especially if  $b$  (or  $b'$ ) is over-estimated. This is due to the modelling

approach in which the impermeable layer is fixed and in which the deepest streamline is always located at the boundaries of the flow domain (Fig. 3.2). Closely spaced streamlines near drain level automatically lead to wider spaced streamlines at greater depth. Or in other words, small values of  $n_e A/dx$  near drain level result in large values of  $n_e A/dx$  near the (hypothetical) impermeable layer. In the field, this phenomenon will not occur. Instead, an effective depth of the impermeable layer will develop which is shallower than  $b$ .

#### Salinity parameters

The parameters used in the solute transport calculations are summarized in Table 5.9. The initial soil  $EC_e$  of  $2 \text{ dS m}^{-1}$  is an estimate. At S-I-B-9, soil salinity is strongly related to land use. Fields which are cropped continuously and irrigated frequently generally have  $EC_e$  values below  $3 \text{ dS m}^{-1}$ . Soil salinity in abandoned fields, on the other hand, may have  $EC_e$  values above  $30 \text{ dS m}^{-1}$  (Hendrickx et al., 1992). Previous applications of the SWAP model on experimental fields at S-I-B-9 resulted in  $\alpha_L$  values of between 3 and 20 cm (Kelleners, 1993; Kelleners, 1996; Sarwar, 2000). In this study, an  $\alpha_L$  value of 10.0 cm was selected for S-I-B-9 (same as for the Sampla site).

**Table 5.9** Parameters for the calculation of solute transport for the central lateral drain of the S-I-B-9 pipe drainage unit of the Fourth Drainage Project.

Initial soil $EC_e$ (0-2.4 m) ( $\text{dS m}^{-1}$ )	2.0
Initial $EC$ groundwater ( $\text{dS m}^{-1}$ )	3.3
Dispersion length, $\alpha_L$ (cm)	10.0
Diffusion coef. in water, $D_w$ ( $\text{cm}^2 \text{ d}^{-1}$ )	0.72
Avg. Saturation Percentage, $SP$ (%)	40
Avg. dry bulk dens., $\rho_b$ ( $\text{g cm}^{-3}$ )	1.62
Eff por. below drain level, $n_e$ (-)	0.30

#### Depth of the groundwater table and cumulative drainage

Simulated depth of the groundwater table,  $d_{gw}$  and cumulative drainage,  $D$  for the 8-year simulation period for the S-I-B-9 unit are shown in Fig. 5.11. A direct comparison with measured values is not possible because the land use at S-I-B-9 has been simplified to one cotton-wheat rotation. Overall, the simulated fluctuation of  $d_{gw}$  seems to concur with the measured fluctuation (Fig. 4.12). Both the measured and simulated  $d_{gw}$  values fluctuate mainly between 100 and 300 cm depth. Again it is stressed that the simulated fluctuations may be somewhat overestimated because it was assumed that the complete area is irrigated at once.

Drain discharge was measured on a daily basis at S-I-B-9 between 19/12/89 and 30/12/92 (Fig. 4.12). Measurements were taken at the collector. Measured cumulative drainage,  $D$  during this period was 371 mm. For the same period (0.6-3.6 years after installation), the simulation yields  $D=254$  mm. These  $D$  values may not be compared directly because the measurements relate to the collector outlet while the simulation relates to the central lateral drain outlet. The collector at S-I-B-9 is perforated and therefore contributes to drainage. Considering the above, finding a simulated  $D$  which is smaller than the measured  $D$ , is a logical result.

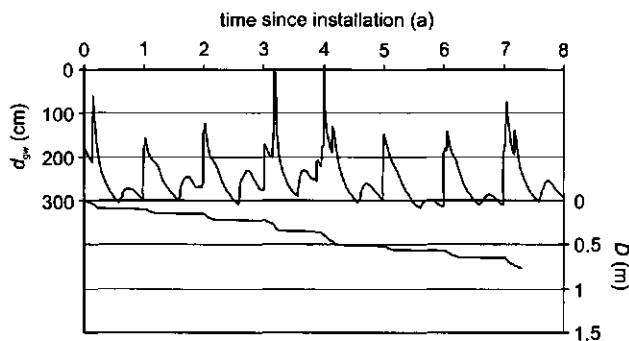


**Figure 5.11** SWAP simulated depth of the groundwater table,  $d_{gw}$  and cumulative drainage,  $D$  for the central lateral drain of the S-I-B-9 pipe drainage unit of the Fourth Drainage Project.

### **Soil and effluent salinity**

Simulated soil and effluent salinity for the S-I-B-9 unit are shown in Fig. 5.12. The salinity of the downward soil water flux at drain level,  $EC_{dp}$  is also given. Soil salinity,  $EC_e$  (0-1 m) drops gradually in response to drainage from  $2.0 \text{ dS m}^{-1}$  to  $< 0.5 \text{ dS m}^{-1}$  in about 3 years. In contrast, the effluent salinity,  $EC_{dw}$  hardly changes during the 8 year period (remains between  $3.3 \text{ dS m}^{-1}$  and  $3.4 \text{ dS m}^{-1}$ ). The simulated trend in  $EC_{dp}$  suggests that  $EC_{dw}$  will eventually start to decrease if the simulation period is prolonged, as will be shown later.

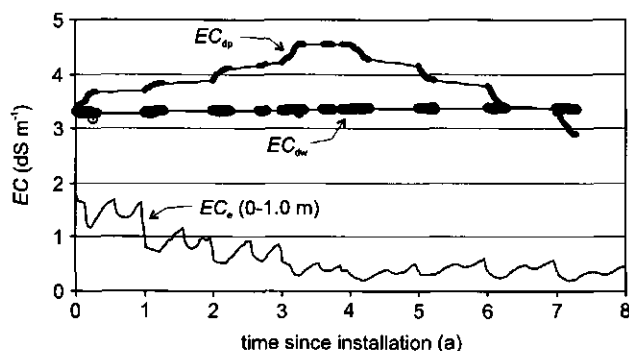


**Figure 5.12** SWAP simulated soil salinity,  $EC_e$ , salinity of the downward flux at drain level,  $EC_{dp}$  and effluent salinity,  $EC_{dw}$  for the central lateral drain of the S-I-B-9 pipe drainage unit of the Fourth Drainage Project.

Inspection of Fig. 4.14 shows that measured  $EC_{dw}$  values indicated a constant  $EC$  of  $\sim 3.0 \text{ dS m}^{-1}$  over the 8-year drainage period. It is difficult to assess the reliability of the simulated  $EC_{dw}$  values. The low average salinity levels at S-I-B-9, the deep aquifer and the large spatial variability in land use, make it impossible to distinguish clear solute breakthrough curves from



the field data. Furthermore, it should be noted that the measured  $EC_{dw}$  values relate to the sump water, while the simulated  $EC_{dw}$  values relate to the central lateral drain. *Both the measured and simulated  $EC_{dw}$  values agree, however, about the fact that no drastic changes can be expected in the salinity of the effluent at S-I-B-9.*

The marginal change in the  $EC_{dw}$  values for S-I-B-9 as compared to Sampla (Fig. 5.7), is due to a combination of factors. (1) Cumulative drainage is relatively low for S-I-B-9 ( $96 \text{ mm a}^{-1}$  against  $205\text{-}210 \text{ mm a}^{-1}$  for Sampla). (2) The thickness of the zone below drain level,  $b$  for Sampla is  $1.25 \text{ m}$ , while for S-I-B-9,  $b' = 87.4 \text{ m}$ . The higher  $b$  (or  $b'$ ) becomes, the more  $f(n_e A/dx)$  will shift towards higher values, implying that more cumulative drainage,  $D$  is needed to transport the solutes to the drains. (3) Drain depth,  $d$  is higher for S-I-B-9 than for Sampla ( $2.4$  against  $1.75 \text{ m}$ ), resulting in longer solute travel times above drain level for S-I-B-9. In addition, initial salinity both above and below drain level is considerably lower for S-I-B-9, which make any changes in effluent salinity more difficult to detect.

#### **Water and salt balance**

The simulated water balance for the central lateral drain of the S-I-B-9 unit is given in Table 5.10. The simulated irrigation water application of  $681 \text{ mm a}^{-1}$  is considerably higher than the actual canal water availability at S-I-B-9 which is  $\sim 450 \text{ mm a}^{-1}$ . Apparently, the selected cotton-wheat crop rotation requires more irrigation water than the actual heterogeneous land use at S-I-B-9. This agrees with actual cropping practices. It was mentioned earlier (Chapter 4) that 25 % of the S-I-B-9 area is abandoned. Furthermore, 25 % of the area is fallow in summer and 9 % of the area is fallow in winter. The abandoned fields are not irrigated and the fallow fields are only irrigated during part of the year. By concentrating their limited irrigation water supplies on the cropped fields, farmers secure at least some crop production.

The above implies that recharge from the agricultural fields at S-I-B-9 is highly localized. Cropped fields may show considerable recharge to the groundwater, especially if rice or sugarcane are grown, which are irrigated intensively. On the other hand, abandoned fields will only contribute to recharge during heavy monsoon rainfall. In the long term, abandoned fields are more likely to constitute a discharge surface than a recharge surface. As a result, the water balance in Table 5.10 may change considerably if a different crop rotation is chosen to represent the land use at S-I-B-9.

**Table 5.10** Simulated water balance terms over 2922 days for the central lateral drain of the S-I-B-9 pipe drainage unit of the Fourth Drainage Project (all values in  $\text{mm a}^{-1}$ ).

---

Rainfall, $P$	307
Irrigation, $I$	681
Interception, $P_i$	15
Surface runoff, $R_s$	0
Crop transpiration, $T$	676
Soil evaporation, $E$	202
Cumulative drainage, $D$	96
Change in water storage, $\Delta W$	0

---

The simulated salt balance is given in Table 5.11. Leaching occurs above drain level (change in storage is  $-1.6 \text{ t ha}^{-1} \text{ a}^{-1}$ ). Salts are however accumulated in the zone below drain level ( $0.3 \text{ t ha}^{-1} \text{ a}^{-1}$ ). At the end of the 2922-day simulation period, only 12.5 % of the *surface area* under the influence of the lateral drain has  $n_e A/dx < D$  (see Fig. 5.17 in Section 5.8). The reclamation rate for the complete soil-aquifer system is mainly related to heavy monsoon showers, as irrigation water is scarce. It can be doubted whether these showers occur frequently enough to complete the reclamation process before the economic life of the drainage system ( $\sim 25$  years) is over. For example: 11,740 mm of cumulative drainage,  $D$  is required so that 50 % of the surface area has  $n_e A/dx < D$ . If the present water balance is extrapolated, this would require  $\sim 122$  years of drainage.

**Table 5.11** Simulated salt mass balance terms over 2922 days for the central lateral drain of the S-I-B-9 pipe drainage unit of the Fourth Drainage Project (all values in  $\text{t ha}^{-1} \text{ a}^{-1}$ ).

Salts in irrigation water	1.0
Salts in drainage water	2.2
Change in salt storage above drain level	-1.6
Change in salt storage below drain level	0.3

## 5.6 New modelling approach for tube-wells

A schematic representation of the modelling approach for tube-wells is shown in Fig. 5.13. Again, the flow region is divided into two zones. The boundary between the two zones is formed by the horizontal plane that coincides with the water level in the well during pumping. This boundary, which will be termed *horizontal boundary plane*, is comparable to drain level for the pipe drainage case. Flow above the horizontal boundary plane is assumed vertical. Flow below the horizontal boundary plane is three-dimensional, assuming radial symmetry around the well-axis. Water flow and solute transport above the horizontal boundary plane is calculated with the SWAP model. The zone below the horizontal boundary plane is characterized by streamlines which are calculated numerically (Section 3.5). In the stream tubes piston flow is assumed. The solute concentration of the tube-well water is determined by convolution, using cumulative pumping,  $Q [\text{L}] (= \int q_d(t) dt)$  as the driving force. Tube-well water salinity  $c_{tw} [\text{ML}^{-3}]$  is calculated as:

$$c_{tw}(t) = \frac{\sum_{i=1}^N c_i(t)(dA)_i}{\sum_{i=1}^N (dA)_i} = \frac{\sum_{i=1}^N c_i(t)(dA)_i}{\pi r_e^2} \quad (5.15)$$

where:

$$c_i(t) = c_0 \quad \text{for} \quad \int_0^t q_d(t) dt < \frac{n_e V_i}{(dA)_i} \quad (5.16)$$

$$c_i(t) = c_{dp} \left( \int_0^t q_d(t) dt - \frac{n_e V_i}{(dA)_i} \right) \quad \text{for} \quad \int_0^t q_d(t) dt \geq \frac{n_e V_i}{(dA)_i} \quad (5.17)$$

where  $(dA)_i$  is the surface area  $[L^2]$  between the two bounding streamlines of tube  $i$ , measured at the horizontal boundary plane and  $V_i$  is the volume  $[L^3]$  of stream-tube  $i$ .

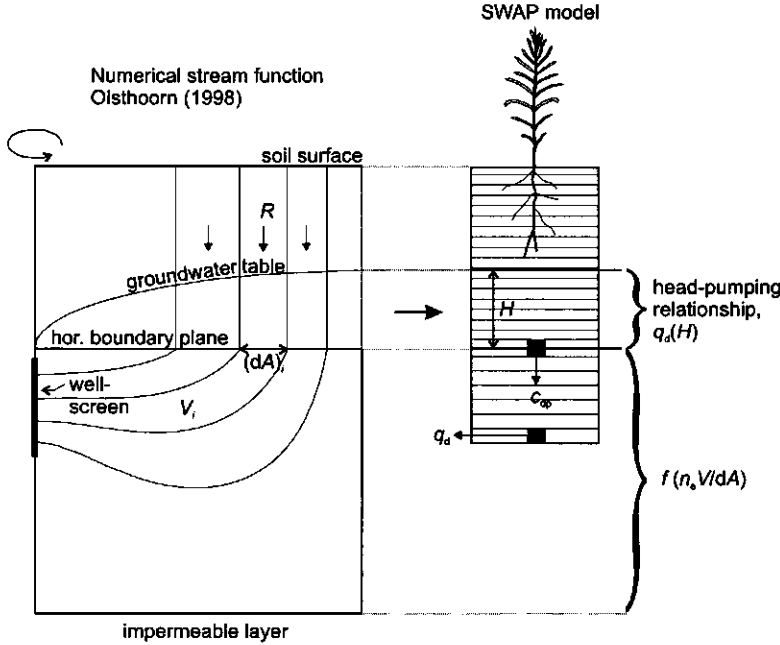


**Figure 5.13** Modelling approach for tube-wells. The right side of the figure represents the SWAP model, with  $f(n_e V/dA)$  representing the solute impulse response function of the zone below the horizontal boundary plane.

The approach assumes that: (1) initial solute concentration,  $c_0$  and effective porosity,  $n_e$  below the horizontal boundary plane are space-invariant, (2) the shape of the stream-tubes is time-invariant (valid under the assumptions made in Section 3.5), (3) solute transport in the zone below the horizontal boundary plane can be described by advection only, neglecting the effects of dispersion and diffusion, and (4) upward vertical solute transport in the zone below the horizontal boundary plane due to depletion of the groundwater by capillary rise, is balanced by downward vertical solute transport during the subsequent recharge period(s).

The value of  $q_d$  is constant during pumping periods:

$$q_d = \frac{Q_v}{\pi r_c^2} \quad (5.18)$$

where  $Q_v$  is the pumping capacity [ $L^3 T^{-1}$ ] on volume basis. In periods with no pumping  $q_d$  is set to zero.

### 5.7 Case 1: Satiana Pilot Project tube-well

A typical Satiana drainage tube-well was simulated (Chapter 4). Pumping capacity,  $Q_v$  is 4893  $m^3 d^{-1}$ . The radial distance to the water divide,  $r_c$ , i.e. half the distance between two neighbouring tube-wells (Fig. 4.7), was assumed to be 750 m. This resulted in a value of  $q_d$  during pumping of 2.8  $mm d^{-1}$  (Eq. 5.18). The simulation period covered 21 years (1/6/1976-31/5/1997), with 1/6/1976 being the estimated starting date of tube-well drainage at the Satiana Project. At the top boundary of the SWAP model, daily values of rainfall, pre-irrigation and potential evapotranspiration were again input. The same cotton-wheat rotation (Table 5.7), and the same irrigation criterion ( $T_a/T_p \geq 0.95$ ), were used as for the S-I-B-9 unit of the Fourth Drainage Project. The additional rainfall data were obtained from a meteorological station at Faisalabad. In the simulations, pumping was initiated when the groundwater table rose above 1.75 m below soil surface. Pumping was terminated when the groundwater table fell below 2.4 m.

The salinity parameters (Table 5.9) and most soil hydraulic parameters (Table 5.8) were the same as for the S-I-B-9 unit. Some of the parameters for the aquifer (the sandy loam subsoil in Table 5.8) were however different. Notably: (1) The thickness of the aquifer contributing to flow; (2) The values of  $K_{rr}$  and  $K_{zz}$  of the subsoil (In Table 5.8,  $K_{xx}$  is used instead of  $K_{rr}$ ); and (3) The position of the horizontal boundary plane (equivalent to drain level). Values for these parameters were derived from a pumping test conducted with Satiana tube-well No. 22a by Moghal et al. (1992). The location of tube-well 22a is shown in Fig. 4.7. The analysis of the pumping test data is explained in Appendix B. The analysis resulted in a horizontal boundary plane of 8.25 m below soil surface, a hypothetical depth of the aquifer base of 231.75 m below soil surface, and  $K_{rr} = K_{zz} = 23.1 m d^{-1}$  for the subsoil.

Calculated streamlines towards the tube-well are shown in Fig. 5.14. Each stream-tube again represents 10 % of the total recharge. Due to radial symmetry, the stream-tubes are no longer spaced equally along the horizontal axis. The effect of partial penetration of the well in the aquifer is clearly visible. At the well-axis the streamlines strongly converge.

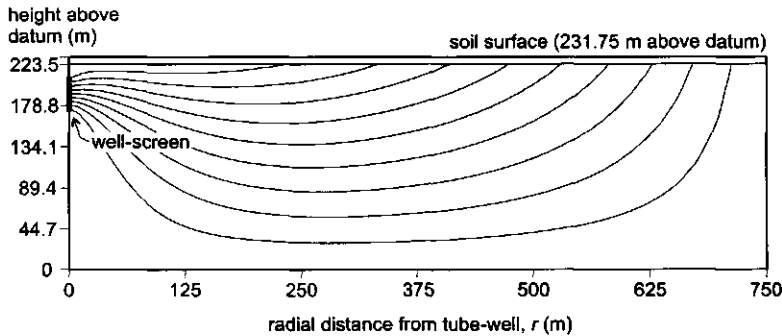


**Figure 5.14** Calculated streamline pattern below the horizontal boundary plane for the Satiana drainage tube-well. Each stream tube represents 10 % of the total discharge. Numerical solution according to Olsthoorn (1998).

#### **Depth of the groundwater table and cumulative pumping**

Simulated depth of the groundwater table,  $d_{gw}$  and cumulative pumping,  $Q$  for the Satiana tube-well are shown in Fig. 5.15. Only the results for the last 8 years of the simulation period are shown which coincides exactly with the simulation period for the S-I-B-9 drainage unit (Fig. 5.11). Comparison between Figs. 5.11 and 5.15 shows that the simulated depths of the groundwater table are approximately the same. The cumulative pumping,  $Q$  of 2.74 m in Fig. 5.15 translates into a total pumping time of 990 days ( $Q_v = 4893 \text{ m}^3 \text{ d}^{-1}$ ). The resulting percentage of operation of 12.9 % is low compared to other public tube-wells in Pakistan. According to Ahmad and Chaudhry (1988), public wells are generally working about 40 % of the time. One reason for this discrepancy is the fact that tube-wells in the field also pump up water that originates from seepage from the irrigation system. In the present analysis only percolation from the agricultural fields is considered.

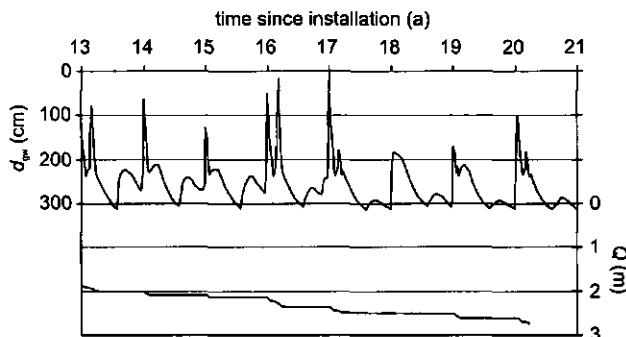


**Figure 5.15** SWAP simulated depth of the groundwater table,  $d_{gw}$  and cumulative pumping,  $Q$  for the Satiana drainage tube-well.

### Soil and effluent salinity

Simulated soil and effluent salinity for the Satiana tube-well are shown in Fig. 5.16. The salinity of the downward soil water flux at the horizontal boundary plane,  $EC_{dp}$  is also given. As in all previous cases, soil salinity,  $EC_e$  (0-1 m) drops quickly in response to pumping from 2.0 to  $< 0.5$  dS  $m^{-1}$  in less than 2 years. The effluent salinity,  $EC_{tw}$  does not change with time. The insensitivity of  $EC_{tw}$  to pumping is due to the depth of the well screen (20 to 60 m below soil surface), combined with the large thickness of the zone below the horizontal boundary plane of 223.5 m. The fact that seepage from the irrigation system is not incorporated in the calculation of  $q_d$  also contributes to the limited temporal changes in  $EC_{tw}$ .

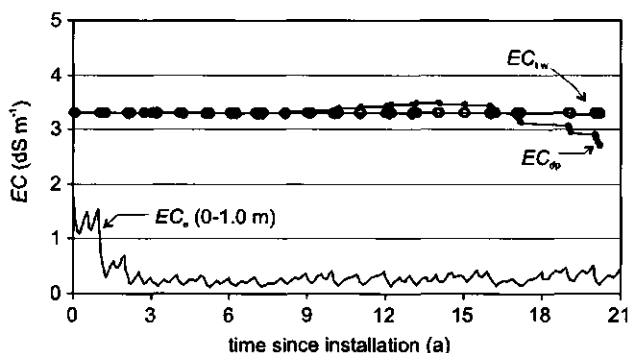


**Figure 5.16** SWAP simulated soil salinity,  $EC_e$ , salinity of the downward flux at the horizontal boundary plane,  $EC_{dp}$  and effluent salinity,  $EC_{tw}$  for the Satiana drainage tube-well.

The effect of the well screen depth on  $EC_{tw}$  can be understood by evaluating  $EC_{dp}$ . Figure 5.16 shows that it takes ~17 years before  $EC_{dp}$  starts to decrease significantly. This implies that 17 years and 2360 mm of cumulative pumping,  $Q$  are needed to leach most of the solutes from the zone above the horizontal boundary plane (at 8.25 m below soil surface). The remaining 4 years in the simulation period are insufficient to notice the reduction in the  $EC_{dp}$  values in the  $EC_{tw}$  values at the well.

Because the average life time of public tube-wells, like the ones in Satiana, is only 12 years (Ahmad and Chaudhry, 1988), it can be forecasted that the Satiana tube-wells will not show any change in effluent salinity during their operational period. This is in accordance with the measured  $EC$  values of the Satiana tube-wells which showed only minor changes over a 10-year period (from 3.3 to 3.1 dS  $m^{-1}$  for drainage tube-wells and constant at 0.6 dS  $m^{-1}$  for irrigation tube-wells (Chapter 4)).

### Water and salt balance

The simulated water balance for the 7670-days simulation period for the Satiana tube-well is given in Table 5.12. The simulated irrigation water application of 675 mm  $a^{-1}$  is slightly lower than the simulated value of 681 mm  $a^{-1}$  for S-I-B-9. The difference is attributed to the higher

## Prediction of Long Term Effluent Salinity of Pipe Drains and Tube-wells

average rainfall for the Satiana tube-well simulation period ( $386 \text{ mm a}^{-1}$  against  $307 \text{ mm a}^{-1}$ ). The relatively high surface runoff,  $R_s$  of  $29 \text{ mm a}^{-1}$  is mainly due to three years with extremely high monsoon rainfall. In the second, third and fifth year of the simulation period, rainfall during the months of July, August and September totalled 422 to 533 mm. Average rainfall during these months is only 224 mm.

**Table 5.12** Simulated water balance terms over 7670 days for the Satiana Pilot Project tube-well (all values in  $\text{mm a}^{-1}$ ).

Rainfall, $P$	386
Irrigation, $I$	675
Interception, $P_i$	16
Surface runoff, $R_s$	29
Crop transpiration, $T$	676
Soil evaporation, $E$	212
Cumulative pumping, $Q$	130
Change in water storage, $\Delta W$	-2

The simulated salt balance over the 7670-day simulation period for the Satiana well is given in Table 5.13. Note that the net removal of salts from the zone below the horizontal boundary plane is  $0.0 \text{ t ha}^{-1} \text{ a}^{-1}$ . Total salt storage in the zone below the plane before pumping started can be calculated as  $1549 \text{ t ha}^{-1}$ . Clearly, reclamation of the complete soil-aquifer system will not be achieved within the lifetime of a single tube-well. Inspection of the solute impulse response function for the Satiana well shows that at the end of the simulation period only 7 % of the surface area under the influence of the tube-well has  $n_e V/dA < Q$  (see Fig. 5.17 in Section 5.8).

**Table 5.13** Simulated salt mass balance terms over 7670 days for the Satiana Pilot Project tube-well (all values in  $\text{t ha}^{-1} \text{ a}^{-1}$ ).

Salts in irrigation water	0.9
Salts in drainage water	3.0
Change in salt storage above the horizontal boundary plane	-2.1
Change in salt storage below the horizontal boundary plane	0.0

### 5.8 The mixing reservoir approach

Several investigators have demonstrated the applicability of the mixing reservoir approach to predict the impulse response of an aquifer to non-point source solute input (e.g. Gelhar and Wilson, 1974; Van Ommen, 1985). Under the assumption of complete mixing in the aquifer, the effluent salinity will be equal to the groundwater salinity ( $c_{dw}$  or  $c_{tw} = c_{gw}$ ) with  $c_{gw} [\text{ML}^{-3}]$  being the groundwater salinity below drain level (or below the horizontal boundary plane). The groundwater salinity can be calculated from the solute mass balance of the reservoir according to (Gelhar and Wilson, 1974):

$$\frac{\partial c_{gw}}{\partial t} = -\frac{q_d}{n_e b} (c_{gw} - c_{dp}) \quad (5.19)$$

where  $b$  [L] is the thickness of the zone below drain level (Fig. 3.2). For tube-wells,  $b$  is the thickness of the zone below the horizontal boundary plane.

The ratio between the horizontal extent of the flow domain ( $1/2L$  or  $r_e$ ) and the vertical extent of the flow domain ( $b$  or  $b'$ ), is of particular importance in this regard. This is called the aspect ratio. Duffy and Lee (1992) investigated the relationship between the aspect ratio of the flow domain and the performance of the mixing reservoir approach to predict outflow concentrations. For drainage systems, which combine non-point sources with a small outflow surface, these investigators found that the mixing reservoir approach worked well for aspect ratios  $> 10$ . Outflow concentrations from flow domains with aspect ratios  $< 4$  should not be described by the mixing reservoir approach. If the mixing reservoir approach is applicable for a particular flow system, then  $n_e A/dx$  and  $n_e V/dA$  are likely to follow an exponential distribution, with  $n_e b$  being the mean of the distribution (e.g. Van Ommen, 1986; Duffy et al., 1990).

Cumulative frequency distributions of  $n_e A/dx$  and  $n_e V/dA$  are shown in Fig. 5.17 for Sampla pipe drains ( $L = 50$  m), the S-I-B-9 central lateral drain and the Satiana tube-well, respectively. In each case, the solid line represents the distribution according to the respective streamline patterns and the dashed line represents the exponential distribution. For Sampla, only the results for drain spacing,  $L=50$  m are given as the results for the other drain spacings were almost the same. Figure 5.17 shows that the distributions for the stream function approach and the mixing reservoir agree well for Sampla. Note that the aspect ratio for Sampla ( $L=50$  m) is 20. Comparison for S-I-B-9 is less favourable (aspect ratio = 2.8). The relatively deep flow pattern at S-I-B-9, combined with the small outflow surface, results in a distribution of  $n_e A/dx$  which differs significantly from the exponential distribution. These findings seem to confirm the earlier mentioned observations of Duffy and Lee (1992). The relatively good comparison for the Satiana tube-well (aspect ratio = 3.4) is due to the relatively large outflow surface of the well. The longer the well-screen, the more the well will resemble a fully penetrating well, and the better the outflow concentrations will fit the exponential distribution (Section 5.1; Van Ommen, 1985).

Predicted effluent salinity according to the stream function approach and the mixing reservoir approach is shown in Fig. 5.18. Effluent salinity is given as a function of cumulative drainage,  $D$  or cumulative pumping,  $Q$ . For Sampla ( $L = 50$  m) the same 5445-day period was simulated as in Section 5.4. For S-I-B-9 and Satiana, a 70-year period was simulated using the rainfall data of 1981, a relatively wet year in the Faisalabad area (rainfall 646 mm). The simulations for S-I-B-9 and Satiana are not representative for the local conditions. The simulations were included only to allow comparison between the stream function approach and the mixing reservoir approach. Figure 5.18 shows that, on average, both approaches agree well. As could be expected, the largest differences are found for S-I-B-9. For values of  $D$  of between 2 and 14 m the mixing reservoir approach over-predicts the  $EC_{dw}$  at S-I-B-9 by about 15 %.



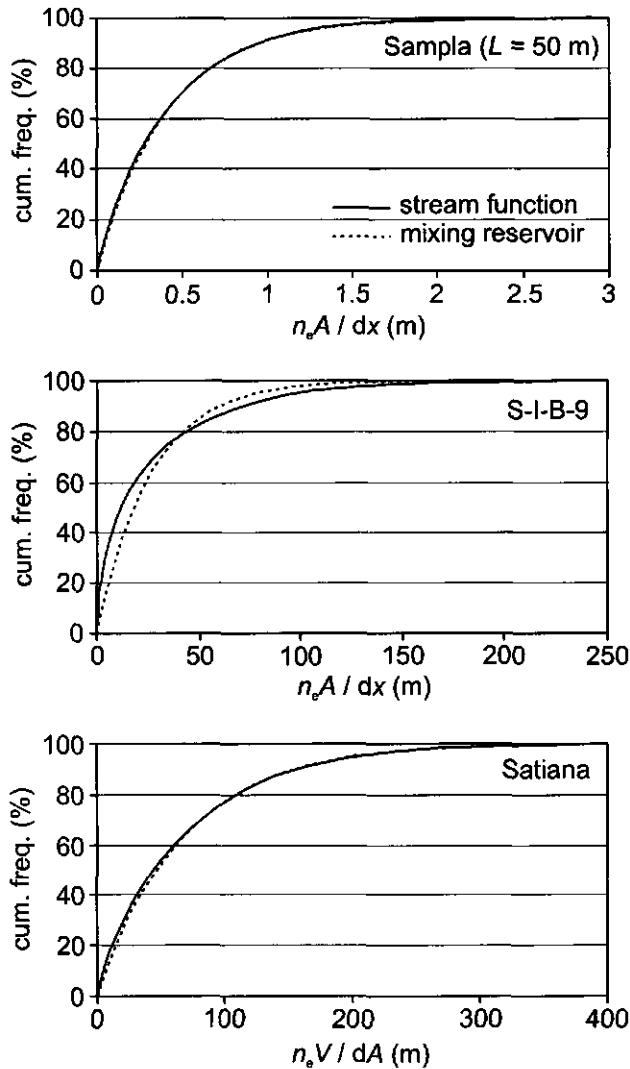


**Figure 5.17** Cumulative frequency distributions of  $n_e A / dx$  and  $n_e V / dA$  according to the stream function approach and the mixing reservoir approach for the Sampla experimental pipe drainage site ( $L = 50 \text{ m}$ ), the S-I-B-9 pipe drainage unit of the Fourth Drainage Project and the Satiana drainage tube-well.

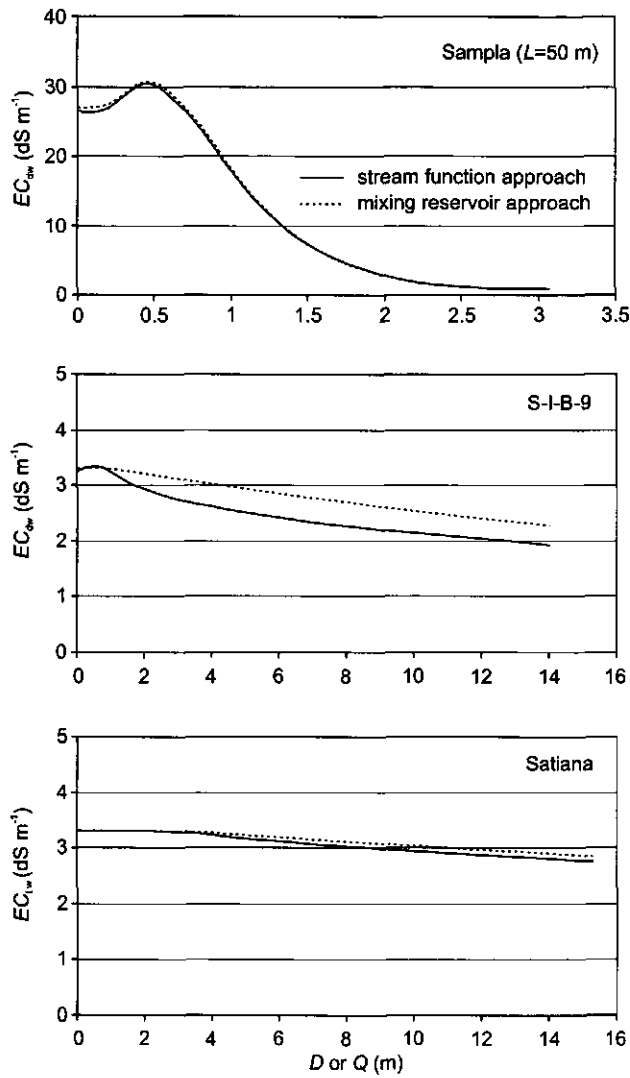


**Figure 5.18** Comparison between the stream function approach and the mixing reservoir approach for the Sampla experimental pipe drainage site ( $L = 50\ m$ ), the S-I-B-9 pipe drainage unit of the Fourth Drainage Project and the Satiana drainage tube-well. Effluent salinity,  $EC_{dw}$  or  $EC_{tw}$  is given as a function of cumulative drainage,  $D$  or cumulative pumping,  $Q$ .

The relationship between the stream function approach and the mixing reservoir approach is investigated further by simulating Sampla ( $L = 50$  m) with different values of the depth of the impermeable layer,  $b$ . To this end the  $b$ -value of 1.25 m (Section 5.4) was increased to 3.75 m and to 6.25 m, where the latter value is the maximum  $b$ -value according to Eqs. (5.13) and (5.14). Note that the new values of  $b$  require a recalculation of the drainage resistance,  $\gamma$  (SWMS\_2D). This resulted in  $\gamma = 65$  d for  $b = 3.75$  m and  $\gamma = 60$  d for  $b = 6.25$  m. The aspect ratios for the newly simulated cases are 6.7 and 4, respectively. Cumulative frequency distributions of  $n_e A / dx$  are shown in Fig. 5.19. Clearly, the differences between the distributions for the two approaches increase as  $b$  increases.

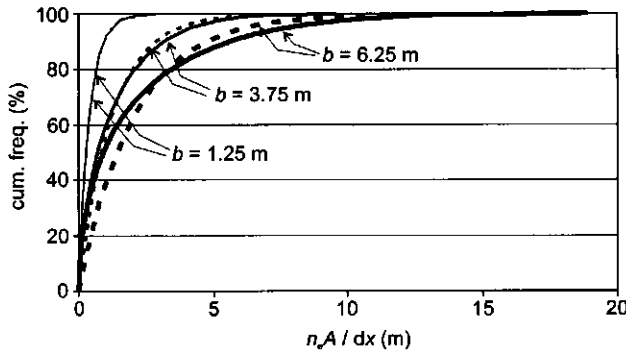


**Figure 5.19** Cumulative frequency distributions of  $n_e A / dx$  according to the stream function approach (solid lines) and the mixing reservoir approach (dotted lines) for the Sampla experimental pipe drainage site ( $L = 50$  m) using different depths of the impermeable layer below drain level,  $b$ .

Predicted effluent salinity for  $b = 1.25$ , 3.75 and 6.25 m is shown in Fig. 5.20. As expected, the comparison between the stream function approach and the mixing reservoir approach is best for  $b = 1.25$  m. The larger the  $b$ -value (and the lower the aspect ratio), the larger the differences between the two approaches. It is interesting to note that the mixing reservoir approach starts to under-predict  $EC_{dw}$  at high  $D$ -values (e.g.  $b = 3.75$  m;  $D > 2.5$  m). This phenomenon is related to an observation made in Section 5.5: Closely spaced streamlines near drain level will automatically lead to wider spaced streamlines at greater depth. Or in other words: Small values of  $n_e A / dx$  near drain level will automatically lead to large values of  $n_e A / dx$  near the (hypothetical) impermeable layer. This artefact of the stream function approach makes that for each case there exists a value of  $D$  at which the over-prediction of  $EC_{dw}$  by the mixing reservoir approach changes into an under-prediction.

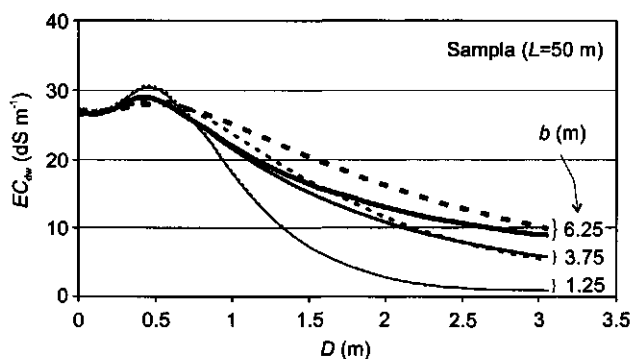


**Figure 5.20** SWAP simulated effluent salinity,  $EC_{dw}$  according to the stream function approach (solid lines) and the mixing reservoir approach (dotted lines) for the Sampla experimental pipe drainage site ( $L = 50$  m) using different depths of the impermeable layer below drain level,  $b$ .

## 5.9 Conclusions

A new modelling approach was developed to study long term soil and effluent salinity. The SWAP model (Van Dam et al., 1997) for water flow and solute transport in the variably saturated zone was coupled with a solute impulse response function for the saturated zone. The solute impulse response function was derived from two-dimensional (pipe drains) and three-dimensional (tube-wells) streamline patterns. The effluent salinity was calculated with a convolution integral, using cumulative drainage or cumulative pumping as the driving force. *Because of a number of simplifying assumptions regarding the flow regime, the modelling approach should only be used for relatively coarse textured soil-aquifer systems.* In case of pipe drains, the depth of the impermeable layer should be clearly below drain level.

The results for the Sampla experimental pipe drainage site show that effluent salinity improves only gradually with time. Complete reclamation of the soil and aquifer, which determines effluent salinity, takes approximately 10 years. In reality, the reclamation time will be longer because of the continuous inflow of saline groundwater from the surrounding area. At Sampla, drain spacing has little effect on effluent salinity due to the impermeable layer at shallow depth which restricts the flow below drain level to a limited part of the upper aquifer. Results for the S-I-B-9 pipe drainage unit show that complete reclamation of soil and aquifer will not be achieved within the economic life of the system (~25 years). Reclamation at S-I-B-9 is relatively slow because of the low cumulative drainage of  $96 \text{ mm a}^{-1}$ , the relatively large drain depth of 2.4 m and the deep groundwater flow (up to 87.4 m below drain level). The modelling results for the Satiana tube-well show that effluent salinity will not change significantly during the operational period of the well. The insensitivity of  $EC_{tw}$  to pumping is due to the low percentage of operation of the tube-well, the depth of the well screen (20 to 60 m below soil surface) and the deep groundwater flow (up to 223.5 m below the horizontal boundary plane).

After the initiation of drainage,  $EC_e$  (0-1 m) levels drop quickly. The simulations for Sampla, S-I-B-9 and Satiana suggest that after 2 years, crops will no longer suffer from soil salinity. *The time lag between the reclamation of the rootzone, and the reclamation of the complete soil-aquifer system (which determines the effluent salinity) appears to be an important feature of agricultural drainage systems in the Indus plain. The implication is that farmers will benefit quickly from the drainage system (reduced soil salinity) but that long term solutions are required for the safe use and disposal of the effluent.* If pipe drains or tube-wells are installed in deep extensive aquifers, large quantities of saline groundwater have to be removed before some improvement in effluent salinity can be expected. If this effluent cannot be used and disposed safely, subsurface drainage systems should not be installed on a large scale.

The solute impulse response function of the saturated zone was also calculated by assuming a completely mixing reservoir. Calculated effluent salinity for the Sampla pipe drains compares well with the results of the stream function approach as long as the depth of the impermeable layer remains shallow ( $b = 1.25$  m). Comparison for Sampla using greater depths of the impermeable layer ( $b = 3.75$  m and  $b = 6.25$  m for  $L = 50$  m) and comparison for the S-I-B-9 central lateral drain is less favourable. The relatively deep flow patterns for these cases, combined with the small outflow surface, result in a distribution of  $n_e A/dx$  which no longer fits the exponential distribution which is implicit in the mixing reservoir approach. In contrast, the mixing reservoir approach performs relatively good for the Satiana well. The large outflow surface constituted by the well screen results in a distribution of  $n_e V/dA$  which remains close to the exponential distribution. *Overall, it may be concluded that for practical purposes, the mixing reservoir approach, which is much simpler than the stream function approach, will suffice for most cases considered in this chapter.*

The implications of the findings in this chapter for drainage planning in the Indus plain are discussed in Chapter 7.



## 6 Density-Dependent Water Flow and Solute Transport to Tube-Wells and Pipe Drains

### 6.1 Introduction

In Chapter 5, it was assumed that pre-drainage groundwater salinity is space invariant. *In the Indus plain, however, groundwater salinity usually increases with depth. The shallow groundwater, which originates from percolation from the irrigated fields and from seepage from the irrigation system, tends to form fresh groundwater lenses on top of the deeper saline groundwater.* The thickness of the fresh groundwater lenses in the Indus plain varies from a few metres at the centre of inter-fluvial areas (doabs) to approximately 150 m near the rivers and canals (Swarzenski, 1968). In water scarce areas, these fresh groundwater bodies may be an important source of irrigation water. In waterlogged areas, where sub-surface drainage is installed to control the groundwater table, the presence of the fresh groundwater bodies may result in a relatively low effluent salinity which reduces disposal problems.

For the Indus plain, several well-configurations have been considered to skim the shallow fresh groundwater, leaving the deeper saline groundwater untouched. A distinction can be made between skimming wells, multi-screen wells and scavenger wells (Fig. 6.1). Skimming wells are conventional tube-wells with a well screen that penetrates only the shallow fresh groundwater. To prevent upconing of the saline groundwater, the drawdown at the well should be balanced by the gravitational forces on the saline groundwater mound below the well (e.g. Chandler and McWhorter, 1975). Generally, a critical pumping rate exists beyond which saline groundwater starts entering the well (Bear, 1979). Multi-screen wells consist of multiple well points that are connected to a common pump. By distributing the pumping from the groundwater over a larger surface area, the upconing below individual well points is kept small (e.g. Hafeez et al., 1986; Shakya et al., 1995). Scavenger wells have two separate well screens. Pumping from the deepest well screen, which is located in the saline groundwater, should prevent upconing below the shallow well screen, which is used to recover the fresh groundwater (Stoner and Bakiewicz, 1993). The subsurface pipe drainage systems in the Indus plain, consisting of laterals, collectors and sumps, could also be regarded as a skimming technology.

Two methods of analysis, the sharp-interface method and the density-dependent water flow and solute transport method, are available to simulate saltwater upconing. The sharp interface method assumes that the fresh-saline groundwater system is composed of two completely immiscible fluids. Thus the problem can be formulated in terms of two distinct systems, the fresh groundwater flow field and the salt groundwater flow field (Reilly and Goodman, 1987). Applications of the sharp-interface method for upconing problems below wells can be found in Bennett et al. (1968), Chandler and McWhorter (1975), Wirojanagud and Charbeneau (1985) and Reilly et al. (1987). Upconing below pipe drains, using the sharp-interface method, was studied by Bear and Dagan (1964) and McWhorter (1972). The sharp interface method is less suitable to study effluent quality because it neglects the transition zone between the fresh and saline groundwater. The transition zone might be approximated however, by superimposing the effect of hydrodynamic dispersion on the position of the interface (Schmorak and Mercado, 1969; Wirojanagud and Charbeneau, 1985).

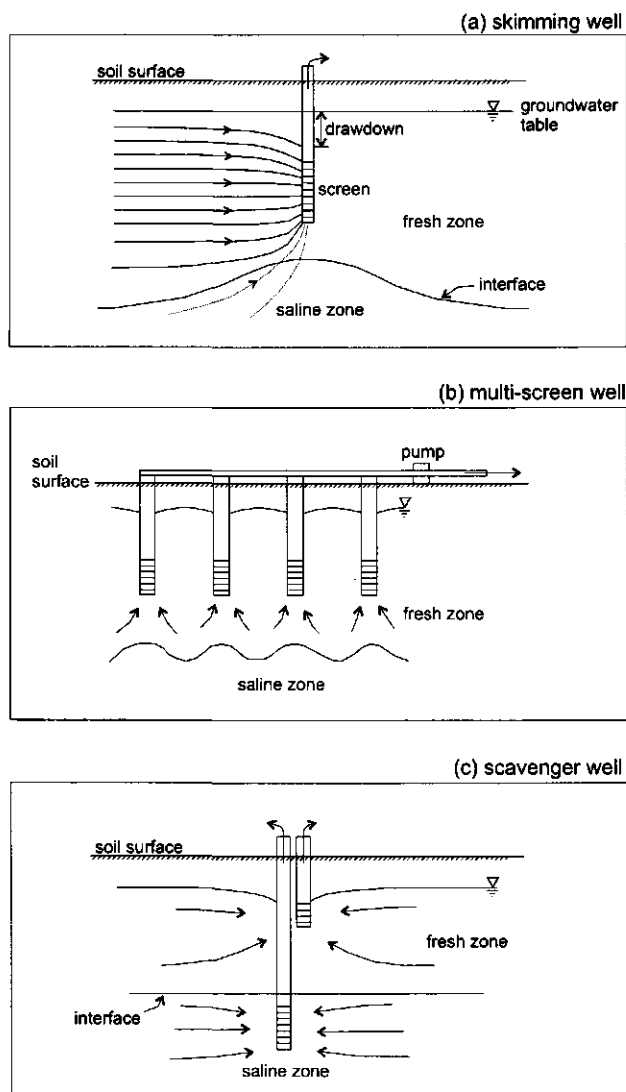


**Figure 6.1** Schematic cross-section of (a) a skimming well, (b) a multi-screen well and (c) a scavenger well in a fresh-saline groundwater system of the Indus plain (after Sufi et al., 1998).

The density-dependent water flow and solute transport method, which is based on a combination of the Darcy equation and the basic mass balance equation, and the advection-dispersion equation (Chapter 2), provides the most complete description of fresh-saline groundwater systems which is currently available (e.g. Voss, 1984; Huyakorn et al., 1987; Kolditz et al., 1998). The



groundwater system is treated as one miscible continuum. The effect of hydrodynamic dispersion on the width of the transition zone is fully accounted for. The density-dependent water flow and solute transport method requires a numerical approach because the water flow and solute transport equations are generally non-linear and have to be solved simultaneously (Thorborg and Jousma, 1989). Applications of the density-dependent method for upconing problems below wells can be found in Reilly and Goodman (1987), Shearer and Van Wonderen (1993), Ma et al. (1997) and Sufi et al. (1998). To the present author's knowledge, the density-dependent method has not been used to study upconing below pipe drains.

Skimming techniques for the Indus plain were studied by the Water Management Research Project of Colorado State University. The work included laboratory experiments with immiscible fluids in a hydraulic model (Sahni, 1972), approximate analytical approaches to calculate the position of the interface between the fresh and saline groundwater (McWhorter, 1972), numerical solution of the groundwater flow problem using the sharp interface method (Chandler and McWhorter, 1975) and field experiments at the Phularwan research farm (Kemper et al., 1976; Hafeez et al., 1986). On the basis of this work, McWhorter (1980) recommended that if no stratification is found during drilling, the screen of a skimming well should penetrate no more than 30 % of the fresh groundwater zone. If vertical permeability is substantially less than the horizontal permeability (e.g. if stratification exists), the length of the screen can be extended to about 50 % of the thickness of the fresh groundwater zone.

More recently, density-dependent water flow and solute transport models have also been used to study skimming techniques for the Indus plain. Aliwi (1993) used the finite-difference model RASIM and Shearer and Van Wonderen (1993) used the model SUTRA to study the design and operation of scavenger wells for a large scale scavenger well project in Sindh Province (376 wells). Both models were tested with data from pilot scavenger wells (see also Beeson et al., 1993). The proportion of recoverable fresh groundwater proved particularly sensitive to the initial depth of the fresh groundwater and to the anisotropy factor of the aquifer. Sufi et al. (1998) used the 3D-finite element model VDGWTRN to study various skimming technologies. This model was calibrated with data from sand tank models and validated with data from the earlier mentioned field experiments carried out at Phularwan farm (Kemper et al., 1976; Hafeez et al., 1986). Data from one of the pilot scavenger well experiments in Sindh were also used for validation. Sufi et al. (1998) concluded that multi-screen wells are suited best for recovering low salinity water from thin fresh groundwater bodies.

*In this chapter, the behaviour of skimming wells and pipe drains in fresh-saline groundwater systems is studied.* Arguably, these two technologies have the greatest chance of finding widespread application in the Indus plain. Scavenger wells and multi-screen wells are relatively costly and are difficult to operate and maintain. An additional disadvantage of scavenger wells is the fact that large quantities of saline groundwater from the lower screen have to be disposed, causing water quality problems downstream. *The density-dependent water flow and solute transport model SUTRA is used to simulate the skimming wells and pipe drains.* Use of SUTRA facilitates the prediction of effluent quality with time. Note that the interaction with crop growth is not included in the model. SUTRA is *calibrated* on data from a skimming well experiment at Phularwan farm (Kemper et al., 1976; McWhorter, 1980; Hafeez et al., 1986). Subsequently, the

model is *validated* on data from a scavenger well experiment at the farm. Parameters for the scavenger well differ from those presented by Sufi et al. (1998) for the same well because spatial discretization in the present study is finer, allowing a more accurate description of the flow processes.

Before continuing, one remark should be made on the use of basic variables. In Chapter 5, pumping rate was expressed in  $\text{m}^3 \text{d}^{-1}$ , recharge in  $\text{m d}^{-1}$  ( $= \text{m}^3 \text{m}^{-2} \text{d}^{-1}$ ) and solute concentration in  $\text{kg m}^{-3}$ . In the SUTRA model, all fluid quantities and solute concentrations are expressed in mass (kg) instead of volume ( $\text{m}^3$ ). For example, pumping rate is given in  $\text{kg s}^{-1}$ , recharge in  $\text{kg m}^{-2} \text{s}^{-1}$  and solute concentration in  $\text{kg kg}^{-1}$  (the subscript s stands for solute). To avoid confusion, and to allow easy comparison between results, volumetric expressions remain to be used in the current chapter. The reader should be aware, however, that implementation in SUTRA requires conversions. For the same reason, the hydraulic properties continue to be expressed in hydraulic conductivity,  $K_{ij}$  [ $\text{L T}^{-1}$ ] instead of permeability,  $k_{ij}$  [ $\text{L}^2$ ] as used in SUTRA. Also the shape parameter  $\alpha_h$  [ $\text{L}^{-1}$ ] in the MVG model is given instead of the parameter  $\alpha_p$  [ $\text{M}^{-1} \text{L T}^2$ ].

## 6.2 Phularwan experimental skimming well site

In the seventies, several skimming technologies were field tested at Phularwan research farm (Fig. 4.1), a part of the Mona reclamation area in Punjab, Pakistan (Kemper et al., 1976; McWhorter, 1980). The experiments were conducted to study the effect of pumping on groundwater systems where fresh water is overlying saline water (McWhorter, 1980). A summary of the system parameters for the three most relevant experiments is given in Table 6.1. The double-screen well was located at the same site as the skimming well, making use of the same pump. The boreholes of the double-screen well were 30 m apart. Pumping rates were generally constant for the well-experiments, except for the lower well screen of the scavenger well. Pumping rates for this *lower* well screen were increased gradually to test how much saline water discharge is required to prevent salt water intrusion in the *upper* well screen (Kemper et al., 1976). In subsequent experiments, also two multi-screen wells were field tested. These wells, however, consisting of 13 well points, proved to be difficult to operate because of suction breaks and because of difficulties with priming (Hafeez et al., 1986).

**Table 6.1** System parameters for three tube-well experiments at the Phularwan research farm, Punjab Province, Pakistan (Kemper et al., 1976).

Parameter	Skimming well	Double-screen well	Scavenger well	
			Upper screen	Lower screen
Screen depth (m)	3.0-18.0	2.4-9.2	3.0-19.2	24.4-30.4
Pumping rate ( $\text{m}^3 \text{d}^{-1}$ )	1223	1223	1223	73-440*
Screen radius (m)	0.1	0.1	0.1	0.05
Pumping period	5-20 Jan 76	2 Jul-3 Aug 76	28 Oct-20 Nov 76	2-20 Nov 76

\* Pumping rate increased during the experiment; no pumping for 5 days (28 Oct - 1 Nov),  $73 \text{ m}^3 \text{d}^{-1}$  for 1 day,  $122 \text{ m}^3 \text{d}^{-1}$  for 4 days,  $183 \text{ m}^3 \text{d}^{-1}$  for 8 days,  $245 \text{ m}^3 \text{d}^{-1}$  for 2 days and  $440 \text{ m}^3 \text{d}^{-1}$  for 3 days.

The aquifer at Phularwan farm is unconfined and consists of medium sand overlain by a loamy sand top-layer of about 3 m depth (McWhorter, 1980; Hafeez et al., 1986). The exact thickness of the aquifer is unknown. Geological cross sections of the Chaj Doab, in which Phularwan farm is located, suggest that non-continuous clay and silt layers can be found in the sub-surface, which may locally reduce the effective size of the aquifer (Greenman et al., 1967). Well-logs and pumping tests at Phularwan farm show that the thickness of the medium sand sub-layer is at least 50 m. Pre-pumping groundwater tables varied between 1 and 3 m below the soil surface. The  $EC$  of the groundwater,  $EC_{gw}$  varied with depth: from 1-1.5  $dS\ m^{-1}$  close to the soil surface to 7-9  $dS\ m^{-1}$  at >35 m depth. The effect of pumping from the wells on the depth of the groundwater table and on  $EC_{gw}$  was monitored with observation wells, installed at 2 to 25 m from the wells. Each observation well contained a set of piezometers, allowing sampling of the groundwater up to 37 m depth. A detailed description of the data collection programme can be found in Kemper et al. (1976) and McWhorter (1980).

During pumping, the well-water salinity was measured almost daily. Values for the skimming well and the double-screen well (Fig. 6.2) show that the  $EC$  of the pumped water,  $EC_{tw}$  was higher for the skimming well than for the double-screen well. This is attributed to the deeper well screen of the skimming well. Both the skimming well and the double-screen well showed an increase in  $EC_{tw}$  with time. The continued rise in  $EC_{tw}$  values at the end of the pumping period, indicates that the fresh and saline groundwater were not yet at equilibrium when pumping stopped. The relatively rapid increase in  $EC_{tw}$  for the skimming well is not surprising, as this well was constructed too deep on purpose, to obtain a clear measurable trend in the well-water quality (McWhorter, 1980).

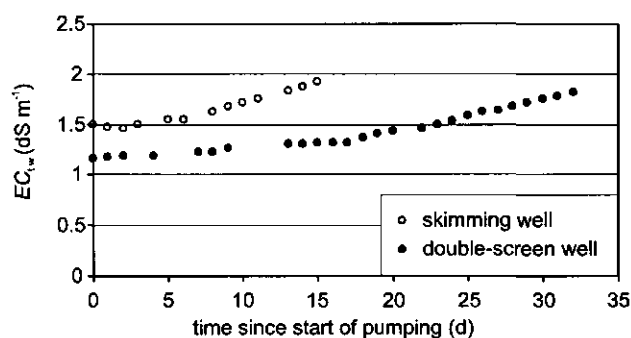


**Figure 6.2** Measured pumped water salinity,  $EC_{tw}$  during the skimming well and the double-screen well experiment (after Kemper et al., 1976).

During the 23-day pumping period for the scavenger well (Fig. 6.3),  $EC_{tw}$  from the upper screen increased from 1.7 to 2.5  $dS\ m^{-1}$ . Over 18 days, the  $EC_{tw}$  values for the lower screen increased from 5.5 to 6.5  $dS\ m^{-1}$  (disregarding the first value of 6.0  $dS\ m^{-1}$ ). The results indicate that a ratio of saline to fresh discharge of 0.4 for the scavenger well is not able to prevent upconing of saline water. *To prevent upconing, pumping rates for the lower well screen should probably be as high or even higher than those for the upper well screen* (Kemper et al., 1976). For comparison: the

pilot wells for the scavenger well drainage project in Sindh had ratios of saline to fresh discharge of between 0.3 and 1.9 (Van Wonderen and Jones, 1993).

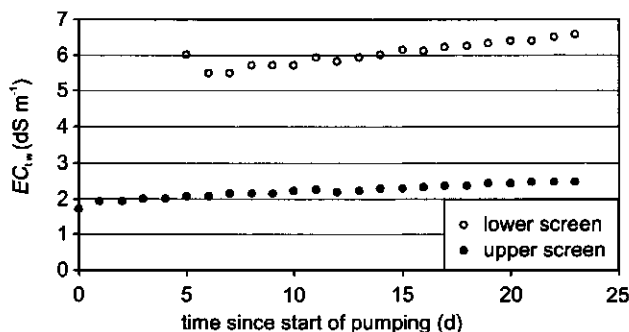


**Figure 6.3** Measured pumped water salinity,  $EC_{tw}$  during the scavenger well experiment (after Kemper et al., 1976).

### 6.3 Calibration of the SUTRA model for the *skimming well* experiment

The SUTRA model was calibrated for the skimming well experiment at Phularwan farm (Table 6.1). The well was described in cylindrical coordinates using a rectangular grid network with 80 nodes along the  $r$ -axis and 240 nodes along the  $z$ -axis. Small grid spacings were used in the upper part of the flow domain and near the well screen. Vertical spacing between nodes for the fresh groundwater zone and the transition zone was 0.2 m at maximum to allow an accurate description of  $EC_{gw}$  with depth. The top 1 m of the soil-aquifer system, which was considered to be the rootzone, was not modelled. The boundary conditions for the SUTRA model and the initial  $EC_{gw}$  are shown in Fig. 6.4.

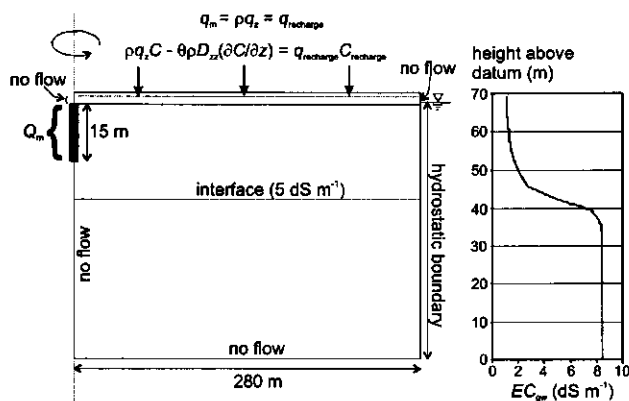


**Figure 6.4** Set-up, boundary conditions and initial groundwater salinity,  $EC_{gw}$  for the calibration of the SUTRA model on the *skimming well* experiment.

Figure 6.4 shows that the outer radial boundary is defined as a specified pressure boundary, assuming hydrostatic conditions. This is the appropriate boundary condition for an isolated well in an unbounded aquifer. To ensure hydrostatic conditions, the radial distance between the partially penetrating well and the outer boundary,  $r_e$  should be  $>2.0(k_r/k_z)^{1/2}B$ , where  $B$  is the saturated thickness [L] of the aquifer (Kruseman and De Ridder, 1990). For the skimming well site,  $B$  was estimated at 70 m at maximum. Furthermore, calibration trials showed that the anisotropy factor,  $k_r/k_z$  for the aquifer is 4. This resulted in  $r_e = 280$  m. Initial depth of the groundwater table was 2.55 m below soil surface.

Note that the well is modelled as a sink boundary and not as a specified pressure boundary. Description of the well screen as a pressure boundary, although more accurate, is not practical in the present case, because it would require many test runs to match the pressure at the screen with the observed well discharge. By employing a sink boundary, it is assumed that the well flow is distributed equally over all screen nodes that contribute to the discharge. Describing the well boundary in this way is likely to underestimate the inflow at the outer sections of the screen, and overestimate the inflow at the middle portions (Muskat, 1937). Because the screen of the skimming well starts at shallow depth, the top of the screen tends to fall dry during pumping. Dry screen nodes do not contribute to the discharge. The fact that these dry screen nodes may act as a seepage boundary was neglected.

**Table 6.2** Values of the input parameters during the calibration of the SUTRA model for the skimming well.

<i>Recharge</i>		
Rate (m d <sup>-1</sup> )	0.0005	
Salinity (dS m <sup>-1</sup> )	1.2	
<i>Water properties</i>		
Fluid viscosity, $\mu$ (kg m <sup>-1</sup> s <sup>-1</sup> )	1.0×10 <sup>-3</sup>	
Porous medium dif. coef., $D_m$ (m <sup>2</sup> s <sup>-1</sup> )	0.0	
<i>Soil and aquifer parameters</i>	Topsoil	Subsoil
Depth of layer (m)	0-3.0	3.0-70.0
Soil texture	loamy sand	sand
Rad. sat. hydr. cond., $K_r$ (m d <sup>-1</sup> )	1.8	35
Anisotropy factor	4	4
Res. water content, $\theta_r$	0.0	0.0
Sat. water content, $\theta_s$	0.33	0.35
Shape parameter, $\alpha_h$ (cm <sup>-1</sup> )	0.028	0.026
Shape parameter, $n$	2.1	2.6
Shape parameter, $\lambda$	0.0	1.0
Longitudinal dispersivity, $\alpha_L$ (m)	0.1	0.1
Transverse dispersivity, $\alpha_T$ (m)	0.005	0.005

A summary of the input parameters for the SUTRA model is given in Table 6.2. The unsaturated soil hydraulic properties in Table 6.2 (see Eqs. 2.24-2.26) were obtained from Smets (1996) who calibrated the SWAP model on a field in the Indus plain with similar soil profile characteristics as at the skimming well site (loamy sand on top of sand). Trial calculations showed that the calibration result is not very sensitive to the values of  $\theta_r$ ,  $\theta_s$ ,  $\alpha_n$ ,  $n$  and  $\lambda$ . Fluid and solid matrix compressibility were neglected in the calculations as well as solute precipitation, adsorption and production/decay processes. A tolerance of  $0.1 \text{ kg m}^{-1} \text{ s}^{-2}$  was used in the pressure solution. An estimated value for  $B$  of 100 m (resulting in a value for  $r_e$  of 400 m) was also tested, but was found to have no effect on the calibration result. *Calibration was achieved by changing the anisotropy factor of the sandy sub-layer, the longitudinal and transverse dispersivities  $\alpha_L$  and  $\alpha_T$  and the porous medium diffusion coefficient  $D_m$ .*

For the final day of pumping, measured and simulated drawdown of the groundwater table at some distance from the well match closely (Fig. 6.5). Close to the well-axis, however, the drawdown is underestimated by the model. This underestimation is attributed partly to the neglect of entrance resistance at the well screen. The measured drawdown *inside* the well, for example, was 3.2 m (McWhorter, 1980), indicating that hydraulic head loss at the well screen is in the order of 2.0 m. The assumption that the well-discharge was distributed equally over all contributing screen nodes may also have resulted in an underestimation of the drawdown at the well. Measured and simulated  $EC_{tw}$  for the skimming well show a good comparison (Fig. 6.6). Both measured and simulated values show an almost linear increase in  $EC_{tw}$  for the 15-day pumping period. The relatively high  $EC_{tw}$  value of  $1.5 \text{ dS m}^{-1}$  at the start of pumping (day 0) is not simulated by the model. This high value is probably due to disturbance of the groundwater at the well-axis during construction of the well which was not described in the initial groundwater salinity (Fig. 6.4).

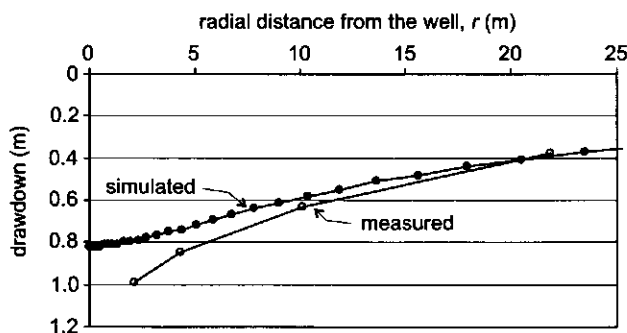


**Figure 6.5** Measured and SUTRA simulated drawdown of the groundwater table for the calibrated skimming well.

*Calibration of SUTRA proved most sensitive to the anisotropy factor of the sandy sub-layer. The final value of 4 is generally considered to be in the range of values for core samples (Smith and Wheatcraft, 1992). The value is of the same order of magnitude as the anisotropy factors of 2 and 1 found for the subsoil at S-I-B-9 and Satiana, respectively (Chapter 5). Regional scale values*

of anisotropy for the Indus plain are in the range of 15 to 90 (Bennett et al., 1967; Mundorff et al., 1976). The discrepancy between the anisotropy factors is explained by differences in scale as the high anisotropy values were obtained from relatively large tube-wells (Pumping rate  $\sim 2400\text{--}8600\text{ m}^3\text{ d}^{-1}$ ; depth borehole  $\sim 45\text{--}90\text{ m}$ ), while no distinction was made between separate aquifer materials. It appears that the sandy aquifer strata in the Northern Indus plain are relatively homogeneous. For comparison: anisotropy values for the subsoil at the pilot scavenger wells in Sindh range between 8 and 19.5 (Beeson et al., 1993). Unfortunately, Sufi et al. (1998), who validated their model on the double-screen well and the scavenger well at Phularwan farm, did not report anisotropy values.

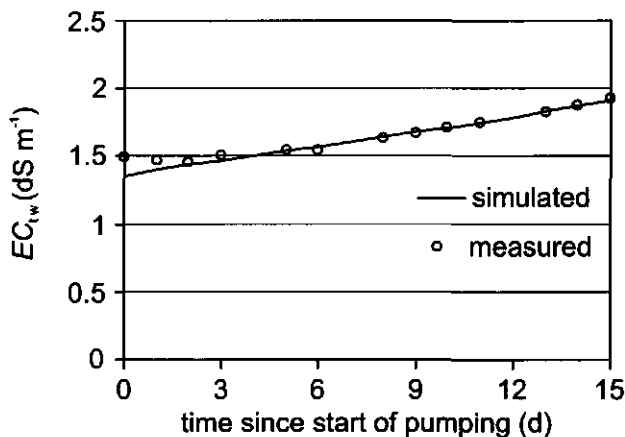


**Figure 6.6** Measured and SUTRA simulated pumped water salinity,  $EC_{tw}$  for the calibrated skimming well.

A vector plot of flow to the skimming well on the final day of pumping (day 15) is shown in Fig. 6.7. Four contour lines are shown in this figure. The top line represents the position of the groundwater table. The bottom three lines represent the positions of the 3, 5 and 7 dS  $m^{-1}$  groundwater salinity contours. *The 5 dS  $m^{-1}$  contour line is assumed to represent the interface between the fresh and saline groundwater at the skimming well site.* The vector plot shows that there is a strong vertical upward flow below the well. This is reflected in the position of the 5 dS  $m^{-1}$  contour line, which moved 10.0 m upwards along the well axis boundary during the 15-day pumping period. The measured (not shown) and simulated position of the 5 dS  $m^{-1}$  contour at the end of the pumping period compared reasonably well; 51.7 m above datum and 52.4 m above datum at the well axis, respectively.

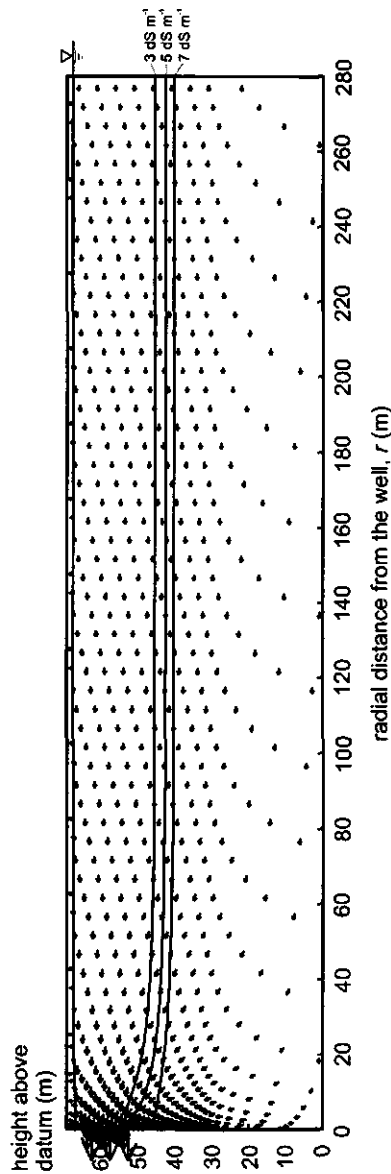


**Figure 6.7** SUTRA simulated flow direction, depth of the groundwater table and groundwater water salinity contours for the calibrated skimming well at the final day of pumping (day 15). Vectors on log-scale; every 25<sup>th</sup> vector is printed.



The sensitivity of  $EC_{tw}$  to the anisotropy of the aquifer was investigated by running SUTRA with anisotropy factors of 1, 10 and 25 for the 15-day pumping period (Fig. 6.8). The factors were obtained by varying  $K_z$  of the sandy sub-layer, keeping  $K_r$  constant at 35 m d<sup>-1</sup>. Anisotropy factors between 1 (isotropic conditions) and 10 clearly influence  $EC_{tw}$ . The higher the anisotropy factor, the lower the effluent salinity. This is due to the fact that the radial upward flow below the well decreases significantly with increasing anisotropy. The effect of anisotropy on  $EC_{tw}$  is non-linear. Changing the anisotropy factor from 10 to 25 hardly influences the results.

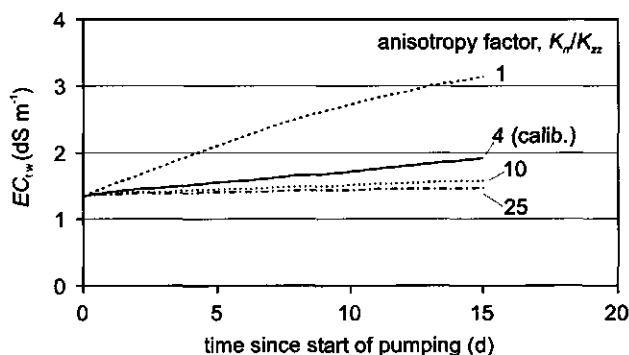


**Figure 6.8** SUTRA simulated pumped water salinity,  $EC_{tw}$  for the skimming well for different anisotropy factors.

After the skimming well was pumped for 15 days, it was not used for 164 days. This recovery period was also simulated with the SUTRA model. During recovery, recharge from the rootzone and radial inflow of *fresh* groundwater will induce a circulation pattern whereby *saline* groundwater will be forced out of the flow domain through the radial boundary. This flow pattern will result in a recession of the saline mound below the well. Unfortunately, under no pumping conditions, a combination of recharge and a hydrostatic boundary in SUTRA will cause outflow of both fresh and saline groundwater through the radial boundary. This phenomenon is due to the fact that, in the model, the values of the hydrostatic boundary are constant with time, while in reality the hydrostatic pressures at the outer radius will gradually rise because of the continuous recharge which raises the regional groundwater table. To circumvent this problem, the 164-day recovery period was simulated in two different ways:

- Mode 1: No flow boundary at the bottom of the rootzone ( $q_m = 0$ ;  $\partial C/\partial z = 0$ ) in combination with a hydrostatic boundary at the outer radius (groundwater table at 2.55 m below soil surface);
- Mode 2: Recharge of 0.5 mm d<sup>-1</sup> from the rootzone ( $EC = 1.2$  dS m<sup>-1</sup>) in combination with a no flow boundary at the outer radius.

The first mode of simulation shows the effect of inflow of fresh groundwater through the radial boundary on the recession of the saline groundwater mound below the well. The second mode clarifies the effect of recharge on the saline mound. The simulated salinity of the well screen nodes for mode 1 is shown in Fig. 6.9. To show the sensitivity to anisotropy, results are presented

again for anisotropy factors 1, 4 (calibrated value), 10 and 25. Note that the results cannot be presented as pumped water salinity,  $EC_{tw}$ , because pumping is assumed to be zero. The results for mode 2 are not depicted because they are practically the same as for mode 1. Figure 6.9 indicates that recovery is a slow process. With an anisotropy factor of 1, for example, > 50 days are required to arrive at pre-pumping  $EC$  levels. The fact that modes 1 and 2 give the same results, indicates that *the recovery process is dominated by the gravitational forces on the saline mound*. The influence of the recharge rate of  $0.5 \text{ mm d}^{-1}$  on the position of the saline mound seems negligible.

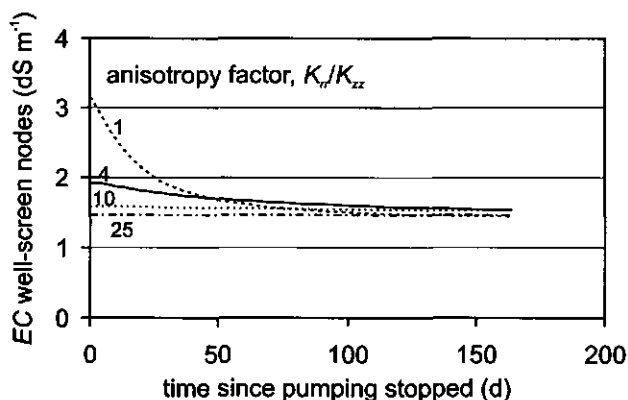


**Figure 6.9** SUTRA simulated  $EC$  of the well-screen nodes for the skimming well for different anisotropy factors. Results for the 164-day recovery period that followed after the 15-day pumping period.

Vector plots for modes 1 and 2 for the final day of the recovery period (anisotropy factor 4; day 164) are shown in Fig. 6.10. At the well axis, the simulated  $5 \text{ dS m}^{-1}$  contour for both modes is 48.0 m above datum. The measured position of the  $5 \text{ dS m}^{-1}$  contour after recovery is 45.6 m above datum (Kemper et al., 1976). If total recession of the  $5 \text{ dS m}^{-1}$  contour line is considered, the results of modes 1 and 2 yield a recession of 4.4 m over 164 days, while the measured recession is 6.1 m. Clearly, the speed of the recession of the saline groundwater mound is underestimated by the model. Numerous test runs were conducted to improve the model performance for the recession period. The present combination, however, with an anisotropy factor for the aquifer of 4, a porous medium diffusion coefficient,  $D_m = 0$  and small values for the dispersivities ( $\alpha_L = 0.1 \text{ m}$ ;  $\alpha_T = 0.005 \text{ m}$ ), showed the best overall results.

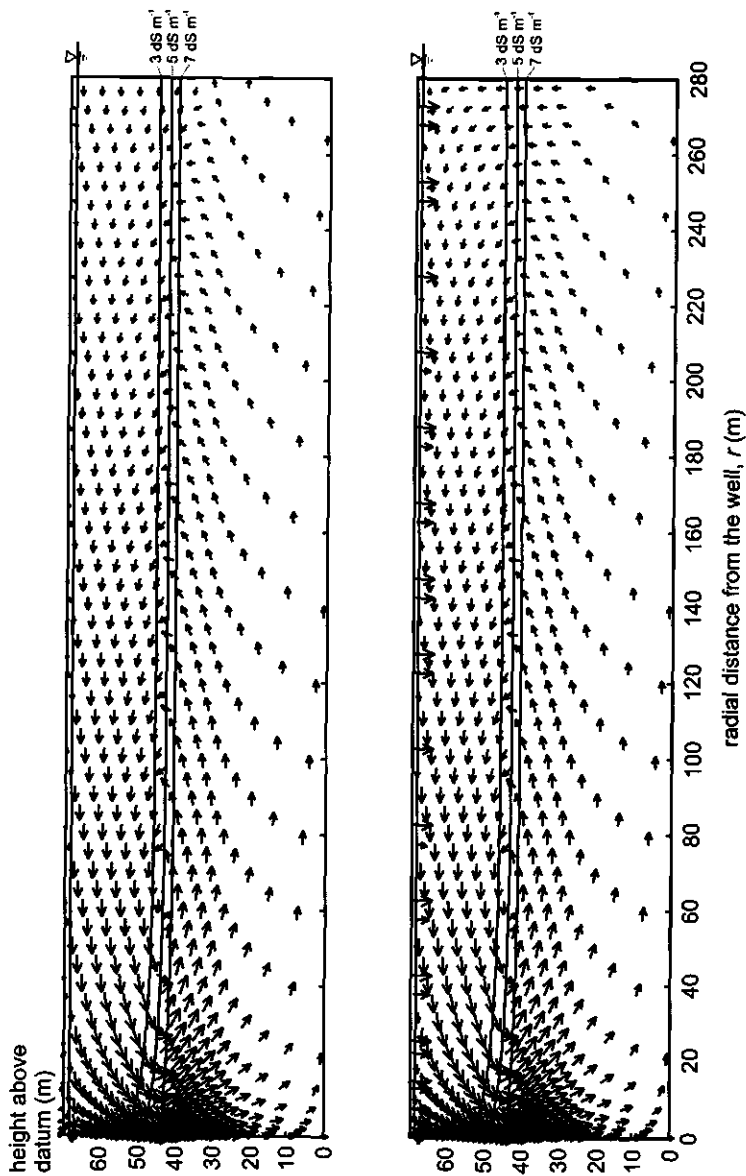


Figure 6.10 SUTRA simulated flow direction, depth of the groundwater table and groundwater salinity contours for the skimming well after the 164-day recovery period. The top figure relates to simulation mode (1) that combines a no flow boundary at the bottom of the rootzone with a hydrostatic boundary at the outer radius. The bottom figure relates to simulation mode (2) that combines a (recharge) flux boundary at the bottom of the rootzone with a no flow boundary at the outer radius. Vectors on log-scale; every 25<sup>th</sup> vector is printed.

Both measurements and simulations indicate that a 164-day recovery period is not enough to reduce the salinity at the well screen nodes to pre-pumping values. Two explanations can be given for the slow recovery: (1) Gravitational forces that result from the differences in the density of the water are the main driving force during recovery. These gravitational forces are low compared to the hydraulic gradients caused by pumping (Kemper et al., 1976); (2) Theory and laboratory experiments on pore-scale dispersion indicate that most of the flow occurs along the centre lines of the larger pore spaces as saline water is drawn up through the fresh water zone. Then ionic diffusion carries dissolved salt to the pore walls and into smaller interstices of the pore structure. When gradients are reversed, and fresh water is drawn back through the system, the inflow of fresh water displaces the saline water along the centre lines of the larger pores. However, inward ionic diffusion from the pore walls or from the smaller pores now causes the fresh water to become saline. Hence, a large volume of fresh water must be circulated back through the saline groundwater mound to reduce salinity levels. The volume of fresh water required may range from 3-10 times the original volume of saline water which was introduced (Bennett, 1990).

#### 6.4 Validation of the SUTRA model for the *scavenger well* experiment

The SUTRA model was validated with data from the scavenger well experiment at Phularwan farm (Table 6.1). The complete 23-day pumping period was simulated. Validation on data for the double-screen well was not possible because no radial symmetry can be assumed for this well. Simulation of the double-screen well would require a fully three-dimensional model (e.g. Sufi et al., 1998). The boundary conditions and the initial groundwater salinity for the scavenger well simulation are shown in Fig. 6.11. Initial depth of the groundwater table was 1.74 m. Electrical conductivity of the recharge was  $1.4 \text{ dS m}^{-1}$  (equal to the salinity of the shallow groundwater). All other input parameters were the same as for the skimming well (Table 6.2).

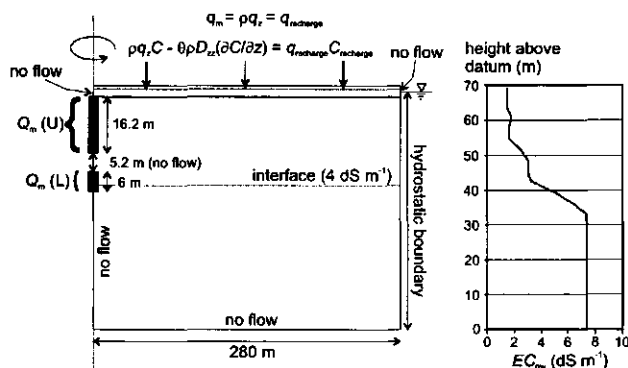
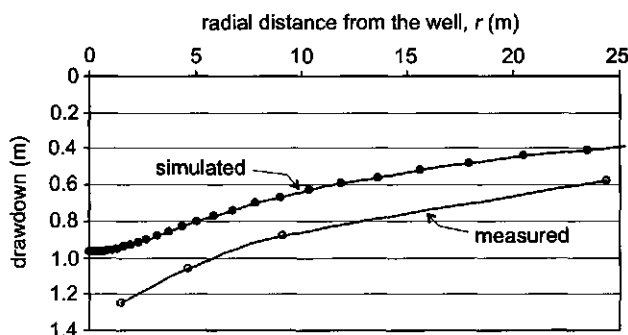


Figure 6.11 Set-up, boundary conditions and initial groundwater salinity,  $EC_{gw}$  for the validation of the SUTRA model on the *scavenger well* experiment.

Comparison between measured and simulated drawdown of the groundwater table after 20 days of pumping (17 Nov.) (Fig. 6.12), shows that the measured drawdown is about 0.2 m more than the simulated drawdown. Close to the well-axis the difference between measured and simulated values increases. The difference close to the well-axis is again due to the neglect of entrance resistance at the well screen and the equal distribution of discharge along the contributing screen nodes. The 0.2 m difference at some distance away from the well is probably due to the assumed steady-state boundary conditions. In the field, recharge and regional depth of the groundwater table will not remain constant over a 20-day period. For example, if during the 20-day pumping period, the regional groundwater table drops from 1.74 m to 1.94 m below soil surface, this would fully explain the difference between the measured and simulated drawdown. Unfortunately, the regional depth of the groundwater table during the scavenger well experiment was not reported (Kemper et al., 1976).



**Figure 6.12** Measured and SUTRA simulated drawdown of the groundwater table for the validated scavenger well.

Measured and simulated pumped water salinity,  $EC_{tw}$  for the scavenger well is shown in Fig. 6.13. The increasing trends in the salinity of both the upper "fresh" screen water and the lower "saline" screen water are simulated correctly by the model. The  $EC_{tw}$  levels, however, are somewhat underestimated. The simulated values are ~10 % too low for both the upper and the lower screen. Inaccuracies in the measurement of the initial  $EC_{gw}$  might be the reason for this discrepancy. Inspection of Fig. 6.11 shows that the distribution of  $EC_{gw}$  with depth at the scavenger well site is indeed less smooth than could be expected for a fresh-saline groundwater system that is at equilibrium. Overall, the SUTRA predictions for the skimming well and the scavenger well are of sufficient quality to use the model for scenario analysis, as will be done in the next sections.

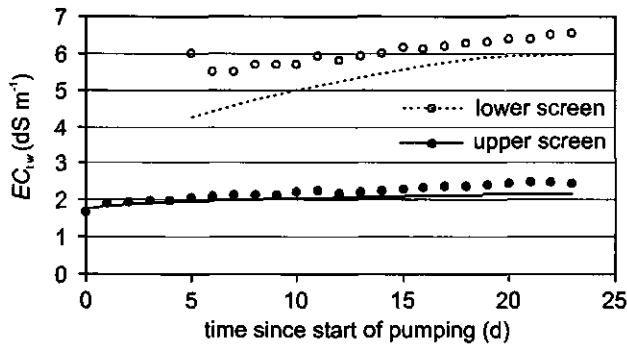


**Figure 6.13** Measured and SUTRA simulated pumped water salinity,  $EC_{tw}$  for the validated scavenger well.

### 6.5 Scenario analysis 1: Effluent salinity of a skimming well

To test the influence of skimming well design on the effluent salinity, three different well designs were simulated (Table 6.3). The well penetration ratios of 0.3 and 0.5 in the simulations follow the recommendations of McWhorter (1980) for aquifers without stratification and with stratification, respectively (Section 6.1). Where well penetration ratio is defined as the ratio between the depth of the well below the undisturbed groundwater table and the undisturbed fresh water thickness. The design of the skimming well used for calibration was not simulated because its screen depth of 3.0-18.0 m is too deep (well penetration ratio of 0.63), causing a quick deterioration of the well water quality (Fig. 6.6).

All three designs were simulated using the same pumping schedule of 1 day pumping followed by 9 days of recovery. This schedule gives a fair representation of the actual pumping schedules for farmer owned tube-wells in the Indus plain (e.g. Malik and Strosser, 1993). Note that the pumping rates mentioned in Table 6.3 of  $612\text{--}1223\text{ m}^3\text{ d}^{-1}$ , are low compared to the average pumping rates used in the Indus plain for farmer tube-wells ( $2447\text{ m}^3\text{ d}^{-1}$ ) and for public tube-wells ( $4893\text{--}7340\text{ m}^3\text{ d}^{-1}$ ). The relatively shallow screens used in the simulations, which are unavoidable because of the thin fresh groundwater zone, do not allow high pumping rates.

**Table 6.3** Design parameters of the simulated skimming wells.

	Pumping rate ( $\text{m}^3\text{ d}^{-1}$ )	Screen depth (m)	Well penetration ratio (-)
Shallow Low-discharge well, S-L	612	3.0-9.8	0.30
Deep Low-discharge well, D-L	612	3.0-14.6	0.50
Deep High-discharge well, D-H	1223	3.0-14.6	0.50

The simulation set-up and the input data for the simulated well are the same as for the calibrated skimming well (Fig. 6.4; Table 6.2) with a few exceptions which are discussed below. The outer radial boundary is treated as a no flow boundary instead of a hydrostatic pressure boundary. This

is the appropriate boundary condition for a well that is part of a complete well field. In other words: The simulation set-up assumes that the entire area is covered with skimming wells. Because the flow domain around the well is now isolated from the remainder of the aquifer, long term discharge should be equal to long term recharge to prevent that the well domain becomes either depleted or overflows. A dynamic equilibrium between discharge and recharge is guaranteed when:

$$\int_{t_1}^{t_2} Q_m dt = \int_{t_1}^{t_3} (q_{\text{recharge}} \pi r_e^2) dt \quad (6.1)$$

where  $t_1$  [T] denotes the start of the pumping cycle,  $t_2$  [T] the end of the pumping period,  $Q_m$  [M T<sup>-1</sup>] the pumping capacity of the well on mass basis,  $t_3$  [T] the end of the recovery period (the start of the next pumping cycle) and  $q_{\text{recharge}}$  [M L<sup>-2</sup> T<sup>-1</sup>] the recharge from the rootzone on mass basis.

Equation (6.1) is used to determine the radial extent of the flow domain,  $r_e$ . This results in  $r_e = 197.33$  m for the low-discharge simulations (pumping rate 612 m<sup>3</sup> d<sup>-1</sup>) and  $r_e = 279.06$  m for the high-discharge simulation (pumping rate 1223 m<sup>3</sup> d<sup>-1</sup>). Initial depth of the groundwater table in the simulations is 1.75 m below soil surface. The simulation period of 1000 days (100 pumping cycles) is a compromise between the objective to study long term trends and the computational requirements. The  $EC$  of the recharge,  $EC_{\text{recharge}}$  of 1.2 dS m<sup>-1</sup> is assumed to remain constant over the simulation period to allow a fair comparison with the effluent salinity of pipe drains (discussed later).

Results for the three skimming well designs (Fig. 6.14), show that  $EC_{\text{tw}}$  is highest for the deep high-discharge well (~2.4 dS m<sup>-1</sup> after 1000 days), and lowest for the shallow low-discharge well (~1.7 dS m<sup>-1</sup> after 1000 days), as could be expected. The simulated number of pumping cycles (100) is sufficient to achieve a dynamic equilibrium in  $EC_{\text{tw}}$  for the low-discharge wells. The  $EC_{\text{tw}}$  for the high-discharge well has not yet reached a dynamic equilibrium, although this point seems not far away. The effect of the recovery periods is clearly visible in Fig. 6.14. At dynamic equilibrium, when salt water upconing has reached its maximum extent, the 9-day recovery period is long enough to reduce the  $EC$  at the well-screen nodes to the initial values of the preceding 1-day pumping period. Because the speed of the recession of the saline groundwater during recovery was found to be underestimated by the model (Section 6.3), it can be expected that in reality the  $EC_{\text{tw}}$  values are somewhat lower than those presented in Fig. 6.14.

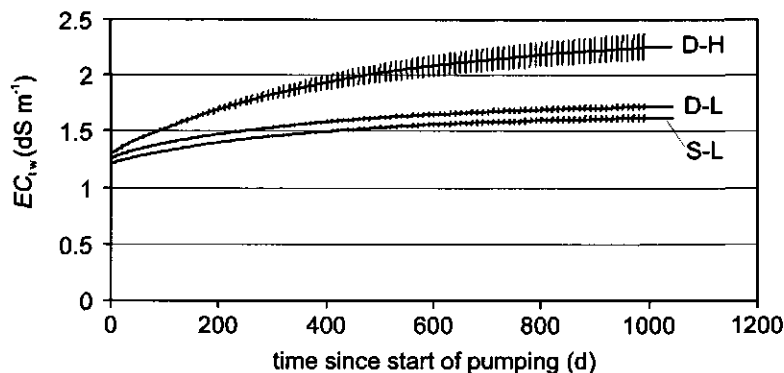


**Figure 6.14** SUTRA simulated pumped water salinity,  $EC_{tw}$  for three skimming well designs; a deep high-discharge well (D-H), a deep low-discharge well (D-L) and a shallow low-discharge well (S-L). For all three designs the pumping schedule consists of 1 day pumping followed by 9 days of recovery. The short, almost vertical lines, represent the 1-day pumping periods. The long solid lines indicate the average  $EC$  of the well-screen nodes.

Vector plots for the final day of pumping (day 991) and the final day in the last recovery period (day 1000) for the shallow low-discharge well are shown in Fig. 6.15. It should be noted that the size of the vectors in both plots in Fig. 6.15 cannot be compared directly, because they are scaled to different maximum values. Flow velocities during pumping (top plot) are much higher than velocities during recovery (bottom plot). The salinity contours show that the salt water upconing is considerable. The  $3 \text{ dS m}^{-1}$  contour line can be found at the bottom of the well screen, which is at 9.8 m below soil surface. This contour line moved 14.7 m upwards along the well-axis since the start of pumping.

Overall, the results indicate that, under the given conditions, a stable pumped water quality can be achieved both with a well penetration ratio of 0.3 and 0.5. All three well designs, however, yield water of marginal quality (Table 1.1), suggesting that the pumped water should only be used for irrigation purposes in conjunction with canal water ( $EC \sim 0.2 \text{ dS m}^{-1}$ ). It should be noted that use of the pumped water for irrigation will result in an increase of  $EC_{recharge}$ . For example, if all pumped water from the shallow-low-discharge well is used for irrigation this will result in a contribution of  $182 \text{ mm a}^{-1}$  ( $EC$  of  $1.7 \text{ dS m}^{-1}$ ). If the relative contributions from canal water and rainfall are  $450 \text{ mm a}^{-1}$  ( $0.2 \text{ dS m}^{-1}$ ) and  $350 \text{ mm a}^{-1}$  ( $0 \text{ dS m}^{-1}$ ), respectively, and a concentration factor of 5 is assumed (evapotranspiration from the rootzone), then the long term  $EC_{recharge}$  will be  $2.0 \text{ dS m}^{-1}$ . In turn this will result in higher long term  $EC_{tw}$  values.



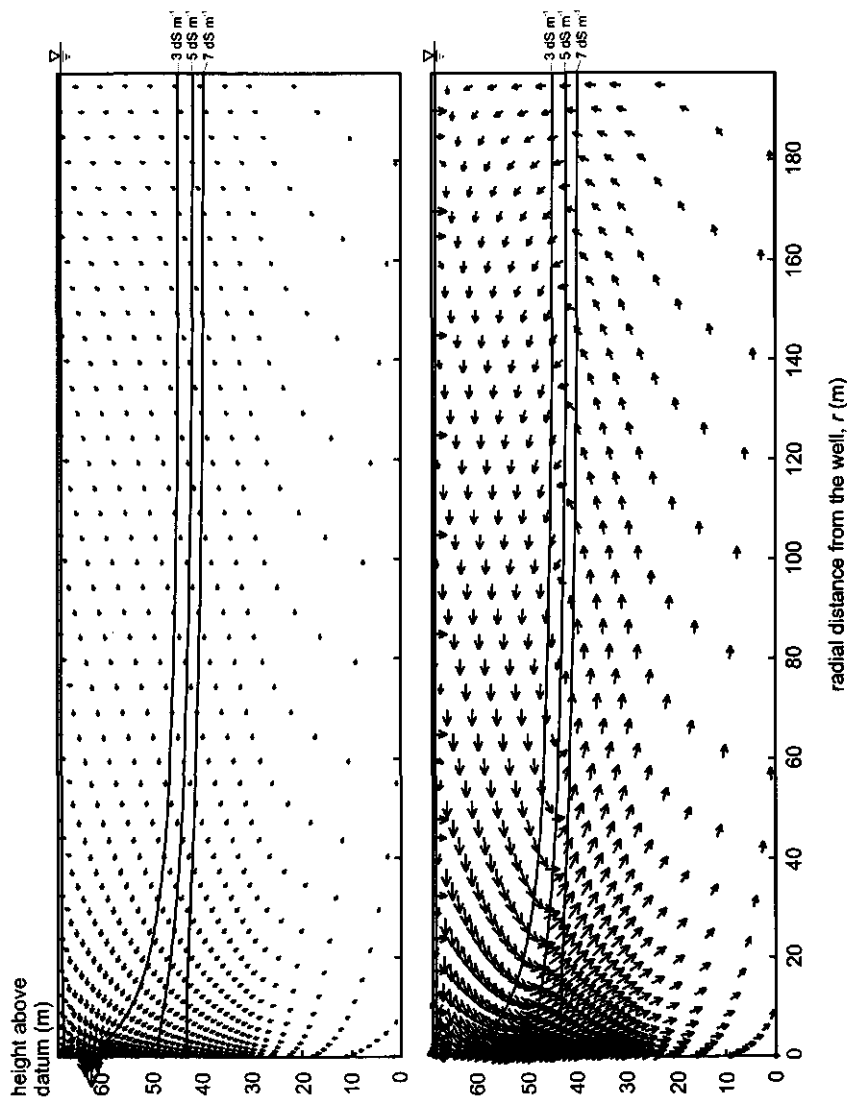


**Figure 6.15** SUTRA simulated flow direction, depth of the groundwater table and groundwater salinity contours for the shallow low-discharge well (S-L). The top plot depicts the soil-aquifer conditions at the final day of pumping (day 991). The bottom plot depicts the soil-aquifer conditions for the final day in the last recovery period (day 1000). Vectors on log-scale; every 2.5<sup>th</sup> vector is printed.

### 6.6 Scenario analysis 2: Effluent salinity of a pipe drain in fresh-saline groundwater

The behaviour of pipe drains was simulated for the same fresh-saline groundwater conditions. Drain depth was fixed at 2.0 m below soil surface and effective drain diameter,  $d_{\text{eff}}$  was fixed at 0.075 m. Three different drain spacings were tested: 75 m, 150 m and 300 m. These combinations of drain depth and drain spacing are more or less representative for actual pipe drainage designs in the Indus plain (Smedema, 1990). The initial depth of the groundwater table of 1.75 m below soil surface and the steady-state recharge of 0.5 mm d<sup>-1</sup> ( $EC_{\text{recharge}} 1.2 \text{ dS m}^{-1}$ ) were similar to those for the skimming well simulations. The simulation period for the pipe drain was 10 years.

The set-up of the pipe drain simulations is shown in Fig. 6.16. Because of symmetry only half of the flow region between two drains has to be analysed. The pipe drain was described in normal ( $x, z$ ) coordinates using a rectangular grid network with 80 nodes along the  $x$ -axis and 240 nodes along the  $z$ -axis. Close to the drain the distance between nodes was 0.05 m. Vertical spacing between nodes for the fresh groundwater zone and the transition zone was 0.2 m at maximum. The top 1 m of the soil-aquifer system was again treated as the rootzone and was not modelled. The pipe drain was represented by a single node (Section 2.6) with a constant pressure of zero. All other boundary conditions were the same as in the skimming well simulations. Note that the vertical extent of the flow domain was not adjusted according to drain spacing (Chapter 5, Section 5.5). To allow a fair comparison between pipe drains and skimming wells the thickness of the aquifer was kept at 70 m.

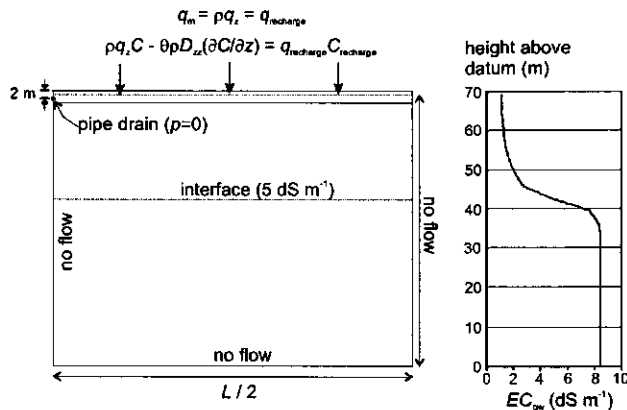


**Figure 6.16** Set-up, boundary conditions and initial groundwater salinity,  $EC_{gw}$  for the simulated pipe drain.

Results for the three drain spacings (Fig. 6.17) show that  $EC$  of the drainage water,  $EC_{dw}$  is highest for drain spacing  $L = 300 \text{ m}$  and lowest for  $L = 75 \text{ m}$ , as could be expected. Larger drain spacings result in deeper flow lines, mobilizing deeper, more saline groundwater. The absolute difference between the final  $EC_{dw}$  values of  $\sim 0.1 \text{ dS m}^{-1}$  is however small and is not significant under field conditions. All three drain spacings deliver water of usable quality (Table 1.1,

Chapter 1). The relatively sharp increase in  $EC_{dw}$  for  $L = 75$  m during the first year of drainage is due to the fact that initial discharge for this drain spacing is relatively high ( $3.8 \text{ mm d}^{-1}$  at maximum), resulting in some additional discharge of saline groundwater. For the three drain spacings it takes 66–113 days before the groundwater table recedes to its equilibrium position. At equilibrium, drain discharge is equal to recharge ( $0.5 \text{ mm d}^{-1}$ ). During the remainder of the simulated period some temporal fluctuations remain in the  $EC_{dw}$  values. The fluctuations are the result of the development of circulation patterns in the saline groundwater (discussed next).

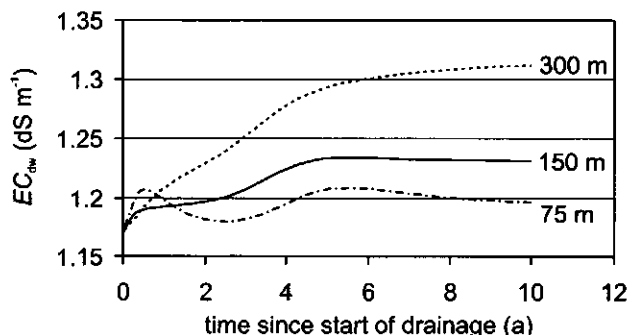


**Figure 6.17** SUTRA simulated drainage water salinity,  $EC_{dw}$  for three pipe drainage designs (drain spacing,  $L=75$  m,  $L=150$  m and  $L=300$  m).

A vector plot for  $L = 150$  m for the end of the 10-year simulation period is shown in Fig. 6.18. Two distinctly different flow regions can be identified. In the shallow "fresh" groundwater, vectors are directed towards the pipe drain. Flow in this region is driven by advection. In the deeper "saline" groundwater, a circulation pattern exists. Flow velocities in the saline zone are small (vectors are on log-scale). The circulation pattern develops during the second year of drainage. This typical pattern is the result of the interaction between dispersion and gravitational forces and is triggered by the flow of relatively fresh groundwater over the saline groundwater body (Santing, 1986; Herbert et al., 1988). There is no significant upconing of saline groundwater below the pipe drain. Groundwater salinity contours remain virtually horizontal. *Overall, the results show that flow towards the pipe drain is restricted to the shallow groundwater where the salinity is low.*

Direct comparison between the simulated effluent salinity of skimming wells and pipe drains is done best on the basis of cumulative drainage,  $D$  and cumulative pumping,  $Q$  (Fig. 6.19). *The superiority of pipe drains over skimming wells with regard to effluent salinity is clearly visible.* The better effluent quality for the pipe drains should be evaluated against the costs for both technologies. In the Indus plain, pipe drainage systems are about 10 times more expensive than tube-wells (roughly US\$1000  $\text{ha}^{-1}$  against US\$100  $\text{ha}^{-1}$ ). Note that the use of conventional deep tube-wells (borehole up to 60 m depth; pumping rate  $4893\text{--}7340 \text{ m}^3 \text{ d}^{-1}$ ), would have resulted in  $EC_{tw}$  values of approximately  $8.4 \text{ dS m}^{-1}$ , being the salinity of the deeper saline groundwater. Clearly, (regional) water management benefits considerably if a skimming technology is used for

drainage of areas where fresh groundwater is overlying saline groundwater.

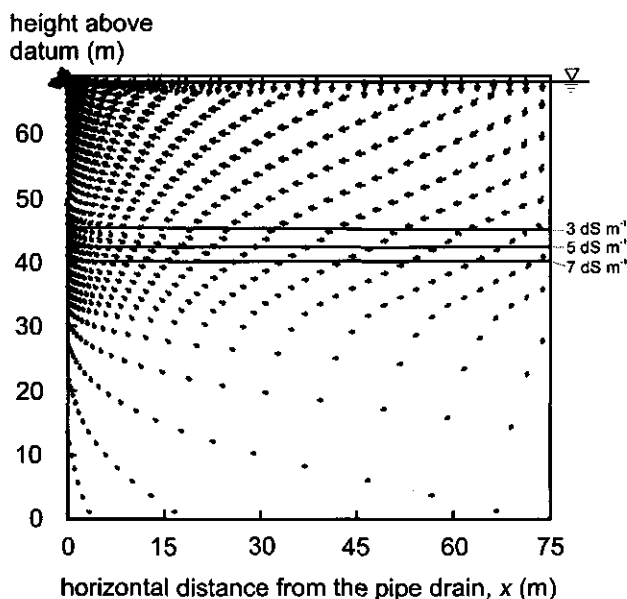


**Figure 6.18** SUTRA simulated flow direction, depth of the groundwater table and groundwater salinity contours for pipe drains with drain spacing,  $L=150$  m after 10 years of drainage. Vectors on log-scale; every 25<sup>th</sup> vector is printed.

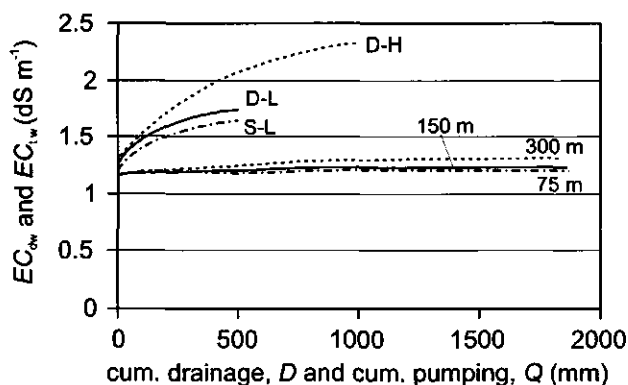


**Figure 6.19** Pumped water salinity,  $EC_{tw}$  for three skimming wells (deep high-discharge well (D-H), deep low-discharge well (D-L) and shallow low-discharge well (S-L)) and the drainage water salinity,  $EC_{dw}$  for three pipe drain spacings (75 m, 150 m and 300 m) as a function of cumulative drainage,  $D$  and cumulative pumping,  $Q$ .

### 6.7 Scenario analysis 3: Effluent salinity of a pipe drain in saline groundwater

The calibrated model can be used to simulate many different drainage situations for the area. One interesting hypothetical case is considered here. It is assumed that the area is completely saline with a uniform soil and groundwater salinity of  $8.4 \text{ dS m}^{-1}$ . Under these conditions pipe drains provide the most attractive drainage solution for two reasons. (1) Farmers will not be inclined to use tube-wells because they cannot use the saline water for irrigation. (2) With pipe drains the mobilization of salts from the deeper groundwater, where they are harmless, is kept to a minimum. As a result, effluent salinity is likely to improve relatively fast.

In all previous simulations the  $EC_{\text{recharge}}$  was kept constant at a value that assumes long term equilibrium with the shallow groundwater (Table 6.2). In the present case as the saline rootzone is reclaimed,  $EC_{\text{recharge}}$  decreases with time. To incorporate this process, it was assumed that the rootzone will act as a completely mixing reservoir. Soil water content is at field capacity. The salinity of the recharge from the reservoir is calculated from (Van Hoorn, and Van Alphen, 1994):

$$C_{\text{recharge}} = f_l C_{fc} + (1 - f_l) C_i \quad (6.2)$$

with

$$C_{fc} = C_i + (C_{0, \text{rootzone}} - C_i) e^{-\frac{f_l t q_{\text{recharge}}}{W_{fc}}} \quad (6.3)$$

where  $C_{\text{recharge}}$  is the solute concentration  $[\text{M M}^{-1}]$  of the recharge,  $f_l$  the leaching efficiency coefficient [-],  $C_{fc}$  the solute concentration  $[\text{M M}^{-1}]$  of the rootzone (at field capacity),  $C_i$  the solute concentration  $[\text{M M}^{-1}]$  of the influent (rainfall and irrigation),  $C_{0, \text{rootzone}}$  the solute concentration  $[\text{M M}^{-1}]$  of the rootzone at time  $t = 0$ ,  $q_{\text{recharge}}$  the flow rate  $[\text{L T}^{-1}]$  through the rootzone and  $W_{fc}$  the depth  $[\text{L}]$  of water stored in the rootzone.

The term root zone is a bit misleading as in Eqs. (6.2) and (6.3) no root water uptake is assumed. Note that the long term  $C_{\text{recharge}}$  value will be equal to  $C_i$ . Theoretically,  $C_i$  is calculated as the weighted average of the solute concentration of irrigation water and rainfall. This would result in a  $C_i$  value  $< 0.2 \text{ dS m}^{-1}$ . Under actual field conditions, however, the long term  $C_{\text{recharge}}$  value will be higher than  $C_i$  because the solutes in the soil water are concentrated due to soil evaporation and root water uptake. To prevent underestimation of the  $C_{\text{recharge}}$  value, and therefore underestimation of the effluent salinity, it is assumed, as in the previous sections, that the  $C_i$  value remains  $1.2 \text{ dS m}^{-1}$ . Conceptually, this can be understood by assuming that soil evaporation as well as root water uptake take place at the soil surface.

Equations (6.2) and (6.3) are incorporated in SUTRA with leaching efficiency coefficient,  $f_l$  is 0.8. All other parameters remain unchanged compared to the pipe drain simulation in the

previous section ( $q_{\text{recharge}}$  is  $0.5 \text{ mm d}^{-1}$ ). Results are shown in Fig. 6.20. The figure shows that for the given situation rootzone salinity decreases quickly. After 2 years,  $EC_e$  has reduced to  $2 \text{ dS m}^{-1}$ . Effluent salinity reduces much slower with time. After 10 years,  $EC_{\text{dw}}$  is still as high as  $5.3 \text{ dS m}^{-1}$ . Figure 6.20 indicates that, if the simulation period is prolonged, the  $EC_{\text{dw}}$  will continue to decrease. It can be expected that the long term equilibrium  $EC_{\text{dw}}$  value will be about  $1.2 \text{ dS m}^{-1}$ . The time lag between the development of rootzone and effluent salinity is typical for alluvial areas as found in the Indus plain (Chapter 5).

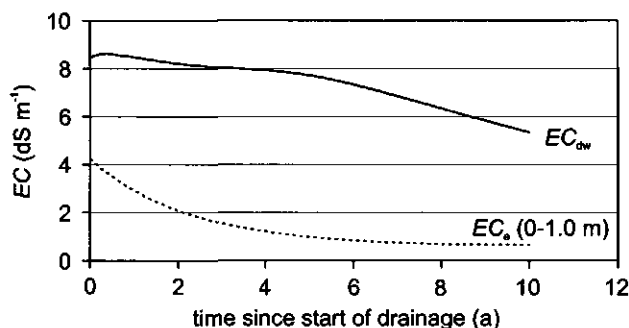


**Figure 6.20** SUTRA simulated soil salinity,  $EC_e$  (0-1.0 m) and drainage water salinity,  $EC_{\text{dw}}$  for a pipe drain ( $L = 150 \text{ m}$ ) in a completely saline soil-aquifer system.

*It should be noted that the speed of the reclamation process is strongly related to the recharge from the agricultural fields overlying the drainage system. The annual average value of  $0.5 \text{ mm d}^{-1}$  is just an estimate for conditions in the Indus plain (in Chapter 5 values ranged between  $0.26 \text{ mm d}^{-1}$  (S-I-B-9) and  $0.57 \text{ mm d}^{-1}$  (Sampla  $L=75 \text{ m}$ )). A lower value for the recharge will increase the time needed for drainage water salinity to be reduced to equilibrium levels. Alternatively, the reclamation process can be sped up by providing additional leaching water to the agricultural fields. This is shown in Fig. 6.21 where the same pipe drain is simulated with  $q_{\text{recharge}} = 1.0 \text{ mm d}^{-1}$  and  $q_{\text{recharge}} = 1.5 \text{ mm d}^{-1}$ . Calculated  $EC_{\text{dw}}$  is given as a function of cumulative drainage,  $D$  (the calculation period remains 10 years). Figure 6.21 shows that the additional leaching water indeed results in faster reclamation (after 10 years  $EC_{\text{dw}}$  is  $3.0$  and  $2.2 \text{ dS m}^{-1}$  for  $q_{\text{recharge}} = 1.0$  and  $1.5 \text{ mm d}^{-1}$ , respectively). The calculations also show, however, that additional salts from the saline groundwater are mobilized. This is due to the increased hydraulic gradients in the flow system.*

Finally, the initial condition with a completely saline soil and aquifer, provides a good opportunity to demonstrate the effect of density differences on the flow system. To this end, the calculations for  $q_{\text{recharge}} = 1.5 \text{ mm d}^{-1}$  were repeated while setting  $\partial\rho/\partial C$  to 0 (Eq. 2.14). By doing this a constant fluid density of  $1000 \text{ kg m}^{-3}$  is invoked, irrespective of the solute concentration. Figure 6.22 shows that the effect of density on  $EC_{\text{dw}}$  is considerable. The  $EC_{\text{dw}}$  after 10 years of drainage is  $4.3 \text{ dS m}^{-1}$  for  $\partial\rho/\partial C = 0$  compared to  $2.2 \text{ dS m}^{-1}$  for  $\partial\rho/\partial C = 700 \text{ kg m}^{-3}$ . Accounting for the density differences results in shallower flow patterns to the pipe drain which in turn results in less mobilization of saline groundwater. The above implies that the temporal changes

in effluent salinity as calculated in Chapter 5 are probably underestimated. This is especially true for the Sampla experimental pipe drainage site where the initial groundwater salinity was  $27 \text{ dS m}^{-1}$ .

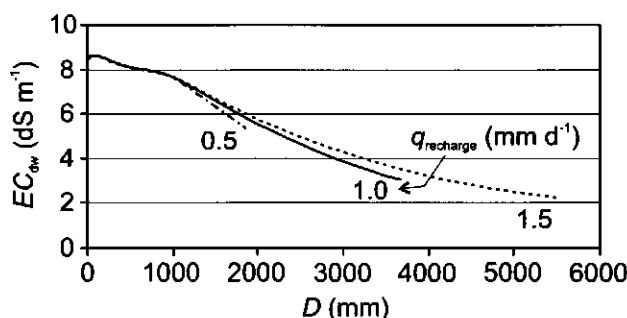


**Figure 6.21** SUTRA simulated drainage water salinity,  $EC_{dw}$  of a pipe drain ( $L = 150 \text{ m}$ ) in a completely saline soil-aquifer system for three recharge values ( $q_{\text{recharge}} = 0.5, 1.0$  and  $1.5 \text{ mm d}^{-1}$ ).

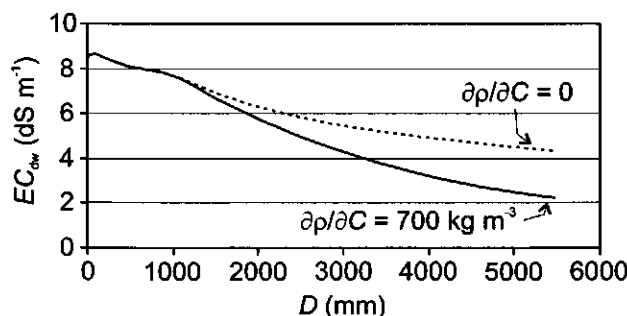


**Figure 6.22** SUTRA simulated drainage water salinity,  $EC_{dw}$  of a pipe drain ( $L = 150 \text{ m}$ ) in a completely saline soil-aquifer system ( $q_{\text{recharge}} = 1.5 \text{ mm d}^{-1}$ ) with and without incorporating fluid density effects.

## 6.8 Conclusions

Predicted pumped water salinity for the calibrated skimming well is sensitive to the anisotropy factor of the aquifer. An anisotropy factor of 4 provides the best results. This value is in the range of values for core samples, implying that the aquifer is relatively homogeneous (no separate soil layers). During no-pumping periods, the saline groundwater mound, that develops during pumping periods, will slowly recede. In order to simulate both pumping and no-pumping periods correctly, small values of the longitudinal dispersivity,  $\alpha_L$  and transverse dispersivity,  $\alpha_T$  are

required (0.1 and 0.005 m, respectively). Both the calibrated skimming well and the validated scavenger well are unable to produce water with a constant low salinity. For the calibrated skimming well this conclusion is not surprising, as this well was constructed too deep on purpose (McWhorter, 1980).

*Comparison between pipe drains and skimming wells shows that, in areas where relatively fresh groundwater is overlying saline groundwater, pipe drains discharge water of lower salinity than skimming wells. With pipe drains, flow is restricted to the shallow "fresh" groundwater. The deeper "saline" groundwater is left untouched. This is an important feature with regard to effluent quality control. It implies that potentially harmful salts from the rootzone and the shallow groundwater can be removed from the system, while limiting the mobilization of salts from greater depth, where they pose no threat to crop production. With skimming wells, the saline groundwater is also contributing to flow. Pumping from skimming wells will bring salts to the surface that would otherwise have remained safely in the deeper aquifer. The better effluent quality for pipe drains as compared to skimming wells must be evaluated against the considerably higher installation costs for pipe drains.*

In areas where soil and groundwater are completely saline, pipe drains provide the best drainage solution. Calculations show that it may take more than 10 years before drainage water salinity has reduced to equilibrium levels. Reclamation of the rootzone goes much faster (in about 2 years according to the presented example). This time lag between the development of rootzone salinity and effluent salinity is typical for alluvial areas as found in the Indus plain (Chapter 5). The reclamation process can be accelerated by providing additional leaching water to the agricultural fields. This, however, increases hydraulic gradients in the flow domain, resulting in deeper flow lines and more mobilization of salts from the saline groundwater.

Exclusion of fluid density effects is shown to have significant influence on the calculated effluent salinity for a pipe drain in saline groundwater ( $EC = 8.4 \text{ dS m}^{-1}$ ). Neglecting fluid density results in deeper flow lines and more mobilization of saline groundwater. This implies that the temporal changes in effluent salinity as calculated in Chapter 5 are probably underestimated. This is especially true for the Sampla experimental pipe drainage site where the initial groundwater salinity of  $27 \text{ dS m}^{-1}$  was high.

The implications of the findings in this chapter for drainage planning in the Indus plain are discussed in Chapter 7.



## 7 Summary and Conclusions

Irrigated agriculture in arid and semi-arid zones often suffers from waterlogging and salinity problems. Excess water in the crop rootzone and high soil salinity reduce transpiration and hence crop yields. Sub-surface drainage systems can be used to control the groundwater table and to facilitate the leaching of salts from the rootzone. The field drainage system may consist of ditches, mole drains, pipe drains or tube-wells. The choice for one of these systems is made on the basis of geo-hydrology, costs and the expected quality of the effluent. With the increasing scarcity of fresh water resources, especially in arid and semi-arid zones, the effluent quality is becoming increasingly important when drainage options are considered. Disposal of the effluent should not detriment the water resources downstream. Furthermore, drainage effluent may be an important source of irrigation water in dry areas, provided that certain water quality criteria are met.

The Indus plain forms a typical example of an irrigated area in an arid to semi-arid zone where sub-surface drainage systems are installed to combat waterlogging and salinity. A distinction is made between fresh and saline groundwater areas. In fresh groundwater areas, irrigation tube-wells take care of the sub-surface drainage requirements. In saline groundwater areas, drainage is provided by either pipe drains or tube-wells. The saline effluent is mostly disposed in surface drains and salt load is the main problem. It is generally assumed that, after a certain reclamation period, pipe drains render a better effluent quality than tube-wells. The flow lines to pipe drains are shorter and therefore originate from usually less saline groundwater layers (Smedema, 1993). *The objective of this study is to review the relationship between drainage technology (pipe drains and tube-wells) and the effluent salinity in the Indus plain. Field data from existing drainage schemes and pilot areas are combined with hydrodynamic models to quantify this relationship.* The hydrodynamic models allow the identification of the most dominant processes and facilitate long term predictions. The results of this study will assist irrigation and drainage engineers with the selection of the proper drainage method, taking into account the expected effluent salinity.

In Chapter 2 the theory of water flow and solute transport in porous media is discussed. The chapter starts however with a section on the calculation of soil evaporation and crop transpiration. The presented relationships are used to determine the water fluxes between the soil profile and the atmosphere in the SWAP model (discussed later). Subsequently, the water flow and solute transport equations are presented. These equations form the basis of the finite-element model SUTRA (Voss, 1984), the finite-element model SWMS\_2D (Šimůnek et al., 1994) and the vertical one-dimensional finite-difference model SWAP (Van Dam et al., 1997). In all three models, water flow is described by a combination of the Darcy equation and the basic mass balance equation. Solute transport in these models is described by the advection-dispersion equation, although this option is not used for the SWMS\_2D model in this study. All three models are applied in cross-sectional mode.

The theory of solute travel time to pipe drains and tube-wells in steady-state flow fields is discussed in Chapter 3. The stream function concept is explained which allows the calculation of streamlines towards the drainage media. The governing equations for two-dimensional flow and axi-symmetrical flow in a vertical cross-section are given. Several investigators derived

analytical expressions for the stream function in pipe drained soils for various conditions. In this study, the expressions for seepage to a pipe drain in a two-layered soil as developed by Töksoz and Kirkham (1971) are used. These expressions can be used for anisotropic soils by employing a coordinate transformation and by re-calculating hydraulic conductivity. The shape of the streamlines in the Töksoz and Kirkham approach is independent of the recharge due to a number of simplifying assumptions. For partially penetrating wells no analytical solutions of the stream function are available. The stream function of this type of well is calculated numerically in a spreadsheet using a finite-difference approach as given by Olsthoorn (1998).

In the remainder of Chapter 3 it is explained how solute travel time can be calculated from the streamline pattern. For pipe drains, this requires that the cross-sectional area of each stream tube is determined by means of numerical integration along the bounding streamlines. For tube-wells, solute travel time is calculated by particle tracing in the flow field using the Euler integration formulas. To calculate solute transport to pipe drains and tube-wells, cumulative outflow can be used as a substitute for solute travel time. This allows the flow regime to be transient. Solute breakthrough follows from a direct comparison of the cross-sectional area (pipe drains) or volume (tube-wells) of the stream tubes on the one hand and cumulative outflow on the other. This requires that the stream tubes are time-invariant, which is true under the assumptions discussed in Chapter 3. For pipe drains, the cross-sectional area of each stream tube follows from the numerical integration discussed above. For tube-wells, the volume of each stream tube is calculated indirectly, after solute travel time has been determined by particle tracing.

A description of the hydrological characteristics of the Indus plain is given in Chapter 4, together with a description of three of the study areas. The climate in the Indus plain ranges from arid in Sindh to semi-arid in the Punjab. Average annual rainfall ranges from ~100 mm to 1000-1400 mm. The aquifer in the Indus plain mainly consists of sand intersected by silt and clay. Thickness of the aquifer ranges from a few metres close to rock outcrops to a few kilometres at the centre of the plain. About 16 million ha fall in the canal commanded areas. Three study areas are discussed in Chapter 4 (a fourth is discussed in Chapter 6). The 9-ha Sampla experimental pipe drainage site represents a case where high soil and groundwater salinity have made the area unfit for crop production. The Sampla site provides a good opportunity to follow the reclamation process after the introduction of pipe drains. The Satiana tube-well Pilot Project (40,000 ha) is representative for a typical public tube-well drainage project in Pakistan. Fifty (drainage) wells are situated alongside main surface drains, and 21 (irrigation) wells are situated alongside irrigation canals. Finally, the Fourth Drainage Project (FDP) is discussed. This large scale pipe drainage project covers 120,000 ha and consists of 79 separate sump units. One of these units, S-I-B-9, is discussed in more detail.

Analysis of the field data results in the following observations. The head-discharge relationships for the Sampla experimental pipe drainage site and the S-I-B-9 pipe drainage unit show that flow to the pipe drains mainly occurs below drain level. This implies that the schematization of Töksoz and Kirkham (1971) is applicable for the relatively coarse textured soil-aquifer system in the Indus plain. The Sampla experimental pipe drainage site shows that soil salinity reduces quickly in response to drainage. In contrast, effluent salinity reacts slowly. At Sampla, it takes approximately 9 years before the *EC* of the effluent has reduced from 20-60 dS m<sup>-1</sup> to 10.5 dS

$\text{m}^{-1}$ . For the Satiana tube-wells and the FDP pipe drainage units, effluent salinity does not change significantly with time. The slow reaction is attributed to the dampening effects of the deep, highly conductive aquifer. The higher average *EC* of  $3.1\text{--}3.3 \text{ dS m}^{-1}$  of the Satiana *drainage* tube-wells as compared to the *EC* of  $2.3\text{--}2.4 \text{ dS m}^{-1}$  of the FDP pipe drainage units is attributed to the fact that tube-wells attract groundwater from greater depths, which is generally more saline.

The prediction of long term effluent salinity of pipe drains and tube-wells is discussed in Chapter 5. The chapter starts by introducing a new modelling approach for pipe drains. The flow region is divided into two zones: one above drain level where only vertical flow is assumed, and one below drain level where flow is two-dimensional. This schematization follows the geometry of the soil-pipe-aquifer system as used by Töksoz and Kirkham (1971). Water flow and solute transport in the zone above drain level are described with the SWAP model. The zone below drain level is characterized by the stream functions of Töksoz and Kirkham (1971). In the stream tubes, piston flow is assumed. The effluent salinity is calculated with a convolution integral, using cumulative drainage as the driving force. In Chapter 5, the SWMS\_2D model is used to simulate head-discharge relationships for pipe drains to help determine some of the soil hydraulic properties.

Modelling results for the Sampla experimental pipe drainage site show that effluent salinity improves gradually with time. Complete reclamation of the soil and aquifer, which determines effluent salinity, takes approximately 10 years. In reality, the reclamation rate will be less because of the continuous inflow of saline groundwater from the surrounding area. At Sampla, drain spacing has little effect on effluent salinity. This is due to the impermeable layer at 1.25 m below drain level which restricts the flow below drain level to a limited part of the upper aquifer. Results for the S-I-B-9 pipe drainage unit of the Fourth Drainage Project show that complete reclamation of the soil and aquifer will not be achieved within the economic life of the system ( $\sim 25$  years). Reclamation at S-I-B-9 is relatively slow because of the low drain discharge of  $96 \text{ mm a}^{-1}$ , the relatively large drain depth of 2.4 m and the deep groundwater flow (up to 87.4 m below drain level).

Chapter 5 continues by discussing a new modelling approach for tube-wells. Again the flow region is divided into two zones. The boundary between the two zones is formed by the horizontal plane that coincides with the water level in the well during pumping. This so-called horizontal boundary plane is comparable to drain level for the pipe drainage case. Flow above this plane is assumed vertical. Flow below this plane is three-dimensional, assuming radial symmetry around the well-axis. Water flow and solute transport above the horizontal boundary plane are calculated with the SWAP model. The zone below the horizontal boundary plane is characterized by streamlines which are calculated numerically. In the stream tubes piston flow is assumed. The solute concentration of the tube-well water is determined again by convolution, using cumulative pumping as the driving force.

Modelling results for a Satiana *drainage* tube-well show that effluent salinity will not change significantly during the operational period of the well. This is due to the low percentage of operation of the tube-well, the depth of the well screen (20 to 40 m below soil surface) and the deep groundwater flow (up to 223.5 m below the horizontal boundary plane). SWAP simulated

$EC_e$  (0-1 m) for Sampla, S-I-B-9 and Satiana suggests that after 1-3 years of drainage, crops will no longer suffer from soil salinity. *The time lag between the reclamation of the rootzone and the reclamation of the complete soil-aquifer system (which determines the effluent salinity) appears to be an important feature of agricultural drainage systems in the Indus plain. The implication is that farmers will benefit quickly from the drainage system (reduced soil salinity) but that long term solutions are required for the safe use and disposal of the effluent.*

Effluent salinity is also calculated by assuming that the zone below drain level (pipe drains) or the zone below the horizontal boundary plane (tube-wells) behaves as a completely mixing reservoir. This implies that the solute impulse response functions for these zones follow a simple exponential distribution. The results of the mixing reservoir approach for the Sampla pipe drains compare well with the results of the stream function approach as long as the depth of the impermeable layer below drain level,  $b$  remains small ( $b = 1.25$  m). Comparison for Sampla using greater depths of the impermeable layer ( $b = 3.75$  m and  $b = 6.25$  m) and comparison for S-I-B-9 is less favourable. The relatively deep flow patterns for these cases, combined with the small outflow surface, result in deviations from the stream function approach. In contrast, the mixing reservoir approach performs relatively good for the Satiana well. This is due to the large outflow surface constituted by the well screen. It is concluded that for practical purposes, the mixing reservoir approach, which is much simpler than the stream function approach, suffices for most cases considered in Chapter 5.

The density-dependent water flow and solute transport model SUTRA is used to study the effluent salinity of tube-wells and pipe drains in Chapter 6. The model is applied to the Phularwan experimental skimming well site, where a fresh groundwater lense with a thickness of about 25 m is overlying saline groundwater with an  $EC$  of  $7-9$  dS  $m^{-1}$ . At Phularwan, several types of skimming wells have been field tested in the past. SUTRA is calibrated on a single-borehole skimming well experiment with a pumping period of 15 days and a recovery period of 164 days. Calibration is achieved mainly by varying the anisotropy factor of the sandy sub-layer, to which the results are very sensitive. The higher the anisotropy factor the lower the effluent salinity. This relationship is strongly non-linear. The model is validated on a scavenger well experiment with a 23-day pumping period.

To test the influence of skimming well design on the effluent salinity, three different well designs are simulated. For convenience these designs are indicated as: a shallow low-discharge well, a deep low-discharge well and a deep high-discharge well. The shallow well depth of 3.0 to 9.8 m below soil surface and the deep well depth of 3.0 to 14.6 m below soil surface correspond to well penetration ratios of 0.3 and 0.5, respectively. All three designs are simulated using the same pumping schedule of 1 day pumping followed by 9 days of recovery. The results from SUTRA indicate that, under the given conditions, a stable pumped water quality can be achieved with all three designs. The long term  $EC$  of the effluent is between  $1.7$  and  $2.4$  dS  $m^{-1}$ , with the lower value for the shallow low-discharge well, and the higher value for the deep high-discharge well. Water with these  $EC$  values is classified as marginal for irrigation purposes.

Subsequently, the behaviour of pipe drains is simulated for the same fresh-saline groundwater conditions as for the skimming well simulations. Three different drain spacings are tested: 75 m,

150 m and 300 m. Drain depth is fixed at 2.0 m below soil surface. Long term effluent salinity is between 1.2 and 1.3 dS m<sup>-1</sup>, with the lower value for the spacing of 75 m, and the higher value for the spacing of 300 m. Water with these *EC* values belongs to the usable category for irrigation purposes. With pipe drains, flow is restricted to the shallow "fresh" groundwater. The deeper "saline" groundwater is left untouched. This is an important feature with regard to effluent quality control. *It implies that potentially harmful salts from the rootzone and the shallow groundwater can be removed from the system, while limiting the mobilization of salts from greater depth, where they pose no threat to crop production or to the environment.* In contrast, pumping from skimming wells will bring salts to the surface that would otherwise have remained safely in the deeper aquifer. The better effluent quality for pipe drains as compared to skimming wells, must be evaluated against the considerably higher installation costs for pipe drains.

In areas where soil and groundwater are completely saline, pipe drains provide the best drainage solution. Calculations show that it may take more than 10 years before drainage water salinity has reduced to equilibrium levels. Reclamation of the rootzone goes much faster (in about 2 years according to the example presented in Chapter 6). This time lag between the reduction of rootzone salinity and effluent salinity is typical for alluvial areas as found in the Indus plain, as noted earlier. The reclamation process can be accelerated by providing additional leaching water to the agricultural fields. This, however, increases the hydraulic gradients in the flow domain, resulting in deeper flow lines and additional mobilization of salts from the deeper groundwater.

## Implications for drainage planning in the Indus plain

The optimum drainage technology for the Indus plain is strongly related to the groundwater conditions. A distinction is made between fresh groundwater areas, fresh-saline groundwater areas (fresh groundwater on top of saline groundwater) and saline groundwater areas. In practice, the differences between these groundwater areas are not so strict. For example, most fresh groundwater areas will be underlain by saline groundwater, only at considerable depth (e.g. > 150 m). Also, many saline groundwater areas will be overlain by thin fresh groundwater lenses of a few metres thick, originating from recent percolation of rainfall and irrigation water.

As explained in Chapter 1, in the fresh groundwater areas, irrigation tube-wells usually take care of the sub-surface drainage requirements. Most of these wells will deliver low salinity irrigation water over a long period of time because of the extensive size of the aquifer in the Indus plain (Chapter 4 and 5). The main challenges for the fresh groundwater areas are to prevent over-pumping both at the local and the regional scale, and to prevent soil sodicity problems at field level (the pumped water contains relatively large quantities of Na<sup>+</sup>). Over-pumping can probably only be prevented by proper legislation and its subsequent enforcement. The occurrence of soil sodicity problems is strongly related to the skills of the farmers and their ability to properly manage the various sources of water (canal, tube-well and rainfall). The availability of amendments like gypsum also plays a role. On the very long term some kind of salt export mechanism may become necessary for these tube-wells.

Fresh-saline groundwater areas will benefit considerably from the use of skimming technologies

(Chapter 6). Pipe drains yield a better effluent quality than skimming wells but are about 10 times more expensive. Skimming wells have the advantage that the pumped water can be used directly for irrigation. The maximum discharge of these wells however, which mainly depends on the thickness of the fresh-groundwater lense and the radial and vertical permeability of the aquifer, is low compared to the discharge from farmer tube-wells in fresh groundwater areas. Farmers need a minimum discharge in the order of  $2500 \text{ m}^3 \text{ d}^{-1}$  in order to irrigate their fields efficiently. Small discharge skimming wells may be combined with sprinkler or drip irrigation to obtain a viable system. At present, field tests of such a system are conducted by several institutes at the Phularwan Research farm in Punjab, Pakistan.

In saline groundwater areas, sub-surface drainage should be provided by pipe drains. The effluent salinity improves relatively fast if there is an impermeable layer at shallow depth or if the drain depth and drain spacing are kept small. Forced leaching by providing extra water to the fields will enhance the improvement of effluent salinity with time. However, additional salts are mobilized from the groundwater and total salt load from the drained area increases. For most practical cases, drainage planners should reckon with the fact that the effluent of pipe drains in the Indus plain remains saline for 10 years or more. This implies that pipe drains should only be installed in areas where an outlet exists for safe disposal. If no outlet is available, sub-surface drainage systems should not be installed at a large scale.

### Concluding remarks on the new modelling approach

In this study a new modelling approach is used to study the effluent salinity of pipe drains and tube-wells (Chapter 5). The approach should only be used for relatively coarse-textured soil-aquifer systems because of a number of simplifying assumptions. Most importantly, the assumption of one-dimensional vertical flow in the zone above drain level (pipe drains) or the zone above the horizontal boundary plane (tube-wells). The neglect of density differences in the groundwater implies that the modelling approach has the tendency to underestimate the reclamation rate of the soil-aquifer system, resulting in an overestimation of the effluent salinity with time (see Chapter 6). This is especially true for areas with a high groundwater salinity, like the Sampla experimental pipe drainage site. In contrast, the exclusion of regional flow processes from the analysis is likely to cause an overestimation of the reclamation rate of the soil-aquifer system, resulting in an underestimation of the effluent salinity with time. The extent to which these two phenomena cancel each other out is dependent on the local geo-hydrological conditions. This issue is not addressed in this thesis and may be a good subject for further study.

The use of the SWAP model to calculate water flow and solute transport in the zone above drain level or in the zone above the horizontal boundary plane provides a state-of-the-art estimate of the percolation from the irrigated agricultural fields to the groundwater. The transient nature of the flow processes in the variably saturated zone and the close interaction with crop growth are fully recognized. A good estimate of the amount of percolation is important because it is one of the main variables determining the speed of the reclamation process. The other key variable determining the development of the effluent salinity is the depth of the active flow domain.

Unfortunately, it is usually not possible to estimate this depth from field data alone. For most cases, this parameter must be approximated with methods as discussed in Chapter 5.

It has been shown in Section 5.8 that the zone below drain level or the zone below the horizontal boundary plane can also be represented as a mixing reservoir. The mixing reservoir approach is much simpler than the stream function approach and is already incorporated in the SWAP model as a tool to assess solute breakthrough from the saturated zone. The mixing reservoir approach works particularly well if a shallow impermeable layer restricts the groundwater flow to the upper aquifer (pipe drains) or if the well screen penetrates a large portion of the aquifer (tube-wells). In case these conditions are not met (e.g. pipe drains in an aquifer allowing deep groundwater flow or shallow partially penetrating wells), the mixing reservoir approach still gives a fair representation of the development of effluent salinity with time.

In principle, the calculations in Chapter 5 could also be done with a two-dimensional numerical model in cross-sectional mode. This would require fewer assumptions about the flow processes in the soil-pipe-aquifer domain. The use of two-dimensional models in transient mode, however, increases the calculation time dramatically and is therefore not advised for the long term calculations as done in Chapter 5.





## Samenvatting en conclusies

De geïrrigeerde landbouw in aride en semi-aride streken heeft vaak last van hoge grondwaterstanden en van verzouting. Teveel water in de wortelzone en een te hoog zoutgehalte in de bodem belemmeren de gewasverdamping en daarmee de gewasoogst. Veld drainage kan worden gebruikt om de grondwaterstand te controleren en om de uitspoeling van zouten uit de wortelzone te vergemakkelijken. De drainagesystemen kunnen bestaan uit sloten, moledrains, drainbuizen of putten. De keuze voor één van deze systemen wordt gemaakt op basis van de geohydrologische omstandigheden, kosten en de verwachte kwaliteit van het drainage water. Met de toenemende schaarste van zoet water in aride en semi-aride streken neemt het belang van drainage waterkwaliteit steeds meer toe. Lozing van het drainage water mag niet ten koste gaan van benedenstroomse waterreserves. Bovendien kan drainage water een belangrijke bron van irrigatiewater zijn, mits voldaan wordt aan bepaalde kwaliteitseisen.

De Indus vlakte vormt een typisch voorbeeld van een geïrrigeerd gebied waar veld drainage wordt geïnstalleerd om wateroverlast en bodemverzouting te bestrijden. Er wordt onderscheid gemaakt tussen gebieden met zoet grondwater en gebieden met zout grondwater. Irrigatieputten zorgen voor de benodigde drainage capaciteit in gebieden met zoet grondwater. In gebieden met zout grondwater worden zowel drainbuizen als putten voor drainage gebruikt. Het zoute drainagewater wordt meestal geloosd in het oppervlakte drainagesysteem. Over het algemeen wordt aangenomen dat drainbuizen, na een zekere reclamatie periode, een betere waterkwaliteit opleveren dan putten. De stroombanen naar drainbuizen zijn korter en komen daarom voort uit lagen met over het algemeen minder zout grondwater (Smedema, 1993). *Het doel van deze studie is om de relatie tussen drainage technologie (drainbuizen en putten) en drainage waterkwaliteit voor de Indus vlakte nader te beschouwen. Veldgegevens van bestaande drainage-projecten en van proefgebieden worden gecombineerd met hydro-dynamische modellen om deze relatie te kwantificeren.* De hydro-dynamische modellen maken het mogelijk om de belangrijkste processen te identificeren en om lange termijn voorspellingen te doen. De resultaten van deze studie kunnen door irrigatie- en drainagedeskundigen worden gebruikt bij het bepalen van het optimale drainage systeem, rekening houdend met de te verwachten drainage waterkwaliteit.

Hoofdstuk 2 behandelt de theorie van waterstroming en stoffentransport in poreuze media. Het hoofdstuk begint echter met een sectie over het berekenen van bodem- en gewasverdamping. De beschreven relaties worden gebruikt om het watertransport tussen de bodem en de atmosfeer te berekenen met het SWAP model. Vervolgens worden de vergelijkingen voor waterstroming en stoffentransport gegeven. Deze vergelijkingen vormen de basis van het eindige-elementen model SUTRA (Voss, 1984), het eindige-elementen model SWMS\_2D (Šimunek et al., 1994) en het verticale één-dimensionale eindige-differentie model SWAP (Van Dam et al., 1997). In alle drie de modellen wordt waterstroming beschreven met behulp van een combinatie van de Darcy vergelijking en de elementaire massa balans vergelijking. Stoffentransport wordt beschreven met de advectie-dispersie vergelijking, hoewel deze optie in deze studie niet wordt gebruikt voor het SWMS\_2D model. Alle drie de modellen worden gebruikt om een verticale dwarsdoorsnede te beschrijven.

De theorie betreffende de reistijd van opgeloste stoffen naar drainbuizen en putten in constante

stromingsvelden wordt besproken in Hoofdstuk 3. De stroomfunctie wordt uitgelegd welke het mogelijk maakt om stroombanen naar het drainagesysteem uit te rekenen. De vergelijkingen voor twee-dimensionale stroming en axiaal-symmetrische stroming in een verticale dwarsdoorsnede worden gegeven. Verschillende onderzoekers hebben analytische uitdrukkingen voor de stroomfunctie in bodems met drainbuizen ontwikkeld. In deze studie worden de uitdrukkingen van Töksoz en Kirkham (1971) gebruikt die de stroming naar een drainbuis in een bodem met twee lagen beschrijven. Toepassing van deze uitdrukkingen op anisotrope bodems vereist een coördinaten-transformatie en het opnieuw uitrekenen van de hydraulische doorlatendheid. De vorm van de stroombanen in de benadering van Töksoz and Kirkham is onafhankelijk van de neerwaartse flux door een aantal vereenvoudigende aannames. Voor gedeeltelijk penetrerende putten is geen analytische oplossing van de stroomfunctie beschikbaar. De stroomfunctie voor dit type put wordt numeriek berekend in een spreadsheet met behulp van een eindige differentie methode zoals weergegeven in Olsthoorn (1998).

In het laatste gedeelte van Hoofdstuk 3 wordt uitgelegd hoe de reistijd van opgeloste stoffen kan worden afgeleid uit het stroombanen patroon. Voor drainbuizen betekent dit dat de oppervlakte van elke stroombuis moet worden uitgerekend met behulp van numerieke integratie. De reistijd van opgeloste stoffen naar putten wordt uitgerekend met behulp van een deeltjes-volg schema dat gebruik maakt van de Euler integratie formules. Bij het uitrekenen van het stoffentransport naar drainbuizen en putten kan cumulatieve afvoer gebruikt worden ter vervanging van reistijd. Dit betekent dat de stroming niet langer constant hoeft te zijn in de tijd. De doorbraak van opgeloste stoffen volgt uit een directe vergelijking tussen de oppervlakte (drainbuizen) of het volume (putten) van de stroombanen aan de ene kant en cumulatieve afvoer aan de andere. Dit houdt in dat de vorm van de stroombanen niet mag veranderen in de tijd, wat waar is zolang de aannames in Hoofdstuk 3 geldig zijn. Voor drainbuizen volgt de oppervlakte van de stroombuizen uit de eerder besproken numerieke integratie. Voor putten kan het volume van de stroombuizen worden uitgerekend nadat de reistijd van de opgeloste stoffen is vastgesteld met behulp van het deeltjes-volg schema.

De hydrologische eigenschappen van de Indus vlakte worden beschreven in Hoofdstuk 4, tesamen met een beschrijving van drie van de studiegebieden. Het klimaat van de Indus vlakte varieert van aride in Sindh tot semi-aride in de Punjab. De jaarlijkse regenval varieert van ~100 mm tot 1000-1400 mm. Het watervoerende pakket in de Indus vlakte bestaat uit zand met daar doorheen silt en klei. De dikte van het pakket varieert van een paar meter nabij rotsuitstulpingen tot een paar kilometer in het centrum van de vlakte. Ongeveer 16 miljoen ha vallen binnen het kanaal-irrigatiesysteem. Er worden drie studiegebieden besproken in Hoofdstuk 4 (een vierde wordt besproken in Hoofdstuk 6). Het experimentele buisdrainage project Sampla beslaat 9 ha en is representatief voor gebieden waar een sterke verzouting van bodem en grondwater heeft geleid tot een lage gewasproductie. Het Sampla project is zeer geschikt voor het volgen van het reclamatie proces dat volgt op de installatie van drainbuizen. Het Satiana putten-proefproject (40.000 ha) is representatief voor een gemiddeld overheids putten-drainage project in Pakistan. Vijftig (drainage) putten staan langs het oppervlakte drainage-systeem en 21 (irrigatie) putten staan langs de irrigatiekanalen. Tenslotte wordt het Fourth Drainage Project (FDP) besproken. Dit grootschalige buisdrainage project beslaat 120.000 ha en bestaat uit 79 aparte eenheden. Een van deze eenheden, S-I-B-9, wordt nader besproken.

Analyse van de veldgegevens leidt tot de volgende waarnemingen. De opbolling-drainafvoer relaties voor het experimentele buisdrainage project Sampla en voor de buisdrainage eenheid S-I-B-9 laten zien dat de stroming richting de drains vooral plaatsvindt beneden drainniveau. Dit betekent dat de schematisering van Töksoz en Kirkham (1971) toepasbaar is op het relatief grofkorrelige watervoerende pakket in de Indus vlakte. Het experimentele buisdrainage project Sampla laat zien dat drainage resulteert in een snelle verlaging van het zoutgehalte in de bodem. Het zoutgehalte van het drainagewater daarentegen verandert slechts langzaam. Het duurt ongeveer 9 jaar voordat de  $EC$  van het drainagewater is gedaald van  $20-60 \text{ dS m}^{-1}$  tot  $10.5 \text{ dS m}^{-1}$ . De putten van het Satiana project en de FDP buisdrainage eenheden laten nauwelijks een verandering van het zoutgehalte van het drainagewater zien. Dit gebrek aan verandering wordt toegeschreven aan het dempende effect van het diepe goed doorlatende watervoerende pakket. De hogere  $EC$  waarden van  $3.1-3.3 \text{ dS m}^{-1}$  voor de *drainage*-putten in Satiana in vergelijking tot de  $EC$  waarden van  $2.3-2.4 \text{ dS m}^{-1}$  voor de buisdrainage eenheden van FDP worden verklaard door het feit dat putten meer diep (zout) grondwater aantrekken.

De voorspelling van het zoutgehalte van drainagewater van drainbuizen en putten op lange termijn wordt besproken in Hoofdstuk 5. Het hoofdstuk begint met de beschrijving van een nieuwe model-benadering voor drainbuizen. Het stromingsgebied wordt opgedeeld in twee zones: één boven drainniveau waar alleen verticale stroming wordt aangenomen, en één beneden drainniveau waar twee-dimensionale stroming wordt aangenomen. Deze schematisering lijkt op de benadering van het bodem-drainbuis-watervoerend pakket systeem van Töksoz en Kirkham (1971). Waterstroming en stoffentransport in de zone boven drainniveau worden beschreven met behulp van het SWAP model. De zone beneden drainniveau wordt gekarakteriseerd met behulp van de stroomfuncties van Töksoz en Kirkham (1971). Er wordt aangenomen dat het stoffentransport in de stroombanen volledig advectioneel is. Het zoutgehalte van het drainagewater wordt berekend met behulp van een convolutie integraal met cumulatieve afvoer als de sturende variabele. Het SWMS\_2D model wordt in Hoofdstuk 5 gebruikt voor het simuleren van opbolling-drainafvoer relaties als onderdeel van een procedure voor het bepalen van de bodemfysische karakteristieken.

De model resultaten voor het experimentele buisdrainage project Sampla laten zien dat het zoutgehalte van het drainagewater slechts langzaam verbetert in de tijd. Complete reclamatie van de bodem en het watervoerend pakket, welke bepalend is voor het zoutgehalte van het drainagewater, duurt ongeveer 10 jaar. In werkelijkheid zal de reclamatie langzamer verlopen vanwege de constante instroom van zout grondwater vanuit het omliggende gebied. De resultaten voor Sampla laten zien dat drainafstand weinig invloed heeft op het zoutgehalte van het drainagewater. Dit wordt veroorzaakt door de aanwezigheid van een ondoorlatende laag op 1.25 m beneden drainniveau die de stroming beperkt tot het bovendste gedeelte van het watervoerende pakket. De resultaten voor de S-I-B-9 buisdrainage eenheid van het Fourth Drainage Project laten zien dat een complete reclamatie van bodem en watervoerend pakket niet haalbaar is binnen de economische levensduur van het systeem (~25 jaar). De reclamatie voor S-I-B-9 is relatief langzaam vanwege de lage drainafvoer van 96 mm per jaar, de relatieve diepe ligging van de drains (2.4 m) en de diepte van de grondwaterstroming (tot 87.4 m beneden drainniveau).

Hoofdstuk 5 vervolgt met de beschrijving van een nieuwe modelbenadering voor putten. Het

stromingsgebied wordt opnieuw verdeeld in twee zones. De grens tussen de twee zones wordt gevormd door het horizontale vlak dat samenvalt met het waterniveau in de put tijdens pompen. Dit zogenaamde horizontale grensvlak is vergelijkbaar met drainniveau in het geval van buisdrainage. Het wordt aangenomen dat de stroming boven het vlak verticaal is. De stroming beneden dit vlak is drie-dimensionaal met radiaal symmetrische stroming rond de put-as. Waterstroming en stoffentransport boven het horizontale grensvlak wordt berekend met het SWAP model. De zone beneden het grensvlak wordt gekarakteriseerd met stroomlijnen die numeriek bepaald worden. Het stoffentransport in de stroombanen is volledig advectioneel. Het zoutgehalte van het opgepompte water wordt opnieuw berekend met behulp van een convolutie integraal waarbij de hoeveelheid opgepompt water de sturende variabele is.

De model resultaten voor een Satiana *drainage*-put laten geen wezenlijke verandering zien in het zoutgehalte van het drainagewater gedurende de operationele periode van de put. Dit wordt veroorzaakt door het geringe gebruik van de put, de diepte van het scherm van de put (20 tot 40 m beneden het bodemoppervlak), en de diepte van de grondwaterstroming (tot 223.5 m beneden het horizontale grensvlak). De door SWAP gesimuleerde  $EC_e$  (0-1 m) waarden voor Sampla, S-I-B-9 en Satiana suggereren dat 1-3 jaar na de aanleg van drainage de gewassen geen last meer hebben van te hoge zoutgehalten in de bodem. *Het tijdsverschil tussen de reclamatie van de wortelzone en de reclamatie van de bodem en het watervoerende pakket (welke bepalend is voor het zoutgehalte van het drainagewater) blijkt een belangrijke eigenschap te zijn van de landbouwkundige drainagesystemen in de Indus vlakte. Dit impliceert dat boeren snel profiteren van de installatie van een drainage systeem (verminderde zoutgehalten in de bodem), maar dat lange termijn oplossingen nodig zijn voor het veilige gebruik en de veilige lozing van het drainagewater.*

Het zoutgehalte van het drainagewater wordt ook berekend door aan te nemen dat de zone beneden drainniveau (drainbuizen) of de zone beneden het horizontale grensvlak (putten) zich gedraagt als een perfect gemengd reservoir. Dit impliceert dat de reactie functies van deze zones op een zoutimpuls kunnen worden beschreven met een simpele exponentiële verdeling. De resultaten van de gemengde-reservoir benadering voor de drainbuizen in Sampla zijn goed vergelijkbaar met de resultaten van de stroomfunctie benadering zolang de diepte van de ondoorlatende laag beneden drainniveau,  $b$  klein blijft ( $b = 1.25$  m). Vergelijkingen voor Sampla met grotere dieptes voor de ondoorlatende laag ( $b = 3.75$  m en  $b = 6.25$  m) en de vergelijking voor S-I-B-9 zijn minder goed. De relatief diepe grondwaterstroming voor deze gevallen, in combinatie met de geringe oppervlakte van het afvoervlak, resulteren in afwijkingen van de stroomfunctie benadering. De gemengde reservoir benadering werkt daarentegen relatief goed voor de Satiana put. Dit komt door de grote oppervlakte van het scherm van de put. Er wordt geconcludeerd dat de gemengde reservoir methode, die een stuk simpeler is dan de stroomfunctie methode, voldoet voor de meeste gevallen in Hoofdstuk 5.

Het dichtheidsafhankelijke waterstromings- en stoffentransport model SUTRA wordt in Hoofdstuk 6 gebruikt om het zoutgehalte van het drainagewater van zowel drainbuizen als putten te bestuderen. Het model wordt toegepast op het Phularwan onderzoeksgebied, waar een zoet water lens met een dikte van ongeveer 25 m bovenop zout grondwater ligt ( $EC$  van 7-9 dS  $m^{-1}$ ). Verschillende typen ondiepe putten zijn in het verleden getest in Phularwan. SUTRA wordt

gecalibreerd op een enkelvoudige ondiepe put met een pompperiode van 15 dagen en een rustperiode van 164 dagen. Calibratie wordt bereikt door de anisotropie factor van de zandige onderlaag, waarvoor de resultaten zeer gevoelig zijn, aan te passen. Hoe hoger de anisotropie factor, hoe lager het zoutgehalte van het drainagewater. Deze relatie is sterk niet-lineair. Het model wordt gevalideerd op een experiment met een tweevoudige put (één scherm in het ondiepe zoete grondwater en het andere scherm in het diepe zoute grondwater). Deze put heeft een pompperiode van 23 dagen.

De invloed van het ondiepe put ontwerp op het zoutgehalte van het drainagewater wordt getest door drie verschillende putten te simuleren. Voor het gemak worden deze ontwerpen als volgt aangeduid: een ondiepe lage-afvoer put, een diepe lage-afvoer put, en een diepe hoge-afvoer put. De ondiepe put diepte van 3.0 tot 9.8 m beneden het bodemoppervlak en de diepe put diepte van 3.0 tot 14.6 m beneden het bodemoppervlak komen overeen met put-penetratie verhoudingen van respectievelijk 0.3 en 0.5. Alle drie de ontwerpen worden gesimuleerd met een pompschema van 1 dag pompen gevolgd door 9 dagen rust. De resultaten van het SUTRA model laten zien dat, onder de gegeven omstandigheden, alle drie de ontwerpen een stabiel zoutgehalte van het drainagewater opleveren. De uiteindelijke *EC* waarden van het drainagewater liggen tussen de 1.7 en 2.4 dS m<sup>-1</sup>, met de laagste waarde voor de ondiepe lage-afvoer put, en de hoogste waarde voor de diepe hoge-afvoer put. Water met deze *EC* waarden wordt geclassificeerd als marginaal voor irrigatie doeleinden.

Vervolgens wordt het gedrag van drainbuizen gesimuleerd voor dezelfde zoet-zout grondwater omstandigheden als voor de ondiepe putten. Er worden drie verschillende drainafstanden getest: 75 m, 150 m en 300 m. De draindiepte wordt vastgelegd op 2.0 m beneden het bodemoppervlak. Het gesimuleerde zoutgehalte van het drainagewater ligt tussen de 1.2 en 1.3 dS m<sup>-1</sup>, met de laagste waarde voor de drainafstand van 75 m, en de hoogste waarde voor de drainafstand van 300 m. Water met deze *EC* waarden is geschikt voor irrigatie doeleinden. De stroming naar de drainbuizen blijft beperkt tot het ondiepe "zoete" grondwater. Het diepe "zoute" grondwater blijft onberoerd. Dit is een belangrijke eigenschap met betrekking tot drainage waterkwaliteit. *Het impliceert dat schadelijke zouten kunnen worden verwijderd uit de wortelzone en uit het ondiepe grondwater terwijl de zouten die zich op grotere diepten bevinden op hun plaats blijven, waar ze geen bedreiging vormen voor de gewassen en voor het milieu.* Ondiepe putten daarentegen brengen zouten naar de oppervlakte die tot dan toe veilig in het diepe watervoerende pakket waren opgeslagen. De betere drainage waterkwaliteit voor drainbuizen in vergelijking tot ondiepe putten moet worden afgezet tegen de beduidend hogere installatiekosten voor drainbuizen.

Drainbuizen vormen de beste drainagemethode voor gebieden waar bodem en grondwater geheel verzout zijn. De berekeningen laten zien dat het meer dan 10 jaar duurt voordat het zoutgehalte van het drainagewater is gedaald tot evenwichtsniveau. Reclamatie van de wortelzone gaat veel sneller (in ongeveer 2 jaar voor het voorbeeld in Hoofdstuk 6). Dit tijdsverschil tussen de verlaging van het zoutgehalte in de wortelzone en de verlaging van het zoutgehalte in het drainagewater is een typische eigenschap van alluviale gebieden als de Indus vlakte, zoals eerder opgemerkt. Het reclamatie proces kan worden versneld door de watergiften voor de velden te verhogen. Dit verhoogt echter de hydraulische gradiënten in het systeem, wat resulteert in diepere stroomlijnen en meer mobilisatie van zouten uit het diepere grondwater.

## Gevolgtrekkingen voor de planning van drainage in de Indus vlakte

De optimale drainage technologie voor de Indus vlakte is sterk gerelateerd aan de grondwater condities. Er wordt een onderscheid gemaakt tussen gebieden met zoet grondwater, gebieden met zoet grondwater bovenop zout grondwater, en gebieden met zout grondwater. In de praktijk zijn de verschillen niet zo strikt. De meeste gebieden met zoet grondwater, bijvoorbeeld, bevatten ook zout grondwater, alleen op grotere diepte (bijvoorbeeld > 150 m). De meeste gebieden met zout grondwater daarentegen hebben vaak een dunne zoetwater laag aan de bovenkant met een dikte van een paar meter. Deze zoetwater laag is het gevolg van recente grondwataanvulling door regenval en irrigatie.

Irrigatie-putten voorzien over het algemeen in de drainagebehoeften van de gebieden met zoet grondwater (zie Hoofdstuk 1). De meeste van deze putten leveren irrigatiewater met een laag zoutgehalte over een lange periode. Dit wordt mogelijk gemaakt door de grote reikwijdte van het watervoerende pakket in de Indus vlakte (Hoofdstukken 5 en 6). Het voorkomen van over-exploitatie van het zoete grondwater op lokaal en regionaal niveau en het voorkomen van bodem-sodificatie op veldniveau (het opgepompte water bevat relatief veel  $\text{Na}^+$ ) vormen de voornaamste uitdagingen in de gebieden met zoet grondwater. Over-exploitatie kan vermoedelijk alleen worden voorkomen door wetgeving en wethandhaving. Het optreden van bodem sodificatie hangt sterk samen met de bekwaamheid van de boeren en hun vermogen om de verschillende soorten water (kanaal, put, en regenval) goed af te wisselen. De beschikbaarheid van toevoegingen zoals gips speelt ook een rol. Op langere termijn kan het noodzakelijk blijken om toch een zekere vorm van zout-export voor deze putten te ontwikkelen.

Gebieden met zoet grondwater bovenop zout grondwater hebben baat bij de toepassing van ondiepe drainage (Hoofdstuk 6). Drainbuizen leveren een betere drainage waterkwaliteit op dan ondiepe putten maar zijn ongeveer 10 keer zo duur. Ondiepe putten hebben het voordeel dat het opgepompte water gelijk gebruikt kan worden voor irrigatie. Echter, de maximale capaciteit van deze putten, die vooral afhankelijk is van de dikte van de laag zoet grondwater en de radiale en verticale permeabiliteit van het watervoerende pakket, is laag vergeleken met de capaciteit van putten van boeren in gebieden met zoet grondwater. Boeren hebben een minimale capaciteit van ongeveer  $2500 \text{ m}^3 \text{ d}^{-1}$  nodig om hun velden op een efficiënte manier te kunnen irrigeren. Ondiepe putten met een lage capaciteit zouden kunnen worden gecombineerd met sproei of druppel irrigatie om tot een bruikbaar systeem te komen. Momenteel voeren verschillende instituten veldexperimenten uit met zo'n systeem op de experimentele boerderij in Phularwan, Punjab, Pakistan.

Drainbuizen vormen de beste drainagemethode in gebieden met zout grondwater. De kwaliteit van het drainagewater verbetert relatief snel indien er een ondiepe ondoorlatende laag aanwezig is en wanneer de draindiepte en drainafstand klein gehouden worden. Met hogere watergiften kan het reclamatieproces versneld worden. Dit resulteert echter in extra mobilisatie van zouten in het grondwater en een hogere totale zout afvoer. In de praktijk blijkt dat het drainagewater van drainbuizen in de Indus vlakte voor zeker 10 jaar zout blijft. Dit betekent dat drainbuizen alleen geïnstalleerd moeten worden in gebieden die beschikken over een afvoermogelijkheid voor

veilige lozing. Grootschalige toepassing van veld drainage systemen in gebieden zonder afvoer is niet verstandig.

## Concluderende opmerkingen met betrekking tot de nieuwe modelbenadering

In dit proefschrift wordt een nieuwe modelbenadering toegepast voor de bestudering van het zoutgehalte van drainagewater van drainbuizen en putten (Hoofdstuk 5). De benadering mag alleen gebruikt worden voor relatief grof-korrelige bodem-watervoerende pakket systemen vanwege een aantal vereenvoudigende aannamen. Dit geldt vooral voor de aanname dat boven drainniveau (drainbuizen) en boven het horizontale grensvlak (putten) alleen één-dimensionale verticale stroming optreedt. Het negeren van dichtheidsverschillen in het grondwater houdt in dat de modelbenadering de neiging heeft om de snelheid van het reclamatieproces te onderschatten, resulterend in een overschatting van het zoutgehalte van het drainagewater (Hoofdstuk 6). Dit geldt vooral voor gebieden waar het zoutgehalte van het grondwater hoog is, zoals voor het experimentele buisdrainage project Sampla. Uitsluiting van regionale grondwaterstroming van de analyse, daarentegen, leidt vermoedelijk tot een overschatting van het reclamatieproces, resulterend in een onderschatting van het zoutgehalte van het drainage water. De mate waarin deze twee processen elkaar neutraliseren is afhankelijk van de lokale geohydrologische omstandigheden. Deze kwestie wordt in dit proefschrift niet nader uitgewerkt en kan een goed onderwerp zijn voor een vervolgstudie.

Het gebruik van het SWAP model voor het berekenen van waterstroming en stoffentransport boven drainniveau of boven het horizontale grensvlak, garandeert een zo nauwkeurig mogelijke schatting van de lekverliezen van geïrrigeerde velden. Het veranderende karakter van de waterstromen in de onverzadigde zone en de interactie met gewasgroei worden volledig in acht genomen. Een goede schatting van de lekverliezen is belangrijk omdat het één van de belangrijkste variabelen is die het verloop van het reclamatieproces bepalen. De andere belangrijke variabele is de diepte van het actieve stromingsgebied. Deze diepte kan helaas zelden worden afgeleid uit de veldgegevens. In de meeste gevallen moet deze parameter geschat worden met behulp van methoden zoals beschreven in Hoofdstuk 5.

In Sectie 5.8 is aangetoond dat de zone beneden drainniveau of beneden het horizontale grensvlak ook beschreven kan worden als een gemengd reservoir. De gemengde reservoir benadering is een stuk eenvoudiger dan de stroomfunctie benadering en is reeds beschikbaar in het SWAP model als een middel om de doorbraak van stoffen uit de verzadigde zone te berekenen. De gemengde reservoir methode is vooral geschikt wanneer een ondiepe ondoorlatende laag de grondwaterstroming beperkt tot de bovendste laag van het watervoerende pakket (drainbuizen) of wanneer het scherm van de put een groot gedeelte van het watervoerende pakket penetreert (putten). De gemengde reservoir methode geeft ook redelijke resultaten wanneer aan deze voorwaarden niet voldaan wordt (bijv. drainbuizen in een watervoerend pakket met diepe grondwaterstroming of ondiepe gedeeltelijk penetrerende putten).

In principe kunnen de berekeningen voor Hoofdstuk 5 ook gedaan worden met een twee-dimensionaal numeriek model (toegepast op een verticale dwarsdoorsnede). Dit zou minder

## Samenvatting en Conclusies

---

aannamen vergen omtrent de waterstroming in het systeem. Het gebruik van een tweedimensionaal model met snel veranderende grensvoorwaarden vergt echter zeer veel rekentijd en is daarom niet aan te bevelen voor het doen van lange termijn berekeningen zoals in Hoofdstuk 5.



## References

- Abrol, I.P., 1999. Sustaining rice-wheat system productivity in the Indo-Gangetic plains: water management-related issues. *Agric. Water Manage.* 40, 31-35.
- Agarwal, M.C., Roest, C.J.W. (Eds.), 1996. Towards improved water management in Haryana State; final report of the Indo-Dutch Operational Research Project on Hydrological Studies. CCS Haryana Agric. Univ., Hisar, ILRI, Wageningen, Alterra, Wageningen, 80 p.
- Ahmad, N. Chaudhry, G.R., 1988. *Irrigated agriculture of Pakistan*, Mirajuddin, Lahore, 800 p.
- Aliawi, A.S., 1993. Numerical simulation of the behaviour of the fresh-saline water transition zone around a scavenger well. PhD thesis, Univ. of Newcastle upon Tyne, 250 p.
- Allen, R.G., Pereira, L.S., Raes, D., Smith, M., 1998. Crop evapotranspiration, guidelines for computing crop water requirements. *Irrigation and Drainage paper No. 56*, FAO, Rome, 300 p.
- Anderson, M.P., Woessner, W.W., 1992. *Applied groundwater modeling; simulation of flow and advective transport*. Academic Press, 381 p.
- Ayars, J.E., McWhorter, D.B., Skogerboe, G.V., 1981. Modeling salt transport in irrigated soils. *Ecological modeling* 11, 265-290.
- Ayars, J.E., 1996. Managing irrigation and drainage systems in arid areas in the presence of shallow groundwater: case studies. *Irrig. Drain. Syst.* 10, 227-244.
- Ayars, J.E., Grismer, M.E., Guitjens, J.C., 1997. Water quality as design criterion in drainage water management systems. *J. Irrig. Drain. Eng.* 123(3), 154-158.
- Ayars, J.E., Hutmacher, R.B., Schoneman, R.A., Soppe, R.W.O., Vail, S.S., Dale, F., 1999. Realizing the potential of integrated irrigation and drainage water management for meeting crop water requirements in semi-arid and arid areas. *Irrig. Drain. Syst.* 13, 321-347.
- Ayers, R.S., Westcot, D.W., 1985. Water quality for agriculture. *Irrigation and Drainage paper No. 29*, FAO, Rome, 174 p.
- Barlow, P.M., Moench, A.F., 1999. WTAQ - A computer program for calculating drawdowns and estimating hydraulic properties for confined and water-table aquifers. *Water-Resources Investigations Rep. 99-4225*, U.S. Geological Survey, 74 p.
- Bastiaanssen, W.G.M., Singh, R., Kumar, S., Schakel, J.K., Jhorar, R.K., 1996. Analysis and recommendations for integrated on-farm water management in Haryana, India: a model approach. *Rep. No. 118*, Alterra, Wageningen, 152 p.
- Bear, J., Dagan, G., 1964. Some exact solutions of interface problems by means of the hodograph method. *J. Geophys. Res.* 69(2), 1563-1572.
- Bear, J., 1972. *Dynamics of fluids in porous media*. American Elsevier Publishing Company, Inc., 764 p.
- Bear, J., 1979. *Hydraulics of groundwater*. McGraw-Hill Inc., 567 p.
- Bear, J., Verruijt, A., 1987. *Modeling groundwater flow and pollution*. D. Reidel Publishing Company, 414 p.
- Beekma, J. Kelleners, T.J., Boers, Th.M., Raza, Z.I., 1995. Application of SWATRE to evaluate drainage of an irrigated field in the Indus plain, Pakistan. In: Pereira, L.S., Van den Broek, B.J., Kabat, P., Allen, R.G. (Eds.), *Crop-water-simulation models in practice (selected papers of the 2<sup>nd</sup> workshop on crop-water-models)*. Wageningen pers, p. 141-

## References

---

- 160.
- Beeson, S., Carruthers, R., Wyness, A.J., 1993. Scavenger wells -2- Field investigations and monitoring. In: Custodio, E., Galofré, A. (Eds.), Proc. 12<sup>th</sup> Salt Water Intrusion Meeting, Nov. 1992, CIMNE, Barcelona, p. 557-571.
- Beg, A., Lone, M.I., 1992. Trend of changes in groundwater quality of SCARP-I. In: W.F. Vlotman (Ed.), Proc. 5<sup>th</sup> International Drainage Workshop, Feb. 1992, ICID, Lahore, Vol. 2, p. 3.66-3.72.
- Belitz, K., Phillips, S.P., 1995. Alternative to agricultural drains in California's San Joaquin Valley: Results of a regional-scale hydrogeologic approach. *Water Resour. Res.* 31(8), 1845-1862.
- Belmans, C., Wesseling, J.G., Feddes, R.A., 1983. Simulation model of the water balance of a cropped soil: SWATRE. *J. Hydrol.* 63, 271-286.
- Bender, F.K., Raza, H.A. (Eds.), 1995. *Geology of Pakistan*. Gebrüder Borntraeger, Berlin, 414 p.
- Bennett, G.D., 1990. Report on a consultancy to develop a research assistance proposal on skimming wells. Tech. Rep. No. 90/10, IWASRI, Lahore, 55 p.
- Bennett, G.D., Rehman, A.U., Sheikh, I.A., Ali, S., 1967. Analysis of aquifer tests in the Punjab Region of West Pakistan. Water-supply paper 1608-G, U.S. Geological Survey, 56 p.
- Bennett, G.D., Mundorff, M.J., Hussain, S.A., 1968. Electric-Analog studies of brine coning beneath fresh-water wells in the Punjab Region, West Pakistan. Water-supply paper 1608-J, U.S. Geological Survey, 31 p.
- Beven, K.J., Henderson, D.E., Reeves, A.D., 1993. Dispersion parameters for undisturbed partially saturated soil. *J. Hydrol.* 143, 19-43.
- Boehmer, W.K., Boonstra, J., 1994. Tubewell drainage systems. In: Ritzema, H.P. (Ed.), *Drainage principles and applications*. Pub. No. 16, ILRI, Wageningen, 931-964.
- Boesten, J.J.T.I., Stroosnijder, L., 1986. Simple model for daily evaporation from fallow tilled soil under spring conditions in a temperate climate. *Neth. J. Agric. Sci.* 34, 75-90.
- Boumans, J.H., 1979. Drainage calculations in stratified soils using the anisotropic soil model to simulate hydraulic conductivity conditions. In: Wesseling, J. (Ed.), Proc. of the International Drainage Workshop, May 1978, ILRI, Wageningen, p. 108-123.
- Boumans, J.H., Van Hoorn, J.W., Kruseman, G.P., Tanwar, B.S., 1988. Water table control, reuse and disposal of drainage water in Haryana. *Agric. Water Manage.*, 14, 537-545.
- Boonstra, J., Moghal, M.A., Ali, S.H., Ahmad, M.I. and Vlotman, W.F., 1991. Collection, processing, and screening of data for the water balance study of Schedule I-B of the Fourth Drainage Project. Rep. No. 30, NRAP, Lahore, 104 p.
- Braden, H., 1985. Ein energiehaushalts- und verdunstungsmodell für wasser- und stoffhaushaltsuntersuchungen landwirtschaftlich genutzter einzugsgebiete. *Mitteilungen Deutsche Bodenkundliche Gesellschaft* 42, 294-299 (In German).
- Bronswijk, J.J.B., Hamminga, W., Oostindie, K., 1995. Field-scale solute transport in a heavy clay soil. *Water Resour. Res.*, 31(3), 517-526.
- Carsel, R.F., Parrish, R.S., 1988. Developing joint probability distributions of soil water retention characteristics. *Water Resour. Res.* 24(5), 755-769.
- Chandler, R.L., McWhorter, D.B., 1975. Upconing of the salt-water-fresh-water interface beneath a pumping well. *Ground water* 13(4), 354-359.
- Christiansen, J.E., 1973. Effect of agricultural water use on water quality for downstream use for

- irrigation. Proc. specialty conf. on agricultural and urban considerations in irrigation and drainage, ASCE, April 1973, Fort Collins, Colorado, p. 753-785.
- Clausnitzer, V., Hopmans, J.W., Nielsen, D.R., 1992. Simultaneous scaling of soil water retention and hydraulic conductivity curves. *Water Resour. Res.* 28(1), 19-31.
- Crane, M.J., Blunt, M.J., 1999. Streamline-based simulation of solute transport. *Water Resour. Res.* 35(10), 3061-3078.
- De Vos, J.A., 1997. Water flow and nutrient transport in a layered silt loam soil. PhD thesis, Wageningen University, 287 p.
- De Vries, J.J., 1975. Some calculation methods for determination of the travel time of groundwater. *Aqua-Vu* 5, 3-15.
- Dieleman, P.J., Trafford, B.D., 1976. Drainage testing. Irrigation and Drainage paper No. 28, FAO, Rome, 172 p.
- Dumm, L.D., 1968. Subsurface drainage by transient-flow theory. *J. Irrig. Drain. Div., ASCE*, 94(4), 505-519.
- Duffy, C.J., Kincaid, C.T., Huyakorn, P.S., 1990. A review of groundwater models for assessment and prediction of non-point-source pollution. In: DeCoursey, D.G. (Ed.), Proc. of the Int. Symp. on water quality modeling of agricultural non-point sources, part 1, June 1988, Logan, Utah, p. 253-275.
- Duffy, C.J., Lee, D-H, 1992. Base flow response from nonpoint source contamination: simulated spatial variability in source, structure, and initial condition. *Water Resour. Res.* 28(3), 905-914.
- Eching, S.O., Hopmans, J.W., Wallender, W.W., MacIntyre, J.L., Peters, D., 1994. Estimation of local and regional components of drain-flow from an irrigated field. *Irrig. Sci.* 15, 153-157.
- El-Atfy, H.E., Abdel-Alim, M.Q., Ritzema, H.P., 1991. A modified layout of the subsurface drainage system for rice areas in the Nile Delta, Egypt. *Agric. Water Manage.* 19, 289-302.
- Ernst, L.F., 1973. De bepaling van de transporttijd van het grondwater bij stroming in de verzadigde zone. Nota 755, Alterra, Wageningen, 42 p (In Dutch).
- Faires, J.D., Burden, R.L., 1993. Numerical methods. PWS Publishing Company, Boston, 503 p.
- Feddes, R.A., Kowalik, P.J., Zaradny, H., 1978. Simulation of field water use and crop yield. Simulation Monographs, Pudoc, Wageningen, 189 p.
- Feddes, R.A., Kabat, P., Van Bakel, P.J.T., Bronswijk, J.J.B., Halbertsma, J., 1988. Modelling soil water dynamics in the unsaturated zone - state of the art. *J. Hydrol.* 100, 69-111.
- Feddes, R.A., Bastiaanssen, W.G.M., 1990. Forecasting soil-water-plant-atmosphere interactions in arid regions. NATO workshop on water saving techniques for plant growth, Sept. 1990, Gent, 29 p.
- Fio, J.L., Deverel, S.J., 1991. Groundwater flow and solute movement to drain laterals, Western San Joaquin Valley, California. 2. Quantitative hydrologic assessment. *Water Resour. Res.* 27(9), 2247-2257.
- Fipps, G., Skaggs, R.W., Nieber, J.L., 1986. Drains as a boundary condition in finite elements. *Water Resour. Res.* 22(11), 1613-1621.
- Fogg, G.E., Senger, R.K., 1985. Automatic generation of flow nets with conventional groundwater modeling algorithms. *Ground water* 23(3), 336-344.

## References

---

- Frind, E.O., 1977. An isoparametric Hermitian finite element for the solution of field problems. *Int. J. Num. Meth. Eng.* 11, 945-962.
- Frind, E.O., Matanga, G.B., 1985. The dual formulation of flow for contaminant transport modeling. 1. Review of theory and accuracy aspects. *Water Resour. Res.* 21(2), 159-169.
- Garcia, L.A., Manguerra, H.B., Gates, T.K., 1995. Irrigation-drainage design and management model: Development. *J. Irrig. Drain. Eng.* 121(1), 71-82.
- Gelhar, L.W., Wilson, J.L., 1974. Ground-water quality modeling. *Ground water* 12(6), 399-408.
- Greenman, D.W., Swarzenski, W.V., Bennett, G.D., 1967. Ground-water hydrology of the Punjab, West Pakistan, with emphasis on problems caused by canal irrigation. Water-supply paper 1608-H, U.S. Geological Survey, 66 p.
- Groen, K.P., 1997. Pesticide leaching in polders; field and model studies on cracked clays and loamy sand. PhD thesis, Wageningen University, 296 p.
- Guitjens, J.C., Ayars, J.E., Grismer, M.E., Willardson, L.S., 1997. Drainage design for water quality management: overview. *J. Irrig. Drain. Eng.* 123(3), 148-153.
- Gureghian, A.B., Youngs, E.G., 1975. The calculation of steady-state water table heights in drained soils by means of the finite element method. *J. Hydrol.* 27, 15-32.
- Hafeez, A., Piracha, Z.A., Ahmad, N., 1986. Multi-strainer tubewells for skimming top layer of fresh water underlain by saline water in the aquifer. Pub. No. 152, Mona Reclamation Experimental Project, Bhalwal, 50 p.
- Hanson, B.R., 1989. A systems approach to drainage reduction in the San Joaquin Valley. *Agric. Water Manage.* 16, 97-108.
- Hendrickx, J.M.H., Baerends, B., Raza, Z.I., Sadig, M., Chaudhry, M.A., 1992. Soil salinity assessment by electromagnetic induction of irrigated land. *Soil Sci. Soc. Am. J.* 56, 1933-1941.
- Herbert, A.W., Jackson, C.P., Lever, D.A., 1988. Coupled groundwater flow and solute transport with fluid density strongly dependent upon concentration. *Water Resour. Res.* 24(10), 1781-1795.
- Heuperman, A.F., 1993. Salinity management in the irrigation areas in Northern Victoria, Australia with special reference to biological management options. *Proc. 15<sup>th</sup> ICID congress, 1993, The Hague, special session R.3*, p. 35-47.
- Hinesly, T.D., Kirkham, D., 1966. Theory and flow nets for rain and artesian water seeping into soil drains. *Water Resour. Res.* 2(3), 497-511.
- Homae, M., 1999. Root water uptake under non-uniform transient salinity and water stress. PhD thesis, Wageningen University, 173 p.
- Hooghoudt, S.B., 1940. Algemeene beschouwing van het probleem van de detailontwatering en de infiltratie door middel van parallel loopende drains, greppels, slooten, en kanalen. *Versl. Landbouwk. Onderz.* 46(14)B. Algemeene Landsdrukkerij, 's-Gravenhage, 193 p (In Dutch).
- Hooja, R., Srinivas, V., Sharma, G., 1995. Waterlogging and salinity problems in IGNP, Rajasthan. In: Rao, K.V.G.K., Agarwal, M.C., Singh, O.P., Oosterbaan, R.J. (Eds.), *Reclamation and management of waterlogged saline soils*. CSSRI, Karnal, CCS Haryana Agric. Univ., Hisar, p. 141-159.
- Hoffman, G.J., Dirksen, C., Ingvalson, R.D., Maas, E.V., Oster, J.D., Rawlins, S.L., Rhoades, J.D., Van Schilfgaarde, J., 1978. Minimizing salt in drain water by irrigation management. *Agric. Water Manage.* 1, 233-252.

- Hopmans, J.W., Stricker, J.N.M., 1989. Stochastic analysis of soil water regime in a watershed. *J. Hydrol.* 105, 57-84.
- Huyakorn, P.S., Andersen, P.F., Mercer, J.W., White, H.O., 1987. Saltwater intrusion in aquifers: Development and testing of a three-dimensional finite element model. *Water Resour. Res.* 23(2), 293-312.
- IFPRI, 1995. A 2020 vision for food, agriculture, and the environment. IFPRI, Washington, D.C., 50 p.
- Johnston, W.R., Tanji, K.K., Burns, R.T., 1997. Drainage water disposal. In: Madramootoo, C.A., Johnston, W.R., Willardson, L.S. (Eds.), *Management of agricultural drainage water quality*. Water Rep. No. 13, FAO, Rome, p. 51-62.
- Jury, W.A., 1975. Solute travel-time estimates for tile-drained fields: I. Theory. *Soil Sci. Soc. Am. J.* 39, 1020-1024.
- Jury, W.A., Roth, K., 1990. *Transfer functions and solute movement through soil, theory and applications*. Birkhäuser Verlag, Basel, 226 p.
- Kamra, S.K., Rao, K.V.G.K., 1985. Selection of representative hydraulic conductivity value for drainage system design. *Irrigation and Power* 42(4), 355-359.
- Kamra, S.K., Singh, S.R., Rao, K.V.G.K., Van Genuchten, M.Th., 1991a. A semidiscrete model for water and solute movement in tile-drained soils. 1. Governing equations and solution. *Water Resour. Res.* 27(9), 2439-2447.
- Kamra, S.K., Singh, S.R., Rao, K.V.G.K., Van Genuchten, M.Th., 1991b. A semidiscrete model for water and solute movement in tile-drained soils. 2. Field validation and applications. *Water Resour. Res.* 27(9), 2449-2456.
- Kelleners, T.J., 1993. Use of SWATRE to simulate the water and salt balance of an irrigated field in the Indus plain, Pakistan. MSc thesis, Wageningen University, 33 p.
- Kelleners, T.J., 1996. Modelling of drain effluent salinity in arid and semi-arid zones; case study for the Fourth Drainage Project, Punjab Province, Pakistan. Unpublished ILRI report, Wageningen, 65 p.
- Kelleners, T.J., Beekma, J., Chaudhry, M.R., 1999. Spatially variable soil hydraulic properties for simulation of field-scale solute transport in the unsaturated zone. *Geoderma* 92, 199-215.
- Kelleners, T.J., Kamra, S.K., Jhorar, R.K., 2000. Prediction of long term drainage water salinity of pipe drains. *J. Hydrol.* 234, 249-263.
- Kemper, W.D., Jahangir, M., McWhorter, D.B., 1976. Skimming well report: Field studies. Pub. No. 67, Mona Reclamation Experimental Project, Bhalwal, 23 p.
- Kinzelbach, W., 1986. Groundwater modelling, an introduction with sample programs in Basic. *Developments in water science* 25, Elsevier, 333 p.
- Khan, M.Y., Kirkham, D., 1971. Spacing of drainage wells in a layered aquifer. *Water Resour. Res.* 7(1), 166-183.
- Khan, M.Y., Kirkham, D., Toksöz, S., 1971. Steady state flow around a well in a two-layered aquifer. *Water Resour. Res.* 7(1), 155-165.
- Kirkham, D., 1949. Flow of ponded water into drain tubes in soil overlying an impervious layer. *Trans. Am. Geophys. Union* 30, 369-385.
- Kirkham, D., 1951. Seepage into drain tubes in stratified soil. *Trans. Am. Geophys. Union* 32(3), 422-442.
- Kirkham, D., 1954. Seepage of artesian and surface water into drain tubes in stratified soil.

## References

---

- Trans. Am. Geophys. Union 35(5), 775-790.
- Kirkham, D., 1958. Seepage of steady rainfall through soil into drains. Trans. Am. Geophys. Union 39(5), 892-908.
- Kirkham, D., Horton, R., 1992. The stream function of potential theory for a dual-pipe subirrigation-drainage system. Water Resour. Res. 28(2), 373-387.
- Kirkham, D., Van der Ploeg, R.R., Horton, R., 1997. Potential theory for dual-depth subsurface drainage of ponded land. Water Resour. Res. 33(7), 1643-1654.
- Kolditz, O., Ratke, R., Diersch, H.-J.G., Zielke, W., 1998. Coupled groundwater flow and transport: 1. Verification of variable density flow and transport models. Adv. Water Resour. 21(1), 27-46.
- Kroes, J.G., Van Dam, J.C., Huygen, J., Vervoort, R.W., 1999. User's guide of SWAP version 2.0; Simulation of water flow, solute transport and plant growth in the soil-water-atmosphere-plant environment. Rep. No. 81, Dep. Water Resources, Wageningen University, 127 p.
- Kruseman, G.P., De Ridder, N.A., 1990. Analysis and evaluation of pumping test data. Pub. No. 47, ILRI, Wageningen, 377 p.
- Kumar, S., Bastiaanssen, W.G.M., 1993. Simulation of the water balance in relation to crop water requirements in (semi) arid zones. Proc. 15<sup>th</sup> ICID congress, 1993, The Hague, Q. 44, R. 28, p. 349-363.
- Kuper, M., 1997. Irrigation management strategies for improved salinity and sodicity control. PhD thesis, Wageningen University, 238 p.
- Leij, F.J., Alves, W.J., Van Genuchten, M.Th., Williams, J.R., 1996. The UNSODA unsaturated soil hydraulic database. User's manual version 1.0. U.S. Salinity Laboratory, Riverside, California, 103 p.
- Luthin, J.N., Fernandez, P., Maslov, B., Woerner, J., Robinson, F., 1969. Displacement front under ponded leaching. J. Irrig. Drain. Div., ASCE, 95(IR1), 117-125.
- Ma, T.S., Sophocleous, M., Yu, Y.-S., Buddemeier, R.W., 1997. Modeling saltwater upconing in a freshwater aquifer in south-central Kansas. J. Hydrol, 201, 120-137.
- Maas, E.V., 1990. Crop salt tolerance. In: Tanji, K.K. (Ed.). Agricultural salinity assessment and management. ASCE manuals and reports on engineering practice No. 71. p. 262-304.
- Maasland, M., 1957. Soil anisotropy and land drainage. In: Luthin, J.N. (Ed.). Drainage of agricultural land. Vol. 7, Am. Soc. Agron., Madison, p. 216-285.
- Malik, S.M., Strosser, P., 1993. Management of private tubewells in a conjunctive use environment: A case study in the Mananwala Distributary Command Area, Punjab, Pakistan. Working Paper No. 27, IWMI, Colombo, 38 p.
- Manguerra, H.B., Garcia, L.A., 1995. Irrigation-drainage design and management model: Validation and application. J. Irrig. Drain. Eng. 121(1), 83-94.
- Manguerra, H.B., Garcia, L.A., 1996. Drainage and no-drainage cycles for salinity management in irrigated areas. Trans. ASAE 39(6), 2039-2049.
- Manguerra, H.B., Garcia, L.A., 1997. Modeling flow and transport in drainage areas with shallow ground water. J. Irrig. Drain. Eng. 123(3), 185-193.
- Matanga, G.B., 1993. Stream functions in three-dimensional groundwater flow. Water Resour. Res. 29(9), 3125-3133.
- McLin, S.G., Gelhar, L.W., 1979. A field comparison between the USBR-EPA hydrosalinity model and generalized lumped parameter models. IAHS Publ. No. 128, p. 339-348.

- McWhorter, D.B., 1972. Steady and unsteady flow of fresh water in saline aquifers. Water Manage. Tech. Rep. No. 20, Colorado State Univ., Fort Collins, Colorado, 49 p.
- McWhorter, D.B., 1980. Summary of skimming well investigations. Water Manage. Tech. Rep. No. 63, Colorado State University, Fort Collins, Colorado, 77 p.
- Millington, R.J., Quirk, J.P., 1961. Permeability of porous solids. Trans. Faraday Soc. 57, 1200-1207.
- Minhas, P.S., Gupta, R.K., 1992. Quality of irrigation water, assessment and management. Indian Council of Agric. Res., New Delhi, 123 p.
- Moench, A.F., 1997. Flow to a well of finite diameter in a homogeneous, anisotropic water table aquifer. Water Resour. Res. 33(6), 1397-1407.
- Moghal, M.A., Ali, S.H., Boonstra, J., 1992. Seasonal net recharge to aquifer underlying the Schedule I-B area, June 85-June 90, Fourth Drainage Project. NRAP Rep. No. 33, Lahore, Pakistan, 127 p.
- Mohammad, F.S., Skaggs, R.W., 1983. Drain tube opening effects on drain inflow. J. Irrig. Drain. Eng. 109(4), 393-404.
- Mohanty, B.P., Bowman, R.S., Hendrickx, J.M.H., Šimůnek, J., Van Genuchten, M.Th., 1998. Preferential transport of nitrate to a tile drain in an intermittent-flood-irrigated field: Model development and experimental evaluation. Water Resour. Res. 34(5), 1061-1076.
- Mualem, Y., 1976. A new model for predicting the hydraulic conductivity of unsaturated porous media. Water Resour. Res. 12(3), 513-522.
- Mundorff, M.J., Carrigan, P.H., Steele, T.D., Randall, A.D., 1976. Hydrologic evaluation of salinity control and reclamation projects in the Indus Plain, Pakistan, a summary. Water-supply paper 1608-Q, U.S. Geological Survey, 59 p.
- Muskat, M., 1937. The flow of homogeneous fluids through porous media. J.W. Edwards, Inc., Ann Arbor, Michigan, 763 p.
- Nieber, J.L., Misra, D., 1995. Modeling flow and transport in heterogeneous, dual-porosity drained soils. Irrig. Drain. Syst. 9, 217-237.
- Nielsen, D.R., Van Genuchten, M.Th., Biggar, J.W., 1986. Water flow and solute transport processes in the unsaturated zone. Water Resour. Res., 22(9), 89S-108S.
- Nour el-Din, M.M., King, I.P., Tanji, K.K., 1987. Salinity management model: I. Development. J. Irrig. Drain. Div., ASCE 113(4), 440-453.
- Olsthoorn, Th.N., 1998. Groundwater modelling: calibration and the use of spreadsheets. PhD thesis, Technical University Delft, 296 p.
- Oosterbaan, R.J., 1998. SALTMOD, description of principles and applications. Unpublished ILRI report, Wageningen, 102 p.
- Oosterbaan, R.J., Nijland, H.J., 1994. Determining the saturated hydraulic conductivity. In: Ritzema, H.P. (Ed.), Drainage principles and applications. Pub. No. 16, ILRI, Wageningen, p. 435-476.
- Oosterkamp, H.C., 1997. Reuse of drainage effluent; a case study of the Fourth Drainage Project, Pakistan. MSc thesis, Wageningen University, 60 p.
- Ortiz, J., Luthin, J.N., 1970. Movement of salts in ponded anisotropic soils. J. Irrig. Drain. Div., ASCE, 96(IR3), 257-264.
- Oster, J.D., 1994. Irrigation with poor quality water. Agric. Water Manage. 25, 271-297.
- Pickens, J.F., Gillham, R.W., Cameron, D.R., 1979. Finite-element analysis of the transport of water and solutes in tile-drained soils. J. Hydrol. 40, 243-264.

## References

---

- Poeter, E.P., Hill, M.C., 1998. Documentation of UCODE, a computer code for universal inverse modeling. Water-Resources Investigations Rep. 98-4080, U.S. Geological Survey, 116 p.
- Pohll, G.M., Guitjens, J.C., 1994. Modeling regional flow and flow to drains. *J. Irrig. Drain. Eng.* 120(5), 925-939.
- Prasad, R., 1988. A linear root water uptake model. *J. Hydrol.* 99, 297-306.
- Prendergast, J.B., Rose, C.W., Hogarth, W.L., 1994. A model for conjunctive use of groundwater and surface water for control of irrigation salinity. *Irrig. Sci.* 14, 167-175.
- Press, W.H., Teukolsky, S.A., Vetterling, W.T., Flannery, B.P., 1992. Numerical recipes in Fortran; the art of scientific computing, 2<sup>nd</sup> edition. Cambridge University Press, 963 p.
- Priestley, C.H.B., Taylor, R.J., 1972. On the assessment of surface heat flux and evaporation using large scale parameters. *Mon. Weather Rev.* 100, 81-92.
- Quinn, N.W.T., 1991. Ground-water pumping for water table management and drainage control in the Western San Joaquin Valley. In: Dinar, A., Zilberman, D. (Eds.). *The economics and management of water and drainage in agriculture*. Kluwer. p.71-97.
- Raats, P.A.C., 1978. Convective transport of solutes by steady flows. I. General theory. *Agric. Water Manage.* 1, 201-218.
- Rao, K.V.G.K., Singh, O.P., Gupta, R.K., Kamra, S.K., Pandey, R.S., Kumbhare, P.S., Abrol, I.P., 1986. Drainage investigations for salinity control in Haryana. *Bul. No. 10, CSSRI, Karnal*, 95 p.
- Rao, K.V.G.K., Leeds-Harrison, P.B., 1991. Desalinization with subsurface drainage. *Agric. Water Manage.*, 19, 303-311.
- Rao, K.V.G.K., Sharma, D.P., Oosterbaan, R.J., 1992. Subirrigation by ground water management with controlled subsurface drainage in semiarid areas. *Proc. Int. Conf. on supplementary irrigation and drought water management*, 1992, Bari, 9 p.
- Rao, K.V.G.K., 1996. Indo-Dutch operational research project (CSSRI) phase II. Final Report Oct. 1990 - Dec. 1994 (Appendix: research results). ILRI, Wageningen, 15 p.
- Rao, K.V.G.K., Sharma, D.P., Kumbhare, P.S., Oosterbaan, R.J., 1996. Impact of subsurface drainage on salt regime of root zone and groundwater. *Proc. 6<sup>th</sup> Drainage Workshop, ICID, 1996, Ljubljana*, p. 657-663.
- Rawls, W.J., Brakensiek, D.L., Saxton, K.E., 1982. Estimation of soil water properties. *Trans. ASAE* 25(5), 1316-1320 and 1328.
- Reilly, T.E., Goodman, A.S., 1987. Analysis of saltwater upconing beneath a pumping well. *J. Hydrol.* 89, 169-204.
- Reilly, T.E., Frimpter, M.H., LeBlanc, D.R., Goodman, A.S., 1987. Analysis of steady-state salt-water upconing with application at Truro well field, Cape Cod, Massachusetts. *Ground water* 25(2), 194-206.
- Rhoades, J.D., Kandiah, A., Mashali, A.M., 1992. The use of saline waters for crop production. *Irrigation and Drainage paper No. 48*, FAO, Rome, 133 p.
- Richards, L.A., 1931. Capillary conduction of liquids in porous mediums. *Physics* 1, 318-333.
- Ritzema, H.P., 1994. Subsurface flow to drains. In: Ritzema, H.P. (Ed.), *Drainage principles and applications*. Pub. No. 16, ILRI, Wageningen, 263-304.
- Rogers, J.S., Fouss, J.L., 1989. Hydraulic conductivity determination from vertical and horizontal drains in layered soil profiles. *Trans. ASAE*, 32(2), 589-595.
- Rycroft, D.W., Amer, M.H., 1995. Prospects for the drainage of clay soils. *Irrigation and*



- Drainage paper No. 51, FAO, Rome, 134 p.
- Sahni, B.M., 1972. Salt water coning beneath fresh water wells. Water Manage. Tech. Rep. No. 18, Colorado State Univ., Fort Collins, Colorado, 168 p.
- Santing, G., 1986. Circulating flow in a confined salt-groundwater body. In: Boekelman, R.H., Van Dam, J.C., Evertman, M., Ten Hoorn, W.H.C. (Eds.), Proc. 9<sup>th</sup> Salt Water Intrusion Meeting, May 1986, Delft University of Technology, Delft, p. 73-84.
- Sarwar, A., 2000. A transient model approach to improve on-farm irrigation and drainage in semi-arid zones. PhD thesis, Wageningen University, 147 p.
- Schmorak, S., Mercado, A., 1969. Upconing of fresh water-sea water interface below pumping wells, field study. Water Resour. Res. 5(6), 1290-1311.
- Seiler, K.P., Stichler, W., Sajjad, M.J., Hussain, S.D., 1988. Study of downward movement of soil moisture in the irrigated area of Faisalabad, Pakistan, the sources of groundwater rise and the salinity of groundwater and soils. In: Proc. Conf. on effects of agriculture and water management on human environment, 1988, ICID, Dubrovnik, Vol. 5, p. 197-211.
- Shakya, S.K., Gupta, P.K., Kumar, D., 1995. Innovative drainage techniques for waterlogged sodic soils. Bul. No. 3, Dep. of Soil and Water Eng., Punjab Agric. Univ., Ludhiana, 34 p.
- Sharma, D.P., Rao, K.V.G.K., Singh, K.N., Kumbhare, P.S., 1995. Recycling of drainage effluent for irrigation. In: Rao, K.V.G.K., Agarwal, M.C., Singh, O.P., Oosterbaan, R.J. (Eds.), Reclamation and management of waterlogged saline soils. CSSRI, Karnal, CCS Haryana Agric. Univ., Hisar, p. 189-204.
- Sharma, D.P., Rao, K.V.G.K., 1998. Strategy for long term use of saline drainage water for irrigation in semi-arid regions. Soil and Tillage Res. 48, 287-295.
- Sharma, D.P., Singh, K., Rao, K.V.G.K., 2000. Subsurface drainage for rehabilitation of waterlogged saline lands: Example of a soil in semi-arid climate. Arid Soil Res. and Rehabilitation 14, 373-386.
- Shearer, T.R., Van Wonderen, J., 1993. Scavenger wells -4- Simulation modelling. In: Custodio, E., Galofré, A. (Eds.), Proc. 12<sup>th</sup> Salt Water Intrusion Meeting, Nov. 1992, CIMNE, Barcelona, p. 583-598.
- Šimůnek, J., Suarez, D.L., 1994. Two-dimensional transport model for variably saturated porous media with major ion chemistry. Water Resour. Res. 30(4), 1115-1133.
- Šimůnek, J., Vogel, T., Van Genuchten, M.Th., 1994. The SWMS\_2D code for simulating water flow and solute transport in two-dimensional variably saturated media. Res. Rep. No. 132, U.S. Salinity Laboratory, Riverside, California, 197 p.
- Šimůnek, J., Suarez, D.L., Šejna, M., 1996. The UNSATCHEM software package for simulating the one-dimensional variably saturated water flow, heat transport, carbon dioxide production and transport, and multicomponent solute transport with major ion equilibrium and kinetic chemistry. Res. Rep. No. 141, U.S. Salinity Laboratory, Riverside, California, 186 p.
- Singh, N.T., 1993. Saline irrigation in the Indian subcontinent. In: Tyagi, N.K., Kamra, S.K., Minhas, P.S., Singh, N.T. (Eds.), Irrigation in saline environment: key management issues, CSSRI, Karnal, p. 40-66.
- Smedema, L.K., 1990. Comparative study of the East Khairpur, Mardan and Drainage IV pipe drainage projects. Pub. No. 8, IWASRI, Lahore, 31 p.
- Smedema, L.K., 1993. Drainage technology and effluent salinity. GRID 3, p. 10.

## References

---

- Smedema, L.K., Poelman, A., De Haan, W., 1985. Use of the Hooghoudt formula for drain spacing calculations in homogeneous-anisotropic soils. *Agric. Water Manage.* 10, 283-291.
- Smets, S.M.P., 1996. The effects of irrigation management on soil salinity and crop transpiration at the field level, by using the agro-hydrological model SWAP93. MSc thesis, Wageningen University, 101 p.
- Smets, S.M.P., Kuper, M., Van Dam, J.C., Feddes, R.A., 1997. Salinization and crop transpiration of irrigated fields in Pakistan's Punjab. *Agric. Water Manage.* 35, 43-60.
- Smith, L., Wheatcraft, S.W., 1992. Groundwater flow. In: D.R. Maidment (Ed.), *Handbook of hydrology*. McGraw-Hill, p. 6.1-6.58.
- Smith, M., 1993. CLIMWAT for CROPWAT. Irrigation and Drainage paper No. 49, FAO, Rome, 113 p.
- Stoner, R.F., Bakiewicz, W., 1993. Scavenger wells -1- Historic development. In: Custodio, E., Galofré, A. (Eds.), *Proc. 12<sup>th</sup> Salt Water Intrusion Meeting*, Nov. 1992, CIMNE, Barcelona, p. 545-556.
- Sufi, A.B., Latif, M., Skogerboe, G.V., 1998. Simulating skimming well techniques for sustainable exploitation of groundwater. *Irrig. Drain. Syst.* 12, 203-226.
- Swain, D.G., 1991. A conceptual planning process for management of subsurface drainage. In: Dinar, A., Zilberman, D. (Eds.), *The economics and management of water and drainage in agriculture*. Kluwer, p.187-205.
- Swarzenski, W.V., 1968. Fresh and saline ground-water zones in the Punjab Region West Pakistan. Water-supply paper 1608-I, US Geological Survey, 24 p.
- Thorborg, B.B.W., Jousma, G., 1989. Development of a knowledge system for modelling fresh- and saline-groundwater flow. In: De Breuck, W., Walschot, L. (Eds.), *Proc. 10<sup>th</sup> Salt Water Intrusion Meeting*, 1988, *Natuurwet. Tijdschr.*, Ghent, p. 200-209.
- Toksöz, S., Kirkham, D., 1971. Steady drainage of layered soils: I, Theory. *J. Irrig. Drain. Div.*, ASCE 97(IR1), 1-18.
- USBR, 1989. Design memorandum subsurface drainage Fourth Drainage Project, Faisalabad, 49 p.
- Van Achthoven, T., Lohan, H.S., Parlin, W., 2000. The reclamation of waterlogged and saline lands with sub-surface drainage: an overview of the Haryana Operational Pilot Project. Unpublished paper, 12 p.
- Van Dam, J.C., 2000. Field-scale water flow and solute transport; SWAP model concepts, parameter estimation and case studies. PhD thesis, Wageningen University, 167 p.
- Van Dam, J.C., Stricker, J.N.M., Droogers, P., 1994. Inverse method to determine soil hydraulic functions from multistep outflow experiments. *Soil Sci. Soc. Am. J.* 58, 647-652.
- Van Dam, J.C., Huygen, J., Wesseling, J.G., Feddes, R.A., Kabat, P., Van Walsum, P.E.V., Groenendijk, P., Van Diepen, C.A., 1997. Theory of SWAP 2.0, simulation of water flow, solute transport and plant growth in the Soil-Water-Atmosphere-Plant environment. Rep. No. 71, Dep. Water Resources, Wageningen University, 167 p.
- Van Genuchten, M.Th., 1980. A closed-form equation for predicting the hydraulic conductivity of unsaturated soils. *Soil Sci. Soc. Am. J.* 44, 892-898.
- Van Genuchten, M.Th., Pinder, G.F., Frind, E.O., 1977. Simulation of two-dimensional contaminant transport with isoparametric Hermitian finite elements. *Water Resour. Res.* 13(2), 451-458.

- Van Hoom, J.W., Van Alphen, J.G., 1994. Salinity control. In: Ritzema, H.P. (Ed.), *Drainage principles and applications*. Pub. No. 16, ILRI, Wageningen, 533-600.
- Van der Molen, W.H., 1987. Van kwantiteit naar kwaliteit: een halve eeuw drainage-theorie. *Cultuurtechnisch tijdschrift*, 26(5), 311-321 (In Dutch).
- Van Ommen, H.C., 1985. Systems approach to an unsaturated-saturated groundwater quality model, including adsorption, decomposition and bypass. *Agric. Water Manage.* 10, 193-203.
- Van Ommen, H.C., 1986. Influence of diffuse sources of contamination on the quality of outflowing groundwater including non-equilibrium adsorption and decomposition. *J. Hydrol.* 88, 79-95.
- Van Ommen, H.C., Van Genuchten, M.Th., Van der Molen, W.H., Dijkema, R., Hulshof, J., 1989. Experimental and theoretical analysis of solute transport from a diffuse source of pollution. *J. Hydrol.* 105, 225-251.
- Van der Ploeg, R.R., Horton, R., Kirkham, D., 1999. Steady flow to drains and wells. In: Skaggs, R.W., Van Schilfgaarde, J. (Eds.), *Agricultural drainage*. Vol. 38, Am. Soc. Agron., Madison, p. 213-263.
- Van Wonderen, J.J., Jones, C.R.C., 1993. Scavenger wells -5- Design criteria and implementation in Sindh. In: Custodio, E., Galofré, A. (Eds.), *Proc. 12<sup>th</sup> Salt Water Intrusion Meeting*, Nov. 1992, CIMNE, Barcelona, p. 599-613.
- Vaughan, P.J., Suarez, D.L., Šimůnek, J., Corwin, D.L., Rhoades, J.D., 1999. Role of groundwater flow in tile drain discharge. *J. Environ. Qual.* 28, 403-410.
- Vimoke, B.S., Tyra, T.D., Thiel, T.J., Taylor, G.S., 1962. Improvements in construction and use of resistance networks for studying drainage problems. *Soil Sci. Soc. Am. J.* 26(2), 203-207.
- Vlotman, W.F., Bhutta, M.N., Ali, S.R., Bhatti, A.K., 1994. Design, monitoring and research Fourth Drainage Project, Faisalabad, 1976 - 1994 (supporting report). Pub. No. 159, IWASRI, Lahore, 223 p.
- Von Hoyningen-Hüne, J., 1983. Die interzeption des Niederschlags in landwirtschaftlichen beständen. *Schriftenreihe des DVWK* 57, 1-53 (In German).
- Voss, C.I., 1984. SUTRA, a finite-element simulation model for saturated-unsaturated, fluid-density-dependent groundwater flow with energy transport or chemically-reactive single-species solute transport. *Water-Resources Investigations Report* 84-4369, U.S. Geological Survey, 409 p.
- Warrick, A.W., Mullen, G.J., Nielsen, D.R., 1977. Scaling field-measured soil hydraulic properties using a similar media concept. *Water Resour. Res.* 13(2), 355-362.
- Westcot, D.W., 1997. Drainage water quality. In: Madramootoo, C.A., Johnston, W.R., Willardson, L.S. (Eds.), *Management of agricultural drainage water quality*. Water Rep. No. 13, FAO, Rome, p. 11-20.
- Willardson, L.S., Boels, D., Smedema, L.K., 1997. Reuse of drainage water from irrigated areas. *Irrig. Drain. Syst.* 11, 215-239.
- Wirojanagud, P., Charbeneau, R.J., 1985. Saltwater upconing in unconfined aquifer. *J. Hydraulic Eng., ASCE* 111(3), 417-434.
- Wolters, W., 1992. Influences on the efficiency of irrigation water use. Publ. No. 51, ILRI, Wageningen, 150 p.
- World Bank, 1997. National drainage program, Pakistan. Rep. No. 15310-PAK, rural

## References

---

- development sector management unit, South Asia Region, World Bank, 119 p.
- Wösten, J.H.M., Lilly, A., Nemes, A., Le Bas, C., 1998. Using existing soil data to derive hydraulic parameters for simulation models in environmental studies and in land use planning. Rep. No. 156, Alterra, Wageningen, 106 p.
- Wösten, J.H.M., Veerman, G.H., De Groot, W.J.M., Stolte, J., 2001. Waterretentie- en doorlatendheids-karakteristieken van boven- en ondergronden in Nederland, de Staringreeks. Rep. No. 153, Alterra, Wageningen, 86 p. (in Dutch).
- Youngs, E.G., Leeds-Harrison, P.B., 2000. Improving efficiency of desalinization with subsurface drainage. *J. Irrig. Drain. Eng.* 126(6), 375-380.
- Yu, S.C., Konyha, K.D., 1992. Boundary modeling of steady saturated flow to drain tubes. In: *Drainage and water table control*, Proc. 6<sup>th</sup> Int. Drain. Symp., Dec. 1992, Nashville, Tennessee. p. 305-313.
- Zaradny, H., Feddes, R.A., 1979. Calculation of non-steady flow towards a drain in saturated-unsaturated soil by finite elements. *Agric. Water Manage.* 2, 37-53.

## Appendix A Application of the SWMS\_2D Model to Simulate the $q_d(H)$ Relationship for Pipe Drains

In Chapter 5, the SWMS\_2D model is used to simulate the  $q_d(H)$  relationship for pipe drains. Main objective is to calibrate the soil hydraulic properties of the soil-aquifer system. The SWMS\_2D model is particularly useful to assess the saturated horizontal conductivity,  $K_{xx}$  [ $L T^{-1}$ ] and the vertical saturated hydraulic conductivity,  $K_{zz}$  [ $L T^{-1}$ ] for the zone below drain level. Because of symmetry, only half the flow region between two drains is modelled (see Fig. 3.2). The pipe drain itself is described by a single node. A correct description of the hydraulic head distribution around the drain is obtained by adjusting the hydraulic conductivity of the elements surrounding the drain (Section 2.6). The following boundary conditions are used in SWMS\_2D (coordinate axis are oriented along the principal directions of the hydraulic conductivity):

Top boundary (soil surface, during irrigation):

$$q_{ir} = -K_r K_{zz} \left( \frac{\partial h}{\partial z} + 1 \right) \quad (A.1)$$

where  $q_{ir}$  is the soil water flux [ $L T^{-1}$ ] due to irrigation.

Top boundary (soil surface, during redistribution):

$$-K_r K_{zz} \left( \frac{\partial h}{\partial z} + 1 \right) = 0 \quad (A.2)$$

Right boundary (water divide):

$$\frac{\partial h}{\partial x} = 0 \quad (A.3)$$

Drain node:

$$h = 0 \quad (A.4)$$

Left boundary (vertical axis through drain):

$$\frac{\partial h}{\partial x} = 0 \quad (A.5)$$

Bottom boundary (impermeable layer):

$$\frac{\partial h}{\partial z} + 1 = 0 \quad (A.6)$$

## Appendix A

---

Only single drainage events are simulated with the model. The initial depth of the groundwater table is always assumed at drain level. Each simulation starts with an irrigation application over the entire soil surface. The quantity of irrigation water is chosen in such a way that no ponding occurs at the soil surface. This limitation was introduced to prevent excessive computation times. Total simulation time is ~100 days, depending on the speed of the redistribution process. To obtain a straightforward  $q_d(H)$  relationship, only  $q_d$ - $H$  values from the redistribution period are considered during the analysis.

## Appendix B Analysis of Pumping Test Data from Satiana Tube-Well No. 22a with WTAQ

The pumping test for Satiana tube-well No. 22a lasted for 121 hours. Drawdown of the groundwater table was measured in the pumping well and in an observation well at 25 m distance from the well. Specific information about the set-up of the test is summarized in Table B.1. Moghal et al. (1992) calculated transmissivity (height of the aquifer times horizontal hydraulic conductivity) using Jacob's method in time-drawdown plots and using the Theis recovery method in time-residual-drawdown plots. The investigators derived the thickness of the aquifer,  $B$  and the specific yield of the aquifer,  $S_y$  [-] from a distance-drawdown plot in a trial and error fashion. No value for the vertical saturated hydraulic conductivity,  $K_z$  could be determined using these methods.

**Table B.1** Specific information on the pumping test for Satiana tube-well No. 22a.

$r$ -value of well (m)	Discharge, $Q_v$ ( $\text{m}^3 \text{d}^{-1}$ )	Depth of well (m)	Length of screen (m)
0.1	5530	63.40	35.36
25		45.00	2.00

In this appendix the pumping test data are re-analysed using the WTAQ model (Barlow and Moench, 1999). WTAQ simulates the drawdown in hydraulic head,  $\phi$  in a confined or unconfined aquifer as a result of pumping from a (tube-)well. The hydraulic properties of the aquifer can be determined through inverse modelling by comparing measured and simulated drawdowns at the well and at a given number of observation wells. The WTAQ code is based on an analytical model of axi-symmetric groundwater flow in a homogeneous and anisotropic aquifer. The number of simplifying assumptions is relatively low compared to the methods used by Moghal et al. (1992). The governing equation of WTAQ can be written as (coordinate axis are oriented along the principal directions of the hydraulic conductivity):

$$\frac{\partial^2 \phi}{\partial r^2} + \frac{1}{r} \frac{\partial \phi}{\partial r} + \frac{K_z}{K_r} \frac{\partial^2 \phi}{\partial z^2} = \frac{S_s}{K_r} \frac{\partial \phi}{\partial t} \quad (\text{B.1})$$

where  $S_s$  is the specific storage [ $\text{L}^{-1}$ ]. Note that  $S_s = \rho_0 g S_{op}$  (Section 2.2).

The following boundary conditions are used in WTAQ. At the top boundary:

$$K_z \frac{\partial \phi}{\partial z} = -\alpha_1 S_y \int_0^t \frac{\partial \phi}{\partial t'} e^{-\alpha_1(t-t')} dt' \quad (\text{B.2})$$

where  $\alpha_1$  is an empirical coefficient [ $\text{T}^{-1}$ ] for drainage from the unsaturated zone (if  $\alpha_1 \rightarrow \infty$ , instantaneous drainage is assumed, if  $\alpha_1 = 0$ , a no-flow condition is obtained) and  $S_y$  is the specific yield [-].

## Appendix B

---

At the outer radial boundary:

$$\phi = \text{constant} \quad (\text{B.3})$$

At the well screen ( $r = r_w$ ):

$$2\pi r_w L_s K_{rr} \frac{\partial \phi}{\partial r} \Big|_{r=r_w} = Q_v + S_{wb} \frac{\partial \phi_w}{\partial t} \quad (\text{B.4})$$

where  $L_s$  is the length [L] of the well screen,  $S_{wb}$  the well bore storage [ $L^2$ ] and  $\phi_w$  the average hydraulic head [L] in the well bore. Note that Eq. (B.4) assumes that the discharge of the well,  $Q_v$  is distributed equally over the well screen nodes.

At the well boundary (above and below the well screen):

$$\frac{\partial \phi}{\partial r} \Big|_{r=r_w} = 0 \quad (\text{B.5})$$

Condition (B.5) implies that a well casing of constant external radius  $r_w$  extends from the top of the screened section to the groundwater table and from the bottom of the screened section to the base of the aquifer.

At the bottom boundary (impermeable layer):

$$\frac{\partial \phi}{\partial z} = 0 \quad (\text{B.6})$$

The above set of equations are solved by Moench (1997) through Laplace transformation using dimension-less parameters. Drawdown is obtained by numerical inversion of the resulting equations (Barlow and Moench, 1999).

The optimization program UCODE (Poeter and Hill, 1998) is used in conjunction with WTAQ. This program minimizes a weighted least-squares objective function using a modified Gauss-Newton method. In the optimization, the value for the thickness of the aquifer is fixed at 230 m, as found by Moghal et al. (1992) to reduce the number of free parameters. The results are given in Table B.2. The values from the original analysis are also shown. Measured and fitted time-drawdown plots for the pumping well and the observation well are shown in Figure B.1.



**Table B.2** Calculated parameter values for the aquifer at Satiana tube-well No. 22a. Values between brackets denote the 95 % confidence interval.

	WTAQ & UCODE	Moghal et al. (1992)
Thickness of the aquifer, $B$ (m)	230	230
Rad. sat. hydr. cond., $K_{rr}$ (m d <sup>-1</sup> )	23.1 (23.0 - 23.3)	24.3 - 25.4
Vert. sat. hydr. cond., $K_{zz}$ (m d <sup>-1</sup> )	25.7 (22.6 - 29.3)	-
Specific storage, $S_s$ (m <sup>-1</sup> )	$2.2 \times 10^{-5}$ ( $1.8 \times 10^{-5}$ - $2.6 \times 10^{-5}$ )	-
Specific yield, $S_y$ (-)	0.11 (0.07 - 0.14)	0.13
Empirical coef., $\alpha_1$ (d <sup>-1</sup> )	0.4 (0.3 - 0.5)	-

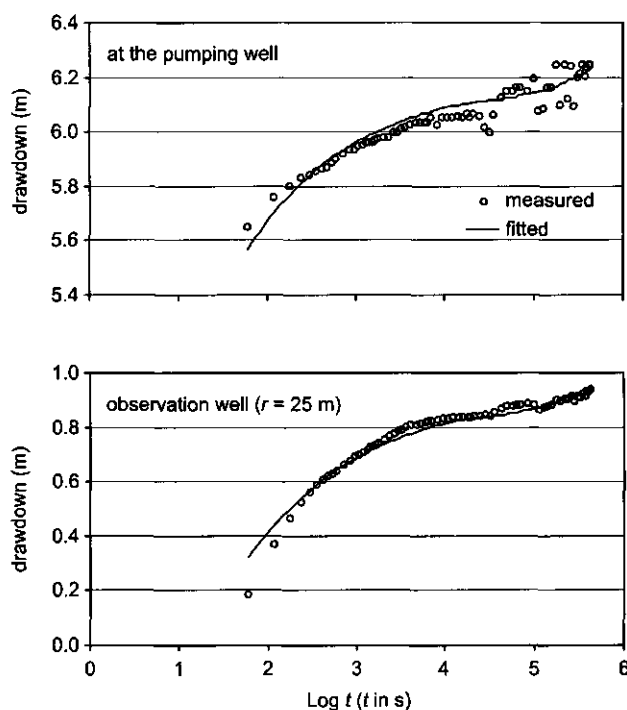
**Figure B.1** Measured and fitted drawdown at Satiana tube-well No. 22a and at the observation well.

Table B.2 shows that the results from WTAQ & UCODE on the one hand, and the results from the analysis of Moghal et al. (1992) on the other hand, agree well. The scatter in the measured drawdown values at the well towards the end of the pumping period (Fig. B.1), is probably due to fluctuations in the well discharge. The calculated  $K_{zz}$  of 25.7 m d<sup>-1</sup> is approximately equal to the calculated  $K_{rr}$  value of 23.1 m d<sup>-1</sup>, indicating that the aquifer is isotropic. In subsequent calculations it is therefore assumed that  $K_{rr} = K_{zz} = 23.1$  m d<sup>-1</sup>. The base of the aquifer is

## Appendix B

---

calculated to be  $230 + 1.75 = 231.75$  m below soil surface, where 1.75 m is the estimated depth of the groundwater table before the pumping test (not reported by Moghal et al., 1992). The depth of the horizontal boundary plane is determined from Fig. B.1. In Chapter 5 the horizontal boundary plane was defined as the water level in the well during pumping. Figure B.1. shows that the drawdown in the well is 6.25 m at maximum. Combined with an average depth of the groundwater table of 2.0 m, this yields a depth of the horizontal boundary plane of 8.25 m below soil surface.

# List of Symbols

## Roman alphabet

$A_i$	Cross-sectional area [ $L^2$ ] or surface area [ $L^2$ ] of stream-tube $i$
$A_{sa}$	Cross-sectional area [ $L^2$ ] of the soil-aquifer system
$a$	Thickness [ $L$ ] of the first layer in the Toksöz and Kirkham (1971) equations
$a_i$	Empirical coefficient [ $L\ T^{-1}$ ] to calculate intercepted precipitation
$B$	Saturated thickness [ $L$ ] of the aquifer
$B_m$	Parameter [-] in the Toksöz and Kirkham (1971) equations
$b$	Thickness [ $L$ ] of the first and second layer in the Toksöz and Kirkham (1971) equations or thickness [ $L$ ] of the aquifer below the horizontal boundary plane
$b_i$	Soil cover fraction [-]
$C$	Solute concentration on mass basis [ $M\ M^{-1}$ ]
$C_0$	Base solute concentration [ $M\ M^{-1}$ ]
$C_{0, \text{rootzone}}$	Initial solute concentration [ $M\ M^{-1}$ ] of the rootzone
$C_d$	Differential water capacity [ $L^{-1}$ ]
$C_{\text{drain}}$	Correction factor [-] as given by Vimoke et al. (1962)
$C_{fc}$	Solute concentration [ $M\ M^{-1}$ ] of the rootzone (at field capacity)
$C_i$	Solute concentration [ $M\ M^{-1}$ ] of the influent
$C_m$	Parameter [-] in the Toksöz and Kirkham (1971) equations
$C_{\text{recharge}}$	Solute concentration [ $M\ M^{-1}$ ] of the recharge
$c$	Solute concentration [ $M\ L^{-3}$ ] on volume basis
$c_0$	Solute concentration [ $M\ L^{-3}$ ] of the resident soil water, initially present in the zone below drain level or in the zone below the horizontal boundary plane
$c_d$	Solute concentration [ $M\ L^{-3}$ ] of the drain flux in the SWAP model
$c_{dp}$	Solute concentration [ $M\ L^{-3}$ ] of the downward flux at drain level or at the horizontal boundary plane
$c_{dw}$	Solute concentration [ $M\ L^{-3}$ ] of the drainage water
$c_{gw}$	Solute concentration [ $M\ L^{-3}$ ] of the groundwater below drain level or below the horizontal boundary plane
$c_i$	Solute concentration [ $M\ L^{-3}$ ] of stream-tube $i$
$c_{ir}$	Solute concentration [ $M\ L^{-3}$ ] of the irrigation water
$c_p$	Specific heat [ $L^2\ T^{-2}\ \Theta^{-1}$ ] of air
$c_s$	Solute concentration [ $M\ L^{-3}$ ] of the surface runoff
$c_{tw}$	Solute concentration [ $M\ L^{-3}$ ] of the tube-well water
$D$	Cumulative drainage [ $L$ ]
$D_{ij}$	Hydrodynamic dispersion tensor [ $L^2\ T^{-1}$ ]
$D_m$	Porous medium ionic or molecular diffusion coefficient [ $L^2\ T^{-1}$ ]
$D_w$	Solute diffusion coefficient in free water [ $L^2\ T^{-1}$ ]
$d$	Drain depth [ $L$ ]
$d_e$	Hooghoudt's equivalent depth [ $L$ ]
$d_{\text{eff}}$	Effective drain diameter [ $L$ ]
$d_{gw}$	Depth of the groundwater table [ $L$ ]
$E$	Cumulative actual evaporation [ $L$ ]
$E_a$	Actual soil evaporation rate [ $L\ T^{-1}$ ]
$E_{\text{emp}}$	Soil evaporation rate [ $L\ T^{-1}$ ] according to an empirical function

## List of Symbols

$E_{\max}$	Maximum soil evaporation rate [ $L\ T^{-1}$ ]
$E_p$	Potential soil evaporation rate [ $L\ T^{-1}$ ]
$EC$	Electrical Conductivity [ $L^{-3}\ M^{-1}\ T^3\ I^2$ ]
$EC_{dp}$	Electrical Conductivity [ $L^{-3}\ M^{-1}\ T^3\ I^2$ ] of the downward soil water flux at drain level or at the horizontal boundary plane
$EC_{dw}$	Electrical Conductivity [ $L^{-3}\ M^{-1}\ T^3\ I^2$ ] of the drainage water
$EC_e$	Electrical Conductivity [ $L^{-3}\ M^{-1}\ T^3\ I^2$ ] of the saturation extract
$EC_{gw}$	Electrical Conductivity [ $L^{-3}\ M^{-1}\ T^3\ I^2$ ] of the groundwater
$EC_{recharge}$	Electrical Conductivity [ $L^{-3}\ M^{-1}\ T^3\ I^2$ ] of the recharge
$EC_{tw}$	Electrical Conductivity [ $L^{-3}\ M^{-1}\ T^3\ I^2$ ] of the tube-well water
$ET_p$	Potential evapotranspiration rate [ $L\ T^{-1}$ ]
$ET_{p0}$	Potential evapotranspiration rate [ $L\ T^{-1}$ ] of the wet crop
$ET_{ref}$	Reference crop evapotranspiration rate [ $L\ T^{-1}$ ]
$e_a$	Actual vapour pressure [ $M\ L^{-1}\ T^{-2}$ ]
$e_s$	Saturation vapour pressure [ $M\ L^{-1}\ T^{-2}$ ]
$f$	Cumulative drainage probability density function [ $L^{-1}$ ]
$f_l$	Leaching efficiency coefficient [-]
$G$	Soil heat flux [ $M\ T^{-3}$ ]
$g$	Gravitational acceleration (gravity vector) [ $L\ T^{-2}$ ]
$g_w$	Weighting function [-] to account for the relative influence of each stream tube $i$ on the effluent salinity
$H$	Height [ $L$ ] of the groundwater table above drain level (pipe drains) or above the horizontal boundary plane (tube-wells)
$h$	Pressure head [ $L$ ]
$h_1$	Pressure head [ $L$ ] below which roots start to extract water from the soil
$h_2$	Pressure head [ $L$ ] below which roots start to extract water optimally from the soil
$h_{3h}$	Pressure head [ $L$ ] below which roots cannot extract water optimally any more, for a high potential transpiration rate
$h_{3l}$	Pressure head [ $L$ ] below which roots cannot extract water optimally any more, for a low potential transpiration rate
$h_4$	Pressure head [ $L$ ] below which no water uptake by roots is possible (wilting point)
$I$	Cumulative irrigation [ $L$ ]
$I_r$	Irrigation rate [ $L\ T^{-1}$ ]
$K_a$	Saturated hydraulic conductivity [ $L\ T^{-1}$ ] above drain level
$K_b$	Saturated hydraulic conductivity [ $L\ T^{-1}$ ] below drain level
$K_{drain}$	Hydraulic conductivity [ $L\ T^{-1}$ ] of elements surrounding the pipe drain
$K_{ij}$	Hydraulic conductivity tensor [ $L\ T^{-1}$ ]
$K_r$	Relative hydraulic conductivity [-]
$K_s$	Saturated hydraulic conductivity [ $L\ T^{-1}$ ]
$k_c$	Crop factor [-]
$k_{drain}$	Permeability [ $L^2$ ] of elements surrounding the pipe drain
$k_{ij}$	Permeability tensor [ $L^2$ ]
$k_r$	Relative permeability [-]
$L$	Drain spacing [ $L$ ]

$L_s$	Length [L] of the well screen
$LAI$	Leaf Area Index [ $L^2 L^{-2}$ ]
$m$	Empirical parameter [-] in the Mualem-Van Genuchten model
$n$	Empirical parameter [-] in the Mualem-Van Genuchten model
$n_e$	Effective porosity [-]
$P$	Cumulative precipitation [L]
$P_i$	Cumulative intercepted precipitation [L]
$P_{ir}$	Intercepted precipitation rate [ $L T^{-1}$ ]
$P_r$	Precipitation rate [ $L T^{-1}$ ]
$p$	Fluid pressure [ $M L^{-1} T^{-2}$ ]
$Q$	Cumulative pumping [L]
$Q_v$	Pumping capacity [ $L^3 T^{-1}$ ] of the well on volume basis
$Q_m$	Pumping capacity [ $M T^{-1}$ ] of the well on mass basis
$q_d$	Drain flux [ $L T^{-1}$ ]
$q_i$	Specific discharge vector [ $L T^{-1}$ ]
$q_{ir}$	Soil water flux [ $L T^{-1}$ ] at the soil surface due to irrigation
$q_m$	Specified fluid mass flux [ $M L^{-2} T^{-1}$ ]
$q_{recharge}$	Specified mass flux [ $M L^{-2} T^{-1}$ ] due to recharge or flow rate [ $L T^{-1}$ ] through the rootzone
$q_v$	Specified water flux [ $L T^{-1}$ ]
$R$	Recharge rate [ $L T^{-1}$ ]
$R_n$	Net radiation [ $M T^{-3}$ ]
$R_s$	Cumulative surface runoff [L]
$R_{sr}$	Surface runoff rate [ $L T^{-1}$ ]
$RSC$	Residual Sodium Carbonate (meq $l^{-1}$ )
$r$	Radial coordinate [L]
$r_0$	Initial radial coordinate [L] of a solute particle
$r_a$	Aerodynamic resistance [ $T L^{-1}$ ]
$r_d$	Radius [L] of a pipe drain
$r_e$	Radial distance [L] to the water divide or to the outer radial boundary for a well
$r_p$	Radial position [L] of a solute particle after a time step $\Delta t$
$r_s$	Crop resistance [ $T L^{-1}$ ]
$r_w$	Radius [L] of the well
$S_a$	Actual soil water extraction rate [ $T^{-1}$ ] by plant roots
$S_e$	Dimensionless saturation [-]
$S_k$	Sink term [ $M L^{-3} T^{-1}$ ]
$S_{op}$	Specific pressure storativity [ $L T^2 M^{-1}$ ]
$S_p$	Potential soil water extraction rate [ $T^{-1}$ ] by plant roots
$S_s$	Specific storage [ $L^{-1}$ ]
$S_w$	Relative saturation [-]
$S_{wb}$	Well bore storage [ $L^2$ ]
$S_{wr}$	Residual saturation [-]
$S_y$	Specific yield [-]
$SAR$	Sodium adsorption ratio ((meq $l^{-1}$ ) $^{1/2}$ )
$SP$	Saturation Percentage [-]

## List of Symbols

---

$s$	Position [L] on a path-line or a streamline
$s_0$	Position [L] on a path-line or a streamline at $t = t_0$
$T$	Cumulative actual transpiration [L]
$T_a$	Actual transpiration rate [ $L\ T^{-1}$ ]
$T_{high}$	High potential transpiration rate [ $L\ T^{-1}$ ]
$T_{low}$	Low potential transpiration rate [ $L\ T^{-1}$ ]
$T_p$	Potential transpiration rate [ $L\ T^{-1}$ ]
$t$	Time [T]
$t_0$	Time [T] to start counting
$V_i$	Volume [ $L^3$ ] of stream-tube $i$
$v$	Advective displacement velocity [ $L\ T^{-1}$ ]
$W$	Water storage [L]
$W_{fc}$	Depth [L] of water stored in the rootzone at field capacity
$w$	Width [L] of a stream-tube
$x$	Horizontal coordinate [L]
$x_i$	Spatial coordinate [L]
$z$	Vertical coordinate or height [L] above datum
$z_0$	Initial vertical coordinate [L] of a solute particle
$z_p$	Vertical position [L] of a solute particle after a time step $\Delta t$
$z_r$	Depth [L] of the rootzone

## Greek alphabet

$\alpha$	Porous matrix compressibility [ $L\ T^2\ M^{-1}$ ]
$\alpha_i$	Empirical constant [ $T^{-1}$ ] for drainage from the unsaturated zone
$\alpha_L$	Longitudinal dispersivity [L]
$\alpha_T$	Transverse dispersivity [L]
$\alpha_{cf}$	Root uptake concentration factor [-]
$\alpha_n$	Empirical parameter [ $L^{-1}$ ] in the Mualem-Van Genuchten model
$\alpha_p$	Empirical parameter [ $M^{-1}\ L\ T^2$ ] in the Mualem-Van Genuchten model
$\alpha_{rs}$	Reduction factor [-] due to salinity stress
$\alpha_{rw}$	Reduction factor [-] due to water stress
$\beta$	Fluid compressibility [ $L\ T^2\ M^{-1}$ ]
$\beta_p$	Boesten parameter [ $L^{1/2}$ ]
$\gamma$	Drainage resistance [T]
$\gamma_a$	Psychometric constant [ $M\ L^{-1}\ T^{-2}\ \Theta^{-1}$ ]
$\Delta_v$	Slope of the saturated vapour pressure curve [ $M\ L^{-1}\ T^{-2}\ \Theta^{-1}$ ]
$\delta_{ij}$	Kronecker delta function [-]
$\zeta$	Width [L] of the slit drain
$\eta$	Unit gravitational vector [-] in the direction of $x_2$ (vertically upward)
$\theta$	Volumetric water content [-]
$\theta_r$	Residual volumetric water content [-]
$\theta_s$	Saturated volumetric water content [-]
$\kappa$	Extinction coefficient [-] for global solar radiation
$\lambda_w$	Latent heat of vaporization [ $L^2\ T^{-2}$ ]
$\lambda$	Empirical parameter [-] in the Mualem-Van Genuchten model

$\mu$	Fluid viscosity [ $M L^{-1} T^{-1}$ ]
$\rho$	Fluid density [ $M L^{-3}$ ]
$\rho_a$	Air density [ $M L^{-3}$ ]
$\rho_b$	Dry bulk density [ $M L^{-3}$ ]
$\rho_0$	Fluid density [ $M L^{-3}$ ] at $C = C_0$
$\rho_w$	Density of water [ $M L^{-3}$ ]
$\tau$	Solute travel time [T]
$\Phi$	Potential function [ $L^2 T^{-1}$ ]
$\phi$	Hydraulic head [L]
$\phi_w$	Average hydraulic head [L] in the well bore
$\psi$	Stream-function ( $[L^2 T^{-1}]$ in two-dimensional flow or $[L^3 T^{-1}]$ in axi-symmetric flow)
$\psi_0$	Stream-function value [ $L^2 T^{-1}$ ] or [ $L^3 T^{-1}$ ] corresponding with the outer boundaries of the flow-system
$\varepsilon$	Porosity [-]

List of Symbols

---



## **Curriculum Vitae**

Thijs Kelleners was born on 7 August 1969 at Vlaardingen, The Netherlands. After secondary school he studied "Westerse Cultuurtechniek" at Wageningen University from 1987 up to graduation in 1993. Major subjects were: soil reconnaissance and land evaluation, soil- and water conservation, agro-hydrology and nature development. Practical training was done at the International Waterlogging and Salinity Research Institute (IWASRI), Lahore, Pakistan. In September 1993 he joined the International Institute for Land Reclamation and Improvement (ILRI) in Wageningen. He worked on various irrigation and drainage related subjects. From April 1997 to April 2001 he did the research work for the present thesis as a PhD student for the sub-department of Water Resources of Wageningen University. In August 2001 he joined the U.S. Salinity Laboratory, Riverside, California where he is conducting research on agricultural drainage problems in San Joaquin Valley in cooperation with the Water Management Research Laboratory in Fresno, California.